Sediment Transport in Combined Sewers

Trevor D. McIlhatton BEng(Hons) MSc

This thesis is submitted in accordance with the requirements of the University of Liverpool for the degree of

Doctor of Philosophy

University of Liverpool

April 2005

ABSTRACT

Watercourses, particularly in urban areas, are polluted by sewage discharges, which convey solids and dissolved contaminants from drains and sewer overflows. In industrialised countries much of the pollution originates from combined sewer systems, from which overflows relieve the highest flows. For more than a decade researchers have been investigating sediment movement in sewers and associated pollutant release. Traditionally impacts from these events have been related to the suspended solids phase of the flow passing through a combined sewer overflow (CSO) structure. It is now apparent that much of the suspended load originates from solids eroded from the bed. The 'near bed solids' which are re-entrained into the flow, together with solids eroded from the bulk bed, account for large changes in the suspended sediment concentration under time varying flow conditions. The Ackers (1991) relationship is widely used in the InfoWorks UK industry standard urban drainage modelling package to predict these suspended solids in transport. This relationship was formulated with data from experiments carried out solely on granular deposits of uniform size and, as shown in this study, is inappropriate for the prediction of suspended transport from cohesive deposits with a range of particle sizes. Deployment of a significant field-monitoring programme in a catchment in Forfar, Northeast Scotland, in conjunction with data from laboratory erosion tests provided good quality in-depth data that was used to examine the behaviour of deposits subjected to increasing rates of bed shear stresses. Investigation of these events enabled an appreciation to be gained of the in-sewer processes that govern the erosion and transport of sediment within combined systems. The results of these tests enabled the veracity of the Ackers (1991) relationship to be examined for the prediction of suspended sediment transport in combined sewers. The results highlighted that, in its unmodified form, the Ackers (1991) relationship did not yield acceptable results. Investigation showed that modifications based on the work of White and Day (1982) and Rushforth (2001) improved the predictions of suspended sediment transport rates (SSTRs). The work also highlighted the importance of consolidation and the effects of cohesion on a deposit's erosional strength.

ACKNOWLEDGEMENTS

The completion of this study has only been possible due to the assistance and encouragement of a great many people. The author would like to extend his gratitude to the following people/organisations.

The Engineering and Physical Sciences Research Council for providing financial support for this project and also for the provision of specialised equipment via the EPSRC loan pool.

Scottish Water (formerly the North of Scotland Water Authority) for providing access to and permitting the instrumentation of the sewerage systems in Dundee and Forfar.

Professor Richard Ashley for providing the opportunity to undertake this study in the first place, and for his continued supervision and support for the duration.

Professor Richard Burrows and Dr Kamil Ali as supervisors who provided valuable contributions and comments throughout the course of the project.

Dr Simon Tait, of the Department of Civil and Structural Engineering at the University of Sheffield whose experience of laboratory testing was invaluable and whose astute comments and observations were much appreciated.

Alex Thomson and his team of technicians, in particular Tony Breen, for whom nothing was too much trouble, no matter how bizarre the request.

The various members of staff of the Urban Water Technology Centre at the University of Abertay, Dundee for their assistance in carrying out the field tests; particularly Mr Robert Peter.

Michelle Clark for analysing countless samples of sewer deposit material and sewage without too much complaint.

Ir John Cornelisse, Mr John Coolegem and Mr Pierre Bosland of WL Delft Hydraulics, for their contributions to the Delft laboratory tests which were funded by an EU TMR programme; the support of which is gratefully acknowledged.

My fellow researchers, Alasdair Fraser and Ruben Sakrabani for providing the '*craic*'. A sense of humour was a prerequisite for carrying out field tests in combined sewers.

Rachel for her understanding and patience while I completed this study.

Finally, I would like to thank my family for the encouragement and support they provided throughout; it was for them that I wished to see this work through to completion.

CONTENTS

Appendices

FIGURES

TABLES

PLATES

ABBREVIATIONS

ADWP	antecedent dry weather period
BOD	biochemical oxygen demand
BSI	British Standards Institute
CIRIA	Construction Industry Research and Information Association
COD	chemical oxygen demand
CSO	combined sewer overflow
DWF	dry weather flow
PFI	private finance initiative
SSTR	suspended sediment transport rate
TS	total solids
TSS	total suspended sediment
VS	volatile solids
VSS	volatile suspended solids
WwTW	waste water treatment works

NOTATION

a reference concentration height in Rouse equation

A cross-sectional area of flow

A_b area of flow influenced by bed

A_w area of flow influenced by pipe wall

A_{gr} value of F_{gr} at threshold of movement

A'_{gr} modified value of F_{gr} at threshold of movement

b coefficient of bed strength profile

B surface width of flow

c_a reference concentration at height a in Rouse equation

C_{ss} suspended sediment concentration

C parameter in Ackers & White equations

C_V volumetric sediment concentration

d depth below bed surface

d particle diameter

d' thickness of "weak layer"

d_A particle diameter of size fraction when $A'_{gr}/A_{gr} = 1$

d_{50}, d_{35} ...particle size of which 50%, 35%...of particles are finer than

d_i particle size of i^{th} fraction

d_{ch} characteristic (minimum) grain diameter

D pipe diameter

D_{gr} dimensionless particle size

D_m hydraulic mean depth

D_* sedimentological grain diameter

E surface erosion rate

F_b mobility parameter based on total bed shear stress

F_D drag force

F_g grain mobility parameter in May equations

F_{gr} sediment mobility parameter in Ackers & White equations

F_r Froude number of flow in May's equations

F_S entrainment function (in Shields)

F_S effective mobility parameter in May's equations

F_W weight force

g acceleration due to gravity

G_{gr} transport parameter in Ackers & White equations

h height in flow above bed surface

H parameter in Ackers & White equations

H distance from bed to flume top plate (in Paganini's equations)

J parameter in Ackers & White equations

k Nikuradse roughness height

k_b Colebrook-White roughness coefficient for bed

K parameter in Ackers & White equations

ℓ Prandtl mixing length

m moisture content in Wotherspoon equations

m parameter in Ackers & White equations

M surface erosion rate when $\tau_b = 2\tau_b$

n parameter in Ackers & White equations

n Manning's roughness coefficient

n_w Manning's roughness coefficient of pipe wall

P total wetted perimeter

P_b wetted perimeter of sediment bed (equal to bed width)

P_w wetted perimeter of pipe wall

q_{si} predicted suspended sediment transport rate for the *i*th size fraction

q_{stot} total predicted suspended sediment transport rate

Q flow rate of fluid

Q_M flow rate when $\tau_b = 2\tau_b$

r pipe radius

R total hydraulic radius

R_b hydraulic radius related to sediment bed

R^2 coefficient of correlation

Re	Reynolds number
Re_b	bed Reynolds number
Re_w	wall Reynolds number
Re_*	particle Reynolds number
R_w	hydraulic radius related to pipe wall
R^*_c	particle Reynolds number based on λc
s	slope
S_G	specific gravity of sediment
s_s	specific gravity of sediment in Nalluri and Alvarez equations
t	time
u	local flow velocity
u_*	shear velocity
$\tilde{u}$	flow velocity at a distance y from the bed [i.e. $\tilde{u} = \tilde{u}(y)$]
v	average velocity of profile
V	mean flow velocity
V_b	flow velocity of bed flow section
V_w	flow velocity of wall flow section
V_L	limiting flow velocity for no deposition
V_t	flow velocity at threshold of sediment movement
W_b	actual width of sediment bed
W_e	effective width of sediment bed
w_s	fall velocity (settling velocity)
y	flow depth
y_o	flow depth parameter in Rouse equation
y_s	sediment depth parameter in modified Ackers relationship
z	thickness of sediment bed
z	coefficient in Rouse equation

α parameter in Ackers & White equations

β parameter in Ackers & White equations

β proportionality factor

γ parameter in Ackers & White equations

δ parameter in Ackers & White equations

Δp_i percentage by weight of i^{th} size fraction in mixture

ε parameter in Ackers & White equations

η transport parameter in May's equations

η sedimentation parameter

θ transition factor in May's equations

θ_{cr} critical mobility parameter

Φ non-dimensional bedload in Einstein's equations

κ Prandtl-von Karman constant

λ Darcy-Weisbach friction factor

λ_b bed friction factor

λ_c composite value of λ

λ_g grain friction factor

λ_s overall friction factor in Nalluri and Alvarez equations

λ_{sb} bed friction factor in Nalluri and Alvarez equations

λ_w pipe wall friction factor

ν kinematic viscosity

ρ_F fluid density (density of water)

ρ_S density of sediment

σ_g geometric standard deviation of grain sorting

τ shear stress

τ_b bed shear stress

τ_c critical shear stress

τ_{cs} erosional strength of bed surface

τ_{cu} erosional strength of uniform layer

τ_o average shear stress

ϕ angle of repose

Ψ shear intensity parameter in Einstein's equations

Chapter One – Introduction

1.1 Background

The primary objective of urban drainage systems is to convey the aqueous and solid wastes emanating from domestic, industrial and storm inputs for treatment and disposal. The solids that enter the system are often a cause for concern as they may settle out to form permanent or temporary deposits in sewer inverts. This can generate problems such as hydraulic overloading due to a decrease in transport capacity which is allied to both surficial flooding and the premature operation of combined sewer overflows (CSOs), often resulting in both acute (short term) and chronic (long term) surface water pollution. A particular threat to surface waters pertains to the solids and associated pollutants within combined sewer systems that can have extremely detrimental effects on receiving watercourses. In extreme storm events a highly polluting phenomenon known as the '*first foul flush*' can occur, although the underlying in-sewer processes and the full extent of the consequences of this in terms of pollution impact are not as yet fully understood. Surface waters are considered important elements of the natural environment and as such efforts should be made to protect these assets from degradation due to impacts from human activities. Increased urbanisation invariably has a detrimental effect on the surface water quality and the challenge for planners and engineers in urban areas is therefore to develop the methods and tools which will enable modern drainage systems to be designed so as to have a minimum impact on society.

In order to meet these demands a number of studies have been carried out both in the laboratory and in the field in an attempt to produce empirical and semi-deterministic models that may be used to assess sewerage systems and their potential polluting discharges. Historically these models have been based on fluvial studies and have concentrated on non-cohesive or inorganic sediment with a uniform size. Subsequently there has been a need for more study into the erosion and transport of cohesive-like sediment mixtures and particularly under extreme 'foul-flush' conditions.

1.2 Aim of Research

The aim of this study was to test the veracity of the Ackers (1991) relationship for the prediction of suspended sediment transport in combined sewers, as used in the quality module (QSIM) of InfoWorks, the UK industry standard urban drainage modelling software. The crux of the work involved the investigation of methods whereby the approach could be improved, in addition to the analysis of specific erosion events, in order to further the understanding of the in-sewer processes that govern the erosion and transport of sediment within combined systems.

1.3 Research Objectives

The specific objectives of the study are as follows:

- Carry out a review of the current state of knowledge relating to the physical in-sewer processes responsible for the erosion and transport of solids in combined sewer systems.
- Undertake a significant field-monitoring programme to provide good quality in-depth data that can be used in conjunction with laboratory data.
- Investigate the nature of the material in suspension during a flush event.
- Analyse the mechanics of the '*first foul flush*' in an attempt to gain an understanding of the physical processes that create the phenomenon and outline a methodology that can be used to identify the origins of a flush.
- Test the Ackers (1991) modelling approach for the transport of suspended solids in combined sewers with data sets derived from both field and laboratory tests.
- Suggest and test modifications to the Ackers (1991) relationship in order to improve the predicted transport rates.
- Utilise the resulting work to recommend a framework for the future development of an integrated in-sewer erosion and transport model.

1.4 Structure of Thesis

The data requirements for this study involved an extensive period of fieldwork to be carried out, first in the Murraygate catchment in Dundee City centre, followed by tests in a combined sewer in Forfar. The fieldwork was supplemented by an

intensive series of laboratory tests in an annular flume carried out at WL Delft Hydraulics in the Netherlands.

Chapter Two provides a review of literature relevant to this study, although given the wealth of literature surrounding the field of sediment transport it was not intended to be exhaustive but rather detail the work most relevant to the current investigation.

Chapter Three outlines the testing that was carried out, both in the laboratory and the field, in conjunction with the analysis that was required to determine the necessary parameters for the data analysis and modelling work.

Chapter Four provides details of the fieldwork test sites and, although the work carried out in the Murraygate catchment did not contribute to the final modelling strategy, Chapter Five outlines the findings from this work as it did provide a valuable insight into the processes involved with sediment transport in combined sewers.

Chapter Six describes the hydrant flush tests carried out in Forfar and presents an analysis of the results. These results were subsequently used to devise a suitable modelling strategy based on existing formulae for the transport of suspended sediment in combined sewers and this methodology is presented in Chapter Seven.

The validation of this modelling technique was carried out using data from the laboratory testing in the Delft annular flume. Chapter Eight describes the laboratory test methodology and presents both the sediment transport results of the Delft tests and the results of applying the modelling methodology outlined in Chapter Seven to predict the aforementioned transport rates.

Chapter Nine outlines the conclusions that were drawn from the study and presents suggestions for further research including the recommendation of a proposed framework for a holistic modelling approach based on future research.

Chapter Two – Literature Review

2.1. Introduction

The problems associated with the build-up of solids in sewer systems such as blockages and subsequent maintenance requirements have been well documented, albeit the management of in-pipe deposits has often not been given a high priority by sewerage network operators (Fraser & Ashley, 1999). In addition, poor flow quality within sewerage systems has been widely recognised as being strongly linked with the movement of sediment in sewers (De Sutter *et al.*, 2000). It is believed that erosion mobilises the surficial material, re-entraining particles and releasing the interstitial liquid trapped in the solids matrix. In an attempt to explain the physical processes for 'foul flushes' in sewers, detailed studies have investigated the effects of disturbance of the bed sediments due to increasing rates of shear stress along the invert. It is for these reasons that for a number of decades now studies have been undertaken throughout Europe with a view to establishing a model capable of predicting the processes involved in the erosion and transport of sediment deposits in sewerage systems (Verbanck, 1995a; Chebbo, 1992; Ristenpart, 1995; Crabtree, 1989; Ashley *et al.*, 1994). In general terms erosion/transport simulation models use mathematical equations to formulate results such as sediment transport rate or depth of erosion and can primarily be sub-divided into two categories; deterministic or empirical.

2.1.1. Deterministic Models

Physically based models or theoretical models include a set of general laws or theoretical principles. These could be used if all the governing physical laws for the processes were well known and could be described by equations of mathematical physics.

2.1.2. Empirical/Semi-empirical Models

If a theoretical/deterministic model simplifies the physical system by including obviously empirical components (e.g., Darcy-Weisbach is an empirical equation and the conservation of momentum equation used to describe surface flow includes an empirical hydraulic resistance term), it may be considered as a semi-empirical model. Empirical models or conceptual models omit the general laws and are in reality a

representation of data. These are employed when modelling from first principles is impractical (due to complexity of the system) or unnecessary, if a simple expression can encapsulate enough of the behaviour of the system.

2.1.3. Model Results

Depending on the character of the results obtained, models are classified as *stochastic* or *deterministic*. If one or more of the variables in a mathematical model are regarded as random variables having distributions in probability, then the model is stochastic. If all the variables are considered to be free from random variation the model is deterministic (even though some "deterministic models" may include stochastic processes to add the dimensions of spatial and temporal variability to some of the sub-processes involved). Additionally, the models may be further sub-divided into those that are chiefly *laboratory* based and those based on extensive *field* measurement programmes.

2.2. Nature of Material Found in Combined Sewer Systems

Sewer sediments are the settleable material which is able to form bed deposits within sewerage systems. The design of these systems strive to transport this material for treatment and disposal in addition to the associated liquid waste (Arthur 1996). Typically sewer sediments are composed of over 50% water (by mass), with the solids fraction often comprised of a 90% inorganic and 10% organic content although these proportions can vary considerably according to ambient hydraulic conditions and the characteristics of the solids entering the system (Arthur and Ashley, 1998). Work carried out at the Water Research Centre (WRc) in the UK investigated the main types of sediment known to occur in sewerage systems (Crabtree, 1989). The classical sewer material classification (Crabtree, 1989) broadly subdivided the material found in sewers based on field observations and sample analysis. This resulted in five categories of sewer sediment being identified in terms of appearance, composition and polluting potential as described in Table 2.1 and illustrated in Figure 2.1.

Type	Description	% by particle size (mm) mean (range)			Bulk S_G	Organics mean %
		<0.063	0.063-2	2-50		
A	Coarse, loose, granular, predominantly mineral material found in the inverts of pipes	6 (1-30)	61 (3-87)	33 (3-90)	1.72	7
B	As for A but concreted by the addition of fat, bitumen, cement, etc. into a solid mass	n/a	n/a	n/a	n/a	50
C	Mobile, fine-grained deposits found in slack flow zones, either in isolation or above Type A material	45 (29-73)	55 (5-71)	0 (0)	1.17	50
D	Organic pipe wall slimes and biofilms around the mean flow level	32 (17-52)	62 (1-83)	6 (1-20)	1.21	61
E	Fine-grained mineral and organic deposits found in combined sewer overflow (CSO) storage tanks	22 (1-80)	69 (1-85)	9 (4-80)	1.46	22

Table 2.1: Crabtree's (1989) sewer sediment classification

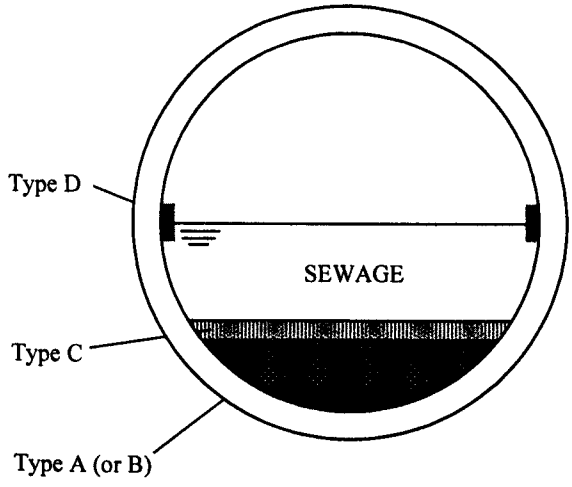

Figure 2.1: In-pipe location of Crabtree's sediment classes

According to Crabtree (1989) the most significant of these in terms of polluting potential were types 'A' and 'C'. The erosion of '*type C*' deposits was considered to be the source of the frequently observed "first foul flush" in many sewerage systems; arising in response to storm events, although, as demonstrated in this study, mass

balances have indicated that erosion of the bulk deposit also contributes to the solids contained in a foul flush (see Section 5.2).

2.3. Origin of Sewer Sediments

Apart from the domestic and industrial inputs, sewer solids and associated pollutants can also be attributed to the surface runoff from contributing catchments (Gromaire *et al.*, 2001; Ashley and Crabtree, 1992). Their origins can be summarised as shown in Table 2.2, adapted from a UK CIRIA report on the design of sewers to control sediment problems (Ackers *et al.*, 1996).

Foul and Combined Sewers
▪ Large faecal and organic matter (gross solids) with a low specific gravity
▪ Slurries and sludges comprised of fine faecal and organic particles
▪ Sewage litter comprising paper, rags and miscellaneous material flushed into sewers
▪ Soil particles and vegetable matter from domestic food processing
▪ Industrial and commercial inputs
▪ Infiltrated soil particles due to leaks and pipe failures
▪ Material due to the decay of sewer fabric
Surface Water and Combined Sewers
▪ Gravels, sands and silts - washed or blown from unpaved areas
▪ Detritus/litter from roads and paved areas (e.g. plastic, paper, cans etc.)
▪ Vehicular particles (exhausts, tyre rubber etc.)
▪ Atmospheric fall-out on roads and paved surfaces (dry and wet)
▪ Erosion of roofing material Road grit (abrasion of tarmac or resurfacing)
▪ Construction works materials
▪ Illegally dumped materials
▪ Vegetable matter (grass, leaves, wood etc.)
▪ Road grit (de-icing operations)
▪ Infiltrated soil particles due to leaks and pipe failures
▪ Material due to the decay of sewer fabric

Table 2.2: Sewer sediment origins (adapted from Ackers *et al.*, 1996)

2.4. Associated Problems of Sewer Sediments

The *direct* effects of sewer solids include a propensity to cause blockages and a reduction in conveyance, accumulation of pollutants, and detrimental effects on wastewater treatment plants (WwTWs) and receiving watercourses via CSOs. CSO spills can also cause increased turbidity, deposition and light reduction in rivers; which can have a detrimental impact on the aquatic life. *Indirect* effects include immediate acute effects or chronic long-term effects due to the conveyance of toxic materials attached to the smaller particulates. Sewer sediments can also lead to hydrogen sulphide (H_2S) generation that can cause fabric corrosion when combined with moisture and oxygen. Solids washout at WwTWs can blind screens and cause other shock loadings. Due to the short time of concentration in sewer systems, high flow rates in CSO spills often precede the rise in watercourse flows and can cause bed and bank erosion and the re-entrainment of contaminated sediments deposited in previous spills.

2.4.1. Hydraulic Considerations

According to Ashley *et al.* (1992), Dinkelacker (1992) and Butler *et al.* (1996), sewer sediments have traditionally been associated with hydraulic problems within wastewater systems which can lead to a decrease in the capacity of the sewer as a result of a reduction in the cross sectional area and an increase in the hydraulic roughness of the pipe. It has been suggested that sediment deposits typically reduce the available storage capacity of a sewer by between 20 and 44%; this can result in a greater chance of surcharging and subsequent surface flooding, in addition to the premature operation of combined sewer overflows (Lindholm & Aaby, 1989). Plates 2.1 and 2.2 illustrate problems that were identified in the main Dundee interceptor sewer during a 'walk-through' of the system that was conducted to establish the severity of the in-pipe deposition. This highlights the problems that can arise due to the ingress of construction works material from large-scale redevelopment programmes such as the work then underway in the Overgate shopping centre in Dundee City centre to which a majority of the aforementioned deposition may be largely attributed.

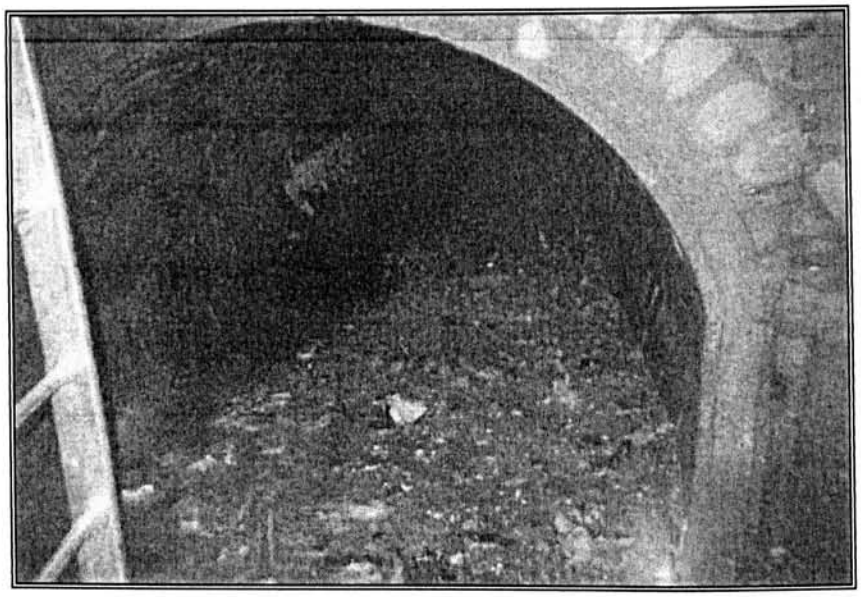

Plate 2.1: Ingress of construction material in the Dundee interceptor sewer (11-08-98)

An appreciation of the severity of the problem and reduction in the hydraulic capacity of the system can be clearly gained from the above illustration. To remedy this situation Scottish Water (formerly the North of Scotland Water Authority) were compelled to spend approximately £10,000 on 'jetting' to remove the deposits from this relatively short section of sewer. Plate 2.2 below highlights the extent of the problem.

Plate 2.2: Coarse deposits in the Murraygate interceptor sewer

2.4.2. Sediment Deposition in Sewerage Systems

The problems illustrated above occur when there is insufficient energy in the sewer flow to maintain a sediment particle in transport and hence a sediment deposit may form. If this deposit is not re-entrained into the flow column it can gain strength by two principal processes:

- **Consolidation**

This occurs due to a combination of a reduction in the void ratio and increased particle interlocking and is similar to the process relied upon by geotechnical engineers for many earth structures to gain strength.

- **Cohesive-*like* strength**

This has different causes in sewer sediments than the electrostatic attraction experienced in clays and fine-grained silts. In sewer systems it is primarily due to the agglutination and cementation effects of the organic substances contained within the deposits. These deposits have higher critical yield stresses than analogous non-cohesive sediments and as a result can resist higher levels of boundary shear prior to erosion taking place (De Sutter, 2001; Arthur & Ashley, 1998; and Wotherspoon & Ashley, 1992).

2.5. Near Bed Solids (NBS)

As reported by Arthur (1996) solids in combined sewers are markedly different to those transported in natural watercourses. Of particular importance are the large organic solids that originate, principally, from domestic sanitary inputs. There is a degree of uncertainty concerning the interface between the solids conveyed in true suspension and those which comprise the bed. Observations using small diameter tubes extracting samples from the flow and near the bed by Ashley *et al.* (1994), Verbanck (1995b), Wöhrle & Brombach (1991) and Ristenpart *et al.* (1995), indicate that there may be a lower zone of highly concentrated material close to the bed which may or may not be in motion, depending upon the hydraulic conditions. Unfortunately studies of the material moving near the bed in real sewers have been limited due to practical measurement difficulties. UK based studies of near bed

solids have principally been undertaken in Dundee, Scotland where field observations of real material moving near the bed have been carried out. At present it is still not possible to precisely define, due to practical constraints, whether this material moves as a true suspension or as a bed load. Results have been based on material collected in bed traps in the UK (Arthur, 1996); material obtained by vacuum extraction of the flow samples (usually with small bore tubes) in France, Belgium and Germany (Ahyerre, 1999; Verbanck, 1995b; and Ristenpart, 1995) or direct observations using specially designed observation boxes in France as shown in Plate 2.3 (Oms, 2003).

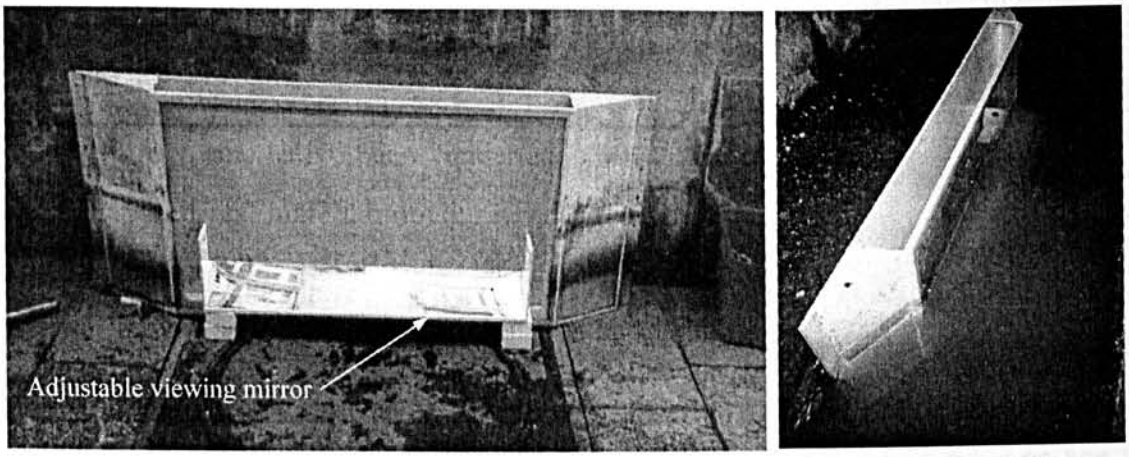

Plate 2.3: French near bed solids observation device

Indirect observations using sonar and thermal conductivity devices to monitor sediment bed erosion have shown the movement of a 'pulse' of dense material moving adjacent to the bed just prior to an eroding event (Ashley *et al.*, 1993). The aforementioned European studies undertaken on NBS indicated some similarities. They showed high organic and moisture content, with weak resistance to erosion. As such, NBS are considered to be an important stock of pollution likely to be entrained into the flow column during rain events (Oms *et al.*, 2002).

2.5.1. Material Characteristics of Near Bed Solids

It is accepted that some of this material, together with organic material from surface inputs, degrades to form the organic fraction of the suspended loads and bed deposits

in sewers (Jefferies & Ashley, 1994 and Bertrand-Krajewski *et al.*, 1995). These large organic fractions are comprised of faeces, textiles, paper, food stuff and surface derived solids (vegetation etc.), and are present at all depths in the flow column due to their low specific gravity. In the UK prevailing hydraulic conditions in sewers are markedly different to those experienced in some of the continental systems such as those found in Paris. Whereas the UK systems tend to have relatively high velocity flows with steep gradients the French sewers tend to be less steep with lower velocities as a result. Thus, after collaboration with French researchers it is now believed that there is more than just one type of near bed solid as had previously been thought. In Paris there has been shown to be a much more visible layer, which can 'survive' due to the lower ambient velocities, whereas the UK systems tend to exhibit a more mobile type of material that may be more difficult to identify.

Additionally observations have led researchers to believe that the material found at the sediment/sewage interface can vary both spatially and temporally, perhaps more significantly than the underlying bulk deposit material (Chebbo *et al.*, 2002). Indeed in the Perth Road catchment in Dundee it has been noted that at times of low flow a white fibrous material, believed to be mainly comprised of tissue paper, can often be found in transport. In contrast, in the Murraygate interceptor sewer the near bed material sampled has typically comprised more faecal/vegetable matter. The terminology, 'near bed solids' (Ashley *et al.*, 1995), is just one of the phrases that has been used to describe this material being transported near the bed. As described by Arthur (1996) other European descriptions of this material have included:

- fluid mud (Simons and Senturik, 1992)
- fluid sediment (Ristenpart *et al.*, 1995)
- dense undercurrents (Verbanck, 1995b)

In addition to the Dundee field studies, the University of Sheffield has carried out experimental laboratory investigations of the erosion and transport of in-pipe, deposited, fine-grained, organic, cohesive-like sediment beds analogous to those found in sewers and corresponding to those categorised as *Type C* material according to the Crabtree (1989) classification. Using synthetic materials such as crushed

olivestone under laboratory conditions a system was established to measure the erosional characteristics of a cohesive-like sediment bed. All the experimental results showed that the cohesive like beds were composed of a weaker surface layer, in which the resistance to erosion of the bed increased with depth, overlying a stronger more stable layer of consistent erosional resistance (Rushforth *et al*, 2003).

2.6. Pollutant Release Considerations

Apart from the hydraulic aspects, the main area for concern regarding sewer sediments is their polluting potential, particularly through re-entrainment and subsequent CSO discharges. The inorganic granular material moving at the bed in sewers, which may be viewed as a true 'bed-load' will very rarely travel in true suspension during DWF (Butler *et al.*, 1995 and Ashley & Verbanck, 1996). Although it is of major importance, as it is found throughout sewerage systems and when arrested, is responsible for the build up of the bulk deposits within sewers, it is the material moving close to the bed that can have disproportionate polluting effects during foul flush events. Work from Denmark has shown that the rate of hydrolysis of organic matter into readily biodegradable substrate is highly dependent upon the nature of the waste and its attachment to sediments (Ashley *et al.*, 1999). The resulting fate of the micro-organisms adsorbed onto the surfaces of particulate matter in sewage is highly attributable to the deposition and transportation of the suspended solids. Under all normal flow conditions particles of very small size or low density may remain in suspension and therefore be transported as a *washload.* Although these particles have a negligible effect on the hydraulic capacity of the sewerage system, they may have a significant impact on the pollutant loading, both in the flow, and at discharge points such as CSOs. Sediments with higher settling velocities may form deposits under low flow conditions but these are usually re-entrained into the flow column with higher velocities due to storms or diurnal variations in flow. In contrast, larger or denser particles may only be transported under peak flow conditions which may be relatively infrequent and therefore may form permanent, stationary deposits near their point of entry (Ackers *et al.*, 1996).

2.7. Solids Transport and Foul Flushes in Combined Sewers

Concerns regarding pollutant release from sewer systems have been well documented, with the contribution from in-sewer solids to the quality of flow during a storm event being especially significant. Current prediction methodologies applied to the movement of sediment in sewers are derived from sediment transport relationships developed in fluvial environments. Given that these models have primarily been developed from studies of non-cohesive sediment these methods are inappropriate where the transport of cohesive near bed solids in sewers is concerned (Ashley & Verbanck, 1996). Notwithstanding these limitations, a number of fluvial sediment transport methodologies have been applied to sewer sediment transport, both in suspension and near the bed (assumed as bed load), with varying degrees of success (e.g. Kleijwegt 1992; Verbanck, 1995a; Ackers *et al.*, 1996, and Arthur, 1996).

It is widely believed that at the beginning of a storm event a 'first flush' of highly polluted stormwater is induced due to a relatively high level of sediments and pollutants being entrained into the flow. This occurs both on the catchment surface, but more importantly, in the pipe itself, due to the erosion and re-entrainment of the in-pipe sediments caused by increased shear stresses accompanying the increased flow velocities (Skipworth, 1996). These events known as 'foul flushes' in combined sewers typically occur in the initial period of storm flows when the concentration of suspended sediments and other pollutants are significantly higher than those observed in the later stages of the storm.

According to Skipworth (1996) the earliest published work in the UK citing the occurrence of a foul flush can be attributed to Wilkinson (1956) while studying a catchment in London. The concentration time of the sewerage system studied was 20 minutes and it was observed that the concentration of polluting matter passed its peak between 20-30 minutes after the onset of the storm. The concentration of pollutant matter in this first flush was approximately twice that of subsequent flows and Wilkinson also noticed that, although for many storms the peak flow and peak suspended solids strength occurred at about the same time, there did not seem to be any correlation between flow and strength. It is the 'near bed solids' that are re-

entrained into the flow, together with solids eroded from the bed, which can account for such large changes in suspended sediment concentration under time varying flow conditions. As yet however, the processes which cause these 'pulses' of solids and pollutants in suspension are not entirely understood (Ashley & Verbanck, 1996). These flushes can be observed when the flow is accelerating either due to storm inputs or during peak flows in dry weather, although flushes are not always observed under what would appear to be identical hydraulic conditions even in the same sewer.

The importance of these flushes should not be underestimated as the entrainment of the solids and subsequent flush gives rise to 'pulses' of highly concentrated suspensions of solids and associated pollutants, notably chemical oxygen demand (COD), which can be conveyed to watercourses via CSO spills. Shock loads at treatment plants is another direct effect of the 'first foul flush' and where no balancing facilities are available the equilibrium in the operation of the plant can be disturbed. As a result a number of the utility services regulators now specify that operators must provide storage systems to retain these foul flushes within the sewer system.

The primary objective for carrying out investigations in the Murraygate test section was to try to gain a greater understanding of the processes involved in the erosion and entrainment of sewer solids during a flush event. The study attempted to collect adequate data in order to develop a reliable methodology for the estimation of the solids that are re-entrained during a flush event. Currently, there are two approaches to the estimation of foul flushes:

(i) Empirical catchment based relationships to predict the representative solids loads and peaks.

(ii) Detailed consideration of the physical processes causing flushes in order to develop deterministic relationships to describe these processes.

Although the increased flow due to rainfall-runoff entering the network usually results in an increase in the solids and/or associated pollutants within the system, dilution can also occur where there is a lack of pollutant supply (i.e. sewer bed

deposit). Moreover, although the phenomena has been termed the '*first foul flush*', in some cases a second flush may also be observed (as shown in Figure 2.2). The second peak is generally attributed to the ingress of surface sediment and the relative time of concentration for the system, compared with the more rapidly occurring local erosion that is responsible for the first flush.

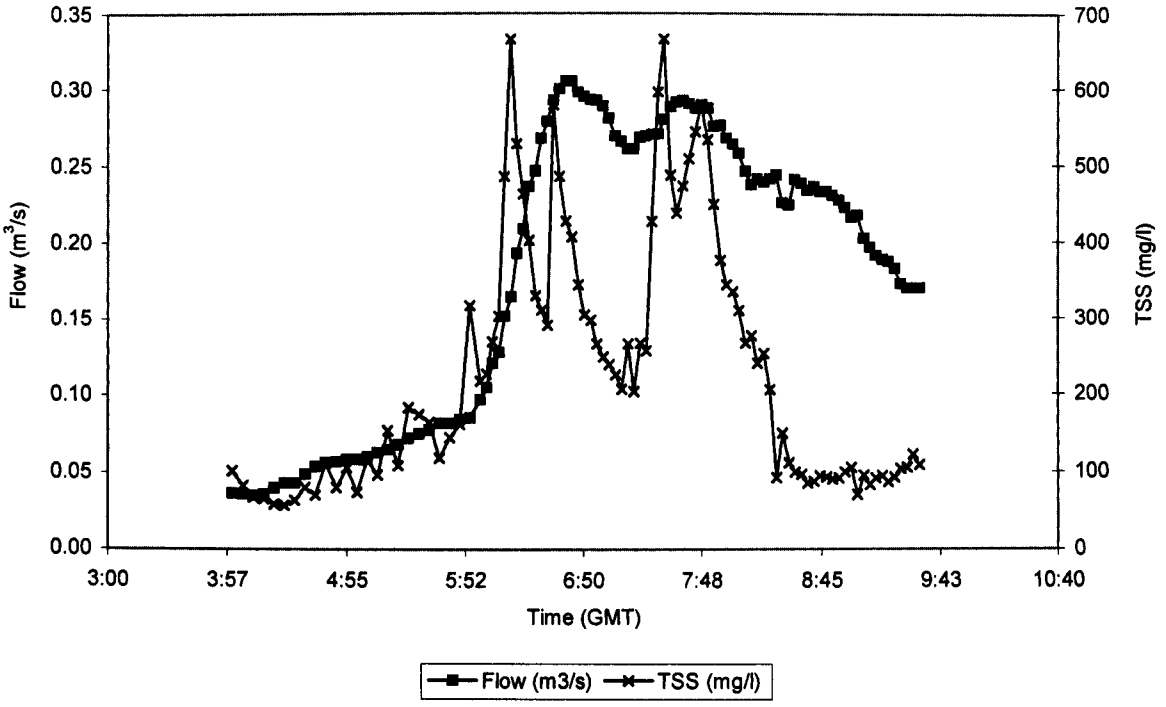

Figure 2.2: First & second foul flush events captured in Dundee interceptor sewer (09-11-94)

[Source: (Arthur, 1996)]

The length of the *antecedent dry weather period* (ADWP) was also found to be an influencing factor on the composition of storm sewage (Arthur, 1996) with evidence suggesting that the scouring of material deposited in dry weather was responsible for the strong first flush. Further work by Ellis (1986) identified that high concentrations of particulate materials were the primary cause of the pollution loads in streams receiving storm water discharges. For a separately sewered development chemographs showed a double peaking of suspended solids concentration with a clear occurrence of a first flush and a second peak occurring on the back of the recession limb of the flood. The fact that for most storms the runoff remained highly turbid for a considerable time after the peak discharge (indicated by the suspended

solids concentration) demonstrated that this first flush of storm water to the sewer system could not actually rapidly clean the catchment area. A ten month study period incorporating the sampling and analysis of storm water flows at the downstream end of the combined sewer system at Great Harwood, Lancashire, was described by Thornton and Saul (1986) who analysed the data for 41 separate storm events. The samples were analysed for suspended solids, chemical oxygen demand (COD), total dissolved solids and ammonia. For the dry weather flow a diurnal pattern was observed for the pollutant concentration whereas for over 75% of the sampled storm events, a distinct 'foul flush' of suspended solids and chemical oxygen demand was observed.

2.8. Generic Definitions of the First Foul Flush

Definitions of foul flushes fall into two distinct groups, which can lead to differing conclusions about their occurrence and characteristics. These may be summarised as follows:

Group 1 Definitions: ***High pollutant concentrations in the initial component of the increased flow due to storm inputs.***

Observations and definitions put forward for the first foul flush that may be categorised as Group 1 have included:

1. The maximum pollution load (kg/min) appears before the maximum water flow (Stotz & Krauth, 1984).

2. Pearson *et al.* (1986) identified two types of flush (Type A and Type B) which occurred during the initial period of a storm flow; during which the concentration of pollutants was significantly higher than those observed during the latter stages of the storm event:

Type A

Suspended solids and COD concentrations were lower than for the ambient DWF conditions and the time of the peak concentration preceded the flow peak.

Type B

The pollutant concentration was in excess of those found in DWF conditions and the timing of observed solids peak generally corresponded with the flow peak. This type of flush was found to occur for larger storms and after an antecedent dry weather period (ADWP) of at least three days.

Group 2 Definitions: ***Specific proportions of total load (mass) occur within a certain cumulative proportion of the total flow.***

Definitions put forward for the first foul flush that may be categorised as Group 2 have included:

1. Geiger (1987) defined a flush as occurring when the initial slope of the cumulative load/flow curve exceeded 45°. If the curve were at an angle of precisely 45° this would represent a constant mass transport rate during the event whereas a curve of less than 45° would constitute dilution of the flow.

2. Saget *et al.* (1995) defined a flush as an event where at least 80% of the pollution load was transferred in the first 30% of the flow volume. Using this definition for an investigation of 197 events in French separate storm and combined sewers it was deduced that only one produced a flush.

3. The Gupta & Saul (1996) definition states that the flush occurs during that part of the storm up to the maximum divergence between the dimensionless cumulative percentage of pollutants and the cumulative percentage of flows when plotted against the cumulative percentage of time. In the example shown in Figure 2.3 it can be seen that at the point of maximum divergence the amount of solids released equates to approximately 80% of the total amount of solids released for the entire event.

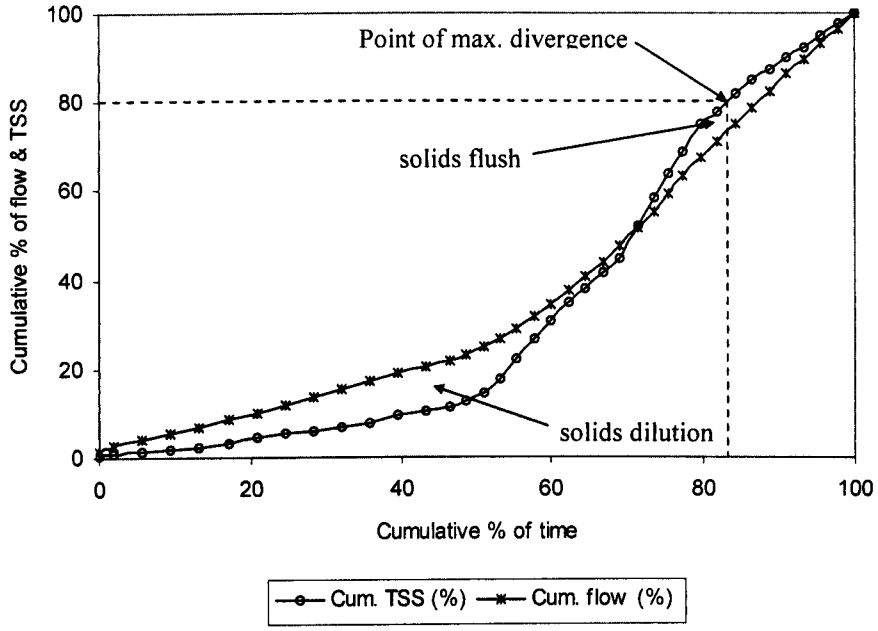

Figure 2.3: Gupta & Saul (1996) definition of a solids flush in a combined sewer

This second group of definitions poses a problem in that the event is deemed to have a start and end point, which influences the computation of the total loads and flows.

2.9. *Investigations into the Inherent Physical Processes of the First Foul Flush*

As already mentioned, it is believed that increasing rates of shear along the inverts of sewers can cause disturbance of the bed sediments. The ensuing erosion results in the mobilisation of the surficial material, due to re-entrainment of the particles, and the subsequent release of any interstitial liquid trapped within the solids matrix. Thus a significant contribution is made to the pollutant load conveyed during periods of peak dry weather and storm induced flows. Previously the 'near bed solids' contribution to the 'first foul flush' has been modelled using field data (Verbanck, 1995b and Arthur & Ashley, 1998). The biochemical pollutant load can also be exacerbated by the concurrent release of wall slimes and biofilms attached to the solids particles although not significantly adding to the solids mass. Arthur (1996) described how the physical process of the erosion and re-entrainment of the near bed material into the flow can be explained by a sewage wave progressing along a 'reach' of the sewer. The flow regimes can be considered segregated into three discrete sections each with a different ambient velocity as illustrated in Figure 2.4:

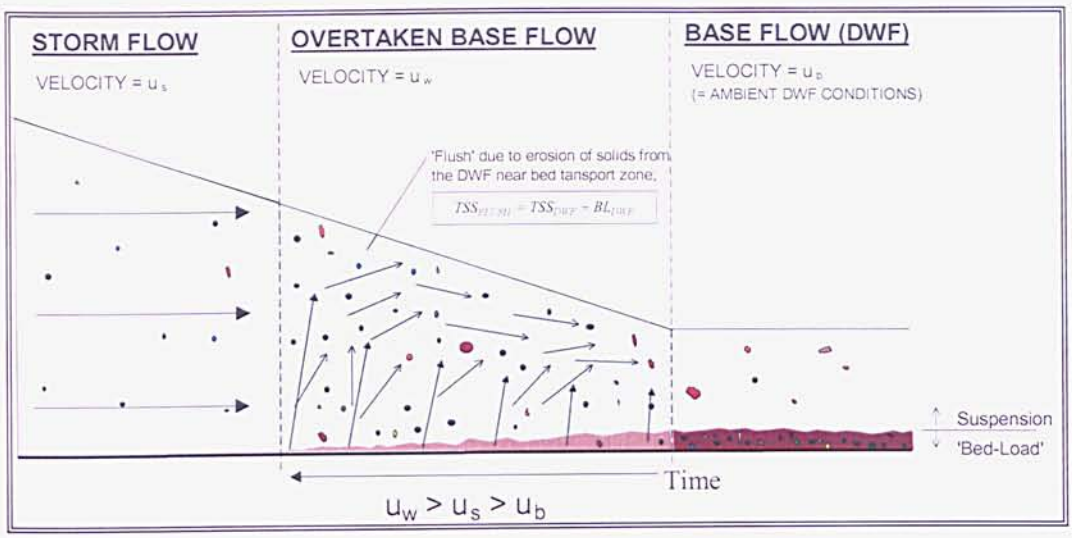

TSS_{FLUSH} = Solids concentration of the 'flush'

TSS_{DWF} = Ambient DWF solids concentration

BL_{DWF} = Near bed solids in transport in ambient DWF conditions

Figure 2.4: Idealisation of storm hydrograph progressing through a combined sewer (Adapted from Ackers *et al.*, 1968; and Davies, 1990)

The advancing part of the storm wave consists of '*overtaken*' base flow which is DWF that is '*forced*' to travel faster than normal due to the surge wave. From experiments using a saline base flow (Harrison & Holmes, 1967) in which it was observed there was negligible dispersion of overtaken base flow into the pseudo-storm water mass, it is therefore possible to presume only limited mixing in this region. The velocity is increased in the 'overtaken' region with the near bed solids being accelerated and entrained into the flow column. The total mass in transport in this region (a 'foul flush') is therefore comprised of the mass transported in suspension in dry weather plus the near bed solids mass. This concept is reinforced by evidence from observations of sewer sediment bed levels in Hildesheim, Germany and Dundee (Ashley *et al.*, 1993) which show a short timescale peak in bed depth 'passing' measurement sections in each sewer during eroding events. As this transient peak was not found to be related to the increase in suspended solids that is usually associated with foul flushes it was believed to be as a result of the near bed solids being 'pushed' in front of the advancing storm wave prior to entrainment into the flow column.

2.10. Origins of the Material Contained within a First Foul Flush

Application of the concepts outlined in Section 2.9 to data collected in Dundee showed that, if all the near bed material in the combined interceptor sewer were entrained into the flow when the base flow is overtaken, then the DWF suspended sediment concentration would have increased by between 0.5% and 9.0% (Arthur & Ashley, 1998). Although a relatively modest increase, the biochemical data indicated that the COD and BOD_5 concentrations would increase by approximately 77% and 120% respectively.

Clearly the role of near bed solids in first foul flushes are of major importance, but flushes also appear to comprise significant amounts of material eroded from the bulk of the underlying bed. According to Verbanck (1995a) there is evidence to suggest that local shear stresses of only $1N/m^2$ are adequate to entrain bed material for first flush contributions. In trying to deduce the origins of a foul flush the total solids load (TSS_{FLUSH}) can be considered as the sum of:

- The total solids in transport during dry weather – TSS_{DWF}
- Dry weather solids moving near the bed that are 'released' - NBS_{DWF}
- Solids eroded from the bulk of the bed as a result of the enhanced bed shear stresses - BES_{WET}

Hence the total solids load in a flush may be represented by:

$$TSS_{FLUSH} = TSS_{DWF} + NBS_{DWF} + BES_{WET} \qquad (2.1)$$

This equation can then be used in an attempt to quantify the individual components of a flush using an approach such as that as outlined in Section 2.10.1.

2.10.1. Quantifying the Individual Components within a First Foul Flush

In order to quantify the individual components contained within a flush the following methodology may be adopted (Ashley & McIlhatton, 1998):

- *Solids transported during dry weather flow – (TSS_{DWF})*

This component can be determined relatively easily as the temporally varying flows and mean suspended solids concentrations throughout the flow column will be known if a pattern of dry weather flow has been established, or assumed based on population.

- *Solids transported near the bed – (NBS_{DWF})*

This parameter is more difficult to estimate as, due to practical constraints, it is not presently possible to define whether the material moves as a true suspension or as a bedload. The concept of the 'near bed solids' contribution to the first flush has been developed using field observations and data (Verbanck, 1995b and Arthur & Ashley, 1998). With a known flow rate and material density the likely contribution of the 'near bed solids' to the first foul flush can be predicted using an empirical transport equation for the organic fraction of the near bed load as developed by Arthur & Ashley (1998). This relationship takes the form described in Equation 2.2:

$$C_v = -105.73 + 2.55\times10^{-3}\left(\frac{I_r^{TSSS}}{D_r}\right) + 0.2023\left(\frac{y_0}{y_{max}}\right) + 47.808\left(\frac{\tau_0}{\tau_b}\right) + 120.45\left(\frac{\rho_d}{\rho_w}\right) \qquad (2.2)$$

where: C_v = Volumetric sediment concentration of the NBS

$\left(\frac{I_r^{TSSS}}{D_r}\right)$ I_r = rainfall intensity; TSSS = time since the start of the last storm and D_r = total depth of rainfall

$\left(\frac{y_0}{y_{max}}\right)$ - Ratio of ave. flow depth : max. flow depth for an ave. DWF day

$\left(\frac{\tau_0}{\tau_b}\right)$ - Ratio of average shear : shear at the bed

$\left(\frac{\rho_d}{\rho_w}\right)$ - Ratio of NBS dry density : sewage density (1000 kg/m^3)

An alternative approach for estimating amount of near bed solids in transport involves utilising results presented by Verbanck (1995b). This approach suggests a two layer model where the near bed solids may be represented by the Coleman (1969) suspended solids distribution relationship:

$$\frac{Cy}{Ca^*} = \left(\frac{y}{a^*}\right)^{-\eta} \qquad (2.3)$$

where: a^* = reference level

C_{a^*} = reference concentration

C_y = concentration at height y

η = sedimentation parameter

This approach assumes that:

- the NBS are transported as a *suspension*
- the lower 25% of the flow column is comprised entirely of NBS

It is acknowledged that certain difficulties are inherent with the application of both methods. As the Arthur (1996) model was an empirical equation developed with multi-regression analysis using field data from a single catchment there is a high likelihood that the method will be very site-specific. Moreover, although it may be more universally applicable, the Verbanck (1995b) method is not straightforward to apply, as it requires a reference concentration from the flow column to be known, prior to the prediction of a suspended solids profile for the entire flow column.

- *Solids eroded from the bed – (BES_{WET})*

The solids eroded from the bed can be determined from the use of current sewer sediment erosion models that have been developed as a result of either field or laboratory based studies or a combination of both.

1. Models based on field studies

The BES_{WET} component can be determined using a sewer erosion model such as that developed and tested after field studies in Dundee and Hildesheim, Germany (Wotherspoon, 1994 and Ristenpart, 1995).

This model was based on a relationship that related bed yield stress (τ_y) to bed moisture content (m):

$$\tau_y = \exp(18.3865) m^{-3.1682} \tag{2.4}$$

By utilising flow loggers τ_b could be determined prior to any erosion taking place and substituted into Equation 2.4 in place of τ_y in order to estimate the deposit moisture content (m) that would be necessary for the initiation of erosion. The erodible bed density (ρ_e) could then be calculated from Equation 2.5:

$$\rho_e = \frac{S_G \rho_w + e\rho_w}{1+e} \tag{2.5}$$

where:

$e = mS_G$ (void ratio)

$S_G = 2.6$ (specific gravity)

ρ_w = density of water

A modified form of the Mehta & Partheniades (1982) relationship for cohesive muds could then be used to determine the depth of erosion as outlined in Equation 2.6:

$$H_e = H_o - \left[H_o \frac{\rho_e}{\zeta \rho_o} \right]^{-\frac{1}{\xi}} \tag{2.6}$$

where:

H_e = erodible depth (m)

H_0 = initial average bed depth (m)

ρ_0 = average initial bed density (kg/m^3)

ξ & ζ = dimensionless calibration coefficients

This model has been successfully used to predict erosion during both dry and wet weather for data from Dundee. Ashley *et al.* (1993) showed an application of the model to an 82m length of main sewer in Dundee yielded good results for the measured mass eroded from the bed during a storm event. The main drawbacks with this model are that it is necessary to calibrate the coefficients ξ and ζ for each event, and it does not cater for deposition or near bed solids.

2. Models based on laboratory investigations

An example of a laboratory-based model that could be used for determination of the BES_{WET} component is the Skipworth (1996) model for predicting suspended sediment transport rates. This model is based on the theory that the sediment bed is comprised of a weak layer of increasing yield strength with depth overlying bed material with uniform strength with depth as described in Section 2.12.3.1.

2.11. Initiation of Motion

The forces that act on a prominent sediment particle in a horizontal bed due to the fluid flow may be represented as depicted in Figure 2.5:

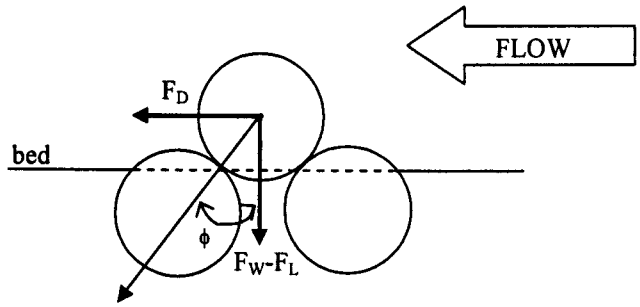

Figure 2.5: Forces acting on a prominent particle resting on a sediment bed

The stream-wise force proportional to the exposed surface area of the particle is termed the drag force, F_D and the vertically acting force is termed the lift force, F_L. The restoring force due to the submerged weight of the particle, F_W, counters these forces and when the particle is just about to move, i.e. at the threshold of motion, it follows that:

$$\frac{F_D}{F_W - F_L} = \tan\phi \qquad (2.7)$$

where: ϕ is termed the angle of repose.

As a result of the stochastic nature of sediment transport due to turbulent fluctuations of the flow, determining this point of 'incipient motion' is difficult to define, and is thus very subjective. As reported by Yang (1996) various studies used various terms to define this threshold state, including:

- initial motion
- several grains moving
- weak movement
- critical movement

Shields (1936) defined the threshold of movement as a *zero transport rate* based on the extrapolation of experimental plots. The plots concerned take the form of a dimensionless entrainment parameter (F_s) plotted against the shear Reynolds number (R_{e*}), as defined in the following equations:

$$F_s = \frac{\tau_c}{\rho g(s_G - 1)d} \qquad (2.8)$$

where: τ_c is the critical bed shear stress, ρ is the density of the sewage, s_G is the specific gravity of the sediment and d is the particle diameter of the uniform sediment.

$$R_{e*} = \frac{du_{*,cr}}{\nu} \qquad (2.9)$$

where: $u_{*,cr}$ is the critical shear velocity and ν is the kinematic viscosity.

The original plot by Shields (1936), now known as the Shields Diagram, was based on work considering the transport of granular spherical solids positioned on a flat

bed. Later work by Rouse (1937) resulted in an extension of the diagram and a line to delineate between motion and no motion as shown in Figure 2.6.

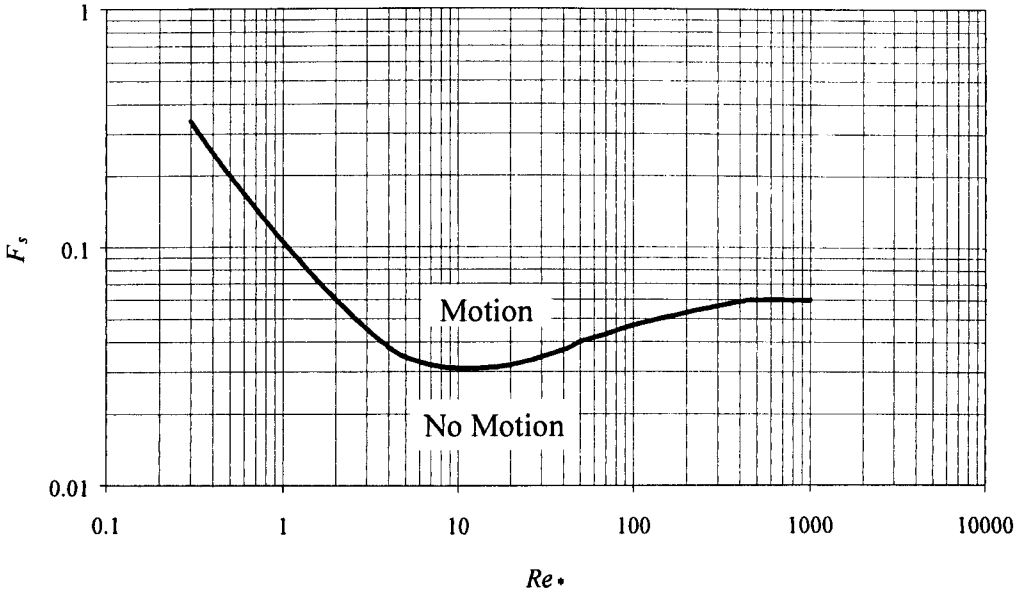

Figure 2.6: Shields diagram with Rouse line (after Yang, 1996)

Studies have shown there is considerable uncertainty at the lower values of particle Reynolds number (Grass, 1970; White, 1970; and Mantz, 1977). A further problem with the Shields curve is that it is an implicit relationship, that is, it requires knowledge of the critical shear velocity $u_{*,cr}$ in order to calculate the critical Shields stress τ_{c*}. To counter this van Rijn (1982) updated the Shields diagram by expressing τ_{cr} in terms of a critical mobility number, θ_{cr},

$$\theta_{cr} = \frac{\tau_{cr}}{(\rho_s - \rho)gd_{50}} \tag{2.10}$$

which was shown by Bonnefille (1963) and Yalin (1972) to be related to the dimensionless particle diameter D_*, and the median particle size d_{50},

$$D_* = \left(\frac{g(s-1)}{\nu^2}\right)^{\frac{1}{3}} d_{50} \tag{2.11}$$

where:

$$\theta_{cr} = 0.24D_*^{-1} \quad \text{for} \quad 1 < D_* \leq 4 \tag{2.12}$$

$$\theta_{cr} = 0.14D_*^{-0.64} \quad \text{for} \quad 4 < D_* \leq 10 \tag{2.13}$$

$$\theta_{cr} = 0.04D_*^{-0.1} \quad \text{for} \quad 10 < D_* \leq 20 \tag{2.14}$$

$$\theta_{cr} = 0.013D_*^{0.29} \quad \text{for} \quad 20 < D_* \leq 150 \tag{2.15}$$

$$\theta_{cr} = 0.055D_* \quad \text{for} \quad D_* \leq 150 \tag{2.16}$$

Although this provides a method of determining the critical shear stress for a sediment deposit there is still great uncertainty about its viability for sediment transport in sewers as sewer deposits, especially fines, tend to act in a cohesive-like manner due to biochemical agglutination effects (Williams *et al.*, 1989 and Wotherspoon & Ashley, 1992). As a result this tends to increase the critical shear stress for these materials above that exhibited by non-cohesive particles. Consequently, the physical and biochemical processes that govern incipient motion in real sewers are not as yet clearly understood and require further research.

2.12. Sediment Transport in Sewers and Cohesive (or "Cohesive-like") and Non-cohesive Sediments

Based on observations in the UK and Europe (Ashley & Verbanck, 1996) three principal modes of solids transport have been defined, although site-specific characteristics may affect the nature of each mode:

- Suspension
- Near-bed (bed-load)
- Semi-permanent deposits

The sediments can be categorised as either cohesive (or 'cohesive-like') or non-cohesive and exhibit different behaviours and as such are often studied separately (Parzonka *et al*, 1997). Where the deposits are comprised mainly of non-cohesive sands (<5% organic) bed-forms can be considered an additional mode of transport as these have been shown to move slowly downstream along the sewer invert

(Kleijtwegt, 1992). A number of transport relationships have been derived, to describe such thresholds as the *limit of deposition* or to estimate the *transport capacity* of the flow. Many of these relationships have been developed at a laboratory scale and have yielded unique estimates of transport rate for sands under a limited range of hydraulic conditions. Most of the sediment used was of a single size and the influence of a limited sediment supply was not taken into account. Ackers *et al.* (1996) demonstrated that in order to achieve reliable predictions, care must be used in the application of these relationships to ensure that the actual conditions were similar to those used in the laboratory. Skipworth *et al* (1999) have stated that previous studies examining the transport of sediment in pipes have concentrated on the movement of non-cohesive sediment with cohesive-like properties being largely ignored by researchers including, May (1993); Nalluri and Ab Ghani (1993), and Ackers (1991).

As stated by Torfs (1995) sediments encountered in sewer systems frequently contain a mixture of both cohesive and non-cohesive sediments and, depending on the mixture composition, can exhibit important mutual interactions between the fractions. Formulations that have emerged for describing the movement of cohesive deposits in sewers have been developed from research that was carried out into cohesive muds in estuarine environments as described in the following section.

2.12.1. Research of Estuarine Muds and Cohesive Mixtures

According to Panagiotopoulos *et al.* (1997) extensive sedimentological investigations, concerning the erosion threshold of estuarine and coastal deposits, have been undertaken into cohesive muds and artificially prepared mud-sand mixtures (Parchure & Mehta, 1985; Raudkivi, 1990; Dade *et al.*, 1992 and Mitchener & Torfs, 1996). Indeed, the theory relating to cohesive sediment transport has an important role within water-related engineering problems as, due to its nature, it not only affects the critical entrainment threshold of sediment deposits but can also have a direct effect on erosion rates and hence transport rates for particular deposits. According to Mitchener & Torfs (1996), the critical shear stress for erosion increases when mud is added to sand, and also when sand is added to mud. However, according to Black *et al* (2002) the difficulty with characterising the entrainment

threshold for a cohesive deposit arises from the fact that cohesive sediment transport is now widely recognised to be governed, not only by hydrodynamic (e.g. drag, lift) and electrochemical forces (e.g., van der Waals bonding, Coulombic repulsion) but also by biological forces.

Many studies (e.g., Kandiah, 1974 and Nalluri & Alvarez, 1992) pertaining to the erosion and transport of cohesive sediments examined the behaviour of clay materials such as kaolin under laboratory conditions. As stated by Black et al (2002) this approach may be too simplistic as clay is only one component within natural sediments and clays are also inherently associated with organic matter. Within the last decade however it has become recognised that the stability of a sediment deposit may also be affected by other factors such as the biomass and bacterial activity within the deposit (Paterson, 1997).

In contrast, the erosion of sediment beds containing non-cohesive sediments relies only on gravitational and frictional forces and are therefore more susceptible to erosion than cohesive sediments, which also exert electrostatic and/or bioagglutination properties (De Sutter, 2001). Section 2.12.2 and Section 2.12.3 detail some of the approaches that are currently available for the modelling of non-cohesive and cohesive sediment respectively in the field of urban drainage.

2.12.2. Studies of Non-cohesive Sediment

Non-cohesive bedload studies that have led to the development of equations for the modelling of sediment transport in sewers include those undertaken by Ab Ghani (1993); Ackers and White (1973); Ackers (1984, 1991); Ackers *et al.* (1996) and May (1993).

2.12.2.1. Ab Ghani (1993)

Ab Ghani (1993) stated that due to the occurrence of in-pipe deposition at low flows the study of sewer sediments needs to encompass both rigid (no deposition) and loose (some deposition) boundary conditions. The experimental programme carried out by Ab Ghani examined sediment transport in both smooth and rough pipes and with rigid and loose boundaries. The resulting transport equations were used to appraise

the UK sewer design methodology, which is based on the minimum velocity (1.0 m/s) criterion and the results of Ab Ghani's research illustrated that this design practice was inadequate for pipe diameters in excess of 300 mm. Ultimately, Ab Ghani's work resulted in two equations that could be used for the prediction of sediment transport at the limit of deposition. It should be noted however that the resultant transport equations are only applicable for non-cohesive bedload moving in clean pipes or for part-full pipes with loose deposited beds.

For rigid boundaries Ab Ghani (1993) proposed the following equation to be used for non-cohesive sediments over a wide range of conditions in sewers with clean inverts:

$$\frac{V_L}{\sqrt{gd_{50}(s_s-1)}} = 3.08C_v^{0.21}D_{gr}^{-0.09}\left(\frac{R}{d_{50}}\right)^{0.53}\lambda_s^{-0.21} \qquad (2.17)$$

where: s_s = specific gravity of sediment

g = gravitational constant (m/s^2)

d_{50} = median particle size

C_v = volumetric sediment concentration (m^3/m^3)

D_{gr} = dimensionless grain size

V_L = flow velocity at limit of deposition (m/s)

R = overall hydraulic radius (m)

λ_s = composite friction factor for flow and sediment bed

$= 1.13\lambda_0^{0.098}D_{gr}^{0.01}C_v^{0.02}$

where:

λ_0 = value of λ for clean pipe (2.18)

Ab Ghani (1993) proposed the following equation should be used in the design of sewers with loose deposited beds:

$$\frac{V_L}{\sqrt{gd_{50}(s_s-1)}} = 1.18C_v^{0.16}\left(\frac{w_b}{y_o}\right)^{-0.18}\left(\frac{d_{50}}{d}\right)^{-0.34}\lambda_s^{-0.31} \qquad (2.19)$$

where: w_b = width of sediment bed (m)

y_0 = depth of flow above sediment bed (m)

2.12.2.2. Ackers and White (1973)

The original Ackers and White (1973) relationship for sediment transport over a deposit was developed as a result of almost 1000 flume experiments with alluvial channels. This work developed a relationship for 'transitional' material (the intermediate grain sizes between the coarse bedload and the fine suspended load) by initially considering the bedload and suspended load separately. The bedload transport of coarse material was related to the net shear force acting on the grains, estimated from the mean flow velocity and the suspended load of fine material was related to the total stream power, estimated from the shear velocity. Subsequently, a general sediment transport function was derived based on three dimensionless groups: particle size, D_{gr}, sediment mobility, F_{gr} and sediment transport rate G_{gr}.

$$D_{gr} = \left(\frac{g(s-1)}{v^2} \right)^{\frac{1}{3}} d \tag{2.20}$$

where d is the representative particle size, for which Ackers and White recommended the use of d_{50} for uniform sediments and d_{35} for graded sediments.

$$F_{gr} = \frac{u_*^n}{\sqrt{g(s-1)d}} \left(\frac{V}{\sqrt{32}\log_{10}(12R/d)} \right)^{1-n} \tag{2.21}$$

$$G_{gr} = \left(\frac{C_V R}{d} \right) \left(\frac{u_*}{V} \right)^n = C \left(\frac{F_{gr}}{A_{gr}} - 1 \right)^m \tag{2.22}$$

where: R = hydraulic radius

V = flow velocity (m/s)

A_{gr} = value of F_{gr} at threshold of movement

The values of n, m, A_{gr} and C are a function of D_{gr}.

For $1 < D_{gr} < 60$:

$$n = 1 - 0.56 \log_{10} D_{gr} \tag{2.23}$$

$$m = 1.34 + 9.66 / D_{gr} \tag{2.24}$$

$$A_{gr} = 0.14 + 0.23 / \sqrt{D_{gr}} \tag{2.25}$$

$$\log_{10} C = 2.86 \log_{10} D_{gr} - (\log_{10} D_{gr})^2 - 3.53 \tag{2.26}$$

For coarse sediments: i.e. $D_{gr} > 60$

(equates to a particle size of approximately 2.5 mm for sand with a density of 2650 kg/m^3)

$$n = 0; \qquad m = 1.5; \qquad A_{gr} = 0.17; \qquad C = 0.025$$

2.12.2.3. Ackers (1984)

In order to render the equations more applicable to pipes and culverts Ackers (1984) made minor modifications to the original equations. The changes accounted for the differences associated with the flow cross-sectional geometry relative to pipe flow when compared with the wide prismatic channels for which the original equations were developed. The changes resulted in the following equations, and with the exception that the coefficient originally referred to as C (in Equation 2.22) was changed to H, all other equations and coefficients remained as originally presented by Ackers and White (1973).

$$F_{gr} = \frac{u_*^n}{\sqrt{g(s-1)d}} \left(\frac{V}{\sqrt{32} \log_{10}(12R/d)} \right)^{1-n} \tag{2.27}$$

$$G_{gr} = \left(\frac{C_V R}{d} \right) \left(\frac{A}{W_e R} \right)^{1-n} \left(\frac{u_*}{V} \right)^n \tag{2.28}$$

where: R = hydraulic radius, and W_e = effective width of sediment bed

2.12.2.4. Ackers (1991)

Using more recent data sets with a greater range of sediment sizes Ackers (1991) derived a new set of equations, principally based on the aforementioned earlier versions, which were also applicable to pipes and culverts, as opposed to open

channels only. A revised power law resistance term and additional coefficients were included:

$$C_V = J\left(W_e \frac{R}{A}\right)^{\alpha}\left(\frac{d}{R}\right)^{\beta}\lambda_c^{\gamma}\left(\frac{V}{\sqrt{g(s-1)R}} - K\lambda_c^{\delta}\left(\frac{d}{R}\right)^{\varepsilon}\right)^{m} \tag{2.29}$$

where: λ_c = composite friction factor of pipe and sediment bed

The new coefficients were:

$$J = \frac{8^{\frac{n(1-m)}{2}} H}{11.3^{m(1-n)} A_{gr}^{m}} \tag{2.30}$$

$$\alpha = 1 - n \tag{2.31}$$

$$\beta = (10 - 4m - mn)/10 \tag{2.32}$$

$$\gamma = n(m-1)/2 \tag{2.33}$$

$$K = 11.3^{(1-n)} g^{\frac{n}{2}} A_{gr} \tag{2.34}$$

$$\delta = -n/2 \tag{2.35}$$

$$\varepsilon = (4+n)/10 \tag{2.36}$$

The revised coefficients were:

$1 < D_{gr} < 60$:

$$m = 1.67 + \frac{6.83}{D_{gr}} \tag{2.37}$$

$$\log_{10} H = 2.79\log_{10} - 0.98(\log_{10} D_{gr})^2 - 3.46 \tag{2.38}$$

$D_{gr} > 60$:

$$m = 1.78.$$

All other coefficients remained the same as for Ackers and White (1973) or Ackers (1984).

2.12.2.5. Ackers et al. (1996)

The InfoWorks sewerage modelling package (Wallingford Software, 2001) utilises a slight modification to the 1991 formulation as recommended by Ackers *et al.* (1996) where the width of the bed deposit W_b was replaced by an effective bed width (W_e) as follows:

$$W_e = \left(0.2 + 3.33\left(\frac{y_s}{D} - 0.01\right)\right)W_b, \qquad \text{when: } 0.01 \le \frac{y_s}{D} \le 0.1 \qquad (2.39)$$

$$W_e = 0.5W_b, \qquad \text{when: } \frac{y_s}{D} > 0.1 \qquad (2.40)$$

where: y_s = sediment depth (m)

D = pipe diameter (m)

All of the aforementioned equations (Ackers and White, 1973; Ackers, 1984; Ackers, 1991 and Ackers *et al.*, 1996) are valid when D_{gr} is greater than unity, which for sand with a density of 2650 kg/m^{3}equates to a particle size of approximately 40 μm.

2.12.2.6. Development of Ackers (1991) Relationship for an Improved Prediction of Bedload (White & Day, 1982 and Rushforth, 2001)

White and Day (1982) examined the sediment transport from mixed-sized gravel river beds and applied the Ackers (1991) relationship on a size fraction basis with a modification made to the value of the threshold mobility parameter (A_{gr}) for each size fraction. The value of the modified threshold mobility parameter, A'_{gr}, was obtained by comparing the measured bedload transport with the predicted bedload transport using Ackers (1991) for each size fraction and adjusting the value of A_{gr} until the predicted bedload transport was equal to the measured transport. Using this technique White and Day (1982) developed a relationship which linked the relative particle stability, A'_{gr}/A_{gr} to particle size, d_i/d_A:

$$A'_{gr}/A_{gr} = 0.4(d_i/d_A)^{0.5} + 0.6 \qquad (2.41)$$

where: d_i = particle size of i^{th} fraction (m)

d_A = particle diameter of size fraction when $A'_{gr}/A_{gr} = 1$ (m)

White and Day also showed a relationship between d_A, and the range of particle sizes in a mixture:

$$d_A/d_{50} = 1.6(d_{84}/d_{16})^{-0.28} \quad (2.42)$$

Work undertaken by Rushforth (2001) at the University of Sheffield studied the erosion and transport of a non-cohesive deposited sediment bed under time-varying hydraulic conditions and utilised the National CSO Test Facility at Hoscar WwTW operated by North West Water near Wigan. As the tests were conducted using real sewer sediments it would seem reasonable to assume the deposits would have been comprised of cohesive material. However, due to the hydraulic regime within the test facility this was not the case, and as described by Rushforth (2001) analysis of the sediment collected during the tests showed the mixture to be inorganic. Flowrates were selected to simulate a typical rise in discharge found in a sewer system during the initial period of a storm event followed by a subsequent period of uniform, steady flow. The temporal response of the sediment bed to these hydraulic conditions was closely monitored over the duration of each test. The test rig consisted of a 60m long, 800mm-diameter glass reinforced plastic (GRP) pipe with an adjustable slope. The inflow to the pipe was raw sewage from the inlet works of the wastewater treatment plant with the pipe outflow returned to the inlet works. The tests were carried out under both uniform and time-varying flow conditions. Bedload traps connected to a load cell at the downstream end of the pipe were used to collect and quantify the material moving on or near the bed with a representative sample of this material also extracted from the boxes for sieve analysis. Rushforth (2001) found that the Ackers (1991) relationship severely under-predicted the bedload transport in the test section. The results from the bedload transport analysis suggested that the behaviour of the sediment mixture within the pipe could best be described by applying the Ackers (1991) relationship on a fractionwise basis with a modified A_{gr} value for each of the fractions under consideration as previously reported by White and Day (1982) for alluvial channels.

2.12.2.7. May (1993)

Another methodology for the transport of sediment over a deposited bed is that reported from work conducted by May (1993). In order to calculate the overall hydraulic resistance the deposit roughness is determined, with subsequent flow conditions then used to determine the sediment transport rate.

The grain mobility is given by:

$$F_g = \sqrt{\frac{\lambda_g V^2}{8g(s-1)d_{50}}} \tag{2.43}$$

where the grain friction factor is given by:

$$\frac{1}{\sqrt{\lambda_g}} = -2\log_{10}\left(\frac{d_{50}}{12R} + \frac{0.6275\nu}{VR\sqrt{\lambda_g}}\right) \tag{2.44}$$

The Froude number of the flow is:

$$F_r = \sqrt{\frac{BV^2}{gA}} \tag{2.45}$$

where: B is the surface width of the flow and A is the cross sectional area of the flow. F_b, the mobility parameter based on total bed shear stress, is selected depending on the limits of F_g and F_r as shown in Table2.3.

F_g	F_r	F_b
$F_g \leq 0.22$	All F_r	$F_b = F_g$
$0.22 < F_g \leq 0.5$	$F_r \leq 0.125$	$F_b = 0.22 + 1.63\,(F_g - 0.22)^{0.44}$
$0.22 < F_g \leq 0.5$	$0.125 < Fr \leq 1.0$	$F_b = F_g + 1.143\,(1 - F_r)\,[1.63\,(F_g - 0.22)^{0.44} - (F_g - 0.22)]$
$0.22 < F_g \leq 0.5$	$1.0 < Fr \leq 1.25$	$F_b = F_g$
$0.22 < F_g \leq 1.0$	$F_r \leq 0.125$	$F_b = 1.15$
$0.22 < F_g \leq 1.0$	$0.125 < Fr \leq 1.0$	$F_b = F_g + 1.143\,(1 - F_r)\,(1.15 - F_g)$
$0.22 < F_g \leq 1.0$	$1.0 < Fr \leq 1.25$	$F_b = F_g$

Table 2.3: Values for F_b based on limits of F_g and F_r

Once an appropriate value has been selected for F_b, the bed friction factor, λ_b is determined from:

$$F_b = \sqrt{\frac{\lambda_b V^2}{8g(s-1)d_{50}}} \tag{2.46}$$

The composite roughness of pipe and sediment bed is given by:

$$\lambda_c = \frac{P_w \lambda_w + P_b \lambda_b}{P_w + P_b} \tag{2.47}$$

where: P_w = wetted perimeter of pipe

P_b = width of sediment bed

λ_w = friction factor of pipe wall from the Colebrook-White equation

To determine the sediment transport, the particle Reynolds number is obtained from:

$$R_{*c} = \left(\frac{\lambda_c}{8}\right)^{0.5} \left(\frac{V d_{50}}{\nu}\right) \tag{2.48}$$

and from this, the related transition factor, θ, can be calculated by:

$$\theta = \frac{\exp\left(\frac{R_{*c}}{12.5}\right) - 1}{\exp\left(\frac{R_{*c}}{12.5}\right) + 1} \tag{2.49}$$

The effective mobility of the particles, F_s, is determined from the value of the transition factor, by:

$$F_s = F_g \sqrt{\theta} \tag{2.50}$$

The value of F_s is used to determine the appropriate value of the transport parameter η, which is found from the following equations, which were revised from the original set after analysis of additional data sets (May, 1994).

The volumetric sediment concentration is then given by:

$$C_v = \eta\left(\frac{W_b}{D}\right)\left(\frac{D^2}{A}\right)\left(\frac{\theta\lambda_g V^2}{8g(s-1)D}\right) \tag{2.51}$$

where: D = pipe diameter

The transport parameter η is dependant upon F_s, which is obtained from the following equations that were a revision of the original set subsequent to the analysis of additional data (May, 1994).

$F_s \leq 0.1$	$\eta = 0$	(2.52)
$0.1 < F_s \leq 0.225$	$\eta = 1.2\ (F_s - 0.1)$	(2.53)
$0.225 < F_s \leq 0.275$	$\eta = 0.15 + 9.0\ (F_s - 0.225)$	(2.54)
$0.275 < F_s \leq 0.4$	$\eta = 0.6 + 3.2\ (F_s - 0.275)$	(2.55)
$0.4 < F_s \leq 0.7$	$\eta = 1 - (F_s - 0.4)$	(2.56)
$0.7 < F_s \leq 0.8$	$\eta = 0.7$	(2.57)

2.12.2.8. The Influence of Bedforms

An added complication when dealing with non-cohesive sediment transport is that prolonged erosion and transport of this material invariably produces bedforms that will have a profound effect on erosion threshold values and transport rates. Although Perrusquia (1995) carried out a series of studies on the formation of sediment beds in sewers, the topic is still not entirely understood and more field investigations are required to form a better understanding of the phenomenon of the generation of bedforms. When the flow-induced shear stresses exceed τ_{crit} a flat sediment bed can generate bed forms, the dimensions of which are related to flow resistance and sediment transport. According to Kleijwegt (1992) experimental observation allowed the sediment beds to be classified as follows:

- Continuous flat mobile bed
- Continuous bed with bed forms (dunes and ripples)
- Discontinuous bed with isolated bed forms

Kleijwegt stated that a continuous bed is present in two opposing stages of extreme flow conditions:

- When there is little or no particle motion
- When there are high shear stresses

Bed forms which travel downstream (relief features) are generated somewhere between these stages due to the interaction of the flow and non-cohesive sediment. The bedforms that move downstream are known as dunes and ripples and move due to erosion at the upstream face and deposition at the downstream face. The geometrical characteristics of dunes and ripples differ as follows:

- Dunes

Regular bed forms with straight crests perpendicular to the flow direction with lengths much greater than the flow depth.

- Ripples

The shape is more irregular with the maximum ripple length approximately equating to the flow depth.

These bedforms may become isolated if the troughs reach the non-erodible sewer invert and the bedforms observed in sewers had crests that were perpendicular to the flow direction (transverse bed forms).

According to Kleijwegt (1992), Perrusquia (1991) studied three aspects of the flow-sediment interaction for partly full pipes; i.e. bed formation, flow resistance and bed-load transport. He concluded that the methods did not yield satisfactory results for the prediction of bedform geometry and recommended that further research should concentrate on the geometric characteristics of pipe channels. He also concluded that

results for flow resistance from using the Engelund-Hansen (1966) and Van Rijn (1984) methods were questionable due to the fact they do not take the pipe geometry into account.

2.12.3. Studies into the Erosion of Cohesive or Mixed Sediment Beds

Skipworth *et al* (1999) noted that field studies have indicated that a significant proportion of the sediments found in UK sewers display significant cohesive properties. Cohesion in clay-like materials is understood to be due to electrostatic forces between the small, plate-like clay particles. The term "*cohesive-like*" has been used to describe sewer sediments that exhibit a resistance to erosion that is much greater than that anticipated from the application of non-cohesive sediment transport models. This increase in resistance is thought to be primarily due to the organic nature of the sediments. Currently, little is known about the mechanisms that create the significant cohesive-like properties of in-sewer sediments and current understanding of the transport of cohesive-like sediment is limited.

- Effects of cohesive-like sediment

A number of studies have been completed which concluded that cohesion had a significant effect on the entrainment threshold and a more limited influence on the transport capacity of the flow in a pipe. Berlamont and Torfs (1996), Nalluri and Alvarez (1992) and Ackers *et al.* (1996) advocated the use of a single figure of 2 N/m^2 to describe the minimum applied shear stress for the erosion of in-sewer deposits, in order to account for the effects of cohesion. However, field studies have indicated a wide variability, both temporally and spatially, in the recorded values of critical shear stress. Reported values have ranged from less than 0.7 N/m^2 to 7.0 N/m^2 (Ristenpart and Uhl, 1993; and Ashley *et al*, 1993).

Experimental laboratory investigations have been carried at the University of Sheffield (Skipworth, 1996) of the erosion and transport of in-pipe, deposited, fine-grained, organic, cohesive-like sediment beds analogous to those found in sewers and corresponding to those classified as T*ype 'C'* material (as classified in Table 2.1). Using synthetic materials such as crushed olivestone under laboratory conditions a

system was established to measure the erosional characteristics of a cohesive-like sediment bed. All the experimental results showed that the cohesive like beds were composed of a weaker surface layer, in which the resistance to erosion of the bed increased with depth, overlying a stronger more stable layer of consistent erosional resistance.

2.12.3.1. Skipworth (1996)

The Skipworth (1996) model for predicting suspended sediment transport rates is based on the theory that the sediment bed is comprised of a weak layer of increasing yield strength with depth overlying bed material with uniform strength with depth as depicted in Figure 2.7.

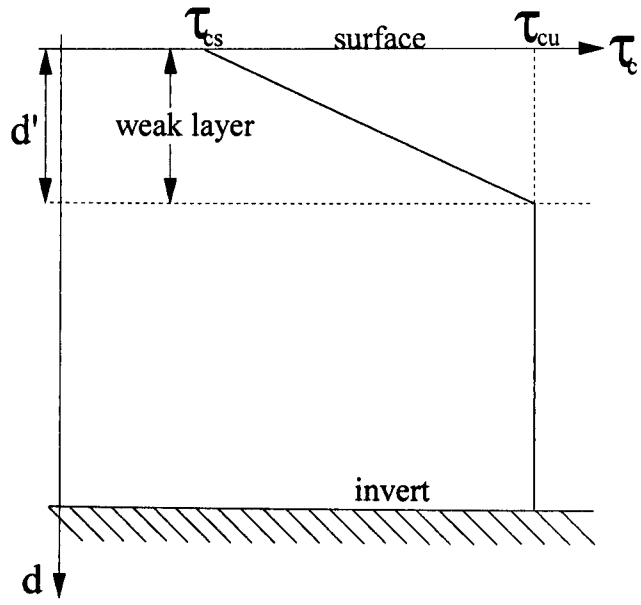

Figure 2.7: Variation of bed strength with depth

where:

d' = depth of weak layer

τ_{cs} = yield strength of bed at surface

τ_{cu} = yield strength of uniform layer

The model is based on research carried out into estuarine soft cohesive sediment deposits by Parchure & Mehta (1985) who proposed the following equation to

describe the erosion of a single size soft cohesive deposit of uniform strength with respect to depth:

$$E = M\left\{\frac{\tau_b - \tau_c}{\tau_c}\right\} \tag{2.58}$$

where:

E = erosion rate

M = erosion rate when $\tau_b = 2\tau_c$

τ_b = applied bed shear stress

τ_c = critical bed shear stress at point of erosion
(constant throughout bed depth)

By assuming the flow to be well mixed and in equilibrium at the measurement position Skipworth (1996) modified this equation by changing *E* from an erosion rate to a transport rate *T*, giving:

$$T = M\left\{\frac{\tau_b - \tau_c}{\tau_c}\right\} \tag{2.59}$$

The model was developed by establishing a relationship between the depth of erosion and bed strength and a relationship linking the transport rate parameter, *M*, to the pipe slope and mass flowrate.

τ_{cs} and τ_{cu} are the yield strengths of the bed surface and uniform layer respectively and the relationship derived by Skipworth to describe the variation of yield strength in the weak layer was given as:

$$\tau_c = \frac{d^{\frac{1}{b}}\left(\tau_{cu} - \tau_{cs}\right)}{d'^{\frac{1}{b}}} + \tau_{cs} \tag{2.60}$$

In the laboratory tests for pipe slopes of 1:500 and 1:1000 the dimensionless power-law coefficient '*b*' was calculated as 0.45, giving:

$$\tau_c = \frac{d^{2.22}(\tau_{cu} - \tau_{cs})}{d^{2.22}} + \tau_{cs} \qquad (2.61)$$

The transport parameter M (i.e. the value of T when $\tau_b = 2\tau_c$) was found to be a function of both slope (s) and mass flowrate (ρQ_m). Utilising a linear regression approach the following equation was formulated:

$$M = 1.89s - 0.001 - 0.135s\rho Q_m \qquad (2.62)$$

where: Q_m = flow rate when $\tau_b = 2\tau_c$

2.12.3.2. *Nalluri and Alvarez (1992)*

Nalluri and Alvarez (1992) found that the bedload transport of non-cohesive sediments (sand) over a loose bed within a circular laboratory flume were comparable with Einstein's bedload curve and could be described by the equation:

$$\varphi = 9.931\ \phi^{-0.123} \qquad (2.63)$$

where the flow transport parameters are given by;

$$\varphi = \tau_b / (\rho_s - \rho) g d_{50} \qquad (2.64)$$

$$\phi = C_v V R / \sqrt{g d_{50}^3 (s_s - 1)} \qquad (2.65)$$

where:

τ_b = bed shear stress (N/m^2)

ρ_s = sediment density (kg/m^3)

ρ = water density(kg/m^3)

g = gravitational constant (m/s^2)

d_{50} = median particle size

C_v = volumetric sediment concentration (m^3/m^3)

V = mean flow velocity (m/s)

R = overall hydraulic radius (m)

s_s = specific gravity of the sediment (-)

However, this governing equation was found to be unsuitable for the transport of cohesive material over a consolidated Type B (Crabtree classification, 1989) deposit. For the cohesive sediment an alternative function (Mayerle *et al.*, 1991) was found to be suitable:

$$\varphi = \tau_b / (\rho_s - \rho) g d_{50} = f(C_v, d_{50} / R, \lambda_s) \tag{2.66}$$

where: λ_s = overall friction factor

As shown in Figure 2.8, Nalluri and Alvarez (1992) showed that regression analysis of this function resulted in an equation suitable for the transport of cohesive sediments (i.e. Laponite clay, sand and water mixtures):

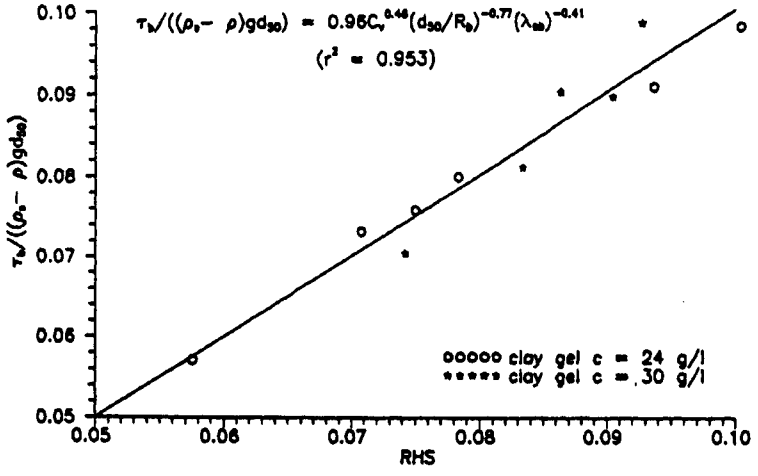

Figure 2.8: Cohesive sediment transport over a fixed bed in a 154mm-diameter flume (where, RHS = right hand side of equation displayed on graph; after Nalluri & Alvarez, 1992)

The resulting relationship for the transport of cohesive sediments was as follows:

$$\tau_b / (\rho_s - \rho) g d_{50} = 0.964 C_v^{0.457} (d_{50} / R_b)^{-0.765} (\lambda_{sb})^{-0.41} \tag{2.67}$$

where: λ_{sb} = bed friction factor

2.13. Summary

Laboratory and field studies have both indicated that during periods of high flow in combined sewers significant amounts of a bed deposit can be eroded into suspension. Until recently most research previously carried out in this area has concentrated mainly on non-cohesive deposits and existing sewer sediment modelling approaches are generally too simplistic. This may be to due to an over-simplification in the computation of the hydraulics combined with a lack of detailed consideration of the bed properties (e.g. consolidation, and cohesive properties, controlled by the finest particles/organics). Indeed the results of laboratory testing have shown that a wide variation in erosion rates can occur even under similar flowrates; and modelling developed from laboratory results indicate the importance of bed properties and varying flow conditions in determining the nature of the erosion/transport that occurs.

The formulations of Ab Ghani (1993); Ackers & White 1973; Ackers (1984, 1991); Ackers *et al.* (1996) and May (1993) were all based on laboratory experiments that utilised inorganic material of a uniform size, which was obviously not representative of the deposit material found in combined sewers. These equations could be used to determine the volumetric sediment concentration for a given set of flow conditions, and in terms of their application, although there is no requirement for calibration, a fairly extensive data set is required, based on deposit characteristics, i.e. d_{50}, bulk density (or specific gravity), sediment depth; and hydraulic conditions, i.e. flow velocity, hydraulic radius and the friction factors relating to the pipe and deposit bed. It should be noted that, of all these data requirements, perhaps the most difficult parameters to ascertain are the hydraulic roughness of the sediment deposit and pipe walls; given the difficulty of estimating these parameters they are the inputs most prone to error.

The Skipworth (1996) and Nalluri & Alvarez (1992) equations were specifically formulated for the transport of cohesive sediments and were determined from laboratory experiments utilising sand/olivestone mixtures in the case of Skipworth and Laponite clay, sand and water mixtures in the Nalluri & Alvarex experiments. Application of the Skipworth (1996) model required the input of values for four parameters to describe the structure of the bed (τ_{cs}, τ_{cu}, d' and b) and a calibration

factor, M, that scaled the erosion rate for the sediment used. The drawback with this model was that it was a site specific model which, prior to use as a predictive tool, required to be calibrated for the sites in question by the use of measured erosion rates from field tests. Initially the five main parameters from the formulation would have to be optimised using a solver which would vary these values of these parameters until a 'match' was achieved between the measured erosion rate and the modelled erosion rate for a specific event. Clearly this would not be a straightforward process as it would obviously entail an extensive data collection exercise to collect the necessary hydraulic and suspended sediment transport data. Moreover, once the model calibration was complete, the data requirements for model input were still onerous and consisted of the pipe diameter and length, deposit characteristics; i.e. bulk density and initial depth and width, in addition to the applied bed shear stress for each time step; this means that the model could never be applied without, not only monitoring of the flow, but also an appreciation of the deposit conditions within the pipe prior to the event. Alternatively the volumetric sediment concentration during an elevated flow event could be determined using the Nalluri & Alvarez (1992) equation for cohesive sediments This method would also require the input of the deposit characteristics, i.e. d_{50}, bulk density (or specific gravity); and prevailing hydraulic conditions, i.e. flow velocity, hydraulic radius and the friction factors relating to the pipe and deposit bed; but again could not be relied on to produce realistic results without comparison against the results of a measured erosion event to assess whether the calibration of the determination coefficients was required.

To date a majority of sediment transport models have been developed and calibrated from laboratory studies of non-cohesive uniform material which would suggest that the behaviour of sediment mixtures is not accounted for in such relationships. Alternatively, synthetic cohesive mixtures that are believed to be representative of real sewer sediments have also been utilised in laboratory sediment transport experiments. To further this area of research it is evident that further study is required into the erosion and transport of cohesive-like sediment beds under elevated flow conditions. To this end good quality field data complemented with the results of laboratory testing programmes using real sewer sediments are required to address

the lack of knowledge surrounding the transport of mixed bed deposits in combined sewers.

Chapter Three: Determination of Study Parameters

3.1. Introduction

In order to examine the processes involved in the transport of sediment in combined sewers, it was necessary to determine a variety of parameters both by monitoring in the field and laboratory analysis. Field instrumentation was employed during the course of this study to monitor the depth and mean velocity of the flow field, whilst simultaneously recording the material in suspension. Further measurements were carried out to measure the depth of the sediment bed, in addition to carrying out laboratory analysis in order to characterise the nature of the deposit material.

3.2. Hydraulic Monitoring

To meet the objectives of the study temporal measurements were made of the hydraulic regime within the test sections of both the Murraygate and Forfar combined sewers. In conjunction with measurements of the total suspended solids (TSS) within the flow column, these were used to evaluate the suspended sediment transport rates (SSTRs) and thresholds of erosion within the test section.

3.2.1. Detectronic Flow Survey Loggers

Three Detectronic flow survey loggers were installed at known points along the principal study length. The loggers calculated the "average" velocity by doppler ultrasonics (the ultrasonic transmission being reflected back by solids and air bubbles in the flow), and depth of flow via a differential pressure transducer. The loggers were inspected and calibrated in the laboratory prior to installation, with velocity re-calibration undertaken on removal using a propeller meter. The adjustment required due to drift in the calibration of an individual logger was evenly distributed with respect to time when applied to the field measurements. An example of the typical drift observed in the velocity data for one of the loggers is illustrated in Table 3.1.

Date	Logged Velocity (m/s)	Measured velocity (m/s)	Velocity Drift (m/s)
18/05/00	0.36	0.40	0.04

Table 3.1: Example of drift in logged velocity data

3.2.2. Liquiflex Level Monitors

In order to monitor the hydraulic gradient within the Murraygate test section Liquiflex level monitors were used, with one positioned at the head of the test section in the Samuels manhole and one in the Bodyshop manhole at the downstream end (see Figure 4.4). This system consisted of two elements; a transceiver with a display and an integral keypad for programming, and the transducer, which was mounted directly above the surface to be monitored. The measurement system operated by the transmission of ultrasonic pulses from the transducer to the surface of the liquid to be monitored which were reflected back to the transducer. As the time period between transmission and reception of the sound pulses was directly proportional to the distance between the transducer and the liquid this allowed the flow depth to be recorded.

3.3. Determination of Bed Shear Stresses

A requirement of this study was to determine the bed shear stresses (and concentration profiles) that were generated during the hydrant flush tests. As discussed by Oms *et al.* (2001), it is difficult to obtain direct measurements of bed shear stress (τ_b) in the field. In flushing tests carried out in a sewerage system in the Marais catchment in Paris (Oms *et al.*, 2001) the discharge was increased in steps and the suspended sediment load was determined by discrete sampling. The resultant bed shear was estimated using an acoustic Doppler velocity (ADV) meter but the measurements showed a lot of scatter. In the present study, as opposed to being directly estimated in the aforementioned manner, the bed shear was computed indirectly using the hydraulics measured by the flow monitors.

3.3.1. Velocity Profiles

Prandtl (1952) and Nikuradse (1933) derived rational formulae for velocity distributions and hydraulic resistance for turbulent flow over flat plates and pipes running full. Prandtl (1952) assumed the total shear stress generated in turbulent flow was approximately equal to the mean shear stress and that the fluctuating velocity components in the axial and transverse directions were equal, thus the general equation of turbulence could be represented by:

$$\tau = \rho \ell^2 \left(\frac{dv}{dy} \right)^2 \qquad (3.1)$$

where ℓ is the mixing length

Prandtl simplified the relationship by assuming:

1. The shear stress (τ) was constant and equal to the boundary shear stress (τ_o); and,
2. The mixing length (ℓ) had a linear relationship with y, the distance from the boundary, that is; $\ell = ky$, where k = the von Karman constant (0.4).

Thus the boundary shear stress could be represented as:

$$\tau_o = \rho k^2 y^2 \left(\frac{dv}{dy} \right)^2 \qquad (3.2)$$

Given that the shear velocity, $u_* = \sqrt{\frac{\tau_o}{\rho}}$ (3.3)

Equation 3.2 could then be rewritten as:

$$\frac{dv}{dy} = \frac{u_*}{k} \frac{1}{y} \qquad (3.4)$$

Integration of Equation 3.4 yields:

$$V = \frac{u_*}{k} \ln y + c \qquad (3.5)$$

From the Nikuradse (1933) velocity profiles Equation 3.5 can be expressed for rough surfaces as:

$$\frac{V}{v_*} = 5.75 \log \left(\frac{33y}{k_s} \right) \qquad (3.6)$$

where k_s is the Nikuradse equivalent sand roughness.

It then follows that for the position of maximum velocity in the flow (i.e. y = h):

$$\frac{V_{max}}{u_*} = 5.75\log\left(\frac{33h}{k_s}\right) \tag{3.7}$$

Subtracting Equation 3.6 from Equation 3.7 yields the velocity-distribution equation:

$$\frac{V_{max} - V}{u_*} = 5.75\log\left(\frac{h}{y}\right) \tag{3.8}$$

3.3.2. Side Wall Elimination

In order to estimate the partitioning of the total shear stress between the sediment bed and the pipe wall the flow column may be partitioned as shown in Figure 3.1.

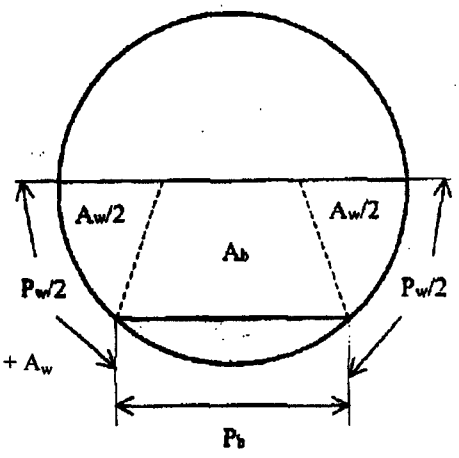

Key:

Flow cross-sectional area (A) = $A_b + A_w$
Wetted perimeter (P) = $P_b + P_w$
w = wall; b = bed

Figure 3.1: Flow partitions for determination of bed shear stress

When the flow cross-section is subdivided as shown in Figure 3.1 the flow in the central section is influenced by the sediment bed only and the pipe wall influences the flow in the outer subsections. This technique assumes that the average velocity and hydraulic gradient is the same in each of the subsections and there is zero shear stress along the surfaces separating the flow sections. The method is based on the concept of an equivalent friction factor for the whole wetted perimeter (λ) as outlined

in Equation 3.9:

$$P\lambda = P_w\lambda_w + P_b\lambda_b \tag{3.9}$$

where: λ = overall friction factor

λ_w = wall friction factor

λ_b = bed friction factor

For open channels the Darcy-Weisbach equation is given by:

$$\lambda = \frac{8gRs}{V^2} \tag{3.10}$$

which may be rearranged to give:

$$\frac{\lambda}{R} = \frac{8gs}{V^2} \tag{3.11}$$

where: s was taken to be equal to the invert slope modified by the sediment deposit.

Based on the assumption that $V_w = V_b = V$ it follows that:

$$\frac{\lambda_w}{R_w} = \frac{\lambda_b}{R_b} = \frac{\lambda}{R} \tag{3.12}$$

where: R_w and R_b = hydraulic radius related to the wall and bed respectively

A successive approximation approach is then used to achieve a solution for R_w and R_b using the Colebrook-White equation so that the hydraulic radius of the bed is given by:

$$R_b = \frac{\lambda_b V^2}{8gs} \tag{3.13}$$

The bed shear stress is then given by:

$$\tau_b = \rho g R_b s \tag{3.14}$$

3.3.3. Determination of Boundary Roughness from Flow Monitoring

From velocities that were logged from flow monitoring that was carried out it was possible to determine the friction factor (λ) from the Darcy-Weisbach equation as given in Equation 3.10. It was then possible to deduce the boundary roughness (k_s) using the Colebrook-White equation (rough channel law):

$$k_s = 14.8R\left(\log_{10} - \frac{1}{2\sqrt{\lambda}}\right) \tag{3.15}$$

An example of the values of k_s that were obtained from flow monitoring in the Murraygate combined sewer is illustrated in Figure 3.2. On this particular day the average value of k_s was approximately 6 mm, with the fluctuations illustrating how the headloss due to friction within the pipe could fluctuate throughout the day. Wotherspoon (1994) noted that minimum values of k_s tended to coincide with periods of greatest flow depths, suggesting that the sediment deposit affected the flows at low depths, with this effect decreasing as the depth of flow increased. In the following example it can be seen that this effect did not appear to be prevalent, although there was a marked decrease in the k_s value when the flow depth suddenly increased from approximately 0.27m to 0.33m.

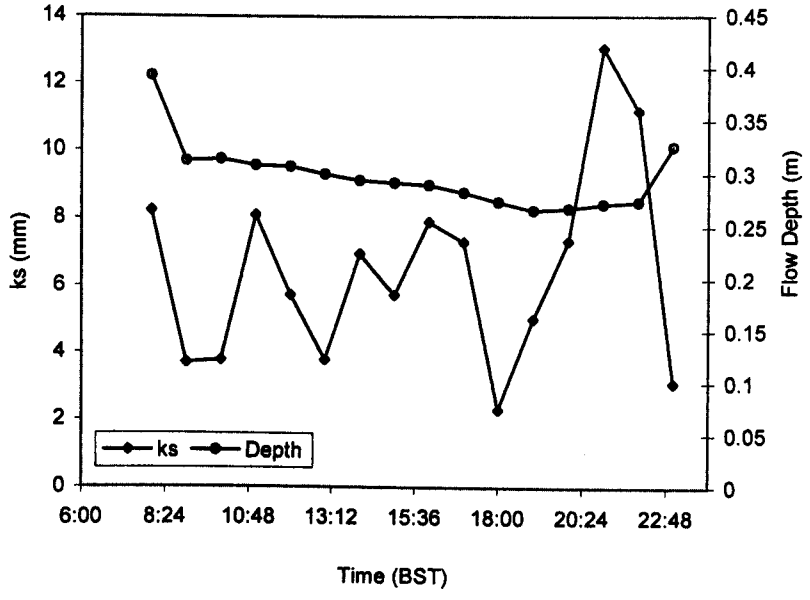

Figure 3.2: Determination of k_s from flow monitoring (Murraygate: 12-06-00)

3.4. Bed Level Measurements

3.4.1. Manual Deposit Measurements

The erosion and deposition of sediment along the study length was monitored using physical profiles of sediment depth present at specific times to produce "snapshots" of the bed profile. This was undertaken by conducting 'walk-throughs' of the test section during DWF using a calibrated bed-measuring device, comprising of a flat plate that rested on the surface of the deposit to which a hollow tube containing a calibrated depth-measuring device was attached. Measurement of the bed depth relative to the free surface of the flow enabled the average bed profile to be determined, and provided a gross estimation of the overall sediment budget within the test section.

3.4.2. Dynamic Depth Monitoring

The erosion and deposition of the sediment bed in the downstream section of the test pipe was also monitored continuously using three sonar devices that were calibrated in the laboratory. The units comprised an ultrasonic transducer within a sealed head that was attached to the end of a rigid tube, which in turn was attached to the soffit of the sewer (see Plate 3.1).

Plate 3.1: Ultrasonic depth deposit monitor

3.5. On-site Sediment and Sewage Sampling

In order to characterise the bed deposit material, samples were extracted from various points along the length of the test section at different times throughout the study period.

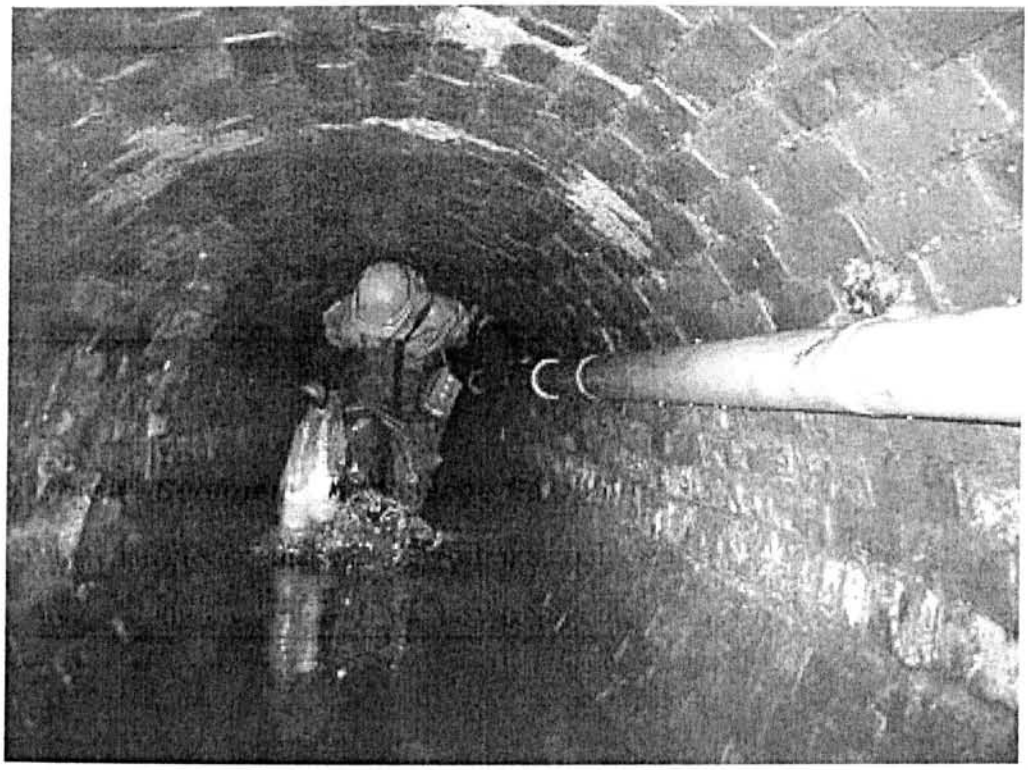

Plate 3.2: Retrieving deposit samples for laboratory analysis

3.5.1. Manual Deposit Sampling

It was found that the most effective and simple method to obtain a deposit sample was to manually force a 1000-ml sample container down through and along the sediment bed. Drainage of the trapped sewage unfortunately enabled fine sediment to escape although this was unavoidable regardless of which sampling method was employed. The sediment samples obtained were tested in the laboratory for particle size distribution, bulk density, dry solids content and were also used in the rheological assessment of yield strength.

3.5.2. EPIC Wastewater Sampling

Sewage samples were also obtained using automatic EPIC samplers with 24 x 500ml capacity containers. At each of the sampling sites a rigid PVC tube was fixed to the sewer wall and oriented into the sewage flow, such that all samples were obtained

from known fixed points above invert level. A flexible PVC hose connected the tube to the sampler at ground level, with the sampling rate varied according to whether DWF or storm conditions were under investigation. For DWF, a sampling interval of 1 hour was selected to cover one full day, while for storm flow conditions, a sampling interval of 2 minutes was used. The sewage samples obtained were analysed in the laboratory for TSS, VSS and particle size distributions.

Plate 3.3: EPIC wastewater samplers (after Arthur, 1996)

3.5.3. Bedload Traps for the Collection of Near Bed Solids

The material moving near the bed at the Samuels site (see Figure 4.4 for location) was sampled using a sediment trap which was fitted in the invert of the 'false' sewer. The sediment trap was compartmentalised into three separate containers (300mm long x 150mm wide x 300mm deep) and was fitted with a cover to prevent the ingress of material outside the sampling times. Flow velocities and depth were recorded at a single point downstream of the sediment trap, at two-minute intervals. The samples obtained were tested in the laboratory for particle size distribution, bulk density and dry solids content.

3.6. Characteristics of Deposit Material

The individual samples retrieved from the study sites were tested, where possible, for each of the following parameters.

3.6.1. Total Solids (TS)

The total solids (TS) were determined by drying the sample at 102° C, with the residue remaining constituting the total solids value, measured in grams.

3.6.2. Particle Size Distribution

Determination of the particle size distribution by dry sieving was primarily undertaken on the inorganic fraction of the material in transport, although for the near bed solids, observational analysis was undertaken on organics. The test undertaken on the mineral fraction was in accordance with BS1377 (BSI, 1990).

3.6.3. Bulk/Dry Density

To give an estimation of the characteristics of particles in transport, the bulk density of each sample retrieved was determined. The dry density, which is used in geotechnics to estimate the degree of compaction in soils (Craig, 1987 & Smith, 1990), was also determined to give a value for the mass of (dry) solids per unit volume of sample.

3.6.4. Moisture Content

Moisture contents were determined by drying the sample in an oven at 105°C. The moisture content was expressed as a percentage ratio of water to dry solids by weight.

3.6.5. Volumetric Solids

A sediment sample is composed of solid mass grains with voids in between the grain. These voids may be either filled with water or air or with both and the term volumetric solids (C_v) refers to the ratio of the volume of solids to the total sample volume. Theoretically;

$$C_v = 1 - \left\{ \frac{e}{1+e} \right\} \qquad (3.16)$$

where: $$e = \frac{S_G m}{100} \quad (3.17)$$

and; S_G is sediment specific gravity; m is sediment moisture content (%)

3.6.6. Inorganic Solids and Organic Solids

The organic fraction of the material retrieved from the field was removed by drying the sample at 102°C, followed by furnacing the dry sample at 550°C. The percentage of dry mass remaining that did not ignite constituted the non-volatile inorganic solid fraction. The dry mass lost in the furnacing procedure was thus the organic fraction, expressed as a percentage of the total dry mass. Arthur (1996) commented that a possible source of error in this procedure could occur where the mass of the inorganic fraction was low, as the results could be affected by the remaining ashed residue of the organic material that was burnt.

3.7. Characterising the Deposit Strength and Estimating the Critical Bed Shear Stress

An important aspect in modelling the erosion of bed deposits in sewer systems is the need for some estimation of the 'strength' characteristics of the material being eroded. The beds' propensity for erosion will depend on several factors such as consolidation period, which is related to the antecedent dry weather period (ADWP), cohesive bonding, porosity and possibly even the biochemical reactions taking place within the bed, related to the ambient temperature. These will determine the so-called critical bed shear stress (τ_{cr}) required for the onset of erosion; the parameter most frequently used to express deposit erosional resistance (De Sutter, 2001). Although the objective of this part of the study was to attempt to quantify the erosional resistance of the sediment beds under investigation, realistically there will be a range of τ_{cr} values. This is due, not only to the difficulties in defining a critical threshold, but also the sensitivity of the measuring equipment and the heterogeneity of sewer sediments (Lavelle and Mofjeld, 1987).

3.8. Investigative Techniques

The current study has examined the strength of sediment deposits using the following experimental techniques:

3.8.1. Erosion Meter Analysis

Samples of sediment collected from the main Dundee interceptor sewer and a combined sewer in Forfar were analysed using an erosion meter (see Figure 3.3). This provided an estimation of the critical bed shear stress for the material in addition to erosion rates for various applied shear stresses.

3.8.2. Rheological Testing

Samples of sediment collected from the main Dundee interceptor sewer and a combined sewer in Forfar were analysed using a Carrimed controlled stress rheometer to provide an indication of their yield strength.

The threshold or critical bed shear stress (τ_{bcr}) of a sewer deposit refers to the transitional point for incipient motion of particles on the bed surface. As documented by Lavelle and Mofjeld (1987), it is actually the instantaneous stress (fluctuating around the mean stress) that is responsible for the motion of individual particles. Various researchers have carried out investigations in order to determine τ_{cr} for different materials. An important aspect of this work is the definition used to describe the incipient motion. The definitions given for the threshold of erosion have been many and varied; thus demonstrating the imprecise nature of the concept (Lavelle and Mofjeld, 1987). In reality there have been three distinct categories of definitions for obtaining τ_{cr} as noted by De Sutter (2001):

3.8.3. Extrapolation of suspended sediment profiles

Sediment fluxes have been measured in flumes with the transport rate extrapolated back to zero to give a corresponding critical bed stress (τ_{cr}); although it should be noted that the actual extrapolation methods used may differ.

3.8.4. Visual observations

This method is highly subjective and the repeatability of results is obviously questionable. This technique relies on personal judgement as to when a few particles are moving, many grains are moving or general transport is occurring (Tito, 1995).

3.8.5. Extrapolation of high erosion rates

Partheniades (1965) noted that during experiments with cohesive sediments often little erosion occurred at low shear stresses, while higher stresses exhibited large changes in erosion rates. Hence it was argued that the high erosion rates could be extrapolated back to zero to give a corresponding critical bed stress (τ_{bcr}) and any erosion occurring below this threshold could be deemed insignificant.

In his study, De Sutter (2001) used an iterative process to determine the transition. With a load cell indicating a steady weight in a sediment trap and a turbidity sensor revealing no suspension for a given steady state discharge step, he concluded that no erosion was taking place. In the next step, using the same method he deduced that erosion was taking place and then defined the critical bed stress as the average for both steps. When using this approach the accuracy of the calculated τ_{bcr} would obviously rely on the magnitude of the difference in discharge steps.

3.8.6. Determination of τ_{bcr} in the Laboratory

In order to determine their critical bed stress, sewer sediments were extracted from the main Murraygate interceptor sewer in Dundee and a combined sewer in Forfar. Controlled erosion tests were then carried out using a specially developed portable erosion meter (based on a design by Liem *et al.*, 1997), which could exert specified shear stresses to the sewer deposits.

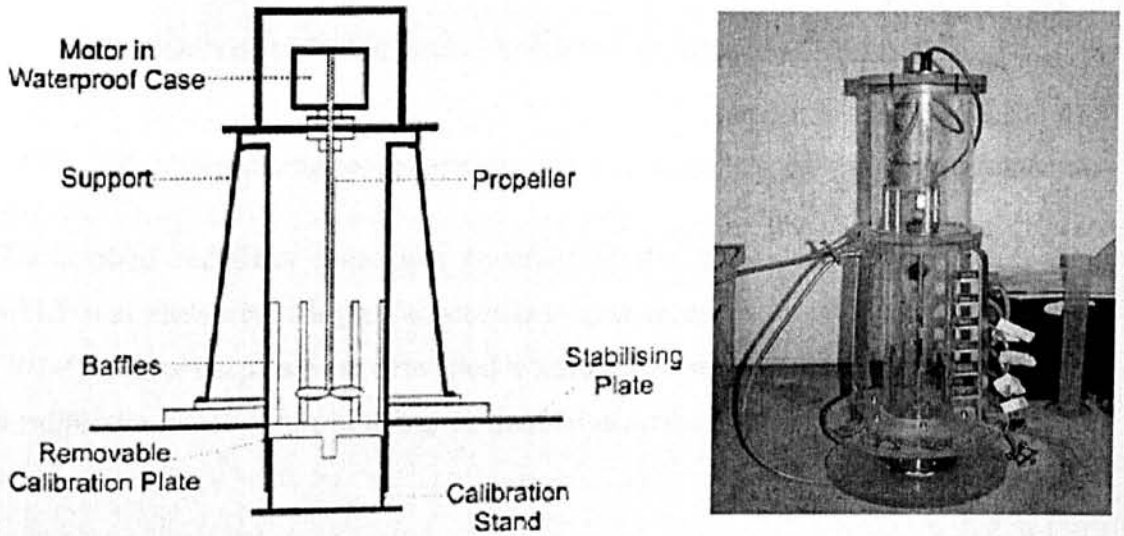

(a) Schematic illustration (Source: Jubb *et al.*, 2000) (b) Extraction ports clearly visible

Figure 3.3: Erosion meter shear stress simulation device

The erosion meter consists of a cylindrical Perspex tube (100mm inner diameter) with a sample container at the bottom (60mm high with a 7238mm^2 surface area). A 50mm diameter propeller, centred 30mm above the sediment bed, exerted a uniform shear stress, with baffle plates (0.2mm thick) fixed perpendicular to the inner wall of the tube, to prevent vortices. A waterproof casing at the top of the erosion meter contained the propeller motor. On the wall of the Perspex tube seven sample extraction ports (7mm diameter) were situated at heights of 40, 80, 120, 160, 200, 240 and 280mm above the bed. These provided the means for drawing off samples that could subsequently be analysed for suspended solids concentration.

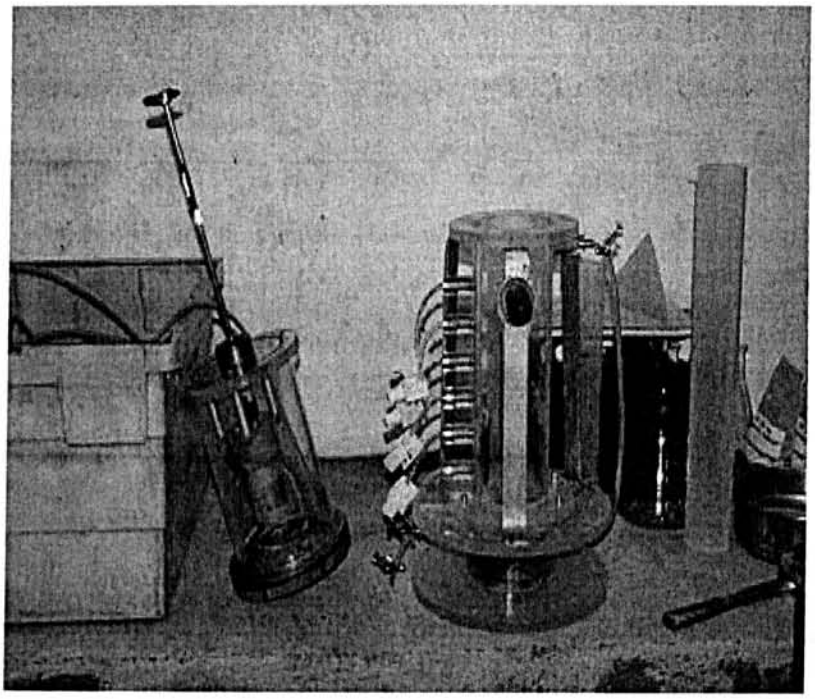

Plate 3.4: Motor casing/propeller assembly and main Perspex unit of erosionmeter

The applied bed shear speed was governed by the angular speed of the propeller, which was measured using a Tachometer to give an output in revolutions per minute (RPM). These outputs were converted to corresponding bed shear stress values using a calibration curve obtained using the method described below.

3.8.6.1. *Instrument calibration*

Prior to carrying out controlled erosion tests to simulate the shear stresses exerted under storm conditions, the erosion meter had to be calibrated. This was achieved using a modified version of the Shields' criterion (1936), as the original was not deemed sufficient when considering fine sand fractions (Licht, 1998). This provided a predictive relationship between the angular velocity of the propeller and the applied bed shear stress (τ_b). The modified Shields' criterion (Van Rijn, 1984) related the sedimentological grain diameter (D_*) to a critical mobility parameter (θ_{cr}).

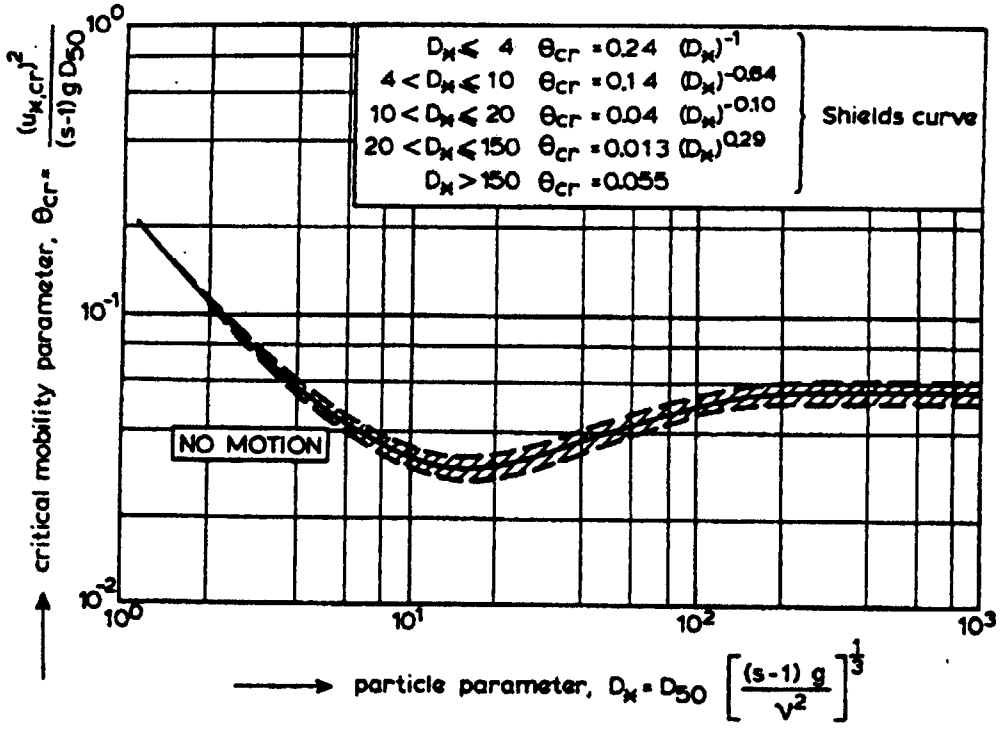

Figure 3.4: Modified Shields' (1936) criterion according to Van Rijn (1984)

Prior to applying the relationships proposed by Van Rijn (1984) a suitable definition for the onset of erosion of the sand particles had to be established. According to Licht (1998), when increasing the angular velocity of the erosion meter propeller, four distinct states of motion related to sediment transport could be observed:

Initialisation: Individual grains begin to vibrate but do not leave their location in the sediment bed.

Surface stabilisation: Grains are excited and may occasionally leave their position in the bed and move to locations that afford more protection from the prevailing current.

Onset of erosion: Grains roll over the surface of the sediment bed and are transported for relatively long distances.

Transport: Increasing the angular velocity of the propeller could increase the rate of grain mobilisation per time and area.

The question may be posed why this observational method was not directly employed during the tests on the sewer deposits to evaluate τ_c. Although the method is viable when dealing with mineral particles such as sand, it was found to be impossible to implement when using real sewer sediments, as, due to the turbidity of the water column, the bed surface was not discernible.

For the calibration procedure five different samples of quartz materials were used with different uniform grain sizes. Each size fraction was assigned a characteristic grain diameter (d_{ch}), which would normally be determined as the average grain diameter for each fraction. In this case d_{ch} was assigned as the minimum grain diameter as this would be decisive for the onset of erosion. The sedimentological grain diameter was then defined as:

$$D_* = d_{ch}\left(\frac{\rho_r g}{\nu^2}\right)^{\frac{1}{3}} \qquad (3.18)$$

where:

d_{ch} = characteristic (minimum) grain diameter [mm];

ν = kinematic viscosity (μ/ρ) [m^2/s];

g = acceleration due to gravity [m/s^2];

and,

$$\rho_r = \frac{\rho_S - \rho_F}{\rho_F} \qquad (3.19)$$

where:

ρ_S = the density of the quartz particles [kg/m^3];

ρ_F = the fluid density (water) [kg/m^3].

And; ρ_S was assumed to be equal to 2650 kg/m^3

(As the material used was comprised of quartz/silicate grains.)

The Froude number may be evaluated from:

$$Fr_* = \frac{u_{*cr}^2}{\rho_r g d_{ch}} \tag{3.20}$$

where, the critical shear velocity u_{*cr} is defined as:

$$u_{*cr} = \sqrt{\frac{\tau_{cr}}{\rho_F}} \quad [\text{m/s}] \tag{3.21}$$

By manipulation of Equations 3.20 and 3.21, the critical bed shear stress becomes:

$$\tau_{cr} = (u_{*cr})^2 \rho_F = Fr_{*cr} \rho_r g d_{ch} \rho_F \qquad [\text{N/m}^2] \tag{3.22}$$

The critical Froude number (Fr_{*cr}) denotes the threshold of motion for non-cohesive grains characterised by sedimentological drain diameter (D_*). Using Van Rijn's (1984) modified Shields' approach this critical mobility parameter may be determined as follows:

$D_* \leq 4$	$Fr_{*cr} = 0.109D_*^{-1}$	(3.23)
$4 < D_* \leq 10$	$Fr_{*cr} = 0.140D_*^{-0.64}$	(3.24)
$10 < D_* \leq 20$	$Fr_{*cr} = 0.040D_*^{-0.1}$	(3.25)
$20 < D_* \leq 150$	$Fr_{*cr} = 0.013D_*^{0.29}$	(3.26)
$D_* > 150$	$Fr_{*cr} = 0.055D_*^{-1}$	(3.27)

Using these equations the critical shear stress was evaluated for five separate grain fractions with particle sizes ranging from 150μm-1.70 mm. This enabled a second order regression curve to be plotted relating the angular velocity of the erosion meter (RPM) to the applied critical bed shear stress (τ_{cr}).

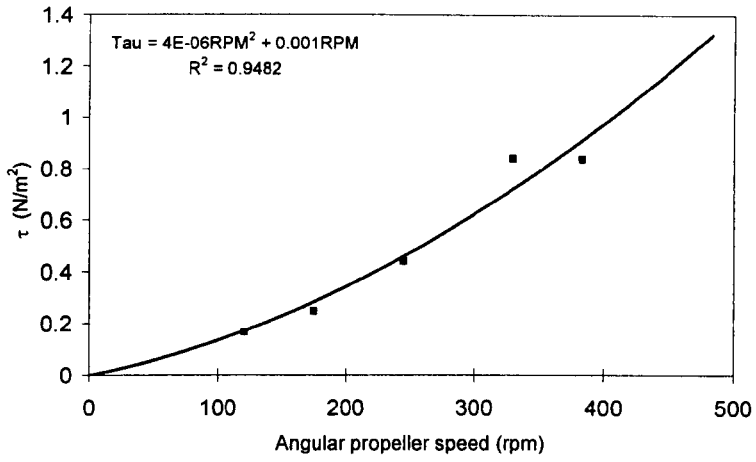

Figure 3.5: Erosion meter calibration using Van Rijn's modified Shields' criterion

3.8.7. Test procedure

Sediment samples were extracted from the sewer using a hand-sampling tool and returned to the laboratory for preparation. The intention was to replicate the conditions that would be found in the field. The sample was placed in the appropriate container and allowed to consolidate for a period of at least twenty-four hours to ensure the bed would have adequate strength and also to allow the turbidity in the water column to subside. The consolidation times were also varied to observe the effect this would have on the erosional resistance of the sediment beds. No effects of temperature were investigated and all tests were carried out at room temperature. Prior to each test the erosion meter was warmed up for thirty minutes to ensure good correlation between the rotational speed of the propeller and the applied bed shear stress. During the actual test a low shear stress was initially applied and progressively increased to avoid increasing the turbidity in the water column. The sampling procedure involved the extraction of samples from each of the seven ports in turn. These were analysed for total suspended solids (TSS) concentration and then averaged for the overall volume contained in the apparatus. The total volume (2027ml) was subdivided into seven partial volumes with the extraction ports located at the top of each partial volume.

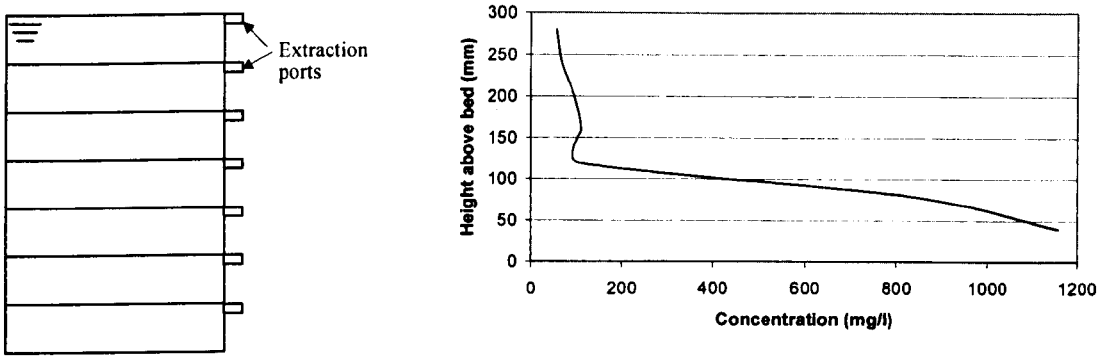

(a) Illustration of partial volumes (b) Typical concentration profile

Figure 3.6: Erosion meter concentration profile

Ideally, the samples would have been extracted simultaneously but as this was not possible, they were withdrawn on a top-down basis, as due to the marked concentration profile (see Figure 3.6(b)) this would have the least effect on the concentration of the next sample to be extracted. Once the concentration of each sample had been established, this was equated to the mass of solids released for that partial volume, which were then summed to give the total solids release for that particular applied shear stress. For each applied shear stress this approach ultimately produced an erosion rate determined from the total mass of solids released per exposed bed surface area per applied stress time. It is acknowledged that the effect of dilution was not accounted for in this study as the water column was replenished between each applied shear stress. This methodology gave some measure of the response of the deposit to applied stress:

$$q = \left(C_{SS,m} - C_{SS,0}\right)\frac{V}{A.\Delta t} \qquad (3.28)$$

where: q = erosion rate [gSS/m^2/s]

$C_{SS,m}$ = current concentration of suspended solid [gSS/m^3]

$C_{SS,0}$ = concentration of suspended solids prior to application of shear stress [gSS/m^3]

V = volume of water column (2027×10^{-3} m^3)

A = exposed surface area of bed (7.238×10^{-3} m^2)

Δt = change in time (s)

3.9. Rheological Properties of the Deposit

As reported by Wotherspoon (1994) studies of combined sewer sediment deposits (Crabtree, 1989) have recognised that these deposits may possess cohesive characteristics as a result of organic binding. It follows then that such deposits may have a higher critical yield stress than a similar non-cohesive deposit and thus require a higher bed shear stress for the onset of erosion. Torfs (1995) stated that it has been attempted to relate the critical bed shear stress (τ_{bcr}) to one or more physical deposit characteristics (grain size, water content, density, surfacial friction angle etc.) without any success. Contrary to this, the current study has confirmed there is a correlation between the rheological yield strength and (τ_{bcr}) as first reported by Wotherspoon (1994). Fundamental studies by Williams *et al.* (1989), Williams and Williams (1987) and Kirby (1988) formed the foundation for the Wotherspoon (1994) rheological work, which was based on the following assumptions:

- Sewer sediments can demonstrate elastico-viscous properties.
- The steady shear methods used by geotechnical engineers to determine yield strength are not appropriate due to the heterogeneous nature of the material.

Based on these assumptions Wotherspoon (1994) tested the yield strength of sediments using direct shear stress and shear wave propagation techniques, utilising a non-standard measuring geometry based on previous investigations carried out by Williams and Williams (1989). This cruciform vane geometry assumes a cylindrical failure surface, which causes the sample to fail via creep deformation.

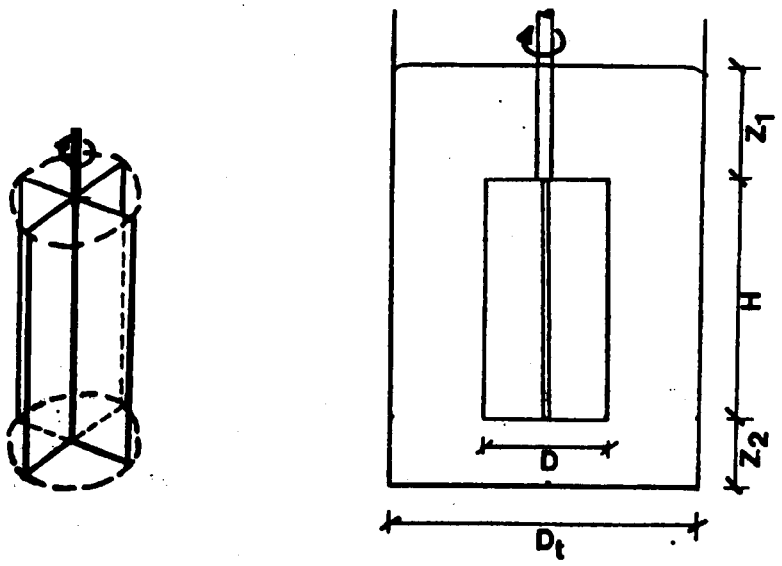

Figure 3.7: Vane geometry

For the current study the vane geometry was identical to that adopted by Wotherspoon (1994) with a 10mm diameter and 20mm height, as this met all the specified limits on dimensions whilst providing the greatest measurement range. This vane allowed for yield strength measurements to be measured from between 25 N/m^2 and 2500 N/m^2 (the limit of measurement of the instrument utilised). The measurement technique employed was the Berger model (gradual increases in the value of constant applied stress) and demonstrated the rapidity of breakdown of the elastic response of the sediment structure with small increases in stress. Wotherspoon (1994) noted that this phenomenon is characteristic of the critical stress reported by researchers using flume studies of sediment bed behaviour, who noted that beyond a certain critical applied bed shear stress, the bed structure breaks down rapidly (Nalluri & Alvarez, 1990)

3.9.1. Apparatus Used for Rheological Testing

The EPSRC loan pool provided the rheometer used, a Carrimed CSL 100 controlled stress rheometer (Carrimed Ltd., Dorking, Surrey), which was controlled by computer software with measurements taken via a direct interface.

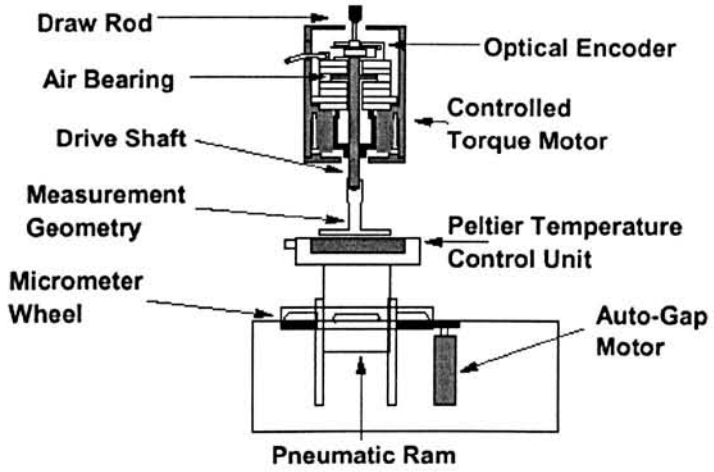

Figure 3.8: Schematic diagram of the Carrimed controlled stress rheometer

The rheometer incorporated a torque motor assembly, the drive shaft of which was supported on an air bearing, providing a virtually frictionless support. An optical encoder mounted on the drive shaft detects angular movements as low as $2x10^5$ of a radian. The computer also managed the temperature control system, with normal operation in the range of 5°C to 60°C.

3.9.2. Test Procedure Adopted

The same testing procedure was used for this study as that adopted by Wotherspoon (1994), that is, the applied stress technique utilised by Williams and Williams (1989). It should be recognised that the measurement is of an apparent yield stress, no attempt being made to measure true yield stress (stress below which no viscous flow occurs). The testing procedure for the individual samples retrieved from the study sites was as follows:

1. The samples retrieved from the study sites were placed in 40mm diameter by 60mm high Pyrex beakers and the sediment structure allowed to reform for 24 hours at 5°C.
2. The air supply to the rheometer was switched on, followed by the water supply to the Peltier temperature control system (all tests were carried out at 20°C).
3. The micrometer on the loading ram was adjusted such that when raised, the sample jar and vane were in positions corresponding to the limits on

dimensions noted previously.

4. The computer was switched on and the system allowed to self-test, after which the spindle restraint was removed and the vane attached.
5. The sample in its container was then placed on the loading ram and fixed into position using adhesive tape (to prevent accidental rotation or movement of the jar).
6. The sample was introduced to the vane by raising the ram via the software package.
7. The sample was then left for 15 minutes until an equilibrium condition had been reached before the first application of stress.
8. A specified torque was applied for 30 seconds and a relaxation time of 30 seconds was also monitored using the creep package within the software.
9. Steps 7 and 8 were then repeated for torques corresponding to higher increments of stress until the sample yielded.

It should be noted that the strain was measured as an angular movement and hence this was not true strain due to the geometry of the vane and the sediment included within the blades. As stated by De Sutter (2001), given the high values of critical yield that have been recorded from rheological tests of sewer sediment, this would suggest it would be impossible for these deposits to be eroded in sewers. As this is obviously not the case then the yield stress value cannot be considered equal to the critical bed shear stress. Nonetheless, this does not mean that a functional relationship could not exist between the two parameters.

3.10. Wastewater Characteristics

The matter transported in sewers can be classified as either *organic* or *inorganic*. The organic matter is those chemical compounds containing carbon, with the inorganic matter making up the remainder. The organic matter includes living biomass and is required as substrate for the microbial processes within the system. It exists both in dissolved forms as well as particulate fractions subdivided into biomass and particles of different sizes and biodegradability. In order to characterise the suspended solids transported in the flow column the individual parameters can generally be determined as outlined in the BSI Standard Methods (1990).

3.10.1. Constituents Associated with the Suspended Material

The various constituents associated with this phase can be determined by the analysis of either filtered or non-filtered samples and, apart from the methods for the determination of the individual compounds such as volatile fatty acids (VFAs) etc., the organic and inorganic material may be quantified as follows:

Parameter	Determination Method	Units
Total solids (TS)	The sample is dried at 102°C. Any parts not evaporated are the total solids.	g TS
Inorganic solids or non-volatile solids (NVS)	The sample is dried at 102°C then furnaced at 550°C – the remainder that cannot be burnt is the inorganic material.	g NVS
Volatile Solids (VS)	This is the difference between the dry and the furnaced weights once the sample has been dried at 102°C then furnaced at 550°C. The burning at 550°C is supposed to give a complete pyrogenic oxidation of the organic matter and therefore VS is a measure of the total organic matter.	g VS
Biological Oxygen Demand (BOD)	The sample is diluted with saturated water and the oxygen concentration measured after a number of days (usually 5) and using the undiluted sample the consumed oxygen is calculated.	g BOD or g O_2
Chemical Oxygen Demand (COD)	The sample is boiled in a digestion solution consisting of sulphuric acid, potassium dichromate, mercury and silver in order to oxidise all the organic matter.	g COD or g O_2

Table 3.2: Measuring procedures for organic and inorganic matter (Metcalf & Eddy, 1991)

3.10.2. Particle Fall Velocity Distributions

The settling velocity distributions of the sample were determined using the Umwelt und Fluid Technik (UFT) method (Michelbach & Wöhrle, 1992) as utilised by Arthur (1996), where pre-settled samples were tested in a relatively short 0.7m column. The method is principally suited for fine (suspended) particles, with the methodology promoted extensively in Germany and further afield (Pisano, 1995). Arthur (1996) reported that the results from this methodology have been widely applied to the design of sewerage ancillary structures and treatment facilities (e.g. Michelbach & Weiss, 1995).

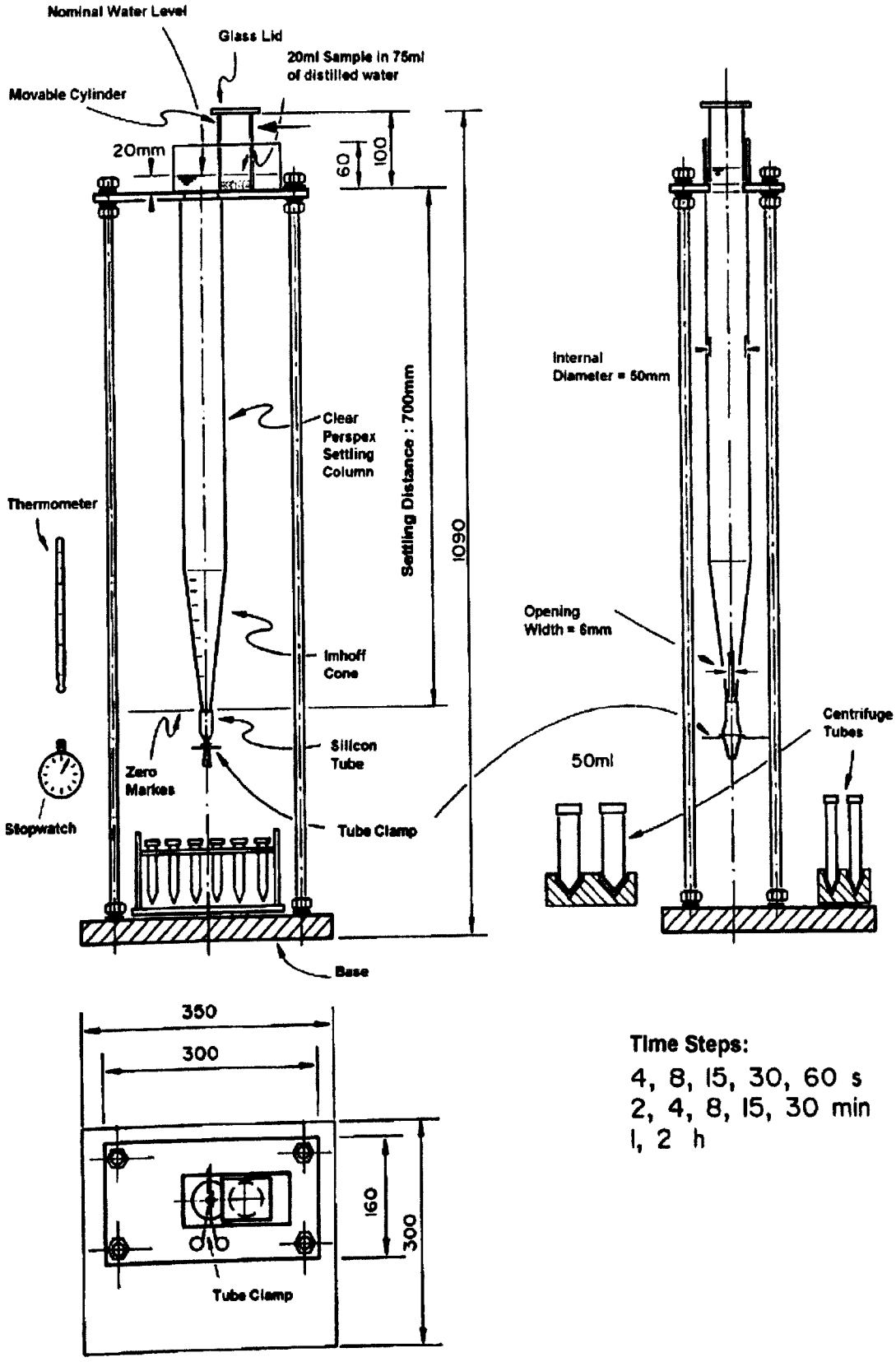

Figure 3.9: UFT settling velocity apparatus

The apparatus (illustrated in Figure 3.9) consists of a 700mm long transparent hollow cylindrical column (50mm diameter) which tapers into an Imhoff cone at the bottom. At the top of the column a second section of open-ended cylinder, of the same internal diameter, is housed inside a small container fixed to the top of the main column. Settled samples are drawn off via a silicon tube, fixed to the base of the Imhoff cone, with flow controlled by a small clamp. The testing procedure was as follows:

1. The column was filled with distilled water to a level 10mm above the top of the cylinder, i.e. filling 10mm of the container at the top of the column and the water temperature was held at 20°C.
2. The small movable cylinder was then placed in the container at the top of the column and filled with the sample to be tested.
3. The top of the small cylinder was sealed using a small sheet of wetted glass, and then moved immediately over the open end of the settling column. At this point timing starts.
4. Once settling had been initiated samples were drawn off at intervals which increased by approximately 100% each time, that is: 4 seconds, 8", 15", 30", 60", 2', 4', 8', 15', 30', 60' and eventually 2 hours.
5. At the end of each time step a sample of 15ml was drawn off, however, for the higher fall velocities larger sub-samples are recommended.
6. Any material that was deposited in the wall of the cone during the procedure was dislodged during each time step by tapping the outside of the cone.
7. The settling velocity was then estimated by dividing the fall distance (700mm) by the settling time. Using the weight of solids in each sub-sample a graph of % cumulative mass settled could then be plotted against settling velocity (an example of which can be seen in Figure 6.43).

Chapter Four – Field Study Catchments

4.1. Introduction

The collection of field data for this study was undertaken in two catchments in Scotland (Dundee and Forfar, shown in Figure 4.1) with supplementary data obtained during laboratory testing in Delft, The Netherlands. The site selection procedures and data collection protocols are discussed in this chapter.

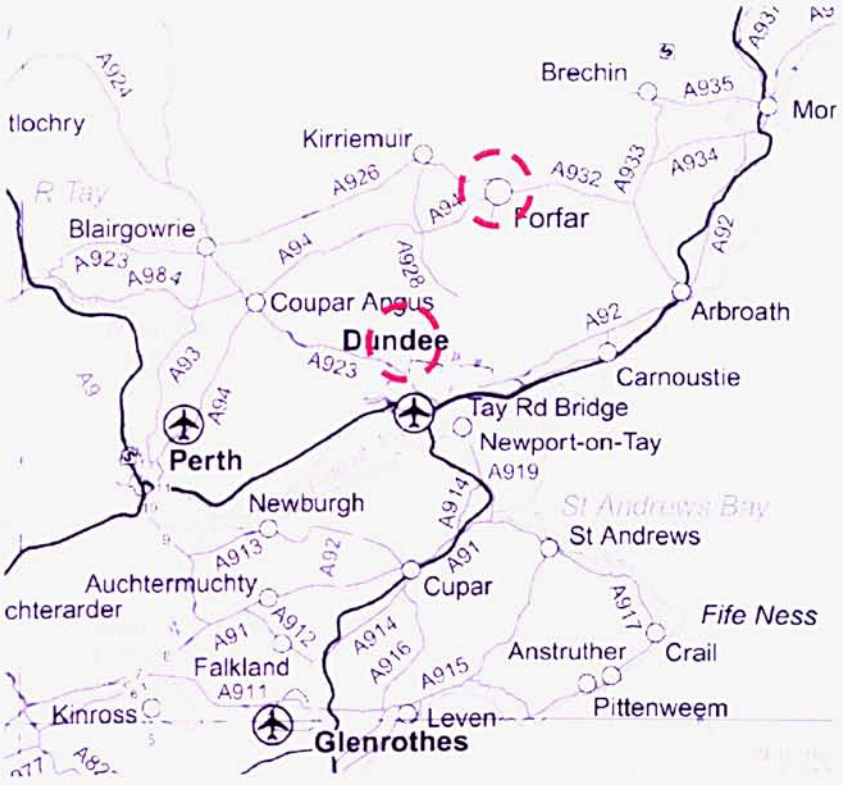

Figure 4.1: Overview of test catchments (circled)

4.2. Dundee Catchment Details

This system has been the subject of many investigations and has therefore been described various times by other researchers (Ashley *et al.*, 1992; Ashley, 1993; Ashley, 1994; Wotherspoon, 1994; Coghlan, 1995; Rennet, 1995 and Arthur 1996). Most of the gravity sewerage system within the City of Dundee is comprised of ovoid sewers; with the Murraygate interceptor (the largest section in the system) having a diameter of up to 1.8m. The system originates from the nineteenth century

and although some sections have undergone rehabilitation there are still some sections where the fabric of the sewer is badly eroded. The combined drainage system historically discharged into the Tay Estuary via more than 30, mostly untreated, outfalls. The completion of the £100m PFI Tay Wastewater scheme in the autumn of 2001 has now resolved the issue of poor water quality within the estuary. This two-year project involved the construction of a 35km pipeline running between Invergowrie (a village on the western outskirts of Dundee) and Arbroath, seven underground pumping stations and a new state-of-the-art treatment plant at Hatton, near Carnoustie.

The drainage system in Dundee is rather complex due to the presence of over 250 control gates and there are usually a number of loops, bypasses and bifurcations in operation in the main system as well as the secondary network. The central area of Dundee experienced flooding approximately every 2 to 3 years prior to the removal of sediment in 1990. The area does still encounter localised flooding in the lower terrace as flows from the steeper catchments around the city centre are rapidly conveyed into the relatively flat lower lying central area. In cases where the combination of an intense storm with a high tide renders the tidal outfalls unable to convey the flows out of the system, backing up, surcharge and eventually flooding occurs (Arthur, 1996). The Murraygate interceptor sewer was utilised for this study for a number of reasons:

- The relatively easy access and safe working area afforded by the site due to its location within a pedestrian precinct.
- The presence of both 'Type A' and 'Type C' sediments (as categorised by Crabtree, 1989 – see Table 2.1).
- The degree of control offered by the presence of gates in the study section.
- The site had historically yielded useful data in other research studies as previously mentioned.

4.2.1. Murraygate Interceptor Sewer Details

The main Dundee interceptor sewer drains the higher catchments of the Law and the Balgay Hills via steep trunk sewers. For the purpose of hydraulic modelling the central catchment has been considered as a number of sub-catchments owing to the

complexity of the system. This is largely due to the numerous control gates in the system; many of which are half gates that can act as internal overflows during storms. The catchments contributing to the interceptor sewer are listed in Table 4.1.

Sub Catchment	Population (× 1000)	Area (ha)	Land Use
Perth Road	4.800	164.9	T, I, P
Constitution Road	2.900	64.6	T, H, I, S, P
Hilltown	1.900	30.3	T, H, I, P
Dens Road	11.500	236.4	T, H, I, S, P
Dura Street	1.600	37.5	T, H, I, S, P
Albert Street	2.200	11.2	T, H, I, S, P
Hawkhill	0.280	6.8	T, I, P
Blackness	1.300	20.2	T, H, S, P
Polepark	5.800	159.9	T, H, I, S, P
Guthrie Street	0.420	19.3	T, I
Lochee	0.200	14.2	T, I, S, P
City Centre	≈ 5.300	≈ 25	T, S, P
Totals	38.200	790.3	-
Land Use: T – Tenements/High Rise H – Housing I – Light Industry/Commercial S – Retail P – Park/Permeable Areas			

Table 4.1: Catchments contributing to Dundee interceptor sewer

The total flow in the catchment is approximately 6875 m^3/day (4479 m^3/day domestic and 2406 m^3/day industrial). Due to the transient nature of the population in the city centre retail area it should be noted that both the population and the flow vary on a micro and macro scale (Arthur, 1996).

4.2.2. Interceptor Sewer Study Section

The chamber at the head of the interceptor is a bifurcation where flows from the Overgate and High Street trunk sewers mix prior to being passed forward. The setting of the half gate situated at the downstream end of the chamber determines whether the flow enters the Dock system or is conveyed into the interceptor sewer. Although the flow is routed through the interceptor sewer under normal operational conditions, during storm events excess flow may enter the Dock System, as the gate acts as an internal overflow. A 6m long silt trap is located downstream of the gate and occupies the full width of the sewer section. A 1.5m section of the sewer upstream of the silt trap has a flat invert for the whole width of the pipe in order to

aid maintenance of the silt trap. The current study used a 6m long test rig which occupied the full width of the sewer section and was constructed for a previous research study (Arthur, 1996). The rig spanned the silt trap and met the upstream and downstream sewer section as closely as possible, so that the ambient flow patterns were affected as little as possible. The rig consisted of a Glass Reinforced Plastic (GRP) flume that was manufactured to the actual shape of the ovoid sewer with a moulded 'brick' surface in order to replicate the existing sewer roughness and flow regime as closely as possible. A drawing of the test rig is shown in Figure 4.2 without dimensions for clarity.

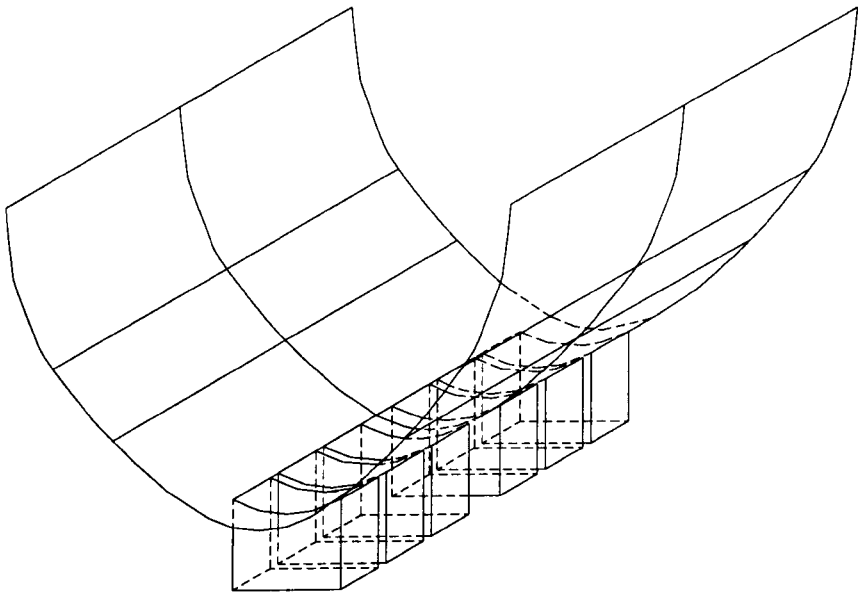

Figure 4.2: Invert trap test rig used for bedload collection

Sedimentation has been a historic problem with deposits in excess of 300mm (~16% of the pipe height) being encountered. The total length of the interceptor is approximately 2500m from head to outfall, and the sewer, which is situated 5m above high tide level on a former river terrace, has an average gradient of 0.07%. The study section has an average gradient of 0.04% although it should be noted that localised backfalls (possibly due to ground settlement) are present along the length as evident in Figure 4.3.

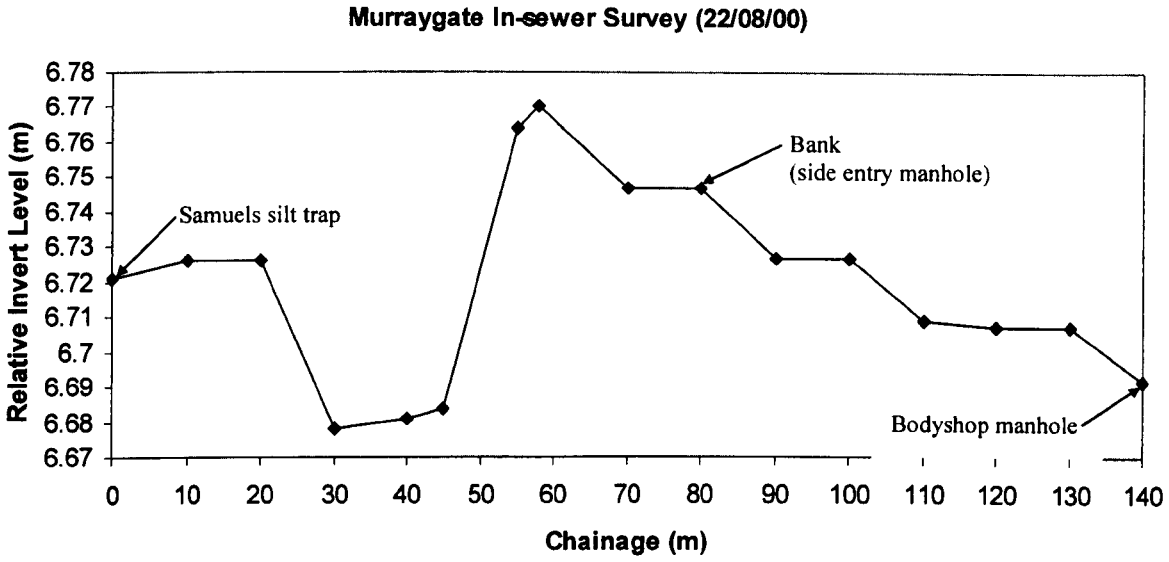

Figure 4.3: Longitudinal profile Murraygate interceptor sewer study section

A plan survey of the test length was also undertaken on 21/08/00 as shown in Figure 4.4.

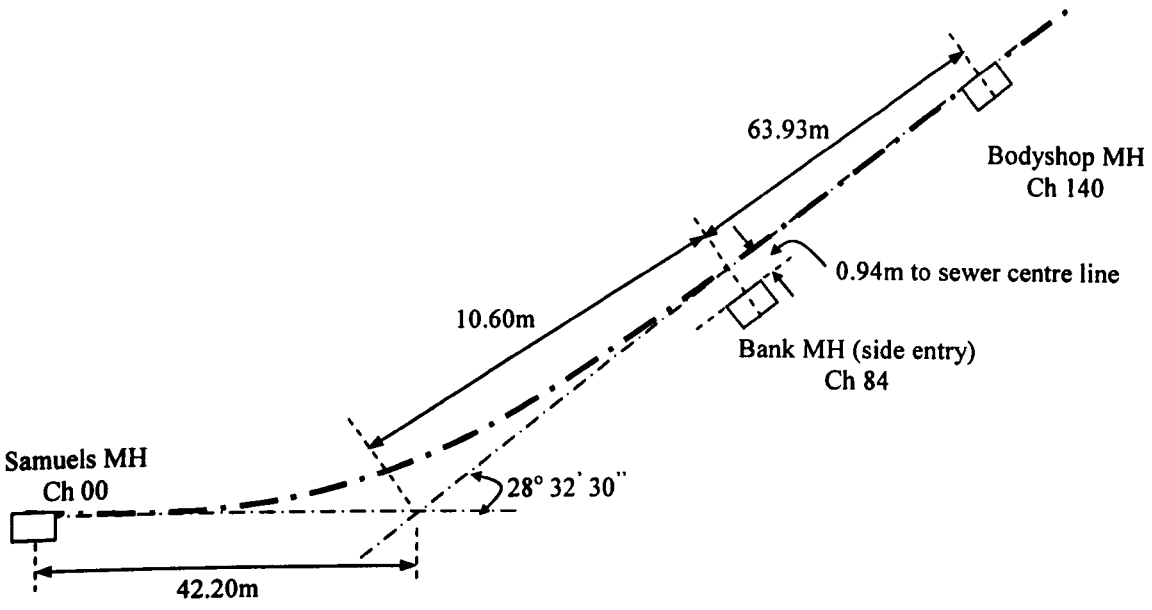

Figure 4.4: Top survey of Murraygate study section (21/08/02)

The study section location is shown in Figures 4.5 and 4.6.

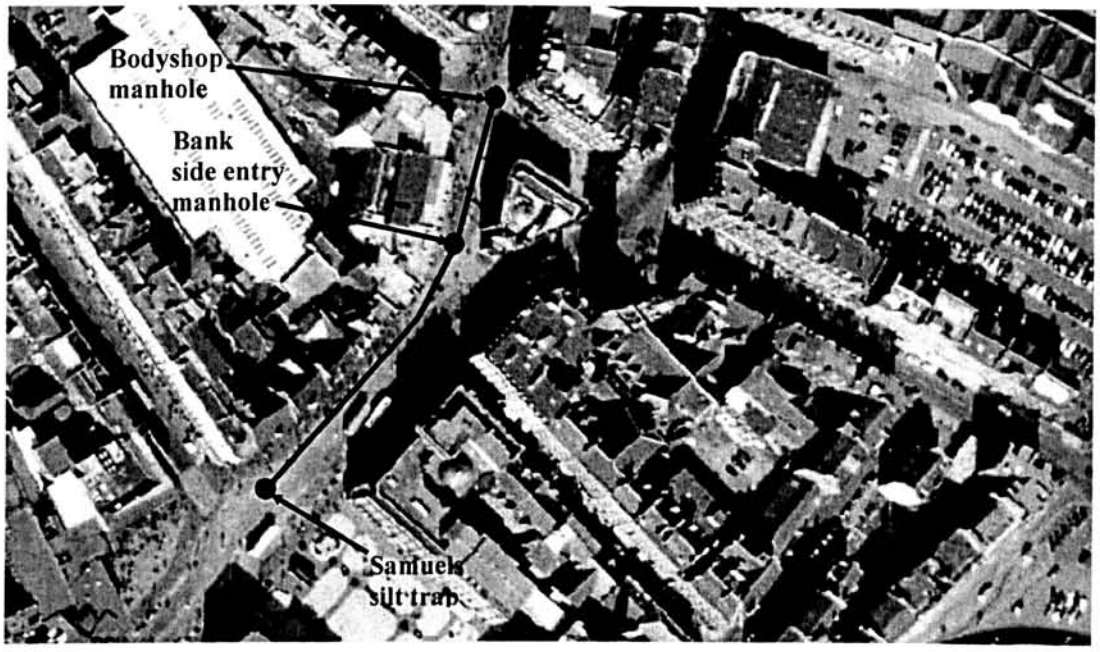

Figure 4.5: Aerial view of city centre pedestrian precinct with test section highlighted

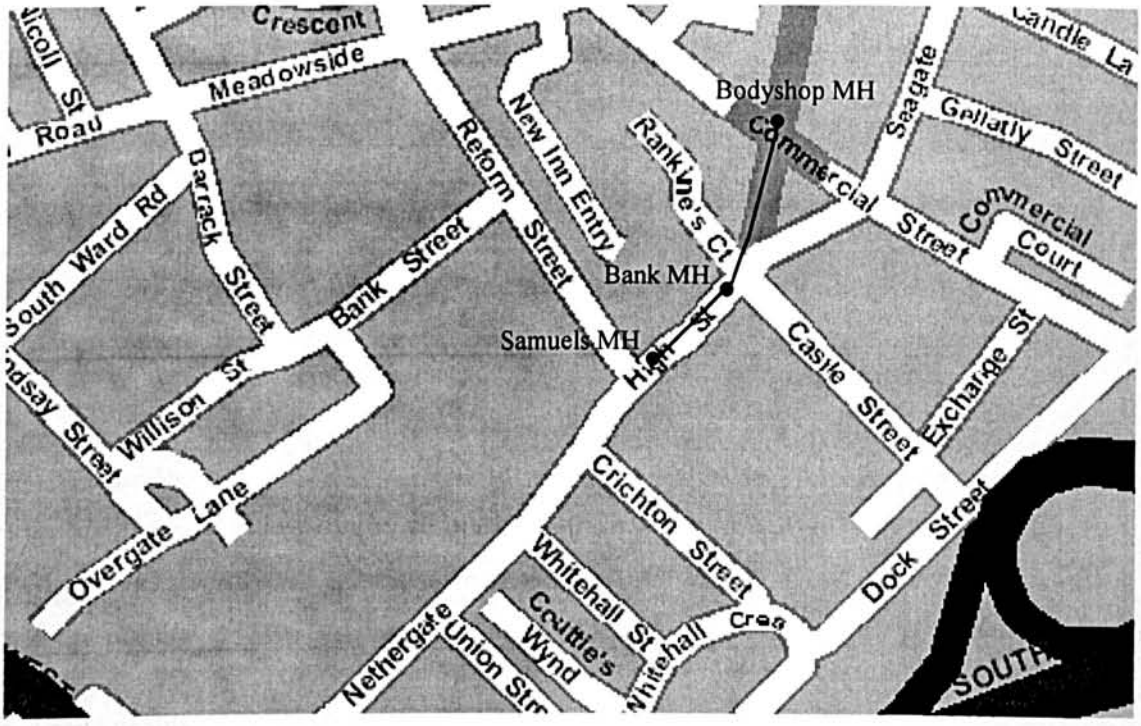

Figure 4.6: Dundee City centre street map with test section highlighted

Reproduced from (2003) Ordnance Survey map with the permission of the Controller of Her Majesty's Stationary Office, © Crown Copyright NC/03/16545.

4.2.3. Study Section Contributing Catchments

The catchments that contribute to the study section are described in Table 4.2.

Sub Catchment	Population (× 1000)	Area (ha)	Land Use
Hawkhill	0.280	6.8	T, I, P
Blackness	1.300	20.2	T, H, S, P
Polepark	5.800	159.9	T, H, I, S, P
Guthrie Street	0.420	19.3	T, I
Lochee	0.200	14.2	T, I, S, P
City Centre	≈ 5.300	≈ 25	T, S, P
Totals	13.300	245.4	-
Land Use: T – Tenements/High Rise H – Housing I – Light Industry/Commercial S – Retail P – Park/Permeable Areas			

Table 4.2: Catchments contributing to the Murraygate study section

4.2.4. Murraygate Measured Parameters

In order to assess the hydraulic characteristics of the study section, the pattern of sediment movement (erosion and deposition) within the pipe and the physical characteristics of the sediment, the principal measurement parameters used in the study are listed in Table 4.3 (see Chapter 3 for detailed description of these techniques).

Parameter	Used in Evaluating
Hydraulic gradient	Flow rate Roughness/friction parameters Shear stresses
Velocity distribution	
Bed depth: - time-varying at 3 points - at 1m intervals at discrete time intervals	Erosion/deposition history Sediment 'type' 'Strength/Yield point' of deposit Solids 'release' characteristics
Sediment physical characteristics: - density - particle size distribution - % organics - moisture content	
Sediment rheology	
Bed stress/concentration curve (Erosion meter)	
Sewage suspended solids concentration	Quantification of suspended solids in transport
Sewage physical characteristics: - fall velocity - particle size distribution	Characteristics of solids in transport under varying hydraulic conditions
Bedload	Quantification of near bed solids in transport

Table 4.3: Murraygate measured parameters

4.3. Forfar Catchment Details

The town of Forfar, situated in Eastern Scotland, approximately 21km north of the city of Dundee, is the main settlement in the county of Angus. It originated from a small market area and developed in a radial pattern from the central High Street during the 19th century. With a population of 12,961 (General Register for Scotland, 2001) between 1984 and 1998, development was mainly concentrated in Westfield and Northampton Place (in the Southwest), Tufbeg (to the Northwest) and Lilybank (to the east). Further development was limited due to lack of capacity in the sewerage system and the redevelopment of existing areas was encouraged. The town was designated a conservation area in 1972 (Angus Council – Finalised Angus Local Plan, 1999). Industry in the area is mainly limited to Orchardloan Trading Estate and the Strathmore Mineral Water Company facilities.

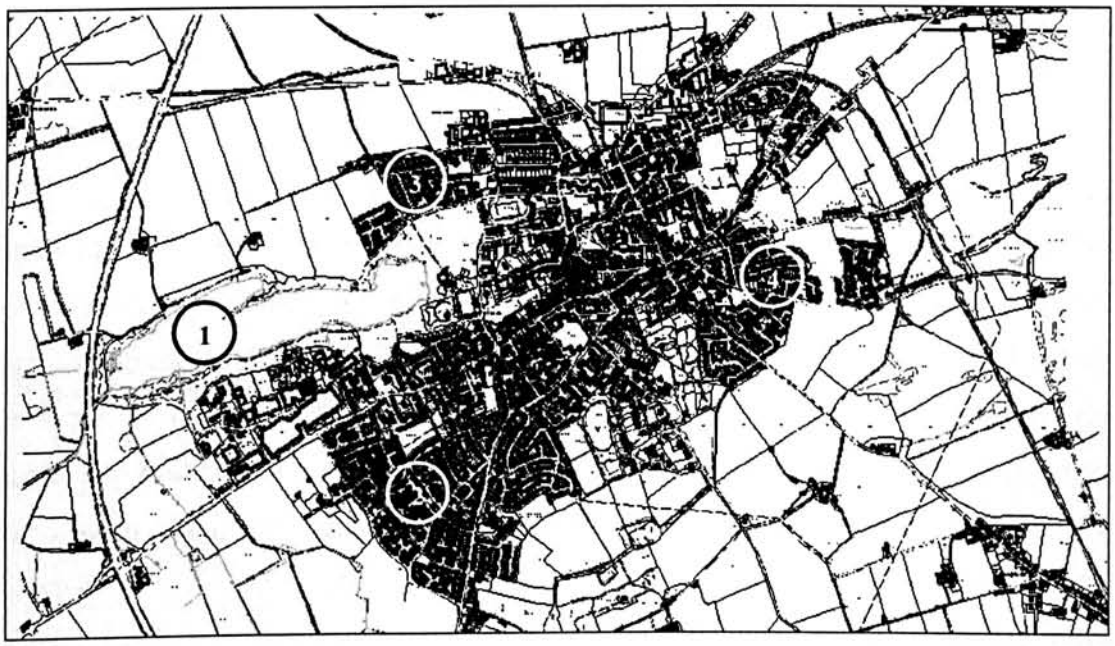

Figure 4.7: Overview of Forfar catchment

(1: Forfar Loch; 2: Westfield & Northampton Place; 3: Tufbeg, and 4: Lilybank)

Two culverted burns (Treacle Burn and Hornie Burn) originate in the surrounding hills and discharge into Forfar Loch, which is located on the west side of the town; with the natural drainage running from east to west (Hyder Consulting, 2002). The Loch is 1.5km long and 9 metres deep and discharges into Dean Water, which flows

past Glamis en route to the River Isla and the sea. The north bank of the Loch is a haven for wildlife.

The sewerage network in Forfar has developed in a number of ways as the town has grown. The southern catchment is served by a combination of separate, combined and dual manhole systems, which drain to the Wastewater Treatment Works (WwTW) and to Forfar Loch. The northern catchment consists of separate and combined systems draining to the Queenswell Road Pumping Station, which transfers flows to the WwTW. The network contains overflows that drain excess flow to Forfar Loch via the culverted watercourses. The sewerage catchment includes the outlying settlements of Kingsmuir, Padanaram and Lunanhead, the resident population, including these villages, is 14,800 (Hyder Consulting, 2002).

Forfar Wastewater Treatment Works was originally constructed in 1953 and consisted of a settlement tank, filter bed and a humus tank. As the town expanded, the council provided separate drainage systems to reduce the load on the plant. In 1967 a substantial section of the trunk sewer was replaced. In the early 1970's an activated sludge process was introduced and secondary settlement tanks were added. By the late 1980's the WwTW could not sustain any further domestic and industrial inputs, which restricted development. The plant was seen to be complex and ageing and only met consent standards 60% of the time. There was also local concern over algal blooms in the Loch and in the Dean Water and it was discovered that significant phosphorus and nitrogen reserves had built up in the sediment in the Loch. In 1994, under the Urban Waste Water Treatment (Scotland) regulations, Forfar Loch was designated 'sensitive'. Babcock Water Engineering Ltd were appointed in 1997 to construct a £5.2 million new treatment works, to address some of these problems.

In 1996, NoSWA carried out an investigation to determine the improvements that were required for the Forfar sewer system. The outcome was a phased improvement strategy to be implemented in three stages. Phase 1 involved the removal of two overflows and upgrading of one other. The programme also involved the construction of silt traps and a new pumping station and storage facility at Queenswell Road. Phase 2 involved the construction of a new sewer along

Queenswell Road. The third phase will involve the construction of two storage tanks at Myre Road and Academy Street. Phases 1 and 2 have been completed, while Phase 3 is proposed for 2004-5.

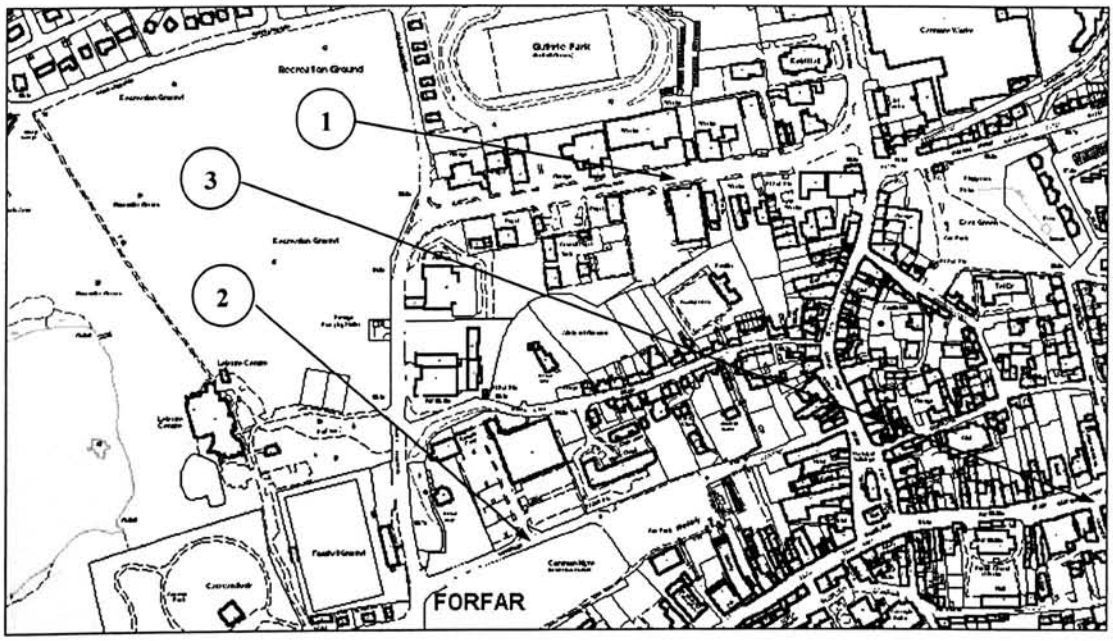

Figure 4.8: Locations of recent Forfar sewerage infrastructure upgrades
(1: Queenswell Road; 2: Myre Road, and 3: Academy Street)

4.3.1. Sedimentation Problems

The upgrading of Forfar WwTW has been at the core of the strategy for addressing the receiving water sensitivity for the adjacent loch. The 600mm and 900mm combined sewers that feed the WwTW via a pump station have shallow gradients and sedimentation therein is ubiquitous, with recurrent deposit depths of 50% of the bore. In an attempt to offset the sedimentation problem and potential effects on the WwTW, sediment traps were constructed on each of the two sewers at locations conveniently identified for ease of construction.

Since construction, it has been found that the trap on the smaller sewer fills rapidly (days) with organic solids and that the larger sewer fills within a few weeks, also with a considerable amount of organic solids. Currently, the flows in the smaller sewer are slow due partially to tree root blocking. In addition to the sediment

problem, there are also rapid pulses in pH (low to high) during wet weather flows (Hyder Consulting, 2002).

4.3.2. Forfar Study Section

This 600mm sewer was chosen due to the shallow gradient and organic deposits as it was believed these conditions were suited to the inducement of a solids flush via an adjacent water hydrant. The study section from the hydrant injection point through to the sampling sites (Site 1 – caravan site manhole, and Site 2 – football pitch manhole) is shown in Figure 4.9.

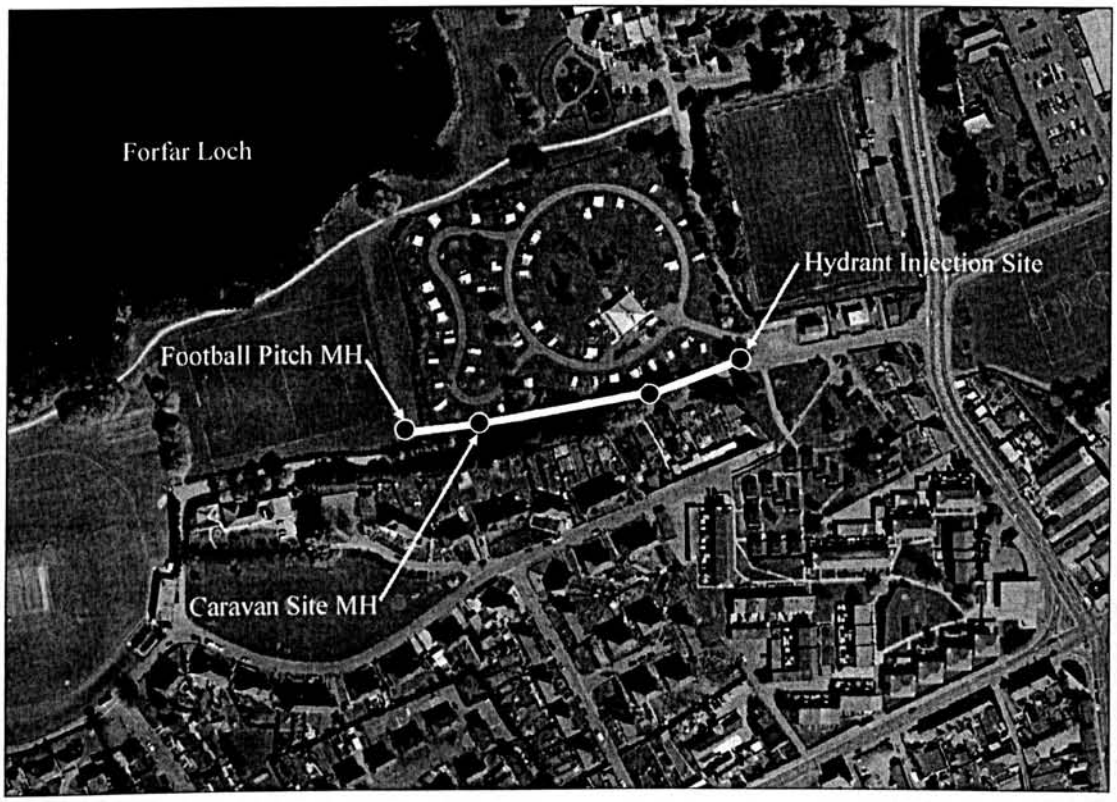

Figure 4.9: Forfar study section (600mm pipe)

The study section was 178m in length with an average invert gradient of 1 in 2254 (0.044%); the individual pipe details are shown in Figure 4.10.

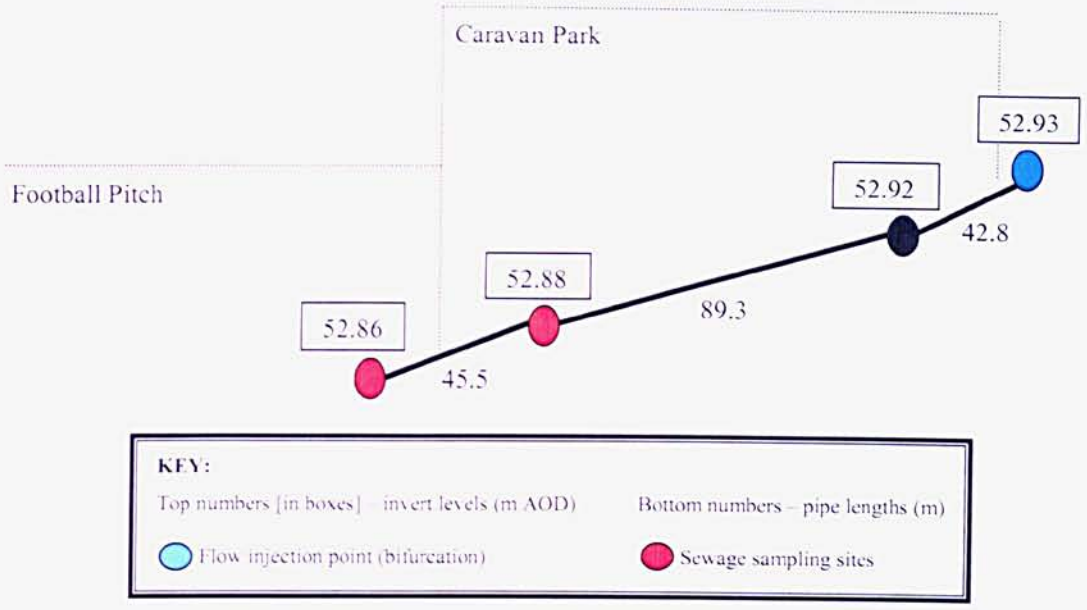

Fig 4.10: Schematic of Forfar study section

4.3.3. Forfar Measured Parameters

As with the Murraygate study section, a range of parameters was measured. The hydraulic characteristics of the study section, the pattern of sediment movement (erosion and deposition) within the pipe and the physical characteristics of the sediment were assessed using various measurement parameters as listed in Table 4.4.

Parameter	Physical Characteristics
Velocity distribution	Flow rate Roughness/friction parameters Shear stresses
Bed depth in manholes before and after flush test	Erosion/deposition history Sediment 'type' 'Strength/Yield point' of deposit Solids 'release' characteristics
Sediment physical characteristics: - density - particle size distribution - % organics - moisture content	
Sediment rheology	
Bed stress/concentration curve (Erosion meter)	
Sewage solids concentration	Quantification of suspended solids in transport
Sewage physical characteristics: - fall velocity - particle size distribution	Characteristics of solids in transport under varying hydraulic conditions

Table 4.4: Forfar measured parameters

4.4. Transport Mode

There was no means available for the collection of bedload transport data in Forfar as the retrofitting of sediment collection traps in the sewer invert was obviously not a viable option. Due to this constraint the field tests were designed with the material transport mode taken into account. The transport of sediment in pipes with clean and deposited beds have been extensively studied in laboratory pipe flume studies. The results of such studies at Hydraulics Research in the UK provided the grounding for the current methods employed for the design of sewers to control sediment problems. Figure 4.11 illustrates the various transport regimes that were observed in circular pipe flows.

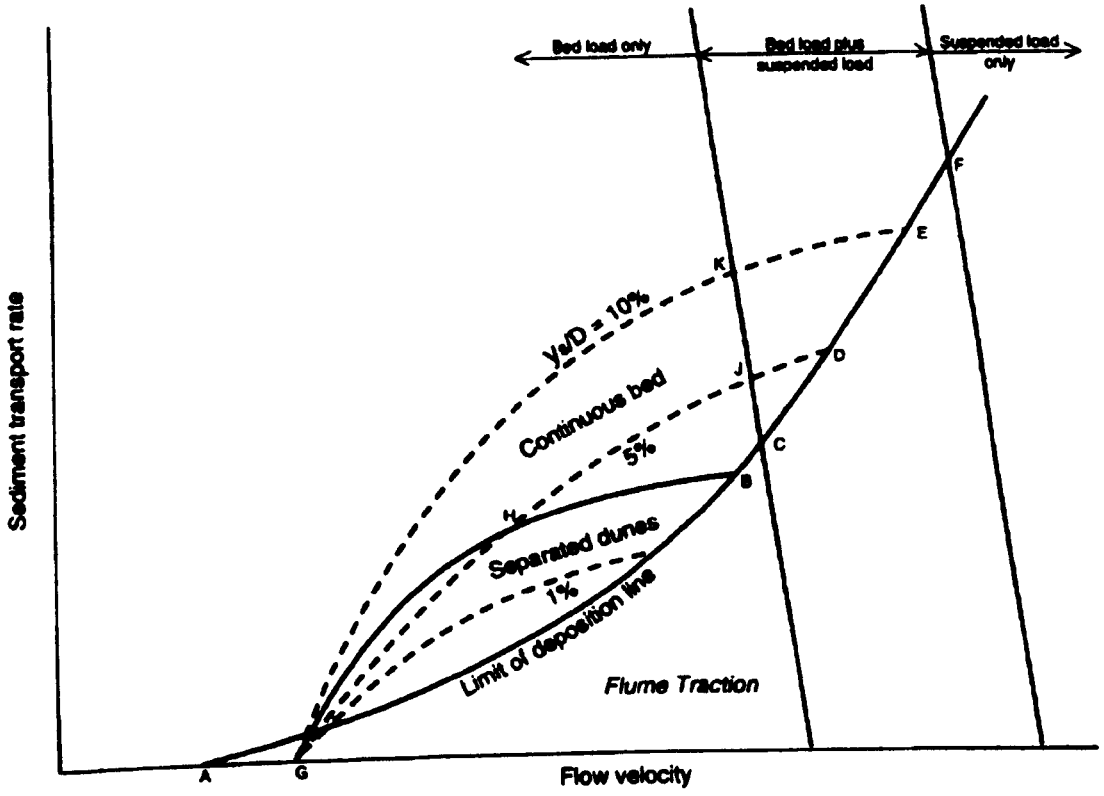

Figure 4.11: Diagrammatic representation of sediment transport regimes in pipes
(Source: Ashley *et al.*, 2003)

A mass of sediment particles is said to be in a state of suspension if eddies of fluid turbulence keep it above the bed. Bagnold (1966) reasoned that suspension occurs when the upward directed components of the turbulent velocity fluctuations (w'_{up}) exceed the fall velocity of the particles (w_s). The criterion for a full suspension is based on the sedimentation parameter, η:

$$\eta = \frac{w_s}{\kappa u_*} \qquad (4.1)$$

When discussing different sewer sediment transport modes Ashley and Verbanck (1996) gave an approximate classification system adapted from fluvial channels (Raudkivi, 1990), based on the sedimentation parameter, η.

bed load	$5 < \eta < 15$	
suspension	$\eta \leq 3$	(4.2)

Ashley *et al.* (1994) successfully used field measurements for the transport of material collected in bed load traps in combined sewers to show that the definition of Equation 4.2 for suspended and bed loads appeared to correspond with the material sampled from suspension and in the traps.

In general, for a full suspension, $\eta \leq 3$ and, based on diffusion considerations, all conditions for which $\eta < 1$ correspond to flow situations where a given particle released in the flow will be unlikely to enter the constant-stress layer close to the bed (Batchelor, 1965). The threshold value for suspended load expressed by equation 4.2 is identical to that recommended in a revised UK sewer design method (Ackers *et al.*, 1996).

The sedimentation parameter (η) was evaluated for the hydraulic conditions generated during the flush tests carried out for this study. The mean fall velocity of the Forfar bed material was evaluated as 0.69 mm/s, with a maximum value of 3.22 mm/s recorded for bed material collected prior to flush Test C on 09/07/01. Even using the maximum value of w_s in conjunction with the lowest generated u_* value (0.018 m/s, also from Test C) the resultant value for the sedimentation parameter was less than unity. As the test conditions corresponded to situations where $\eta < 1$ the material in transport was deemed to be travelling as a full suspension (with no bedload transport occurring). Consequently, it followed that evaluation of the suspended load was representative of the total load in transport, and thus application of the Ackers (1991) total load relationship should provide representative results of the suspended loads observed during the Forfar tests.

The results obtained from the investigations carried out in the Murraygate test section in Dundee are discussed in Chapter 5 while Chapter 6 presents the results of the hydrant flush tests that were conducted in the Forfar test section.

Chapter Five – Murraygate Field Investigations

5.1. Introduction

The purpose of this chapter is to describe initial investigative work that was carried out in the Murraygate catchment. Originally it was intended to carry out all the field studies for this project within this catchment. Ultimately the investigations in the Murraygate were abandoned due to the unsuitability of the hydraulic regime for generating flush events. Thus, the analytical work presented in this chapter only pertains to the preliminary findings of this study and does not feature in the modelling strategy for solids flushes in combined sewers as described in Chapter Seven. Eventually the decision was taken to abandon the fieldwork in Dundee and transfer the investigations to a more suitable site in Forfar, approximately fifteen miles north east of Dundee. Although the data collected from the Murraygate interceptor sewer was not actually used in the development of the modelling strategy it nevertheless provided a valuable insight into some of the phenomena related to sediment erosion and transport within a combined sewer. This chapter provides a summary of the findings of these investigations.

5.2. Determining the First Foul Flush Components for a Storm Event

Using the concepts outlined earlier in Chapter 2 an individual event that was captured by Arthur (1996) in the main Dundee interceptor sewer on 09/11/94 between 05.00 and 07.15 (GMT) (see Figure 5.1) was analysed to determine how the individual components each contributed to the total solids load within the flush. It was decided to use the Gupta and Saul (1996) definition to define the first foul flush for the event. That is, "...that part of the storm up to the maximum divergence between the cumulative percentage of TSS and flow plotted against the cumulative percentage of time", as shown in Figure 5.1.

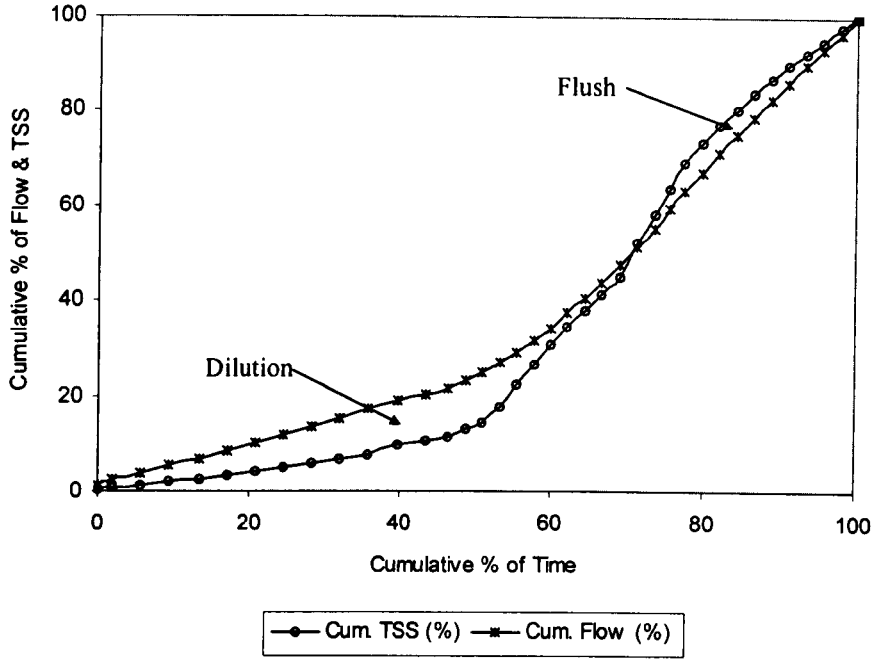

Figure 5.1: Parameters used for the definition of the first foul flush (09/11/94)

By using the method described by Section 2.8 and Figure 2.3, examination of Figure 5.1 confirmed that, according to the Gupta & Saul (1995) definition, the TSS load in the flush comprised approximately 78% of the cumulative total load in the event. The cumulative total load during the event (05:00 - 07:15) was determined from the product of the cumulative flow and the cumulative solids in transport as 426kg, hence:

$$TSS_{FLUSH} = 0.78 \times TSS_{EVENT}$$
$$= 0.78 \times 426$$
$$= 332 \text{ kg}$$

Hence the "missing" solids that could be attributed to the erosion of the underlying bed (BES_{WET}) were determined as follows:

$$TSS_{FLUSH} = TSS_{DWF} + NBS_{DWF} + \mathbf{BES_{WET}}$$

5.2.1. Solids Transported During Dry Weather Flow (TSS_{DWF})

This value was estimated from an average dry weather flow TSS concentration of 90mg/l taken from previously recorded data (Arthur, 1996). This TSS concentration was combined with an average flow of $0.04m^3/s$ throughout the duration of the storm; i.e. $TSS_{DWF} = TSS \times Q \times t$, in order to calculate the final value:

$$\mathbf{TSS_{DWF}} \approx 29kg$$

5.2.2. Solids Transported Near the Bed – (NBS_{DWF})

This figure was determined using an average near bed solids concentration of 10mg/l for this event as previously determined by Arthur (1996):

$$\mathbf{NBS_{DWF}} \approx 14\ kg$$

5.2.3. Solids Eroded from the Bed – (BES_{WET})

Assuming that the "missing" solids could be accounted for by erosion of the underlying bed, they were determined as follows:

$$\mathbf{BES_{WET}} = TSS_{FLUSH} - (TSS_{DWF} + NBS_{DWF})$$

$$\mathbf{BES_{WET}} = 332 - (29 + 14) = 289kg$$

5.2.4. Relative Contributions to the Foul Flush

The allocation of the total solids load for this first foul flush event (TSS_{FLUSH}) may be summarised as follows:

Component	% of Total
TSS_{DWF}	9
NBS_{DWF}	4
BES_{WET}	87

Table 5.1: Example of TSS loads in a foul flush event

This approach can be used to define the 'typical' sources of solids within a 'first foul flush' event illustrating the domination of bed erosion in terms of contribution to the total solids load. Although the near bed solids comprise a relatively minor part of the total solids load it must also be taken into account that, as reported by Ashley *et al* (1999), the biochemical load within a flush event is not so distributed, with the near bed solids component comprising a much higher proportion.

5.2.5. Volume of Eroded Bed

For this event it was established that the mass of 'missing' solids was approximately 289kg. Therefore by assuming a constant bulk density one could equate this to a volume of bed required to be eroded to produce this quantity of solids:

Bulk density of Murraygate deposit material ≈ 1500 kg/m^3

$\Rightarrow$ Required volume of eroded bed = BES_{WET}/Bulk density

$= 289/1500$

$= 0.192$

≈ 0.2 m^3 of bed

5.2.6. Determination of Contributing Pipe Length

If the overall volume of eroded bed was estimated as 0.2m^3, this information could then be used to calculate the depth of bed eroded in order that a contributing pipe length could be determined.

Volume of sediment eroded = 0.2m^3

Average bed width = 0.5m (Dundee interceptor sewer)

Depth of erosion = 10mm

Contributing length = volume of sediment eroded/(bed width x depth of erosion)

$= 0.2/(0.5 \times 0.01)$

$= 40$m

This approach would then suggest that a contributing pipe length of approximately 40m would be required to 'yield' the necessary amount of solids.

5.2.7. *Possible Inaccuracies within the Concept*

When making use of the approach outlined in section 5.3 several simplifications inherent within the procedure need to be taken into account:

Due to the attenuation of the storm wave as it travels along the sewer reach the same depth of sediment will not be eroded along the bed length. As a result this introduces an immediate degree of error into the concept, as the contributing pipe length will be under-estimated. In addition, as reported by Skipworth (1996), there will be variability in the erosional resistance of the deposit material with depth.

The uncertainties of this method are compounded by the fact that spatially varying flows were also not taken into account. In addition to the attenuation of the storm surge, the flows in different sections of the pipe prior to the arrival of the wave would differ in magnitude, and this would also cause varying rates of erosion along the sewer reach, i.e.:

$$FLOW_{TOT} = FLOW_{AMB} + FLOW_{WAVE}$$

This would mean that as the storm wave progresses down the pipe then, at a 'snapshot' in time, the total flow at that particular point will comprise the original flow ($FLOW_{AMB}$) plus the 'extra' flow from the storm wave ($FLOW_{WAVE}$). Apart from the fact that the storm wave would be subsiding (temporal variation) the original flow would also be different in particular sections in the pipe (spatial variation) so that the total flow will be affected by both temporal and spatial variations, leading to varying degrees of erosion along the length of the sewer.

5.3. Further Findings of the Murraygate Research

In the event of a flush, given the polluting potential of the material moving near the bed, it was decided to try and collect near bed solids samples during dry weather. It was hoped that characterisation of these solids would aid the understanding of the processes involved with the erosion and transport of the NBS and whether they moved as a true suspension or as a bedload. Unfortunately, due to the hydraulic characteristics experienced in the test section, it was not possible to collect reasonable amounts of sample for analysis, even by leaving the collection traps in the sewer for a number of hours. Although not enough solids could be collected for any detailed analysis to be carried out, for the solids that were collected an overall mean bulk density of 1090 kg/m^3 was recorded; which was comparable with the Arthur (1996) average value of 1096 kg/m^3 for the bulk density of NBS collected at this site.

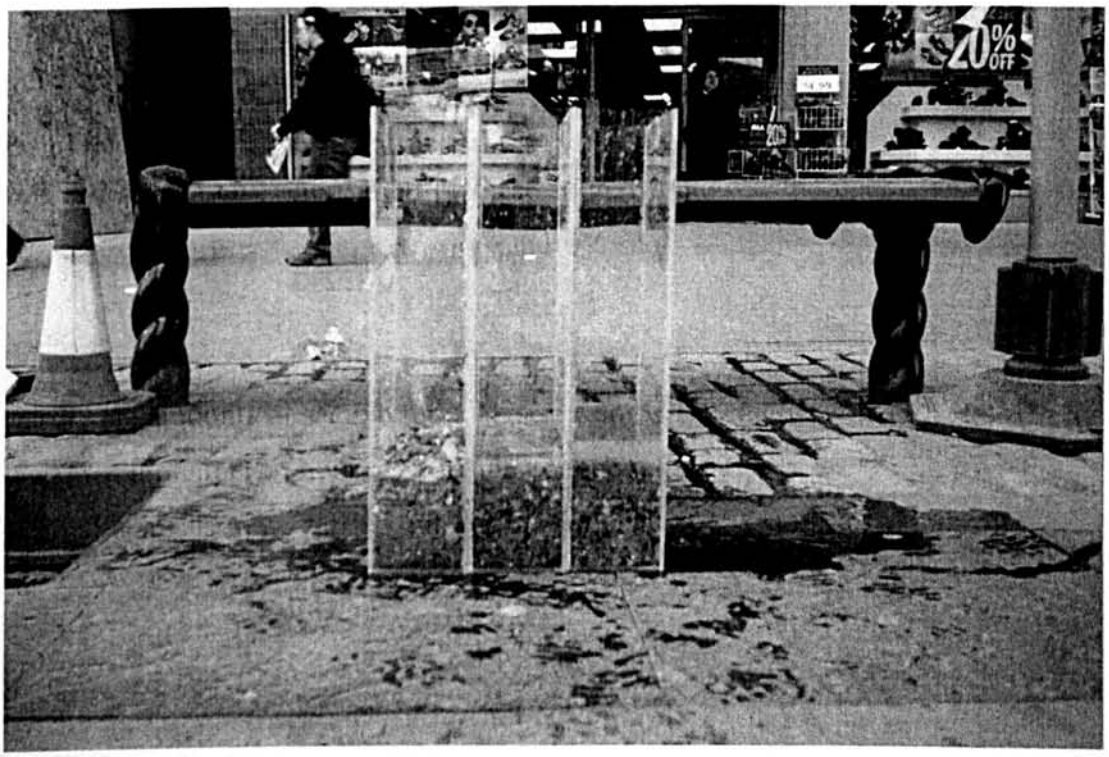

Plate 5.1: Near bed solids collection in Murraygate interceptor sewer

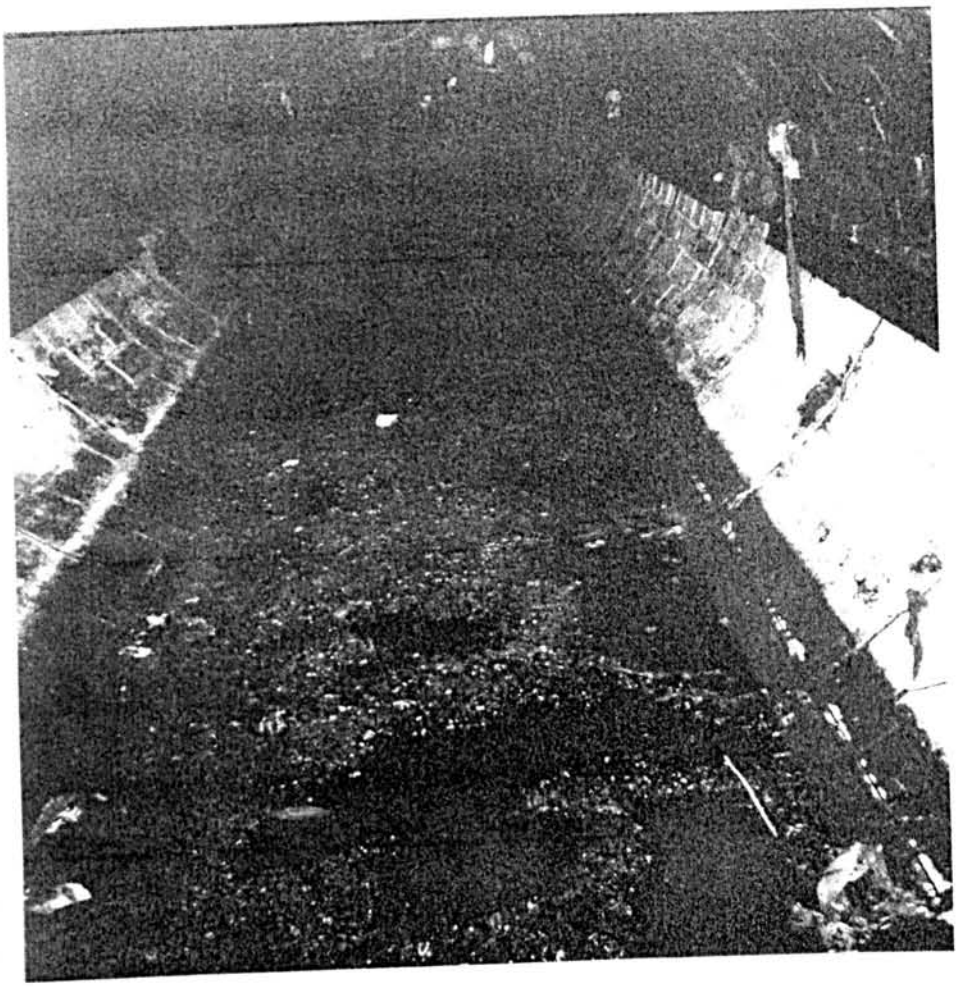

Plate 5.2: Samuels invert trap cover

In addition, the problem of the hydraulic regime in the Murraygate also manifested itself in an inability to generate reasonable amounts of suspended solids from flush events at this location.

5.3.1. Murraygate Hydraulic Regime

The fieldwork was undertaken in a 150m length of the main interceptor sewer in Dundee with an average gradient of 1:2500 and a gradient of 1:500 in the downstream section (see Figure 4.4). The average dry weather flow velocity in the test section was ≈0.35 m/s, which could be elevated to ≈0.5 m/s with the introduction of a hydrant input. Hydraulic analysis has shown that the flow regime was controlled by downstream conditions and was always sub-critical for free surface conditions (Ashley, 1993). The sewer was instrumented for the measurement of hydraulic

gradient, and via bed traps, for near bed solids transport rate measurement, with additional instrumentation installed to monitor bed erosion. Sediment built up in the study sewer over a period of more than a year, until an equilibrium depth was reached for conditions prior to August 2000. The incoming flow from a confluence at chainage 150 acted as a downstream control so that, when extra flow was introduced upstream, the water level would rise but the velocity would actually decrease, resulting in negligible erosion. This was verified by sampling programs carried out under both wet weather conditions and simulated storm events where extra flow was introduced into the upstream manhole via an adjacent water hydrant. Figure 5.2 shows how the stage discharge altered with the closure (by a gate structure) of the incoming connection downstream at chainage 150.

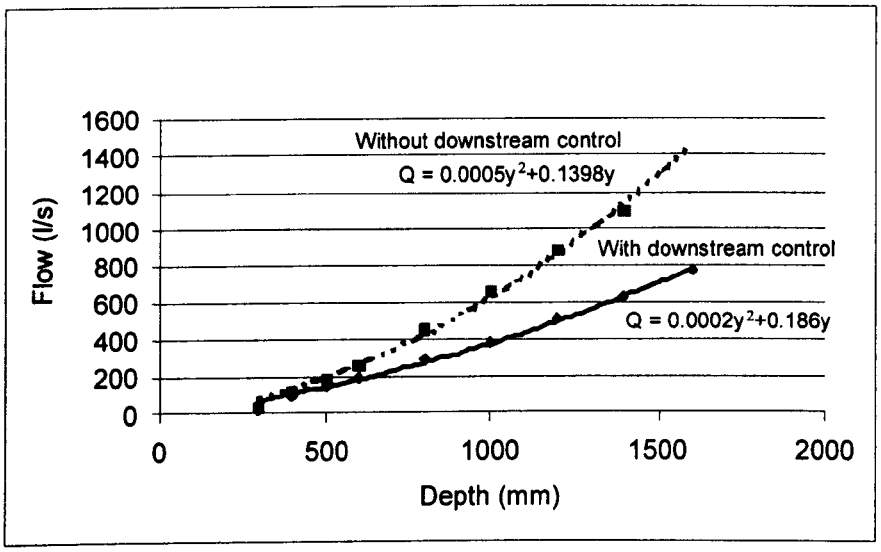

Figure 5.2: Stage discharge with/without downstream control

Previous fieldwork studies (Wotherspoon, 1994) have shown the bed shear (τ_b) in this sewer to vary between approximately 0.5N/m^2 in dry weather to approximately 1.5N/m^2 during periods of elevated flows. By carrying out manual depth surveys it was possible to estimate the bed erosion rate over a period of time. Figure 5.3 illustrates the movement of the bed during a twenty-week period, following the removal of the main downstream hydraulic control on 24 April 2000.

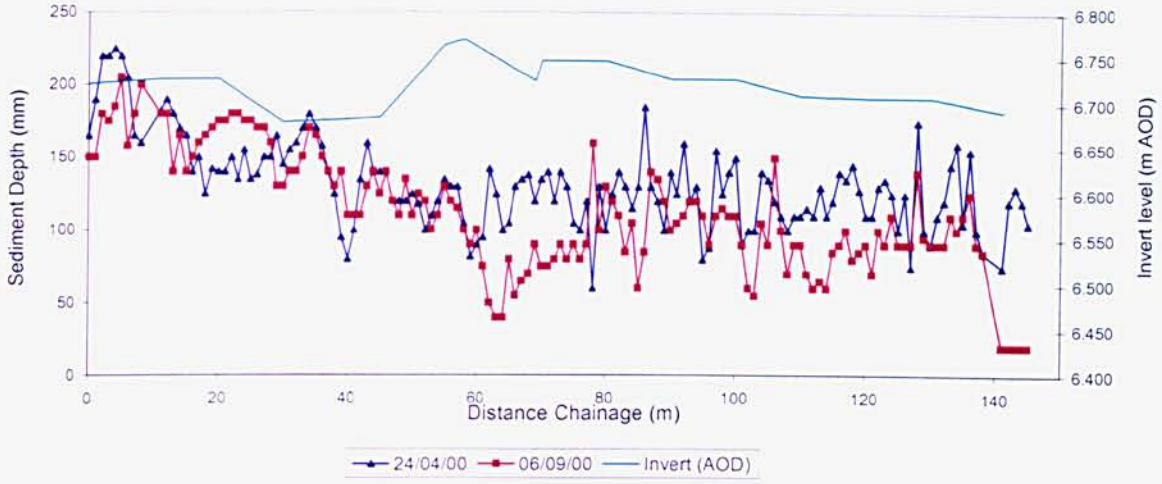

Figure 5.3: Monitoring of deposit depth in Murraygate

5.3.2. Dynamic Monitoring of Deposit Depth

Figure 5.4 illustrates the sediment movement as a result of extra flow from the hydrant input that was injected to simulate a flush event. It can be seen that the bed under the upstream monitor was depleted and the bed under the downstream monitor (3m further downstream) increased as the solids moved downstream.

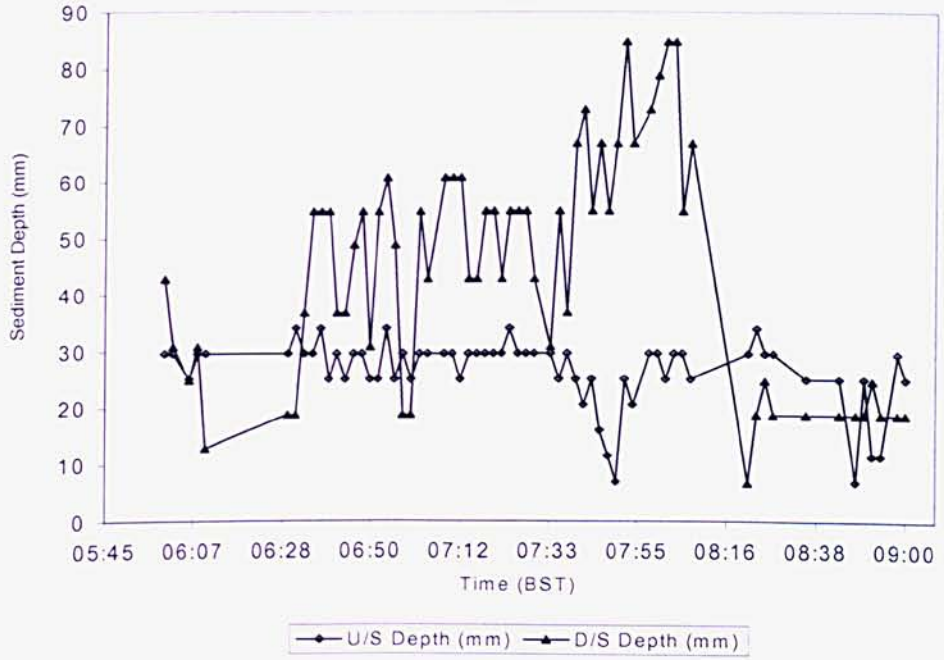

Figure 5.4: Hydrant induced sediment movement in the interceptor – sonar bed depth results (09/10/00)

5.3.3. *Rheological Properties of Murraygate Deposits*

Further to the results of the bed depth monitoring, samples of the deposits within the Murraygate were also analysed in terms of their physical and rheological properties. The main sediment characteristics recorded during this study are presented in Table 5.2 for various chainages.

	0m	40m	83m	120m	135m	140m
Bulk Density (Kg/m^3)	1859.3	1727.2	1827.2	1682.65	1952.55	1608.55
M C (%)	16.26	24.43	26.27	34.68	21.70	22.55
T.D.S (%)	83.74	75.57	73.73	65.32	78.30	77.45
Liquid Content (%)	19.42	32.32	35.62	53.09	27.72	29.11
Volatile Solids (%)	2.15	13.00	4.05	8.19	17.35	12.09
Dry Density (Kg/m^3)	1556.95	1305.30	1347.25	1099.15	1528.75	1245.90

Table 5.2: Physical characteristics of Murraygate sediments

This study also examined the rheological properties of the deposit material; previous investigations (Williams & Crabtree, 1989) found sewer sediments to be non-Newtonian materials exhibiting elastico-viscous behaviour, compatible with applied stress rheometry techniques. Wotherspoon (1994) carried out initial sample tests and established that the structural strength of a sediment bed is related to the proportion of the liquid phase. The work undertaken for this study involved collecting and analysing samples from various locations along the length of the 150m study section of the Murraygate combined sewer and a combined sewer in Forfar. Sixty-three samples were tested using a Carrimed controlled stress rheometer (see Section 3.9.2 for a detailed description) with the resultant yield strengths compared with various physical properties of the sediment in order to investigate correlation. The results were compared with the samples analysed for the previous study (Wotherspoon, 1994) with all samples included in the analysis. Those samples that did not fail were assigned a yield strength of 2650N/m^2 (the maximum that could be exerted by the apparatus) even though this was known to be an underestimate.

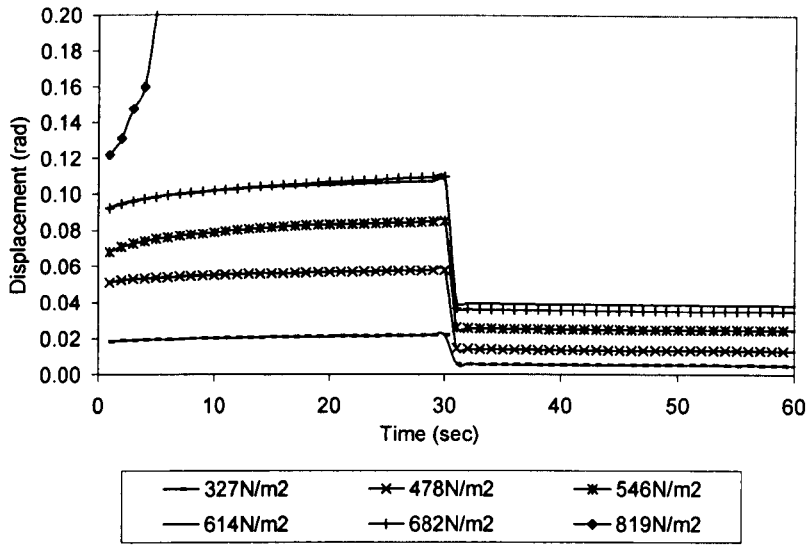

Figure 5.5: Results from creep test on Dundee sample

Figure 5.5 illustrates the results obtained for one such test performed on a sample taken from the interceptor sewer in Dundee. It can be seen that the sample failed somewhere between 682N/m^2 and 819N/m^2. In addition to the parameters examined in the Wotherspoon (1994) study, the volatile solids content of the samples were also compared with the yield strength, as it was believed that the organic content could possibly have a significant effect on the yield strength. Unfortunately, as the samples tested with the Carrimed were so small (40 ml) an individual volatile solids content could not be obtained for each sample. Although far from ideal, an average value was assigned, based on previous analyses, dependent upon where the sample had been extracted from in the sewer. In addition, it was also decided to examine whether a relationship existed between yield and the median particle size (d_{50}), although, as before, average values had to be assigned due to the limited sample size. The test results are summarised in Table 5.3.

Parameter	Regression Equation	R^2
Volumetric Solids	$\tau_y = 76.275\exp(5.0365.C_v)$	0.575
Bulk Density	$\tau_y = 21.041\exp(0.0025.\rho)$	0.208
Moisure Content	$\tau_y = 7462.64\exp(-0.05.m)$	0.77
Voids Ratio	$\tau_y = 3667.6\exp(-1.1823\ e)$	0.481
Dry Solids	$\tau_y = 18.724\exp(0.0034.\rho_d)$	0.680
Volatile Solids	$\tau_y = 3800.9\exp(-0.2856\ vs)$	0.322
Average d_{50}	$\tau_y = 654.81\exp(0.8228 d_{50})$	0.427

Table 5.3: Results from Carrimed rheometer tests

It can be clearly seen that, as in the previous study, the moisture content exhibited the greatest correlation with yield strength. In contrast, the volatile solids did not exhibit a high correlation with yield, suggesting that the organic content of a sediment bed did not have much influence on deposit strength. Although the results of the Carrimed tests confirmed the findings of the earlier study, the R^2 values were significantly lower. This can be explained by the high number of samples whose yield strength exceeded the stress that could be exerted by the apparatus and the fact that the samples were collected over a wide range of temporal and spatial conditions. In the Wotherspoon (1994) study, four out of sixty-one samples exceeded the maximum value in comparison with thirty-two out of sixty-three samples in the latest study. There is no explanation for this disproportionately high number of 'strong' samples, which skewed the results. Although it may have seemed more appropriate to remove any samples with a yield stress in excess of 2650 N/m^2 from the analysis, these samples were included in order that the results from the present study could be directly compared with those obtained in the Wotherspoon (1994) study. Figure 5.6 illustrates how, by removing three of the outlying points (highlighted), the analysis enhanced the R^2 value for the moisture content relationship.

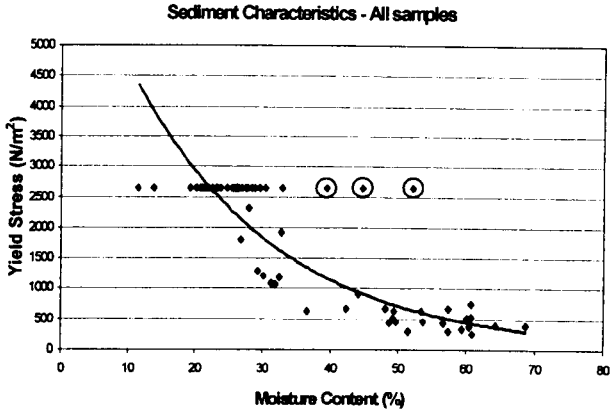

Figure 5.6: Correlation of moisture content and yield strength

After the three significant outlying points evident in Figure 5.6 had been omitted from the analysis the R^2 value increased from 0.77 to 0.86 and the yield strength relationship became:

$$\tau_y = 7689.3\exp(-0.0492.m)\ [N/m^2]$$

where '*m*' is equal to the moisture content, defined here as the mass of water divided by the mass of sediment.

5.3.4. Shear Stress Simulation

The information from the rheological testing was used in conjunction with controlled erosion tests carried out using a specially developed portable 'erosionmeter' (see Figure 3.3). This device was previously used by Jubb *et al* (2000) to investigate oxygen utilisation rates in rivers and was used in this study to simulate the shear stresses exerted under storm conditions.

Controlled erosion tests were carried out on the sewer sediment and a typical example of the results attained using this device is shown in Figure 5.7, illustrating how the critical shear stress (τ_{cr}) could be obtained.

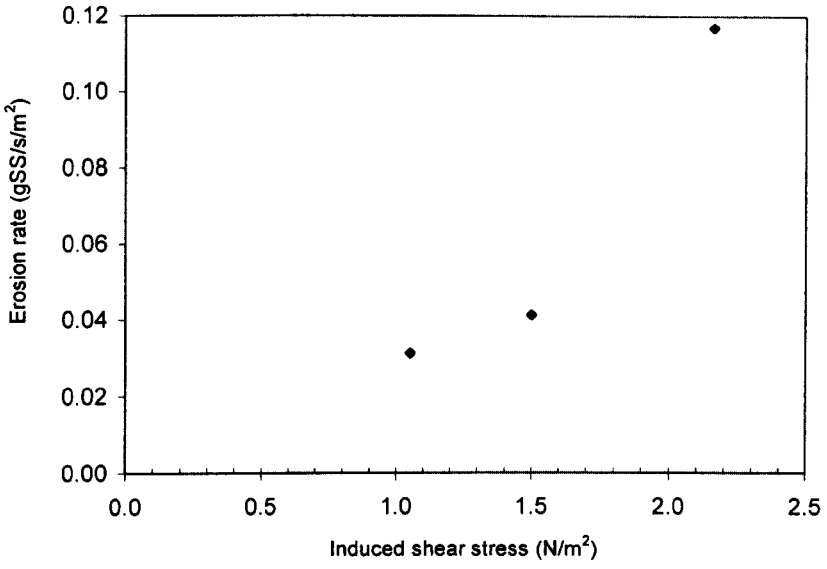

Figure 5.7: Murraygate deposit erosion rate analysis (21/08/00)

Section 3.8.7 details the erosionmeter test procedure and for the example shown in Figure 5.7, three samples were tested with seven sub-samples (one from each of the extraction ports) analysed for total suspended solids (TSS) concentrations, which were then equated to an erosion rate for that particular shear stress. Using such an approach τ could be back predicted to a point where the onset of erosion was deemed to be taking place. Although this is a subjective process it could be used to estimate a value for critical bed shear stress (τ_{cr}), information that could then be employed in an erosion model in conjunction with the bed strength properties ascertained from the rheological testing. Due to the great variability of sewer sediments there will be a range of τ_{cr} values for any one sediment class, dependent on factors such as cohesive-like behaviour (Ashley & Crabtree, 1992) and consolidation periods.

5.4. Conclusions

As illustrated by this study, the foul flush phenomenon can be described by a number of physical processes, with the total pollutant load subdivided into components corresponding to different physical processes. It is proposed that the total load is comprised of contributions from the suspended and near bed solids already present during dry weather flow, and material eroded by the storm flow from existing bed

deposits. Field observations have indicated that the re-suspended material which is moving as near bed solids during dry weather flow provides the bulk of the chemical and biochemical fraction and is therefore highly polluting. Comparison with field measurements of the total amount of material moving during dry weather flow, as both near bed solids and in suspension, with that measured during storm flows suggests that a significant amount of material is unaccounted for. As the erosion of bed deposits is believed to make a significant contribution to the total load within a foul flush this may explain the field observations that flushes are not always identical even under what would appear to be identical hydraulic conditions in the same sewer. From a river impact point of view it is the near bed solids that constitute the major pollutant source and therefore have an important role in CSO intermittent discharges. It is evident that more research is required into the erosion and transport of cohesive-like sediment beds during storm conditions and good quality field data is required to validate the results of laboratory testing programs.

The laboratory tests have demonstrated that shear stresses of less than $1N/m^2$ are adequate for initiating the onset of erosion in sediment samples, as previously reported by a number of researchers. The work described here has confirmed that a definite relationship exists between the moisture content of a sewer sediment bed and its yield strength. It has also demonstrated that there is very little correlation between yield strength and the organic content of the sediment. In addition it has demonstrated that it is possible to simulate hydraulic shear stresses in the laboratory using an erosimeter in order to attain realistic values for the τ_{cr} of the sediment.

Chapter Six – Forfar Field Study Results

6.1. Introduction

The results from the initial field investigations in the Murraygate test section indicated that, due to limitations in the flow rate that could be obtained from the three hydrants, the range of bed shear stresses that were generated were insufficient to produce suitable conditions in order to achieve measurable erosion of the in-pipe deposits. As efforts to capture a sufficiently severe storm event were also unsuccessful it was decided to find a more suitable site. After a brief desktop study it was decided to relocate to a 600mm circular combined sewer in Forfar. The smaller diameter sewer combined with the finer, less stable nature of the deposit material at this site would ensure that a suitable range of shear stresses would be generated, thus making the observation of a range of erosion behaviours much more likely.

Previous experience when conducting tests in the Murraygate illustrated the difficulties that would be encountered if data were only collected during infrequent and essentially unforeseen natural storm events. With this in mind it was decided to continue the practice of introducing extra flow to the test section by means of an adjacent water hydrant rather than attempting to wait and carry out measurements during storm events of unknown, and possibly unsuitable, intensities and durations.

The main objective from this series of tests was to gain a better understanding of the physical processes affecting the entrainment and transport of the suspended sewer solids during unsteady flows as would be observed during natural storm events. The sampling procedures were also designed to examine whether or not the mechanism of sediment transport and erosion within a combined sewer was selective or non-selective. That is, once a certain hydraulic threshold had been reached, did the individual fractions within the sewer deposit exhibit different levels of erosion and thus transport? To enable such an assessment to be made it was necessary to examine a number of parameters within the pollutographs (charts detailing temporal variation in suspended sediment concentration) in conjunction with the temporal pattern of hydraulic parameters. It was then possible to determine whether there was any correlation with the prevailing hydraulic conditions and the physical

characteristics of the sewer sediment particles in transport. This required the relevant hydraulic and sediment parameters to be consistently sampled at a high frequency throughout the flush event. This approach necessitated some form of physical particle characteristic to be determined that could provide a good representation of the heterogeneous material in transport at any given time step. If the sewer sediment had been comprised of a material of similar density then particle size would have been an appropriate characteristic to select. However, due to the heterogeneous nature of sewer sediments particle size alone would not have provided sufficient information on particle properties, and for this reason it was decided to utilise the particle fall velocity as the representative parameter as it would also take into account material density and particle shape. Given the aim to obtain a range of responses from the in-pipe deposit the temporal pattern of the tests was largely determined by the antecedent dry weather period (ADWP). This was especially important as, in order to generate the best possible flush, it was decided to fully open and hence impose the maximum flow-rate at the onset of each test, rather than use a stepped hydrograph approach. In addition to the ADWP the times of day were also varied for the tests. Table 6.1 provides a summary of the key flush test characteristics, Site 1 and Site 2 refer to the sampling sites as described in Section 4.3.2. The hydraulic parameters for each test were measured using Detectronic loggers and bed shear stresses were then determined using the method outlined in Section 3.3.2.

Test	Date/Time	Samples Obtained	ADWP (hrs)	Duration of Hydrant Input (min)	Peak Bed Shear (N/m^2)
A	23/05/01 (10:30)	Site 2 (top & bottom)	94.9	34	0.69
B	04/06/01 (10:50)	Site 2 (top & bottom)	23.75	44	0.76
C	09/07/01 (15:15)	Site 1 (top & bottom) Site 2 (top & bottom)	32.72	40	0.55
D	07/08/01 (07:50)	Site 1 (bottom) Site 2 (top & bottom)	16.93	36	0.564

Table 6.1: Summary of Forfar hydrant flush tests

6.2. Physical Characteristics of the In-pipe Deposits

The characterisation of the original bed material within the test section was accomplished by the recovery of various sediment samples from the sewer invert for the purpose of analysis. In order to preserve the deposit for the purpose of erosion the samples were not recovered on the same dates that the flushing tests took place. Due to the fine nature and limited depth of the deposit the samples were recovered simply by dragging a container through the deposit so that the entire bed was sampled, rather than just a surface scrape. This procedure was found to be the most efficient method of recovering samples although it was inevitable that some fines would be lost whatever sampling technique was used. Using the procedures described in Section 3.6 the results of these laboratory tests yielded values for the physical properties as described in Table 6.2.

Physical Property	14/06/01 (S1)	16/07/01 (S1)	24/7/01 (S1)	24/7/01 (S2)	01/08/01 (S2)	01/08/01 (USM)	Average
Bulk density (kg/m^3)	1660.00	1506.88	1591.50	1625.50	1465.50	1832.50	1613.65
Moisture content (%)	34.04	31.94	32.05	25.22	28.08	22.21	28.92
Total dry solids (%)	65.96	68.06	67.95	74.78	71.92	77.79	71.08
Volatile solids (%)	4.71	5.06	6.66	8.43	7.21	8.52	6.77
Dry density (kg/m^3)	1095.00	1025.63	1081.50	1215.50	1054.00	1425.50	1149.52

Key:
S1 – Site 1 (upstream sampling point) S2 – Site 2 (downstream sampling point) USM – Upstream manhole

Table 6.2: Physical characteristics of Forfar sediments (see Figure 4.9 for sampling location)

It can be seen that the moisture content of the in-pipe deposit at Site 2 was lower than that for Site 1 in conjunction with a higher organic content. Although there was no obvious explanation for this, the particle size distributions also exhibited spatial differences between Sites 1 and 2 as shown in Figures A1-A7 in Appendix A.

6.2.1. Particle Size Distributions of the In-Pipe Deposits

In order to obtain the particle size distribution of the bed material the samples were oven dried at 105°C and then sieved to the BS1377 – Part 2 standard (BSI, 1990) using sieve sizes of 10mm, 6.3mm 5mm, 3.35mm, 2mm, 1.18mm, 0.6mm, 0.425mm, 0.3mm, 0.212mm, 0.15mm, and 0.063mm. In addition to providing information that could be directly utilised in various predictive relationships for sediment transport, these distributions were also used to determine an approximate mean fall velocity distribution for the bed material using relationship 6.10. The results of these tests are shown in Figure A.1 through to Figure A.7 in Appendix A.

It was decided to obtain a single representative mean particle size distribution for the bed material in order that the data could be input to a sediment transport model and used to model the sediment transport at any of the sampling sites. Thus, the percentage distribution from each location and date were averaged to provide the distribution shown in Figure 6.1.

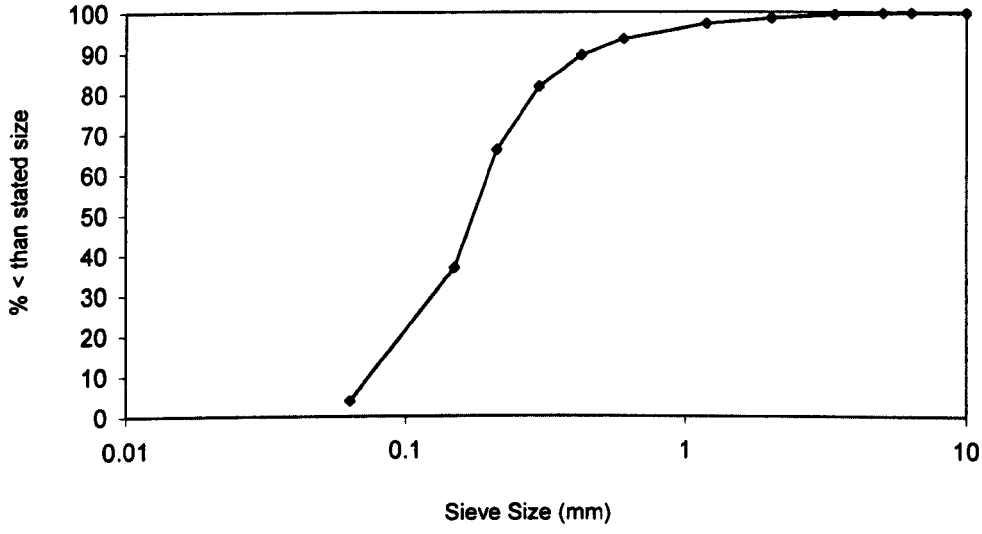

Figure 6.1: Representative mean particle size distribution of Forfar bed sediments

The median particle size, d_{50}, (in addition to the d_{16} and d_{84} particle sizes) was derived from the particle size distribution plots. It was then possible to determine the geometric standard deviation (σ_g), where $\sigma_g = (d_{84.1}/d_{15.9})^{0.5}$, with the results shown in Table 6.3.

Sample	d_{84}	d_{50}	d_{16}	σ_g
14/06/01 (S2)	0.259	0.164	0.089	1.706
14/06/01 (S1)	0.411	0.197	0.116	1.882
16/07/01 (S1)	0.336	0.179	0.095	1.881
24/7/01 (S1)	0.336	0.180	0.095	1.881
24/7/01 (S2)	0.212	0.140	0.081	1.618
01/08/01 (S2)	0.256	0.150	0.085	1.735
01/08/01 (USM)	0.673	0.270	0.159	2.057
Mean	0.336	0.180	0.095	1.881

Key:
S1 – Site 1 (upstream sampling point) S2 – Site 2 (downstream sampling point) USM – Upstream manhole

Table 6.3: Forfar particle size distributions

Upon examination of the data presented in Figure A.1 through to Figure A.7 it is clearly evident that the Forfar pipe deposit material did not contain considerable amounts of sediment with a particle size of less than 63 μm. This would suggest significant cohesive effects could be discounted, albeit Torfs (1995) demonstrated that even if a few % of clay was present in a sample it could significantly affect transport. The d_{50} values tended to be higher in the samples obtained from Site 1 than Site 2, which, in conjunction with the higher moisture contents and lower organic contents of the samples from Site 1, demonstrated the significant spatial differences observed in the sediment deposits. Although it was acknowledged there was a relatively significant spatial variation in d_{50}, it was decided to determine a mean value that could be used in order to simplify any subsequent modelling, even though a temporally varying d_{50} would probably have been more appropriate. It should also be noted that, due to the limited deposit depths, the samples were not extracted on the same dates that the tests were carried out.

6.2.2. *Dry Weather TSS Profiles*

The temporal variation of suspended solids in dry weather was recorded so that ambient conditions could be assessed, although a full 24-hour profile was not obtained due to sampler failure. This data would be useful to compare with the magnitude of the suspended solids recorded during the flush events.

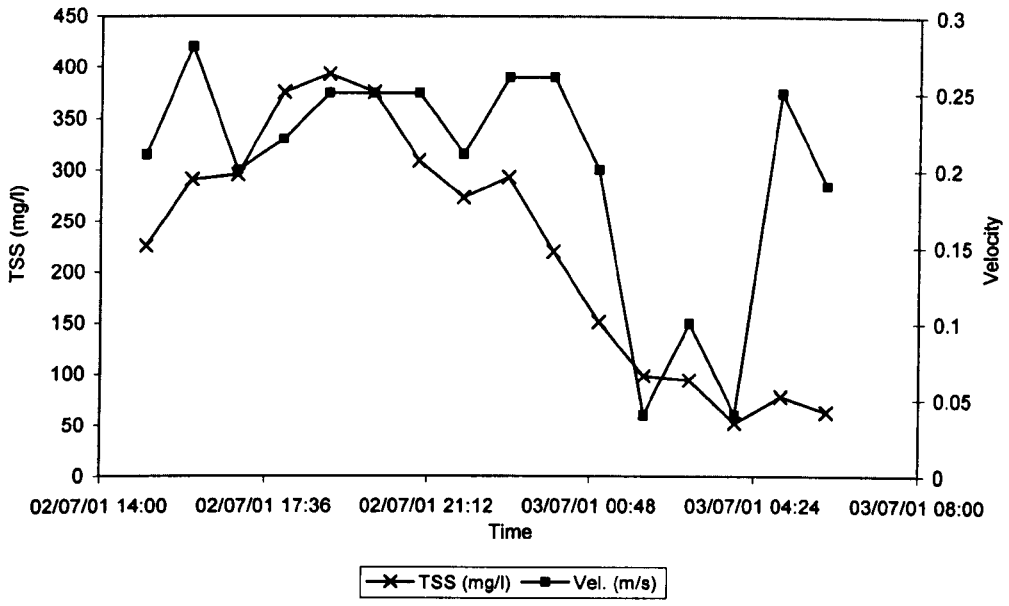

Figure 6.2: Dry weather flow TSS profile (Site 2, 02/07/01)

Figure 6.2 represents the first of the DWF profiles to be recorded which shows that between 15:00 and midnight the TSS values fluctuated around 300 mg/l (corresponding to a mean velocity of approximately 0.25 m/s) before dropping to values of between 50 and 100 mg/l (corresponding to velocities fluctuating between 0.05 and 0.1 m/s) in the early hours of the morning.

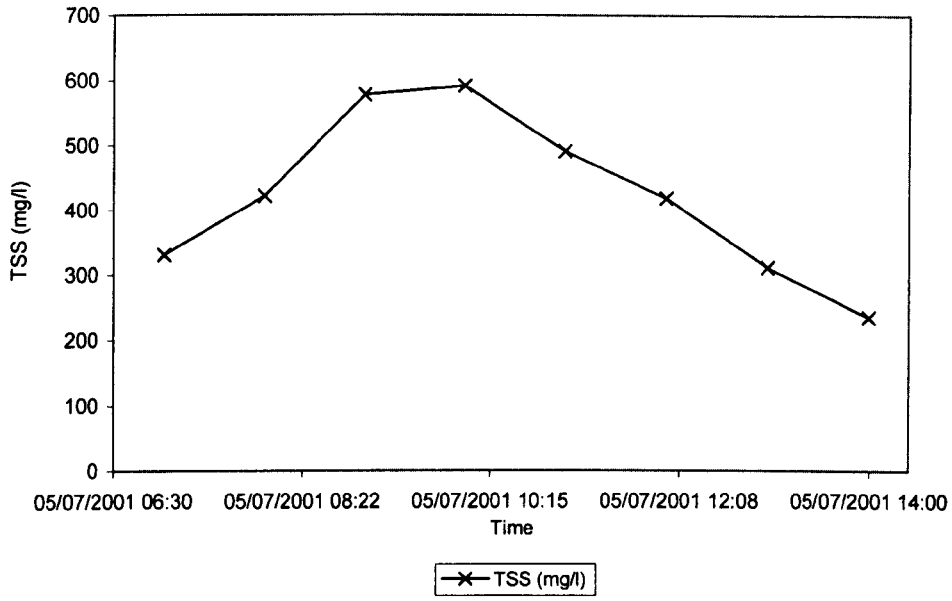

Figure 6.3: Dry weather flow TSS profile (Site 2, 05/07/01)

Further dry weather sampling on 05/07/01 recorded the suspended solids from 07:00 until 14:00, as data for this period had not been captured previously. Unfortunately, no corresponding velocity data was available due to a monitor failure but the TSS data proved useful as it illustrated that the values varied between approximately 300 mg/l and 600 mg/l during this time of the day. A further attempt was made to obtain dry weather samples on 07/08/01 as shown in Figure 6.4.

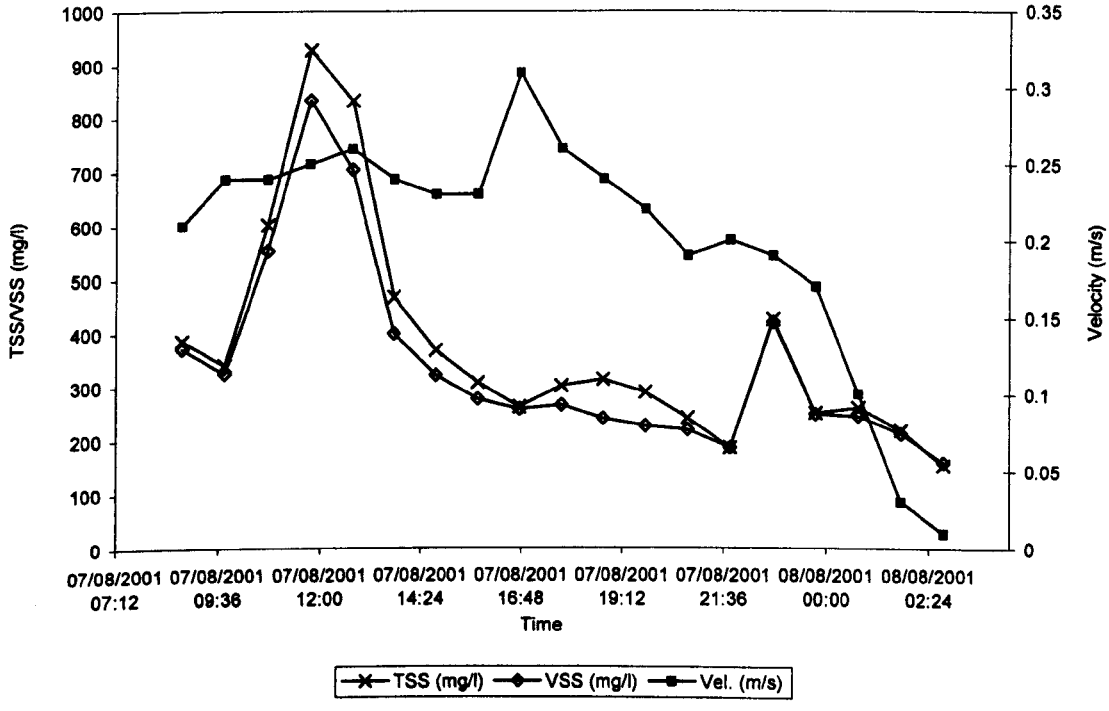

Figure 6.4: Dry weather flow TSS profile (Site 2, 07/08/01)

Sampling commenced at 08:45 and finished at 02:45 on 08/08/01 as, due to a problem with the suspended solids sampler, a full 24-hour profile could not be obtained. Again a problem was experienced with the velocity logger, which started to malfunction (either due to ragging or the velocity magnitude being outwith its operational capabilities) close to midnight. An average velocity of approximately 0.25 m/s was recorded and the TSS values once again tended to approximate to 300 mg/l. It is unclear why a peak occurred at 11:45, as there was no significant corresponding rise in the recorded velocity. Table 6.4 presents the ambient TSS levels recorded during times of day corresponding to when the flush tests were carried out

Test	Date/Time	Corresponding Ambient TSS (mg/l)
A	23/05/01 (10:30)	≈ 550
B	04/06/01 (10:50)	≈ 550
C	09/07/01 (15:15)	≈ 290
D	07/08/01 (07:50)	≈ 400

Table 6.4: Forfar ambient suspended solids concentrations

6.3. Hydrant Flush Tests

In order to replicate flushes of suspended solids additional flow was introduced to the test section of the combined sewer from an adjacent water hydrant through an arrangement as shown in Plate 6.1.

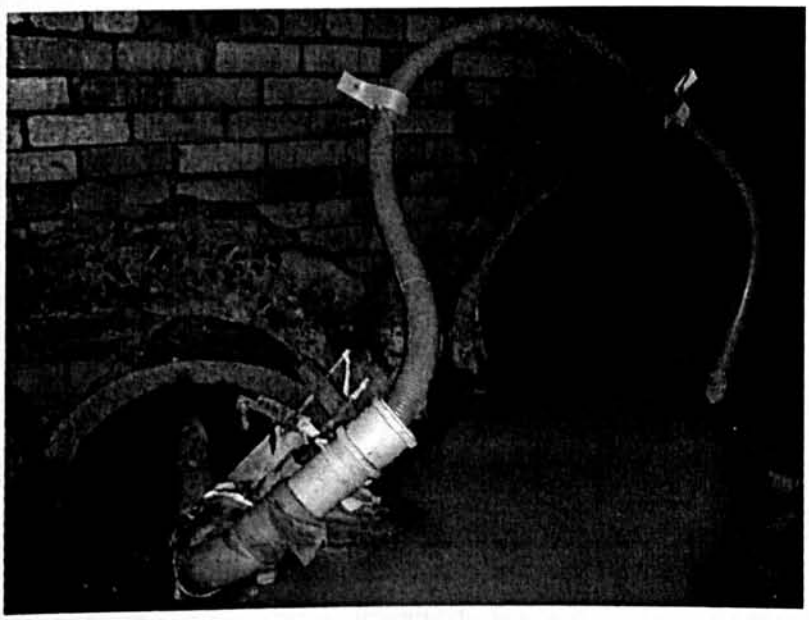

Plate 6.1: Injection of hydrant flow into test section of Forfar 600mm combined sewer

Using this arrangement it was possible to generate flushes with peak suspended solids concentrations that ranged from approximately 800 mg/l to 2500 mg/l compared to the ambient conditions in the pipe which ranged from approximately 150 mg/l to 900 mg/l.

6.3.1. Results of Flush Test A (Site 2, 23/05/01)

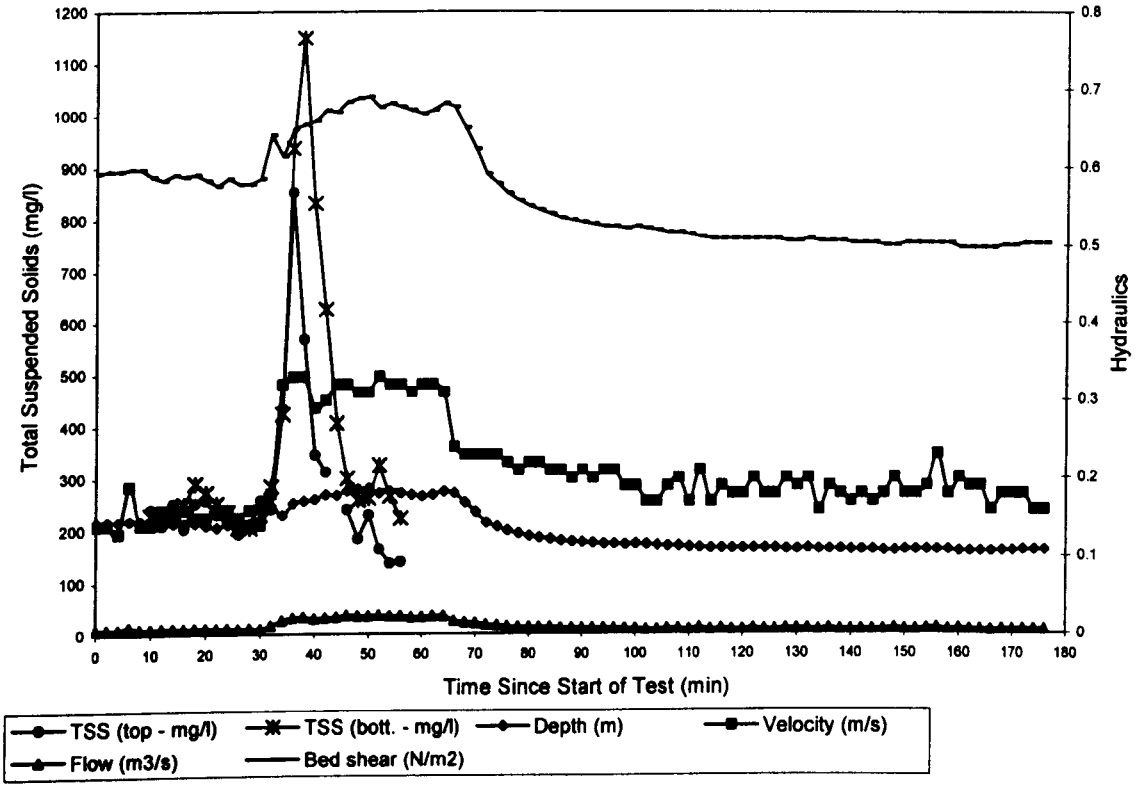

Figure 6.5: Summary of hydraulic and TSS results of Forfar hydrant Test A (Site 2, 23/05/01)

A summary of the results from the first test recorded in Site 2 (i.e. the downstream manhole) is shown in Figure 6.5. The results from the two sampling heights were consistent and exhibited the response of a classic solids flush in a combined sewer, with a sudden increase in TSS at both heights as the flow rate increased suddenly due to the hydrant opening. The TSS values reached a peak then declined, even though the hydraulic conditions were now steady. It was also noted that the TSS concentration was also consistently higher in the samples extracted from the lower sampling point as would be expected. This pattern of behaviour has also been observed in "first foul flushes" in a number of combined sewers. From a long series of measurements in Germany, Geiger (1987) deduced that, even in the same sewer,

storm events could produce either a dilution response or a flushing effect, resulting in either a decrease or increase in concentrations. The flushing was attributed either to surface source inputs (obviously not applicable in the Forfar field tests) or the scouring of the in-pipe deposits.

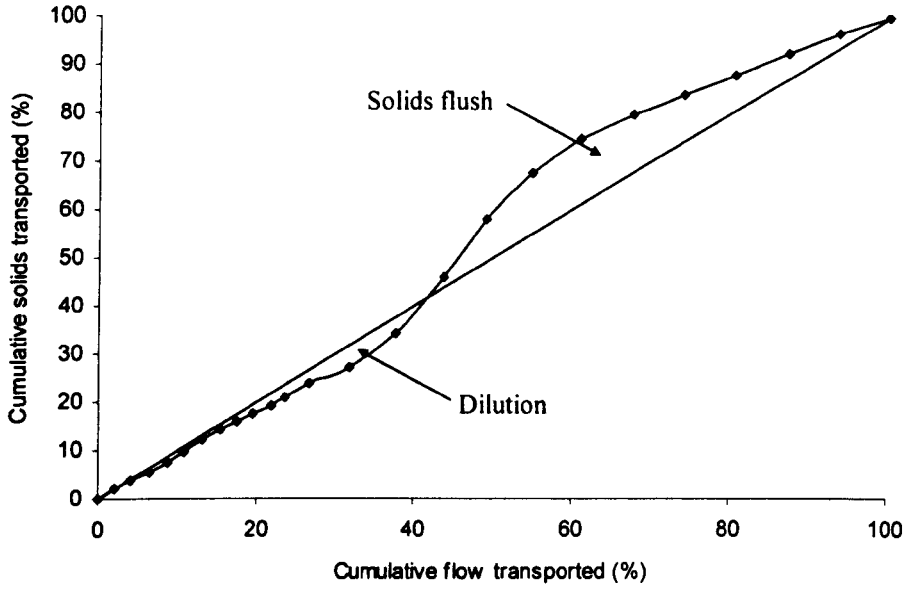

Figure 6.6: Dilution followed by flush response of Forfar hydrant Test A (Site 2, 23/05/01)

By plotting the cumulative load against the cumulative flow Figure 6.6 shows the typical response to the hydrant input. Had the plot been linear this would have intimated that no change had taken place and the situation would have been described as the equilibrium condition (Geiger, 1987). During this test however it can be seen that there was an initial dilution effect due to an inundation of flow from the hydrant followed by a flush of solids that were eroded from the pipe deposit.

The overall pattern of these results in comparison with the pattern observed at a number of other field sites (Arthur, 1996, Geiger, 1987, Stotz and Krauth, 1984 and Pearson *et al.*, 1986) suggested that the artificially created flushes in Forfar had a number of characteristics in common with flushes observed in storm events in a number of different combined sewers.

6.3.2. Results of Flush Test B (Site 2, 04/06/01)

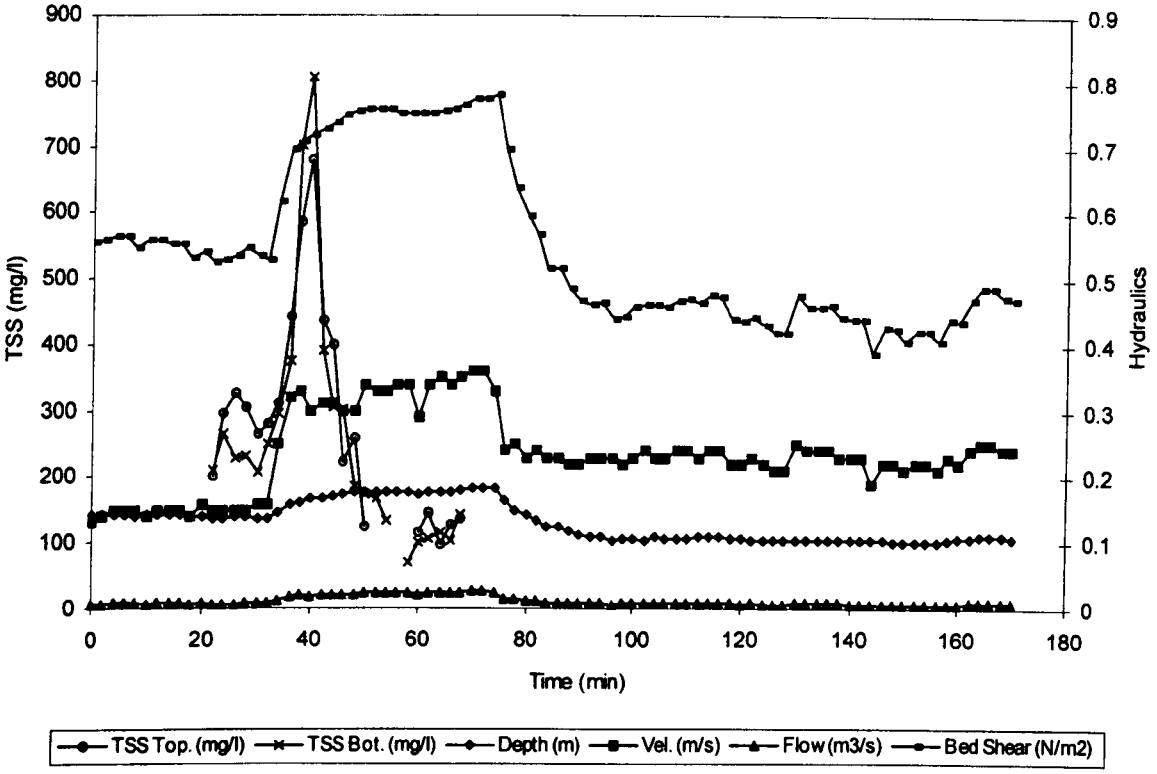

Figure 6.7: Summary of hydraulic and TSS results of Forfar hydrant Test B (Site 2, 04/06/01)

As with the first test the results shown in Figure 6.7 illustrate the marked flush that was attainable by introducing extra flow to the test section using the hydrant. Again the TSS sampling exhibited a rise in suspended solids concentration with the corresponding rise in bed shear stress and showed the TSS dropped even though the levels of shear stress were still high. It is interesting to note that during the ambient conditions prior to the introduction of the hydrant flow the top sampling point exhibited a higher solids concentration than the bottom point.

6.3.3. Results of Flush Test C (Sites 1 & 2, 09/07/01)

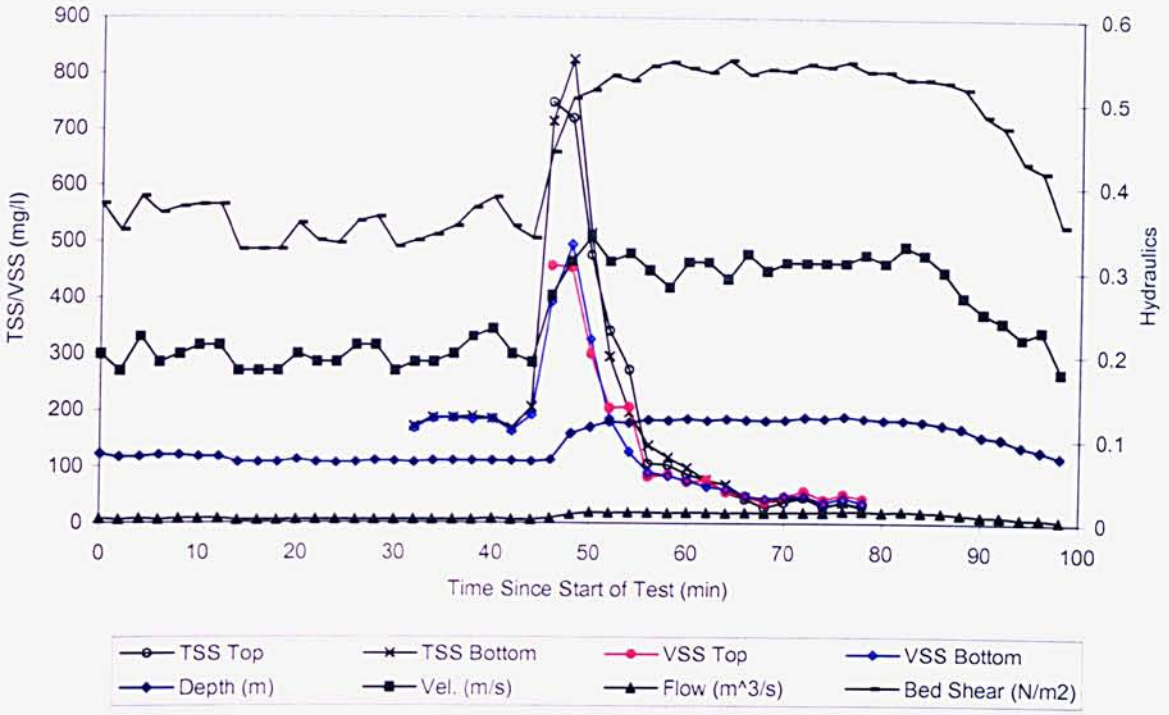

Figure 6.8: Summary of hydraulic and TSS results of Forfar hydrant Test C (Site 2, 09/07/01)

The flush test carried out on 09/07/01 was recorded simultaneously both in Sites 1 and 2. Figure 6.8 shows the results obtained from the downstream manhole and it was noticeable there was no strong differentiation in TSS between the top and bottom sampling points. This was also the case in the previous test although Test A did show a marked difference in the levels of TSS recorded. Also noteworthy is the apparently high proportion of inorganic material present in the first part of the flush as shown by the relatively large difference in the VSS and the TSS levels.

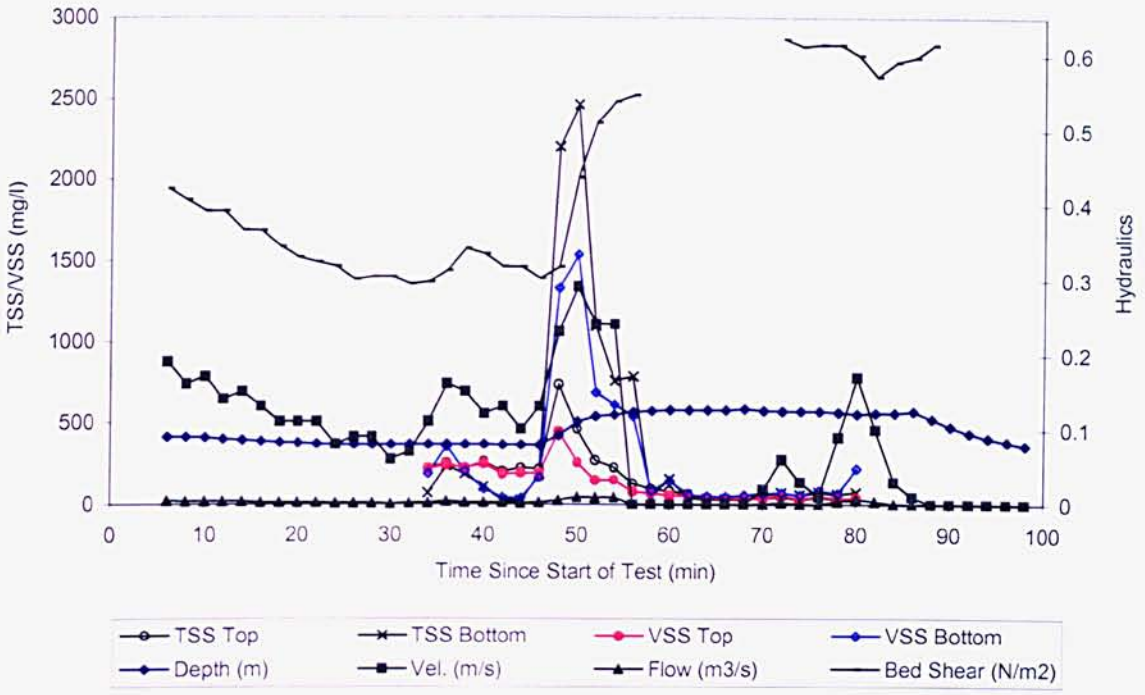

Figure 6.9: Summary of hydraulic and TSS results of Forfar hydrant Test C (Site 1, 09/07/01)

As with the results from Site 2 the first set of results obtained from the upstream sampling point (Site 1) also showed a classic flush. There was a marked difference in the TSS levels between the top and bottom sampling points. Although the TSS levels observed at the top sampling points were similar in magnitude between Sites 1 and 2, there were significantly larger TSS levels recorded from the bottom sampling point at Site 1 when compared with the Site 2 values. As the temporal pattern of these TSS profiles were similar it is unlikely that the difference was due to dispersion.

The ratio of VSS and TSS observed at both sampling heights followed the same general pattern, with a similar magnitude at the start of the event with a marked deviation during the flush, prior to returning to similar magnitudes once the flush had subsided. This would suggest that prior to the increased bed shear stress the material in transport was comprised mainly of organic material, whereas more inorganic material was transported during the flush itself, before the composition returned to a mainly organic mixture once the flush had subsided.

6.3.4. Results of Flush Test D (07/08/01)

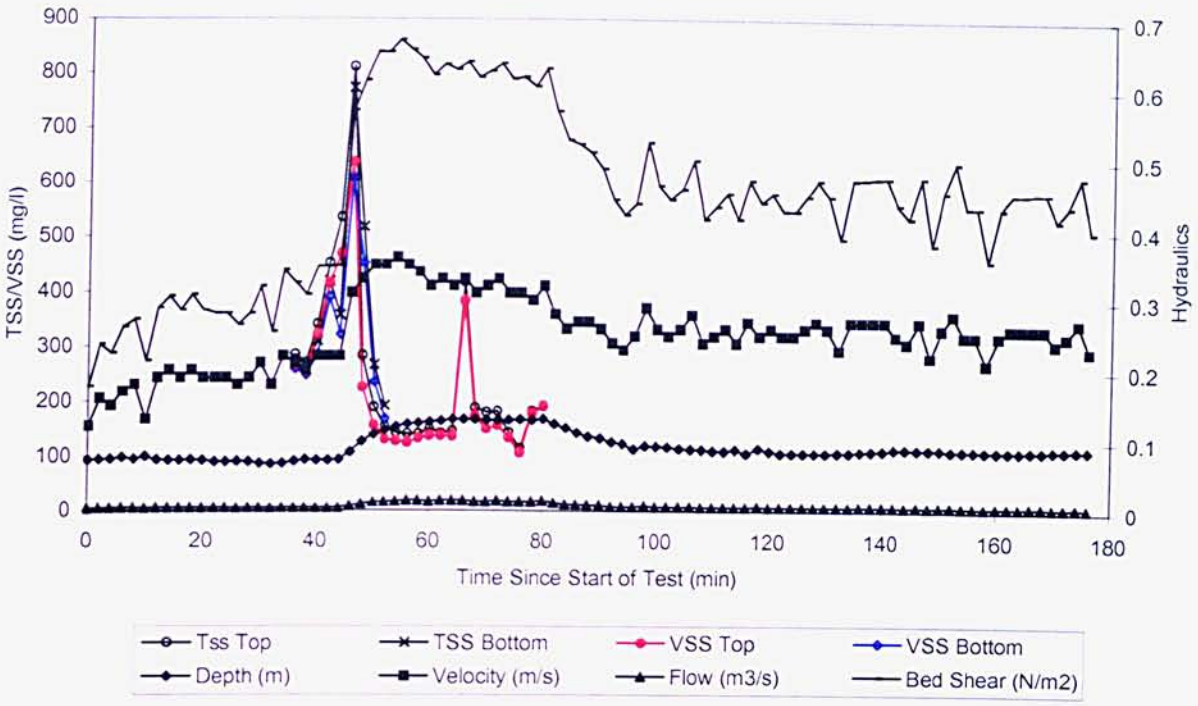

Figure 6.10: Final Forfar hydrant test (Site 2, 07/08/01)

The final flush test carried out on 07/08/01 was again recorded both in Sites 1 and 2. As can be seen in Figure 6.10, there appeared to be an anomaly with the suspended solids results from Site 2. The results from a point closer to the bed showed the peak concentration to be lower than the results from a point higher in the flow column, in addition to being offset. This may have been due to a problem with the sampling tube becoming blocked and hence it was deemed more appropriate that the results from the top sampling tube should be used for the purposes of the suspended sediment transport rate SSTR calculation.

The magnitudes of VSS and TSS observed at the top sampling point were of a similar magnitude at the start of the event but then exhibited a marked deviation during the flush, prior to returning to similar magnitudes once the flush had subsided. The magnitudes of the VSS and TSS at the bottom sampling point on the other hand showed very little deviation and were also almost identical even at the peak values.

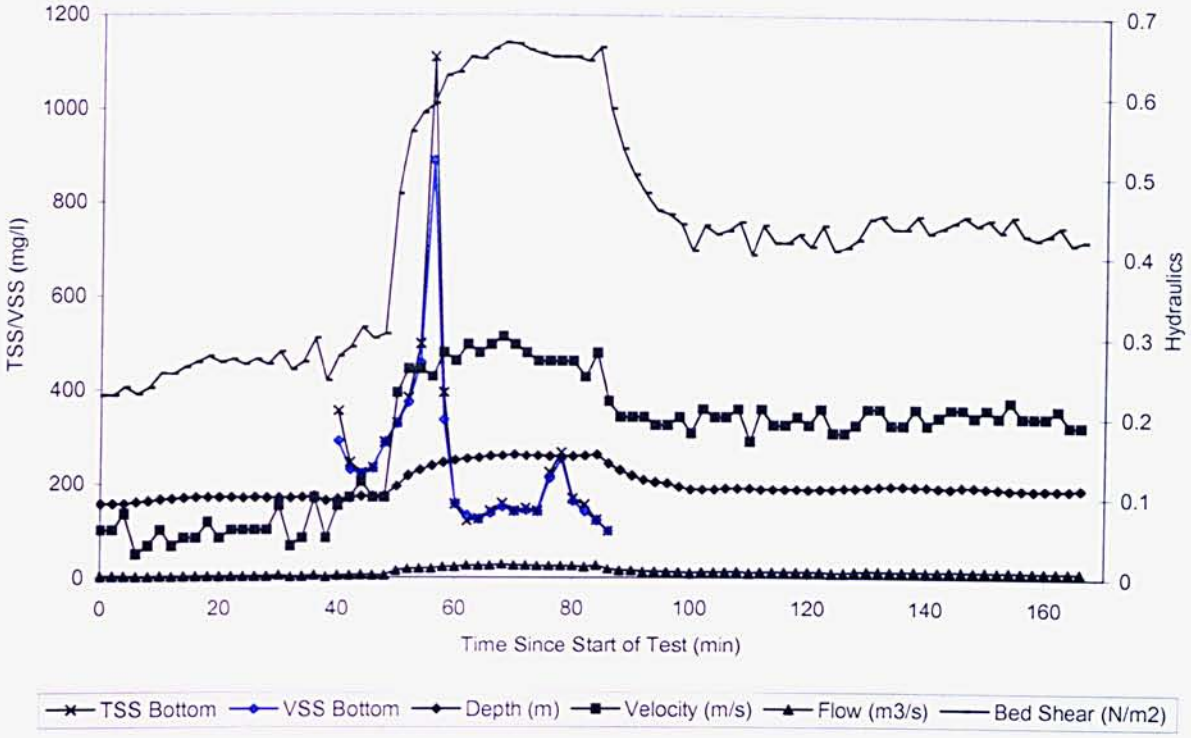

Figure 6.11: Final Forfar hydrant test (Site 1, 07/08/01)

Only samples from the bottom sampling point were obtained at the upstream site with the results again exhibiting a marked flush of suspended material. As in Test 3 there were significantly larger TSS levels recorded from the bottom sampling point at Site 1 when compared with the Site 2 values.

The observed magnitudes of VSS and TSS were again similar at the start of the event with a marked deviation during the flush prior to returning to similar magnitudes once the flush had subsided. As previously suggested, this may have been as a result of more inorganic material being transported in suspension during the flush itself, before the composition returned to a mainly organic mixture once the flush had subsided.

6.3.5. Summary of Flush Test Results

There seemed to be some discrepancy with the timing of the flush in each of the tests. In Test A the flush occurred after the rise in bed shear stress, in Test B the flush occurred just prior to the rise in bed shear while in Test C the flush corresponded with the rise in bed shear stress. It is probable that this was due to an error in the time keeping of the TSS samples due, either to watches not being precisely synchronised, or human error in the recording of the sample times. Rather than modify the results to match up with the rise in bed shear it was decided to leave the results as they were in case any other reason may be evident in the results that would explain the discrepancies.

It was interesting to note that at the end of each test the ambient TSS was lower than that observed prior to the operation of the hydrant which may have been due to either of, or a combination of the following reasons. The most likely explanation would be that most of the deposit upstream of the sampling sites was washed away during the test resulting in a narrower bed width leaving less bed area prone to erosion and hence less material that could be entrained into the flow column. Another possibility may have been that a 'weaker' surface layer could have been eroded exposing a more stable deposit underneath so that the drop observed in the TSS values would actually have been a measure of the increase in bed strength due to a change in the deposit character.

Also of note is the observation that after the peak hydrograph had been exceeded in each test there was a decline in TSS even though the bed shear stress remained at a similar magnitude. This may also have been due to the reasons outlined above or it may have been as a result of a different composition of material in suspension. That is, the organic material may have been flushed from the deposit leaving a more granular deposit and hence a lower level of TSS that could be entrained and sustained in the flow column.

6.4. Evaluation of Mass Transport and Erosion Rates

Rather than simply evaluating the suspended sediment transport rates (SSTRs) as a product of the average flow velocity and average suspended sediment concentration of the flow column, the SSTRs were determined by generating a suspended sediment concentration profile which was then used in conjunction with a calculated velocity profile to estimate the total SSTR for a particular time interval during the flush tests. Erosion rates were calculated by examining SSTRs at consecutive sampling locations.

6.4.1. Determination of Concentration Profiles

In order to determine the mass transport and erosion rates assumptions had to be made when estimating the TSS profile throughout the flow column. Several of the tests contained only one extraction point for the TSS samples and thus only limited data was available on the vertical variation in suspended sediment concentration. This necessitated a suitable approach be adopted for determining the suspended solids concentration profile. Alternative concentration profiles have been proposed including the concentration profile proposed by Rouse (1937), or the methodology adopted by Verbanck (2000) which incorporates the Coleman (1982) profile relationship for the bottom quarter of the flow. These approaches all require a known TSS concentration at a known distance above the bed and an estimate of a representative fall velocity. The main drawback with these methods is their high reliance on an accurate value of the representative particle fall velocity. This has been shown to be a highly sensitive parameter when using the relationship proposed by Verbanck (2000).

For this study it was decided to use the Rouse (1937) formulation and confidence was gained in this methodology when the theoretical profiles were matched with the tests where two measurement points had been taken (see section 6.4.5). The Rouse distribution equation was expressed as:

$$\frac{c}{c_a} = \left[\frac{a(y_o - y)}{y(y_o - a)}\right]^{\frac{w_s}{ku_*}} \qquad (6.1)$$

where: c is the sediment concentration at a distance y above the bed [mg/l]

c_a is the reference concentration at a distance a above the bed [mg/l]

y_o is the flow depth [m]

w_s is the particle fall velocity [m/s]

κ is the von Kàrmàn constant

u_* is the shear velocity [m/s]

The von Kàrmàn constant was assumed as 0.4 and a value of 0.00322 m/s was assumed for w_s, which was the median fall velocity of the bed material. This was deemed to be a reasonable assumption as w_s contains uncertainty due to the large range of settling velocities for the bed material. Skipworth (1996) showed that a variation in the choice of w_s could have a significant effect on the vertical transport rate profile but it had a negligible effect on the overall cross-sectional transport rate at a particular point in time.

6.4.2. Determination of Velocity Profiles

In order to determine the velocity distribution throughout the flow column the Prandtl-von Kàrmàn universal-velocity-distribution law for flow over rough surfaces was used. This approach assumed that:

- the velocity profile was constant laterally across the flow cross section
- the shear velocity (u_*) was that obtained from the bed shear stress (calculated using the Side Wall Elimination method) as outlined in Section 3.3.2
- the Nikuradse roughness height (k) was taken as the average grain size of the bed material (0.18mm).
- at any point in time any accelerations due to the time varying flow could be discounted

The velocity distribution was then determined from the Prandtl-von Kàrmàn law:

$$u = 2.5u_* \ln\left(\frac{30y}{k}\right) \qquad (6.2)$$

The estimated velocity field was verified by determining the average velocity (u) of the profile and multiplying it by the cross sectional flow area. This was then checked in order to ensure that the resulting calculated flow rate was comparable with the measured flow rate.

6.4.3. Determination of SSTRs

The suspended sediment transport rate was determined by integrating the product of local flow velocity (u) and local concentration (c) throughout the total flow depth (Y):

$$SSTR = \int_0^y ucdA \qquad (6.3)$$

The total flow area was subdivided into discrete strip cross sectional areas (CSAs) using the following trigonometric functions

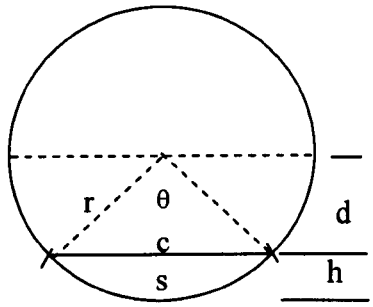

where:	cross sectional area = ½ (rs - cd)	[m^2]	(6.4)
	$\theta = 2 \arccos d/r$	[rad]	(6.5)
	$c = 2 r \sin ½ \theta$	[m]	(6.6)
	$d = r - h$	[m]	(6.7)
	$s = r \theta$	[m]	(6.8)

The flow area was subdivided into n strips with a height of 5mm and an area of dA_n, with n being the strip number at a particular height h above the sediment bed. The corresponding discrete velocity for each strip, v_{nt} and the corresponding discrete suspended sediment concentration, c_{nt}, were then used to determine the transport rate dT/dt (mass per unit time) for each of the strips at time t:

$$(SSTR)_{nt} = v_{nt} c_{nt} dA_n \qquad (6.9)$$

This approach was used to produce a matrix of SSTRs at two-minute time intervals for each of the cross sectional strip areas throughout each flush test. These transport rates were then summed throughout the flow depth to give the total SSTR for each time step, with integration of these transport rates over time yielding the cumulative suspended load for each of the flush events.

6.4.4. Problems Experienced in Determination of SSTRs

In the sewer it was impossible to monitor the temporal changes in bed depth during the tests and initial bed conditions were either estimated or measured prior to the test. It should be noted that any errors in the estimation of the bed position at the beginning and during the test would have had an effect on the calculated concentration profile and velocity profiles, and the estimated cross sectional area of flow. These errors would also have affected the calculated SSTRs. Rushforth (2001) showed that these errors would on average cause a 10% difference in the cumulative SSTRs depending on whether the initial or final bed levels were used; with lower estimated bed levels giving a higher peak SSTR

Other errors were related to practical problems experienced with the hydraulic monitoring equipment in Test D:

Test Test D (07-08-01)

The velocities and flow depths from the hydraulic monitor at Site 2 were used in conjunction with the suspended sediment concentrations from Site 1 as the hydraulic monitor at Site 1 malfunctioned.

The velocities from the Site 1 monitor were unreliable mainly due to siltation, which quickly built up around the sensor head during the tests. For this reason the velocities and depths acquired from the downstream monitor (Site 2) were used with a suitable travel time to account for the distance between the two monitor locations.

Although not ideal this was the only practical option to provide hydraulic data that could be used in conjunction with the concentration data collected at Site 1.

6.4.5. Analysis of SSTR Results

Using the aforementioned techniques the results from each of the tests were analysed and a comparison carried out to ascertain whether any common factors or trends were present. An example velocity profile (generated from Prandtl-von Kàrmàn law) for a particular time-step from Test A is shown in Figure 6.12.

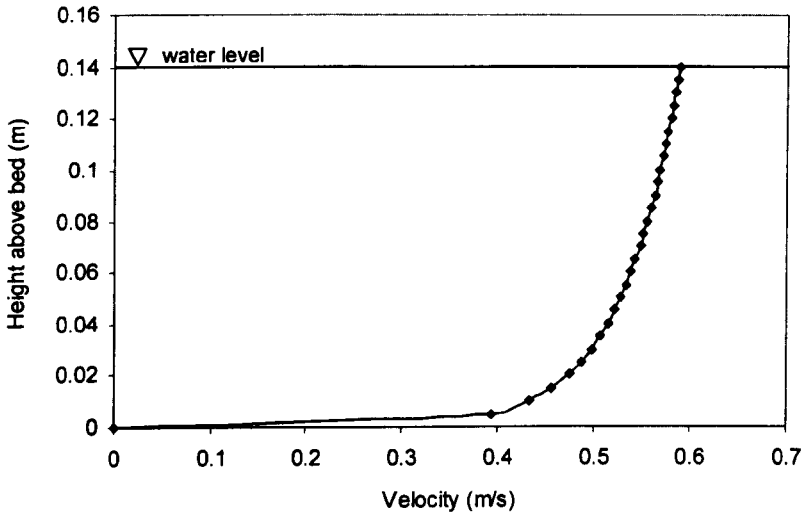

Figure 6.12: Example of calculated velocity profile from Site 2 (Test A)

An example concentration profile at a height of 30mm above the bed generated using the Rouse formula (with c_a = 230 mg/l) for the same time-step of Test A is shown in Figure 6.13.

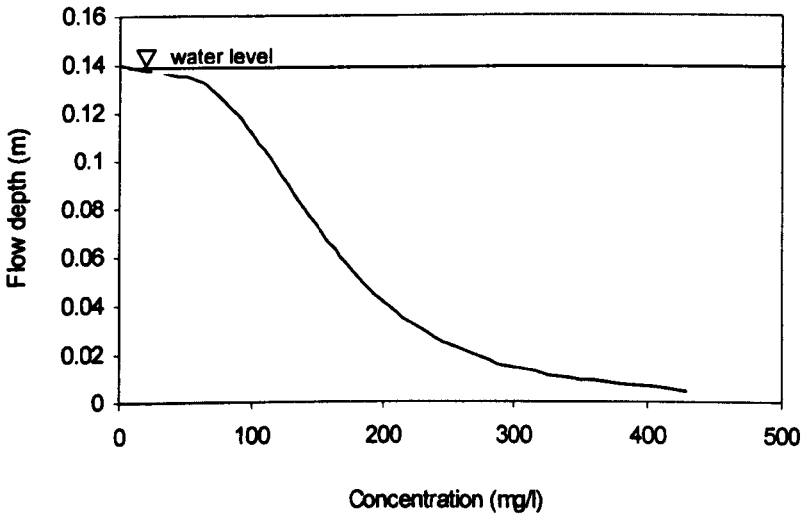

Figure 6.13: Example concentration profile from Site 2 (Test A)

The time-varying concentration profiles during this test were determined using the Rouse theory in conjunction with the observed data from the lower sampling point which was set 30mm above the invert as the reference concentration position. The resulting calculated concentration profiles were checked using the TSS data obtained from the other sampling point (50mm above the invert) as shown in Figures 6.14–6.17.

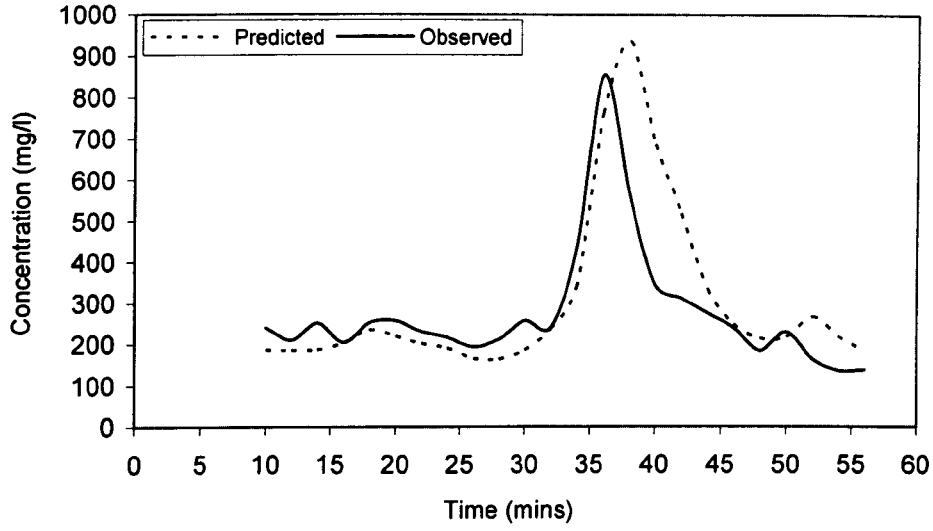

Figure 6.14: Predicted and observed point concentrations (Test A, 50mm above invert)

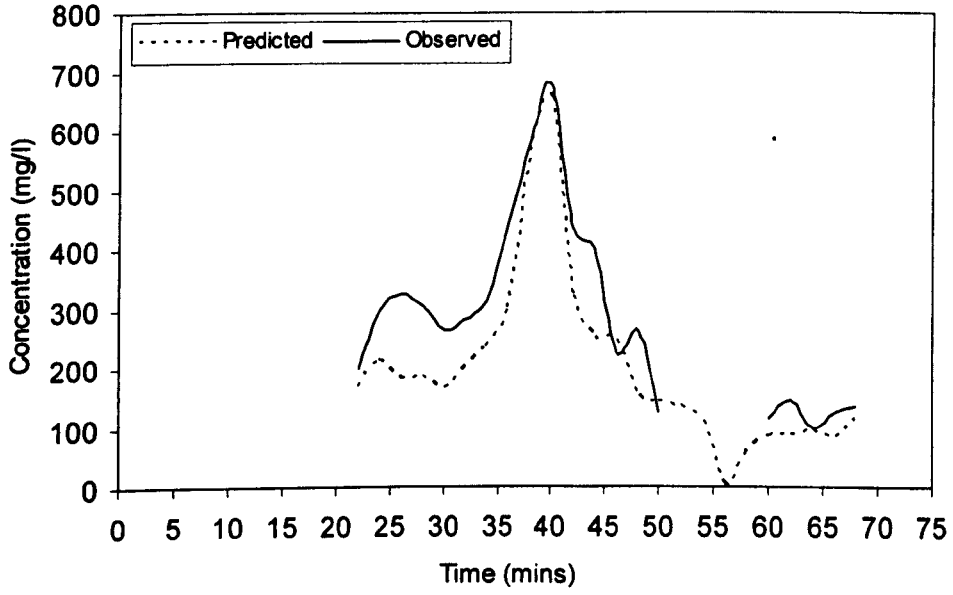

Figure 6.15: Predicted and observed point concentrations (Test B, 50mm above invert)

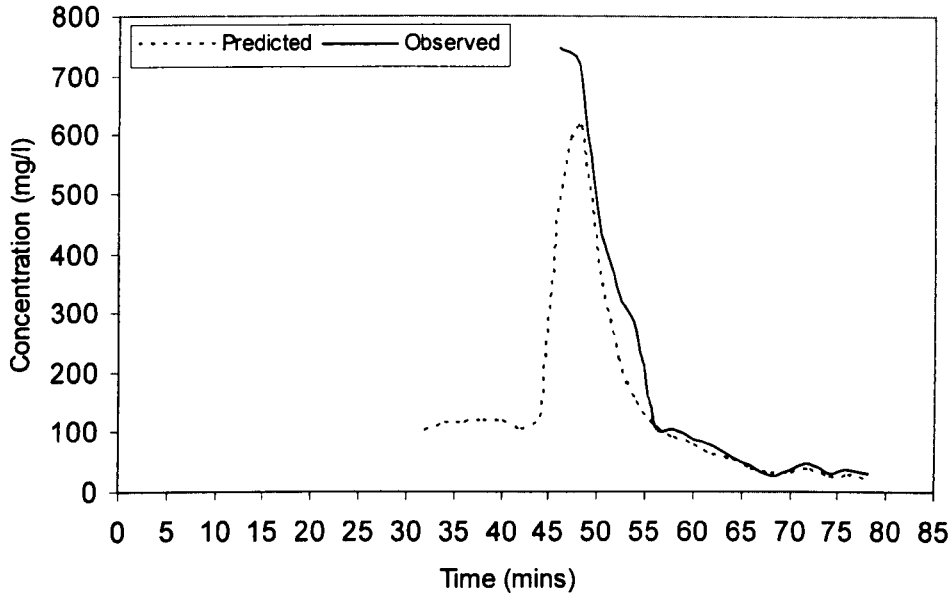

Figure 6.16: Predicted and observed point concentrations (Test C, 50mm above invert)

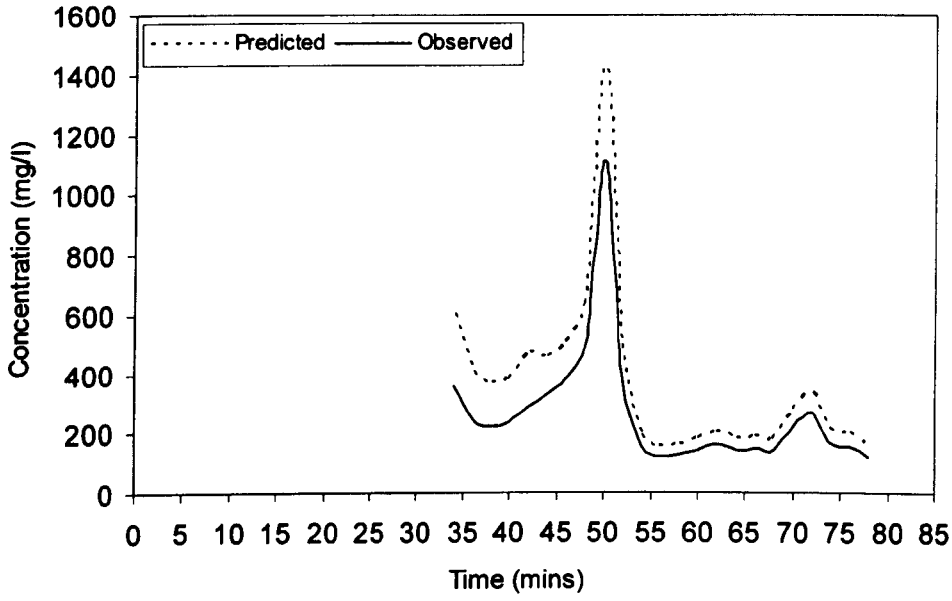

Figure 6.17: Predicted and observed point concentrations (Test D, 30mm above invert)

Note: During Test D the results from the bottom sampling tube showed the peak concentration to be lower than the results from a point higher in the flow column. As this may have been due to a problem with the sampling tube becoming blocked it was deemed more appropriate that the results from the top sampling tube (50mm above the bed) be used to generate the Rouse profiles for this test.

At the beginning of the Test A it was clear that the suspended solids concentration estimated by the Rouse distribution theory at the upper sampling height under-predicted the concentration by an average of 15% over the duration of the test. However the observed data followed the estimated concentrations more closely during the rising limb of the flush (with an average under-prediction of 11.5%) than when the concentrations started to fall. For the remainder of the test, after the peak suspended solids concentration had been reached, the concentration was generally over-predicted by an average of 42% with the peak concentration being over-predicted by a margin of 9.5%. The peak estimated and observed concentrations were also offset by approximately five minutes. The average overall difference between the Rouse-predicted and observed concentrations for this test was 27%.

Examination of Figures 6.15-6.16 showed that over-prediction of the peak also occurred in the remainder of the tests except for Test B. Integration of the product of the Rouse concentration and velocity profiles with respect to the flow depth yielded the cross-sectional SSTR pattern for each of the flush tests (see Equation 6.9). A sensitivity analysis was carried out to ascertain what effect varying the main parameters within the Rouse formulation would have on SSTRs (Fraser, 1998). The analysis was carried out on three main parameters:

- Reference concentration (c_a)
- Settling velocity (w_s)
- Shear velocity (u_*)

As the reference concentration (c_a) is used purely as a constant of multiplication, its effect on the overall transport rate is directly linear. Conversely, the settling velocity (w_s) influences the concentration profile via the power term η:

$$\eta = \frac{w_s}{\kappa u_*}$$

Fraser (1998) reported that the SSTR was found to be highly sensitive to changes in this parameter in excess of a 25 % increase.

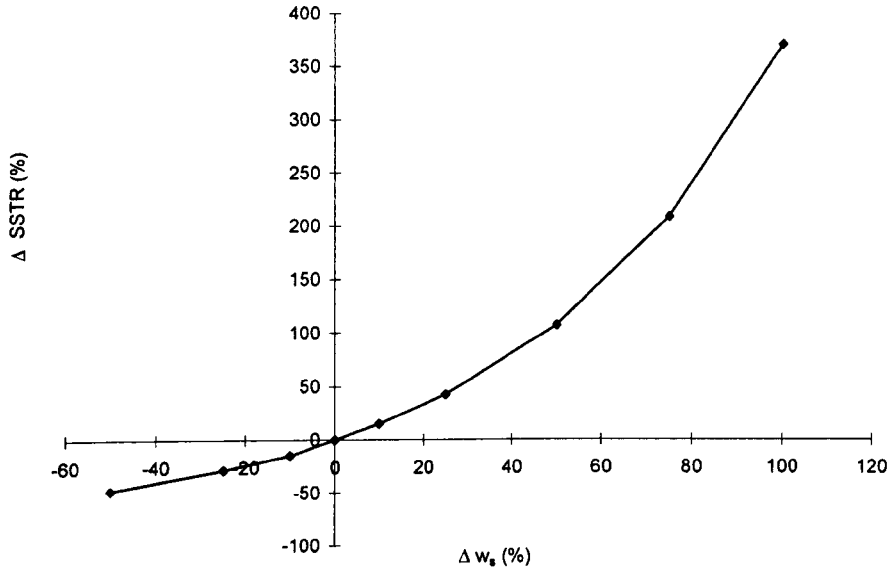

Figure 6.18: SSTR sensitivity to changes in settling velocity (w_s)

Changes in the value of the shear velocity (u_*) were found to have a much more complex effect on the calculated transport rate. This is a result of how u_* is used to calculate the SSTR:

- it is initially used to determine the power term 'η' of the concentration profile
- it is subsequently used as a direct multiplier to calculate the transport rate

The SSTR sensitivity to changes in u_* is illustrated by Figure 6.19.

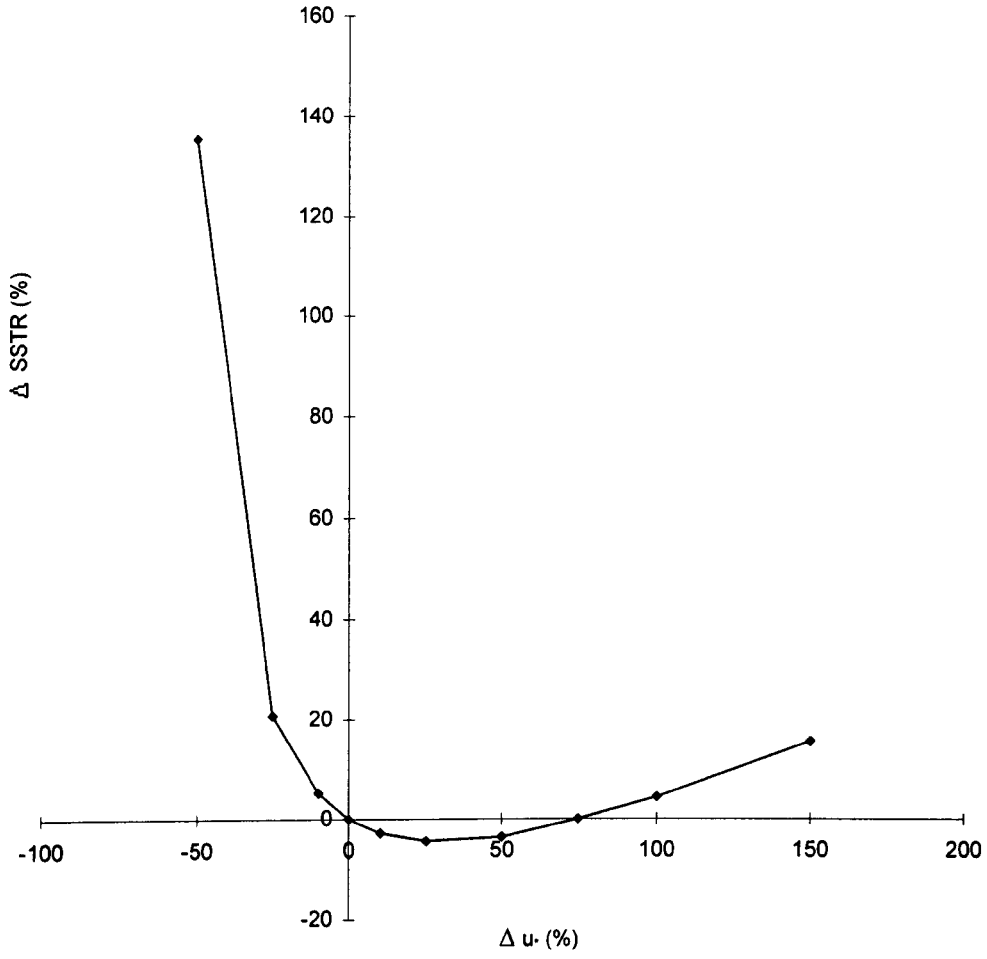

Figure 6.19: SSTR sensitivity to changes in shear velocity (u_*)

The effect on the SSTR stems from the fact that; a reduction in the shear velocity results in an increase in the TSS concentration, coupled with a reduction in the velocity of the particles. As shown by Figure 6.19, at low values of shear velocity, the overall transport rate increases as it is dominated by the high TSS concentration produced, indeed a decrease of approximately 50% in shear velocity can lead to an overestimate in SSTR of approximately 135%. If the shear velocity is increased to approximately +75% a slight reduction in the total transport rate is observed, due to a combination of reduced concentrations and increased velocities. Although further increases in shear velocity result in an increased SSTR, the results illustrated in Figure 6.19 suggest that an overestimate of the shear velocity (by up to +150%) could still be used to yield reasonable results, therefore it would be preferable to use an over-estimate of shear velocity to an under-estimate. As previously mentioned, as c_a is used purely as a multiplication constant, its effect on the overall transport rate is directly linear; however, the cumulative effect due to combined worst case errors in w_s and u_* is an over-estimation in transport rate of 1.614×10^4 %.

6.4.6. SSTR Results (Test A – 23/05/01)

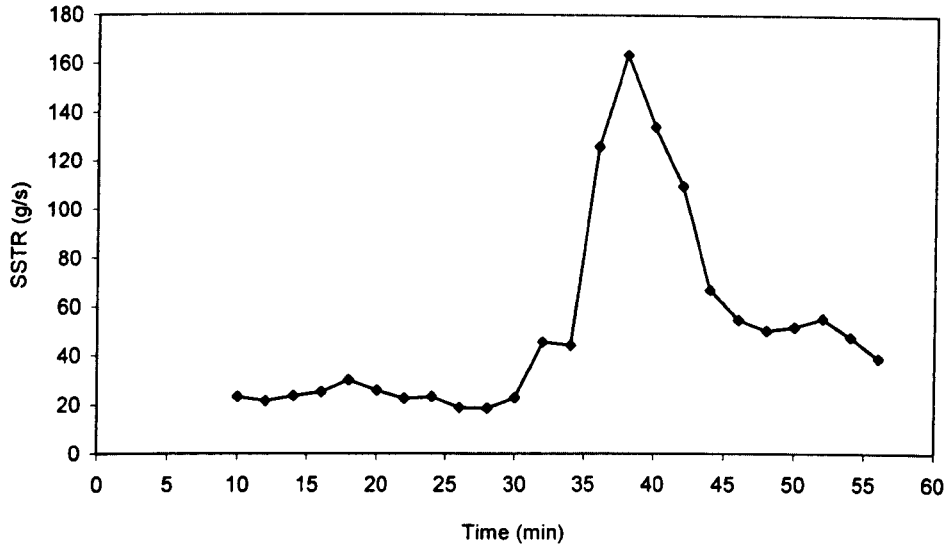

Figure 6.20: SSTR pattern from Test A (Site 2)

Figure 6.20 shows the temporal SSTR pattern during Test A. This test had an average SSTR during the dry weather portion of the test (from 10 to 30 minutes) of 23.35 g/s. During the test the transport rate rose sharply to a peak of approximately 164 g/s, followed by a gradual decline in SSTR until a stable value of approximately 39 g/s was achieved even though the flow rate was approximately constant at 0.022 m^3/s.

The status of the system prior to the flush was used to determine the background SSTR, as this would have been characteristic of the dry weather flow and the contributing sediments from the part of the system upstream of the test section (see Figure 4.6). The SSTR due to the elevated flow shown in Figure 6.21 was then determined by subtracting the ambient background SSTR, with the time-base adjusted to zero to signify the start of the increasing SSTR.

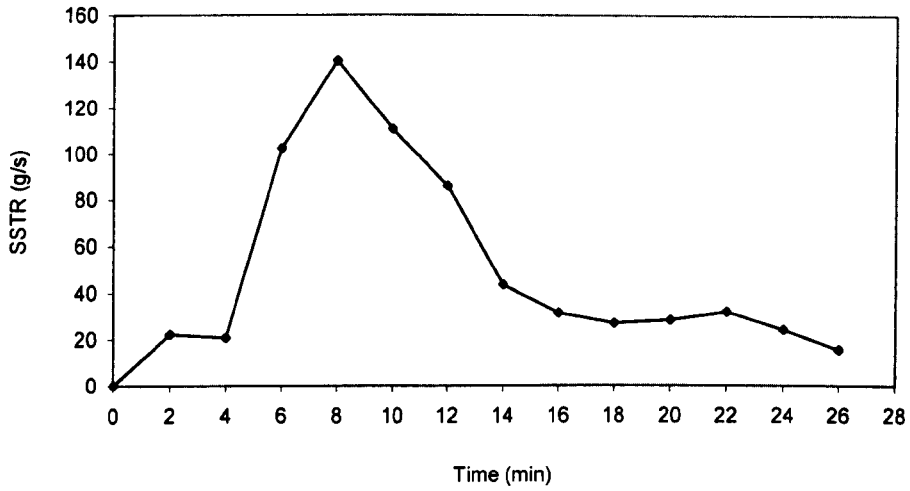

Figure 6.21: SSTR pattern at Site 2 due to increased bed shear (Test A)

Integration of the transport rate with respect to time enabled the cumulative suspended sediment load to be evaluated.

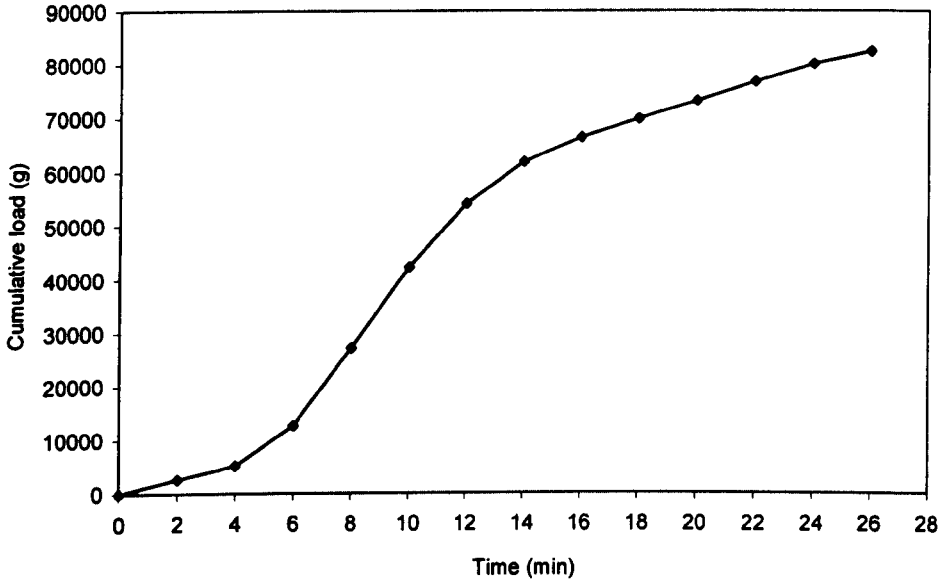

Figure 6.22: Temporal pattern of cumulative suspended load from Site 2 (Test A)

Figure 6.22 was plotted on the same time-base as Figure 6.21 as it represented the cumulative load due to the enhanced flow only, with the DWF portion subtracted. It can be seen that, in the first part of the test, 4 minutes had elapsed before the cumulative load increased significantly. After approximately 14 minutes the gradient

of the cumulative load slackens, indicating that solids were being released at a lower rate into the flow column.

6.4.7. SSTR Results (Test B – 04/06/01)

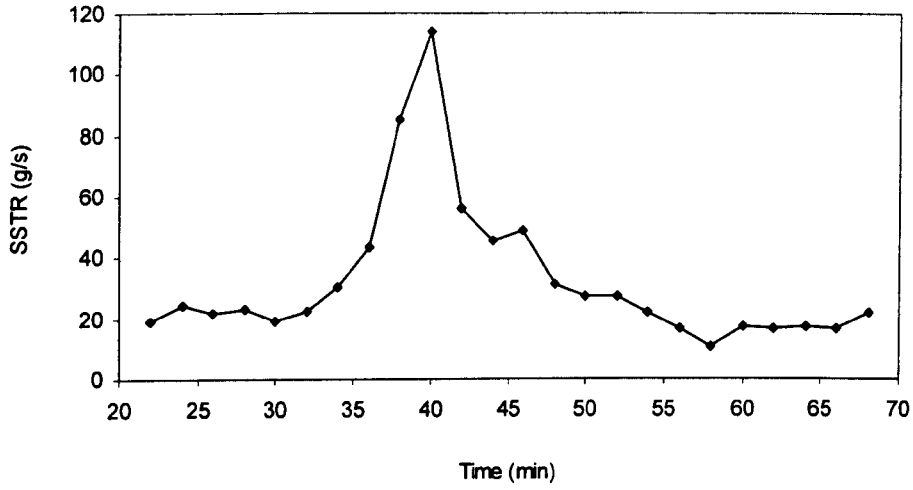

Figure 6.23: SSTR pattern from Site 2 (Test B)

The average SSTR during dry weather observed during the initial part of Test B (21.6 g/s) was of a similar magnitude to that observed in Test A (22.04 g/s). During the eroding part of this test the transport rate again rose rapidly until it peaked at approximately 114 g/s, prior to a more gradual decline to an average value of approximately 17 g/s, which was lower than the original ambient transport rate.

The status of the system prior to the flush was again used to determine the background SSTR. The cumulative load was then determined for the eroding portion of the test as indicated in Figure 6.24, with the background SSTR subtracted in order to determine the suspended load that originated from the bed during the flush event. Again the time-base was adjusted to zero to signify the start of the increasing SSTR due to the increasing flow input.

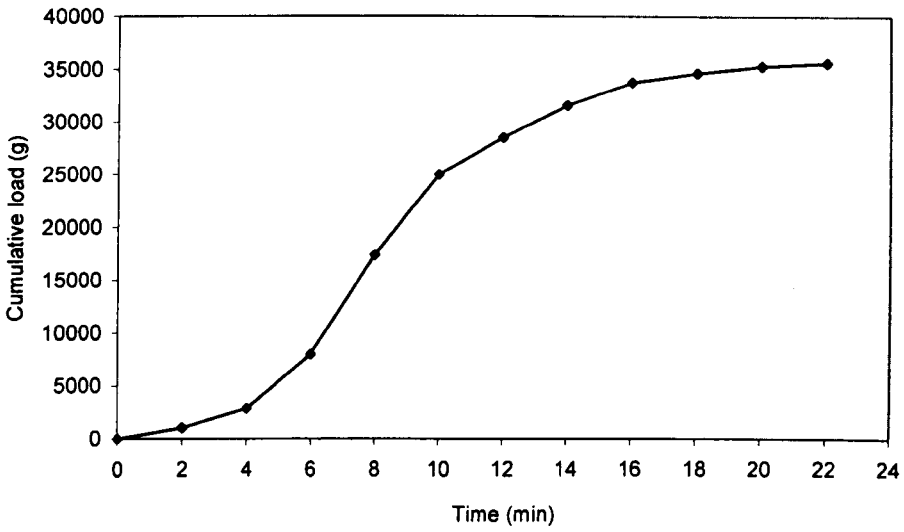

Figure 6.24: Pattern of cumulative suspended load from Site 2 (Test B)

As with Test A the load did not increase significantly until approximately 4 minutes of the eroding part of the test had elapsed, this corresponded with a rise in the bed shear stress. Again, after approximately 16 minutes the gradient of the cumulative load slackened, indicating that fewer solids were being released into the flow column. As shown in Figure 6.24 this was not due to the bed getting stronger with depth but instead corresponded with a decrease in the bed shear stress.

6.4.8. SSTR Results (Test C – 09/07/01)

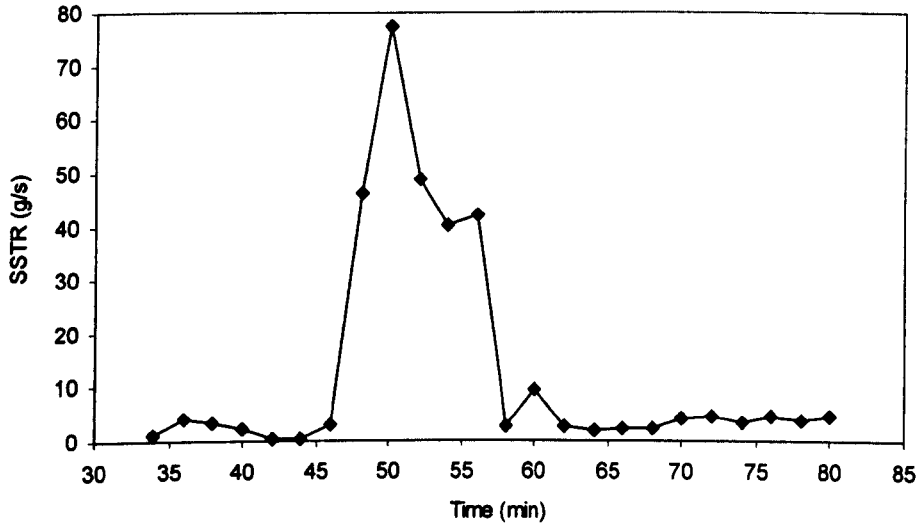

Figure 6.25: Temporal SSTR pattern from Site 1 (Test C)

During Test C the average SSTR during dry weather at Site 1 was 1.97 g/s. This was approximately an order of magnitude lower to that observed in Tests A and B in which the dry weather flow SSTR approximated to 22 g/s. Although the antecedent dry weather period (ADWP) prior to Test C was significantly less than that for Test A, it was slightly longer than for Test B so this factor could not be used to explain the different character of the bed. The contributory factor was more likely to be the dry weather shear stress (as shown in Figure 6.9) which was lower in this test than those observed in Tests A and B. During the initial part of this test the transport rate again rose until it peaked at approximately 78 g/s, prior to a more gradual decline to an average value of approximately 4.1 g/s, which was higher than the original ambient transport rate.

The cumulative load was determined for the eroding portion of the test as indicated in Figure 6.26, with the background SSTR subtracted in order to determine the suspended load that originated from the bed deposit and not from sediment contributed from upstream of the hydrant injection point.

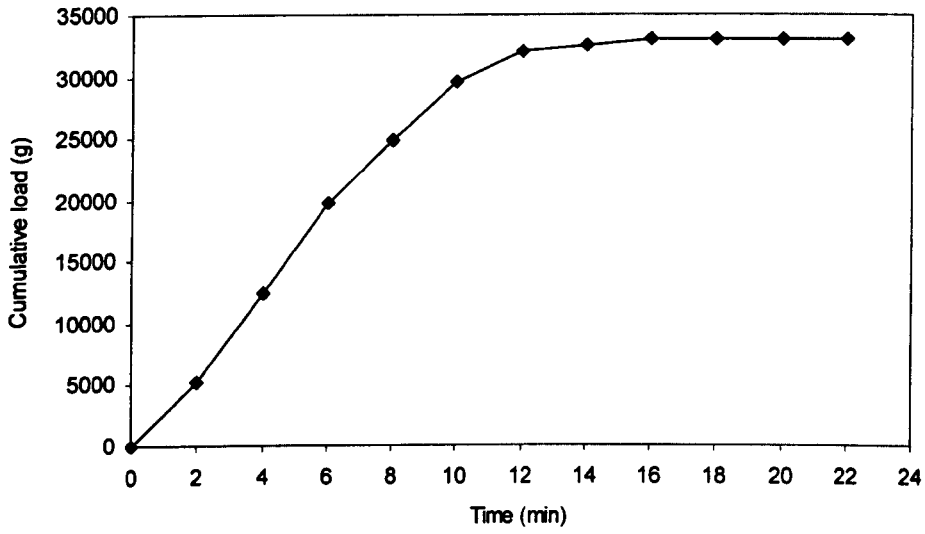

Figure 6.26: Cumulative suspended load from Test C (Site 1)

The cumulative load pattern with time differed somewhat from the pattern in Tests A and B. The cumulative load did increase immediately during the eroding part of this test. As with the previous tests the gradient of the cumulative load progressively

reduced after approximately 14 minutes, indicating that fewer solids were being released into the flow column. The cumulative suspended load yielded from Site 1 during the test was approximately 33.08 kg.

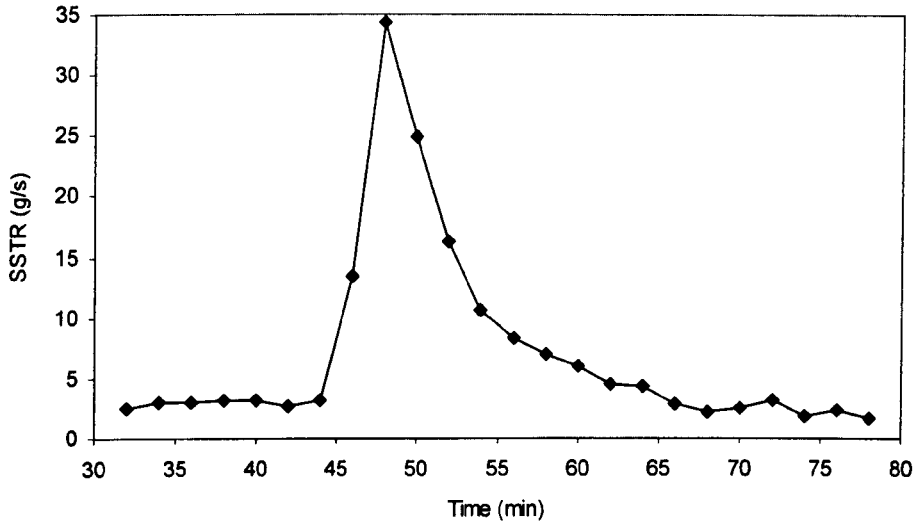

Figure 6.27: SSTR pattern from Test C (Site 2)

At Site 2 the average ambient dry weather SSTR from Test C was 2.9 g/s in comparison with the 1.97 g/s from Site 1. During the eroding part of this test the transport rate again rose until it peaked at approximately 31.5 g/s, prior to a more gradual decline which took approximately 15 minutes to reach an average value of approximately 2.25 g/s, which was slightly lower than the initial ambient transport rate.

The cumulative load was determined for the eroding portion of the test as indicated in Figure 6.28, with the background SSTR subtracted in order to determine the suspended load that originated from the bed.

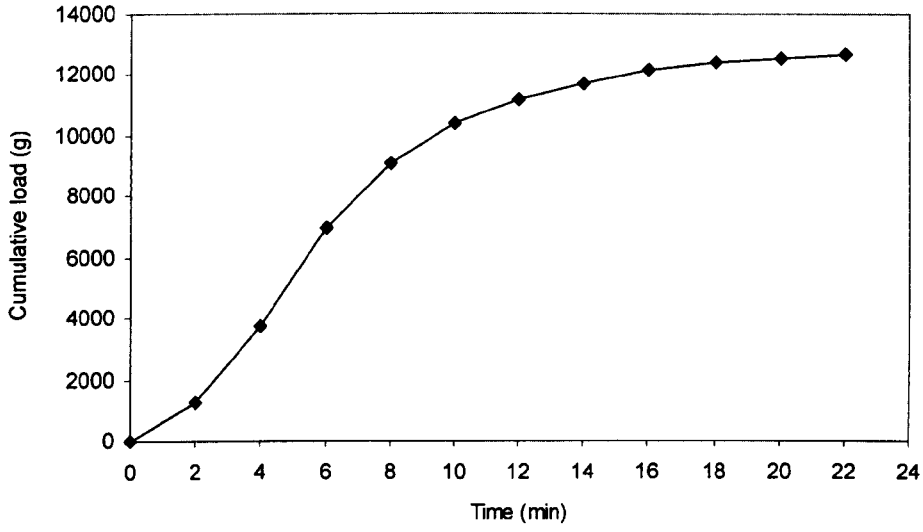

Figure 6.28: Cumulative suspended load from Site 2 (Test C)

As with Tests A and B there was an initial rise followed by a marked increase in the cumulative load during the eroding part of the test. As with the previous tests the gradient of the cumulative load reduced after approximately 14 minutes, indicating that fewer solids were being released into the flow column. The cumulative suspended load yielded from Site 2 during the test was approximately 12.67 kg. This posed a challenge to explain as it represented a net decrease of almost 20kg of suspended material between Site 2 and Site 1 approximately 45m upstream. This net loss of material in suspension may have been due to deposition occurring between Sites 1 and 2 and would equate to an increase in bed depth of approximately 2mm between the two sites.

Examination of Figure 6.27 in conjunction with Figure 6.25 showed similar ambient SSTRs at the beginning and end of the tests and would suggest this deposition occurred throughout the duration of the test with Site 1 consistently exhibiting a higher SSTR than Site 2. This deposition may have been due to a higher shear stress being exerted at Site 1 than Site 2; unfortunately this deduction cannot be verified as the hydraulic conditions during Test C were only recorded at Site 2 for the reasons outlined in Section 6.4.4. However, this hypothesis is supported by the fact that the incoming pipe to Site 1 was slightly steeper (1 in 2232) than the pipe between Site 1 and Site 2 (1 in 2275).

6.4.9. SSTR Results (Test D – 07/08/01)

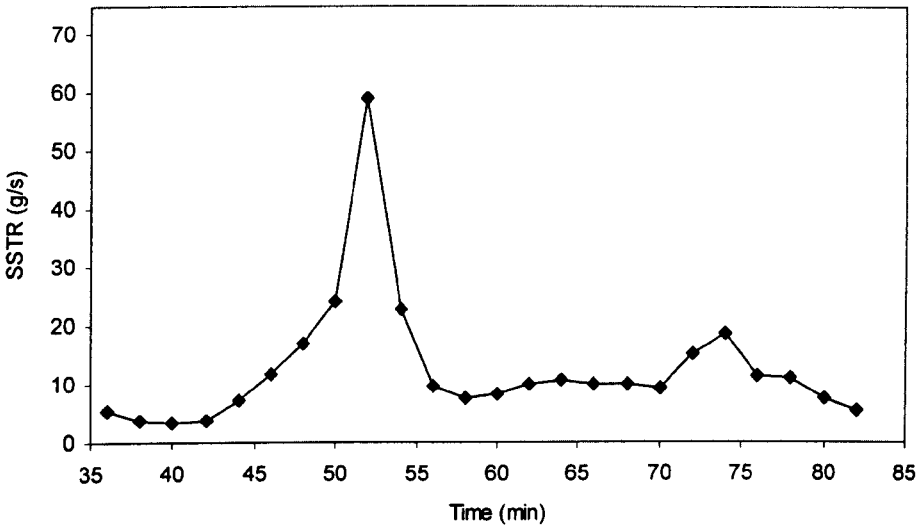

Figure 6.29: SSTR pattern from Site 1 (Test D)

At Site 1 the average ambient dry weather SSTR from Test D was 4.2 g/s, again a relatively low value that was comparable with that observed in Test C. During the eroding part of this test the transport rate again rose until it peaked at approximately 60 g/s, prior to a decline to an average value of approximately 10.6 g/s, which was higher than the initial ambient dry weather transport rate.

The cumulative load was determined for the eroding portion of the test as indicated in Figure 6.30, with the background SSTR subtracted in order to determine the suspended load that originated from the bed deposit between the hydrant injection point and Site 1.

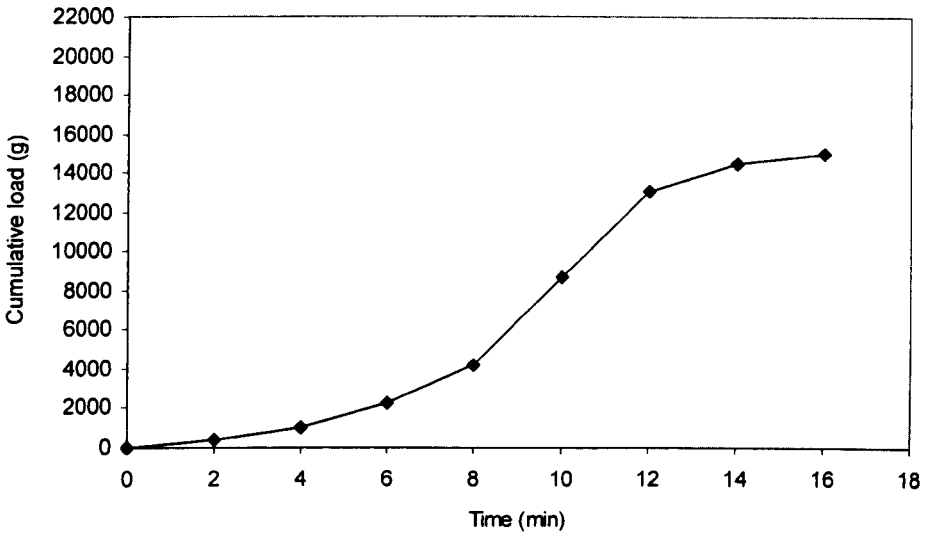

Figure 6.30: Cumulative suspended load from Test D (Site 1)

As with Tests A and B there was an initial rise followed by a marked increase in the cumulative load during the initial part of the test. In this test also the gradient of the cumulative load reduced after approximately 12 minutes, indicating that fewer solids were now being released into the flow column. The cumulative suspended load yielded from Site 1 during the test was approximately 15.1 kg.

At Site 2 the mean ambient dry weather SSTR from Test C was approximately 7 g/s. During the initial part of this test the transport rate again rose until it peaked at approximately 48 g/s, prior to a more gradual decline to a stable value of approximately 13.7 g/s, again higher than the initial ambient dry weather transport rate.

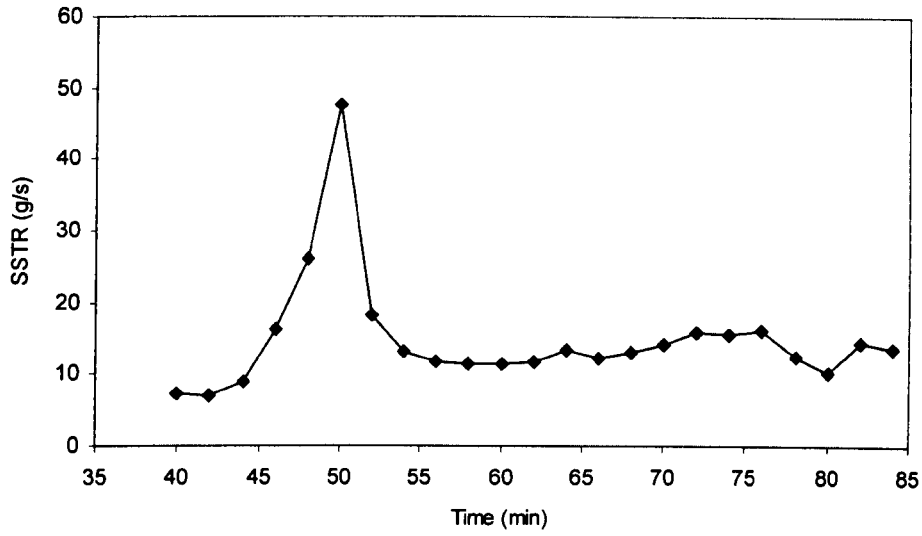

Figure 6.31: SSTR pattern from Site 2 (Test D)

The cumulative load was determined for the eroding portion of the test as indicated in Figure 6.32, with the background SSTR subtracted in order to determine the suspended load that originated from the bed.

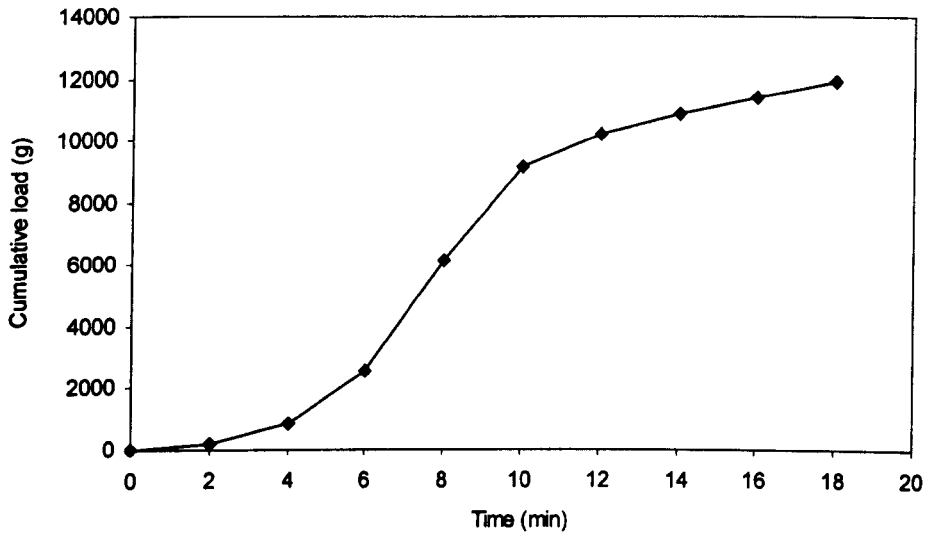

Figure 6.32: Cumulative suspended load from Site 2 (Test D)

As with Tests A and B there was an initial rise followed by a marked increase in the cumulative load during the eroding part of the test. The cumulative suspended load yielded from Site 2 during the test was approximately 11.9 kg. This represented a net decrease of approximately 3 kg of suspended material between Site 2 and Site 1

approximately 45m upstream (equating to an approximate increase in deposit depth of less than a mm). This net loss of material from the flow column provided more evidence that there was a net deposition of material between Site 1 and Site 2 during the flush tests.

6.5. General Test Observations and Erosion Thresholds

In order to investigate the critical levels of bed shear stress (τ_{cr}) the suspended sediment transport rates from each test (up to the peak value) were plotted against the corresponding bed shear stresses. These were then extrapolated back to a zero transport rate in order to determine the threshold of motion values. During the receding limb after the peak SSTR value had been exceeded it would have been useful to increase the bed shear to a level where the SSTR again started to rise. The SSTR could then have been plotted against the corresponding bed shear in order to determine the elevated critical stress value relating to the stronger material underlying the initial bed surface. Unfortunately this approach would have required a stepped hydrograph with greater flow rates. This was not possible as the hydrant was operated at its capacity and there were no further hydrants in the vicinity of the test section.

In these tests the peak SSTR usually occurred prior to the peak bed shear, suggesting that the initial bed conditions had permitted the maximum amount of solids release within the applied bed shear range. Alternatively, what could have been observed was the exhaustion of the sediment budget within the pipe resulting in the entire solids being flushed down the pipe with no more solids available from upstream to replenish the suspended load

6.5.1. Bed Shear Analysis

From the experimental data for each test that was carried out the bed shear stress (τ_{bed}) was plotted against the SSTR (up to the maximum observed value). As a result, it was readily apparent there was a discernible relationship that could be used to describe the correlation between the two parameters, and, as can be seen from Figure 6.33 overleaf, inspection of the data showed that it could be represented by a traditional power-law relationship.

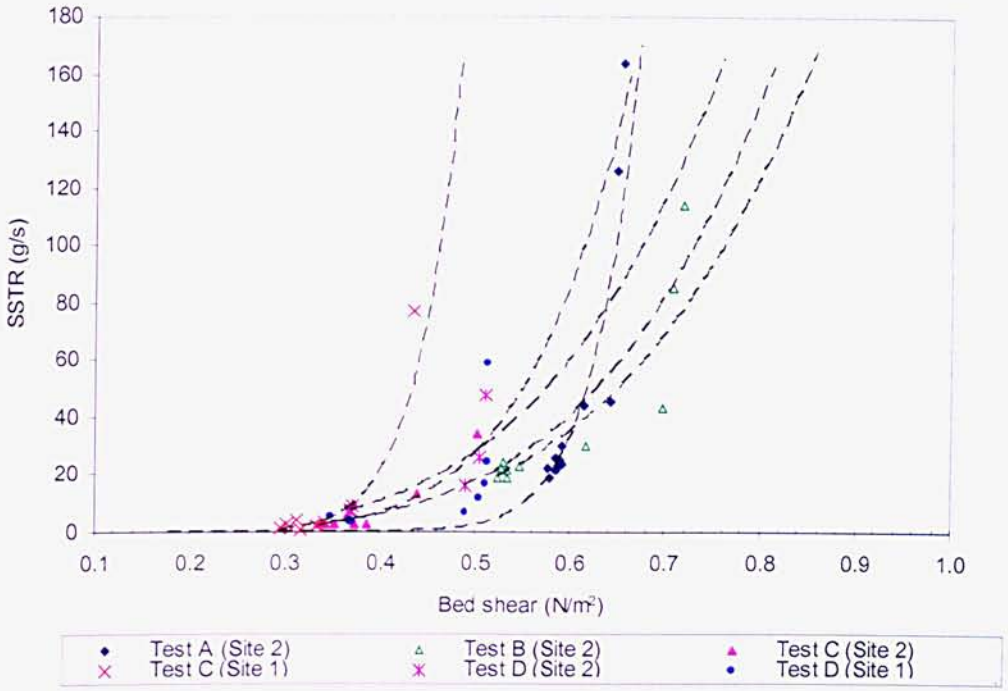

Figure 6.33: SSTR correlation with bed shear

In order to determine a critical bed shear stress the SSTR relationships had to be extrapolated to a 'negligible' transport rate. The elected limit was 2 g/s, which was chosen as it corresponded to the lowest observed average dry weather transport rate. The resulting estimates of critical bed shear stress and corresponding relationships are presented in Table 6.5.

Test	Relationship	τ_{crit} (N/m^2)	Regression Fit (R^2)
Test A (Site 2)	$S = 49539.\tau_b^{14.329}$	0.5	0.89
Test B (Site 2)	$S = 328.91.\tau_b^{4.3747}$	0.3	0.86
Test C (Site 1)	$S = 162010.\tau_b^{9.6044}$	0.31	0.39
Test C (Site 2)	$S = 2101.3.\tau_b^{6.274}$	0.33	0.91
Test D (Site 1)	$S = 421.81.\tau_b^{4.5881}$	0.3	0.68
Test D (Site 2)	$S = 532.67.\tau_b^{4.2763}$	0.27	0.86

where 'S' represents the suspended sediment transport rate (SSTR)

Table 6.5: Power law relationships between SSTR and τ_{bed}

As can be seen from Table 6.5, with the exception of Test C (Site 1), all of the relationships exhibited regression fits with an R^2 value of 0.68 or greater. Although

the estimated value of critical bed shear stress from this test seemed reasonable it was decided to reanalyse the results with the outlying data point removed (circled in Figure 6.34).

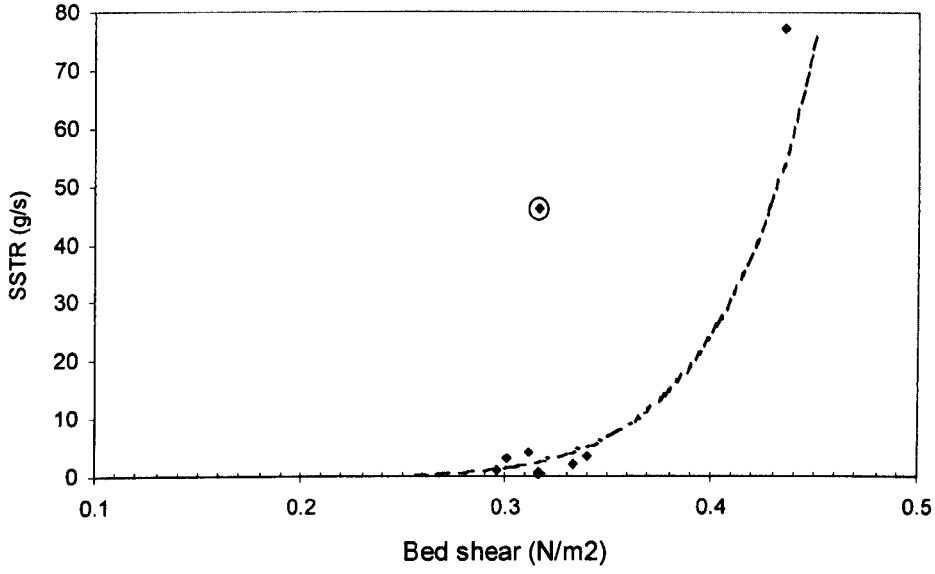

Figure 6.34: SSTR correlation with bed shear from Site 1 (Test C)

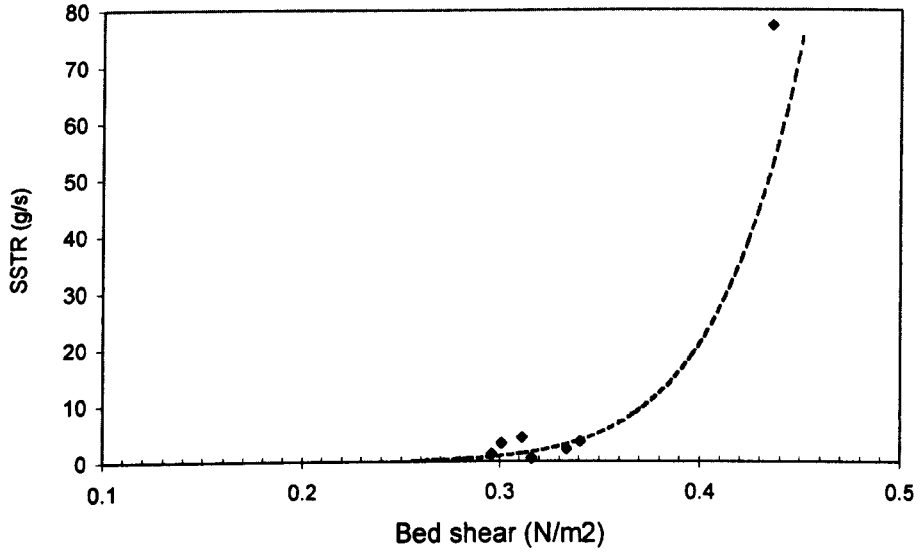

Figure 6.35: Test C SSTR correlation with bed shear from Site 1 (outlier removed)

With the outlying data point removed the relationship exhibited a better fit and the estimated critical bed shear stress was marginally altered to 0.32 N/m^2. The resulting relationship is presented in Table 6.6.

Relationship	τ_{crit} (N/m^2)	Regression Fit (R^2)
$S = 374935.\tau_b^{10.684}$	0.32	0.67
where 'S' represents the suspended sediment transport rate (SSTR)		

Table 6.6: SSTR and τ_{bed} relationship at Site 1 with outlier removed (Test C)

6.6. Further Investigations of Erosion Thresholds

The range of critical bed shear stresses (0.27 N/m^2 - 0.5 N/m^2) estimated from the observed transport data was relatively narrow. Hence it was decided to investigate further in an attempt to ascertain if a general relationship could be derived that could adequately represent the threshold of motion criteria for all tests.

6.6.1. Combined Data from all Tests

The combination of the observed data from all tests led to an overall power law relationship.

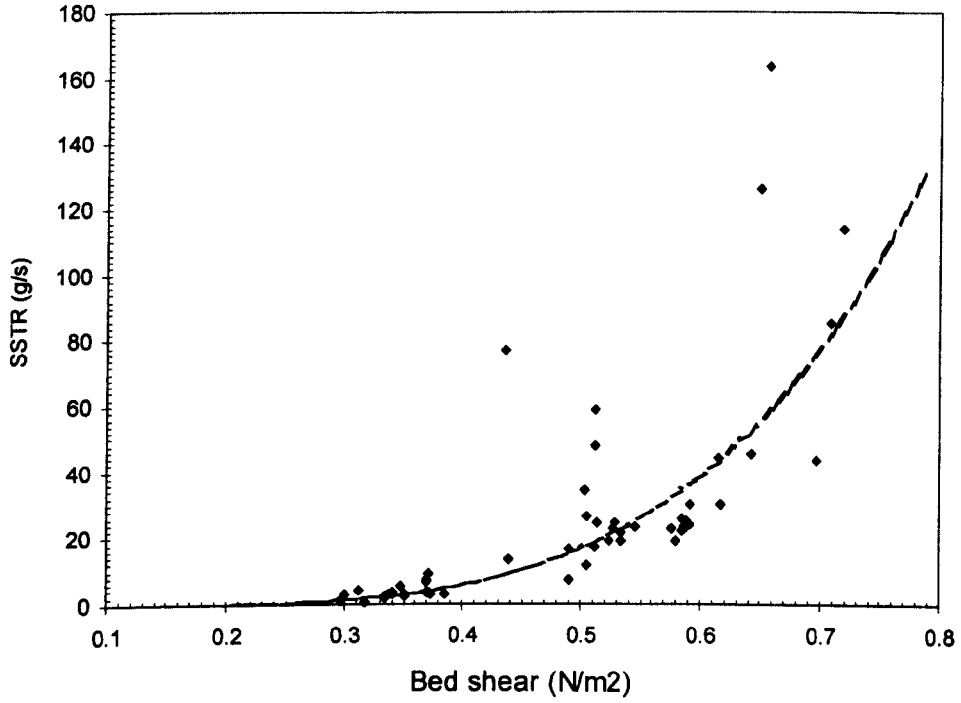

Figure 6.36: Combined results of SSTR versus bed shear stress (All tests)

Extrapolation of the data to a negligible transport rate (2 g/s) yielded an estimated critical bed shear stress of 0.3 N/m^2. The resulting relationship is presented in Table 6.7.

Relationship	τ_{crit} (N/m^2)	Regression Fit (R^2)
$S = 387.73.\tau_b^{4.5231}$	0.3	0.797
where 'S' represents the suspended sediment transport rate (SSTR)		

Table 6.7: Power law relationship between SSTR and τ_{bed} (All test data)

6.6.2. Site Specific Data

The previous analysis showed that it was possible to derive a relationship that could adequately represent the data from all tests. It was decided to investigate the combined data from both Site 1 and Site 2 separately to see if the relationships would exhibit a better fit. Site 1 data was recorded in Tests C and D whereas Site 2 data was available for all tests.

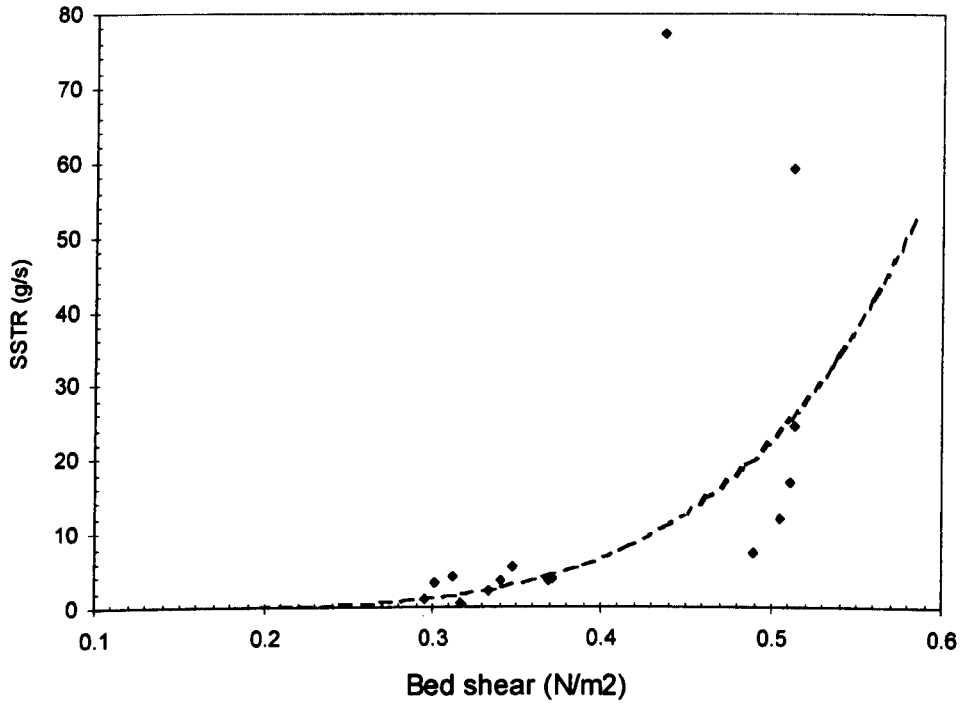

Figure 6.37: SSTR versus bed shear stress correlation (Site 1 data – Tests C & D)

As can be seen from Figure 6.37 combining the Site 1 data only from Tests C and D did not result in a stronger relationship than the combination of the entire data set.

Extrapolation of the data to a negligible transport rate (2 g/s) yielded an estimated critical bed shear stress of 0.32 N/m^2. The resulting relationship is presented in Table 6.8.

Relationship	τ_{crit} (N/m^2)	Regression Fit (R^2)
$S = 1016.3.\tau_b^{5.4969}$	0.32	0.64
where 'S' represents the suspended sediment transport rate (SSTR)		

Table 6.8: Power law relationship between SSTR and τ_{bed} (All Site 1 data)

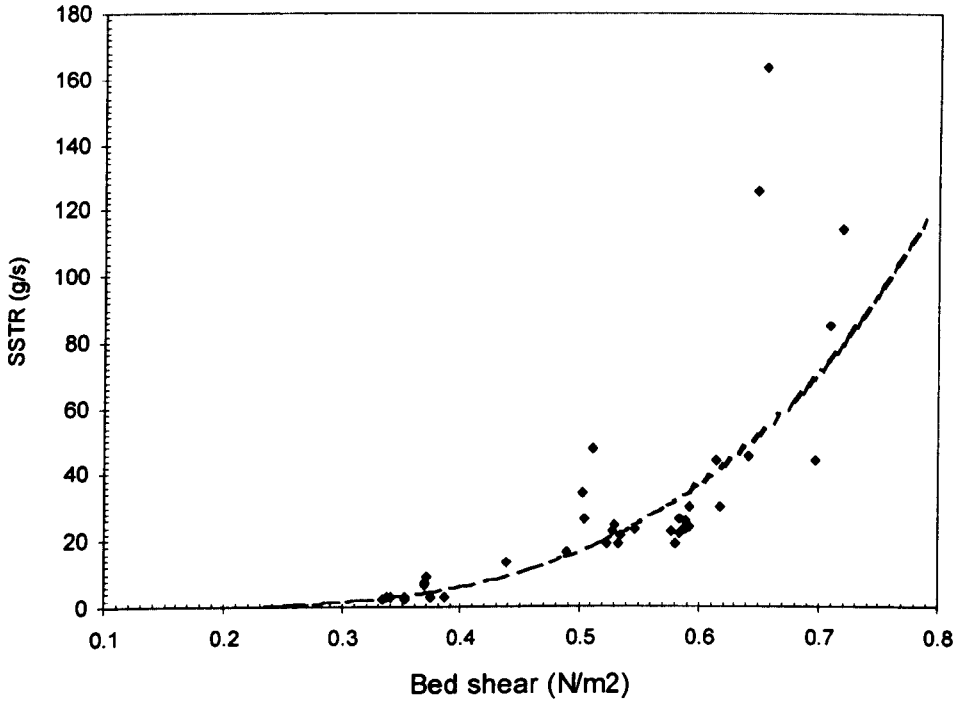

Figure 6.38: Combined results of SSTR versus bed shear stress (Site 2 – All tests)

Figure 6.38 illustrates how combining all of the Site 2 data did result in a stronger relationship than the combination of the entire data set. Extrapolation of the data to a negligible transport rate (2 g/s) yielded an identical critical bed shear stress (0.3 N/m^2) to that observed for the entire data set. The resulting relationship is presented in Table 6.9.

Relationship	τ_{crit} (N/m^2)	Regression Fit (R^2)
$S = 322.33.\tau_b^{4.2652}$	0.3	0.84
where 'S' represents the suspended sediment transport rate (SSTR)		

Table 6.9: Power law relationship between SSTR and τ_{bed} (All Site 2 data)

6.6.3. Summary of Combined Results

Table 6.10 outlines the summary of results obtained from combining the test data. It can be seen that the erosion threshold for this material was approximately 0.3 N/m^2.

Results	Relationship	τ_{crit} (N/m^2)	Regression Fit (R^2)
All results	$S = 387.73.\tau_b^{4.5231}$	0.3	0.797
Site 1 (Tests C & D)	$S = 1016.3.\tau_b^{5.4969}$	0.32	0.64
Site 2 (all tests)	$S = 322.33.\tau_b^{4.2652}$	0.3	0.84
Where: 'S' represents the suspended sediment transport rate (SSTR)			

Table 6.10: SSTR and τ_{bed} power law relationships for combined test data

6.6.4. Influence of ADWPs on Erosion Threshold Results

Although the previous analysis showed the in-pipe material in Forfar generally exhibited a critical shear stress of approximately 0.3 N/m^2, the sewer deposit present in Test A was apparently considerably 'stronger' with an estimated shear stress observed at the threshold of transport of 0.5 N/m^2. In an attempt to explain this anomaly it was decided to investigate the history of the deposits prior to the tests. It is widely believed that the antecedent dry weather period (ADWP) may significantly alter the structure of a sediment bed and impact upon its propensity for erosion. The underlying physical and/or biochemical processes that alter the 'strength' of the sediment bed are not as yet clearly understood, but may be due to a number of factors such as consolidation, biochemical processes related to the depletion of oxygen and/or other factors. Table 6.11 summarises the erosion thresholds observed in the Forfar flush tests along with the corresponding ADWPs.

Test	ADWP (hrs)	τ_{crit} (N/m^2)	Regression Fit (R^2)
A (23/05/01, Site 2)	94.9	0.5	0.89
B (04/06/01, Site 2)	23.75	0.3	0.86
C (09/07/01, Site 1)	32.72	0.32	0.67
C (09/07/01, Site 2)	32.72	0.27	0.86
Test **C** mean	32.72	0.295	n/a
D (07/08/01, Site 1)	16.93	0.3	0.68
D (07/08/01, Site 2)	16.93	0.27	0.86
Test **D** mean	16.93	0.285	n/a

where: 'ADWP' refers to the antecedent dry weather period

Table 6.11: Antecedent dry weather periods for Forfar hydrant tests

As no tipping rain gauge data was available at Forfar, the UK Meteorological Office was contacted in an effort to obtain the relevant data. The only data that the Met. Office could provide was either, tip rain gauge data from Mylnefield (National Grid Reference: NO 339301) which was approximately 20 miles south-southwest of Forfar and 31 metres above mean sea level, or hourly rain gauge data from Inverbervie (National Grid Reference: NO 839734) which was approximately thirty miles north-east of Forfar and 134m above mean sea level. Approaches for rainfall data were also made to local schools in the area, in addition to the Scottish Environment Protection Agency and the Scottish Crop Research Institute, however both organisations did not possess such data. Due to the distance of the Met. Office measurement sites from the field site it was decided to use data collected via a tipping gauge located in Dundee to estimate the ADWPs. This was not ideal but as Dundee was located approximately 15 miles southwest of Forfar this was the best option available, the rainfall corresponding to the test period is shown in Figure 6.39.

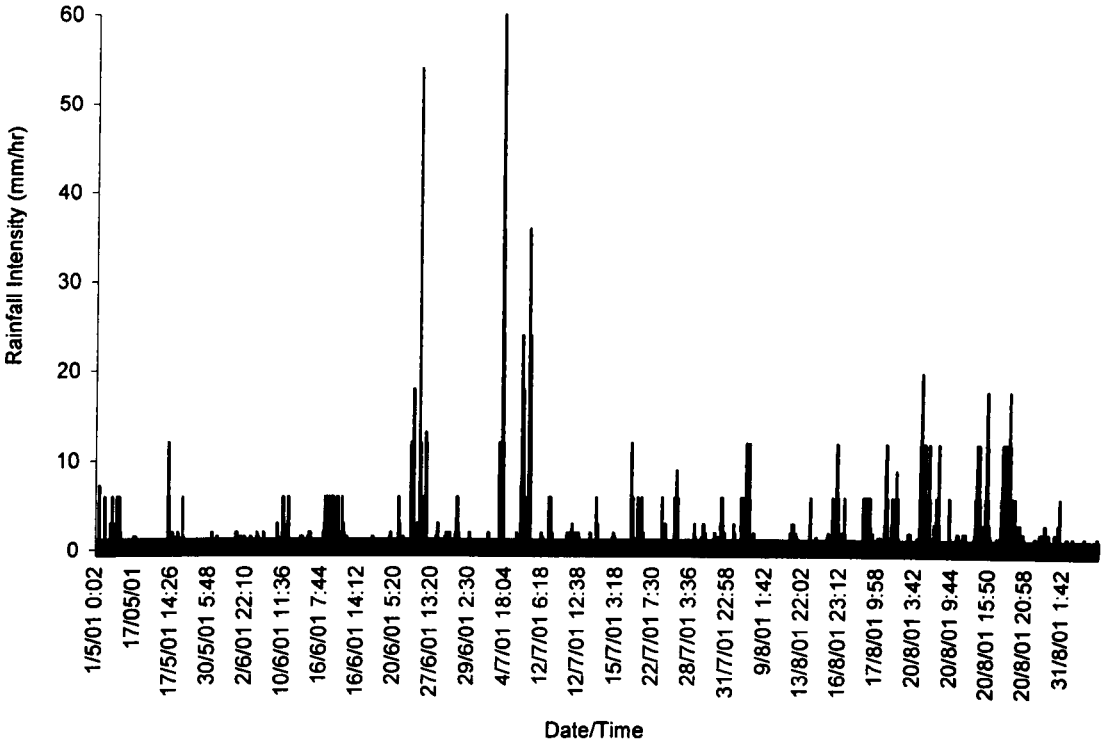

Figure 6.39: Dundee rainfall data used to determine event ADWPs

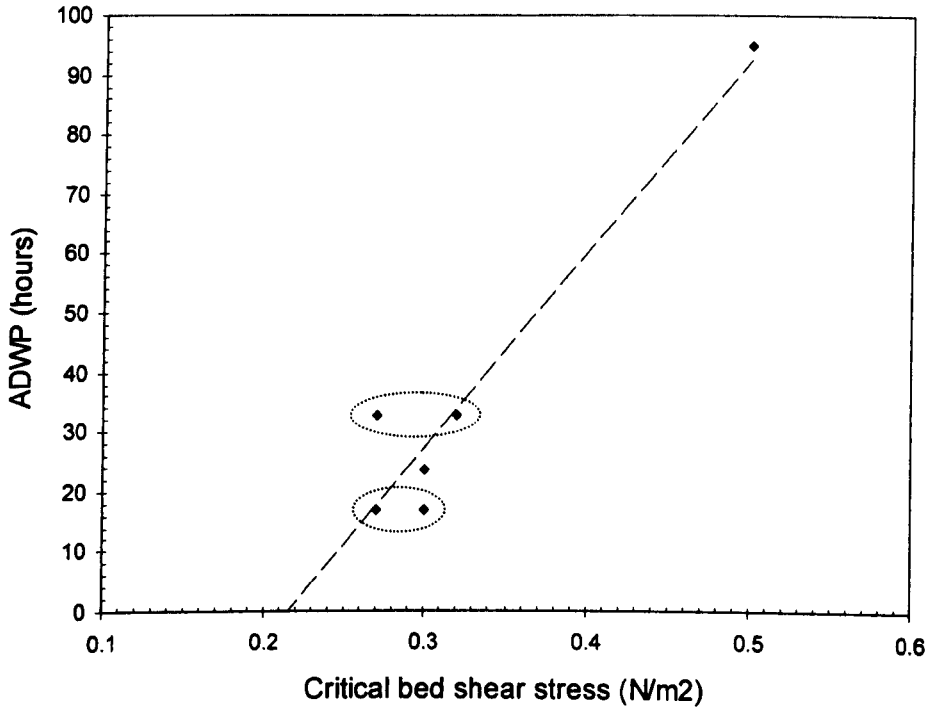

Figure 6.40: Linear relationship exhibited between ADWP and τ_{crit}

As shown in Figure 6.40 there was an apparent linear relationship between the ADWP and the observed values of shear stress at the threshold of transport. The parallel data points (encircled in Figure 6.40) represent the inclusion of data from Tests C and D when two sites were used. Given these sites were approximately only 45m apart in the same combined sewer it was deemed appropriate that the data should be reanalysed using a mean value to combine both sites.

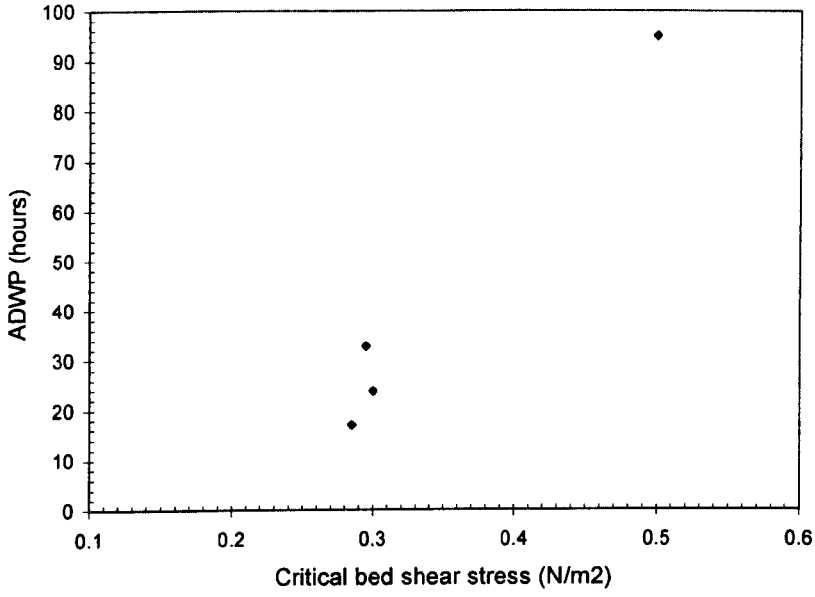

Figure 6.41: Relationship between ADWP and τ_{crit} (Site 1 & 2 combined for Tests C & D)

Using mean critical shear stress values to combine the data from Sites 1 and 2 in Tests C and D appeared to produce a linear relationship between the ADWP and the threshold shear value, although it is acknowledged that this was based on only four data points. This analysis suggests that the ADWP may have an effect on the 'strength' of a sediment deposit in a combined sewer. It is not known why this occurs or what effect varying ADWPs would have on the deposit strength. For example, it may be that although a longer ADWP initially strengthens the deposit, an even greater ADWP may actually weaken the bed due to biochemical and physical processes. The data has been summarised in Table 6.12 and illustrates the minimum critical bed shear stress that would be required to generate material transport if a fresh bed deposit was present.

Data	Min. τ_{crit} (N/m^2)	Relationship	Regression Fit
Individual site data	0.21	$\tau_{crit} = \frac{(ADWP + 69.881)}{325.12}$	0.92
Mean data used for Tests C & D	0.22	$\tau_{crit} = \frac{(ADWP + 75.487)}{341.8}$	0.98

Table 6.12: Relationship between ADWP and τ_{crit}

6.7. Analysis of Settling Velocity Data

As outlined in Section 6.4, the SSTR results showed that during the flush tests there was a net deposition of material between Site 1 and Site 2. The extraction of samples at various time-steps enabled the settlability of the material in the flow column to be determined for different stages of the tests. This would enable an assessment to be made of whether the coarser solids settled out between Sites 1 and 2, and establish whether there was any increase in the fine fraction in transport. The samples were tested using the UFT method (discussed in section 3.10.2) in order to ascertain the fall velocity distribution of the suspended sediment. As no samples were available to determine the settling velocity of the pre-eroded bed material Stokes (1851) law was applied to achieve an estimated fall velocity distribution of the parent bed material.

6.7.1. Determination of Fall Velocity of Original Bed Material

In order to be able to compare the distribution of the fall velocity of the eroded material at various stages of the flush test with that of the original bed material it was first necessary to determine an average fall velocity distribution for the pre-eroded bed. Sedimentation methods for evaluating particle size distributions take advantage of the fact that large particles in a liquid suspension settle more quickly than small particles. Stokes' Law (Stokes, 1851) relates the terminal velocity of a spherical particle to its diameter. As non-spherical particles have a lower mean terminal velocity than spherical particles of equivalent volume sedimentation methods of particle size measurement based on Stokes' Law will undersize non-spherical particles.

Van Rijn (1993) outlined the following formulae based on Stokes law for evaluating the terminal fall velocity of non-spherical sediment particles.

$$w_s = \frac{(s-1)gd^2}{18\nu} \qquad \text{when: } 1 < d \leq 100\ \mu m \qquad (6.10)$$

$$w_s = \frac{10\nu}{d}\left[\left(1 + \frac{0.01(s-1)gd^3}{\nu^2}\right)^{0.5} - 1\right] \qquad \text{when: } 100 < d \leq 1000\ \mu m \qquad (6.11)$$

$$w_s = 1.1[(s-1)gd]^{0.5} \qquad \text{when: } d > 1000\ \mu m \qquad (6.12)$$

where:

w_s = fall velocity (m/s)

ν = kinematic viscosity (m^2/s) [$1x10^{-6}$ for water]

g = acceleration due to gravity (9.81 m/s^2)

d = sieve diameter (m)

s = specific gravity (= 2.65)

Using the aforementioned approach it was not only possible to derive fall velocity distributions for the original bed deposit samples that were collected during periods of dry weather, it was also possible to estimate particle sizes for the material in suspension. The particle size distributions for these samples are shown in Figure B.1 through to Figure B.7 in Appendix B with the w_{s50} values summarised in Table 6.13.

Site	Sample Date	w_{s50} (mm/s)
1	14/06/01	0.78
2	14/06/01	0.63
2	16/07/01	0.7
1	24/07/01	0.68
2	24/07/01	0.5
Upstream manhole	24/07/01	1.08
2	01/08/01	0.59

Table 6.13: Fall velocity values of suspended material sampled during dry weather

In order to provide a 'benchmark' distribution, against which the eroded particles could be compared, the profiles of the 'parent' deposit material were combined to yield a mean fall velocity distribution as shown in Figure 6.42. The mean settling velocity distribution for the initial Forfar bed material had a w_{s50} of 0.69 mm/s.

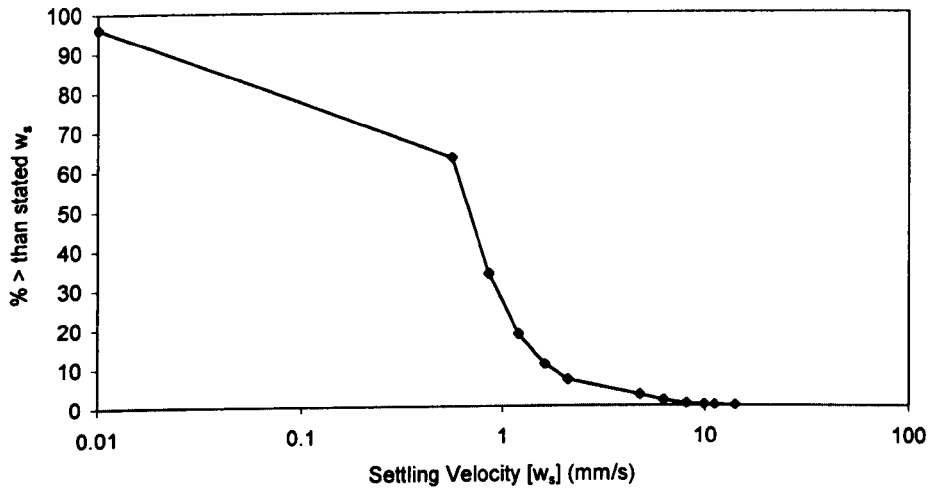

Figure 6.42: Estimated mean fall velocity distribution of Forfar bed material

6.7.2. Fall Velocity Distribution Profiles from Flush Events

It was decided not only to compare the w_{s50} values of the samples extracted during the tests but also the shape of the profiles. It was hoped this approach would provide some idea of the dynamics of the erosion and transport system to investigate, for example, if there was some form of particle selection taking place or if all particles had an equal chance of being eroded and thus transported (equal mobility). This

information would be invaluable when modelling the erosion events, as it would dictate whether it would be necessary to model the sediment population within the deposit as a series of fractions or by using a single representative parameter.

6.7.2.1. *Fall Velocity Distribution from Test A (23/05/01)*

As previously described, the first hydrant-induced flush event was carried out on 23rd May 2001 in Forfar.

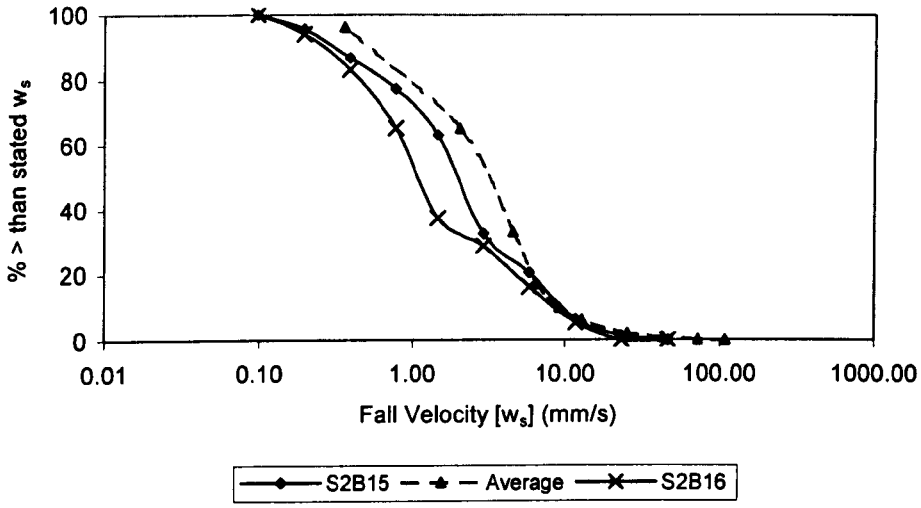

Figure 6.43: Fall velocity distributions from hydrant test (23/05/01)

The name allocated to each distribution refers to the location and sequence in which it was extracted. For example, S2B15 refers to TSS sample number 15, extracted from the Site 2 sampling point. In order to deduce whether any particle selection was taking place during the flush events the w_{s50} relative to the prevailing shear stress was deemed to be the most significant data and has been collated in Table 6.14.

Distribution	Test Time (min)	Sample Height (mm)	Prevailing τ (N/m^2)	w_{s50} (mm/s)
S2B15	38	30	0.655	2.09
S2B16	40	30	0.660	1.15
Mean	N/A	Bed sample	N/A	0.69

Table 6.14: Key fall velocity data from Test A (23/05/01)

Figure 6.44 illustrates the chronology of the fall velocity samples in relation to the flush event.

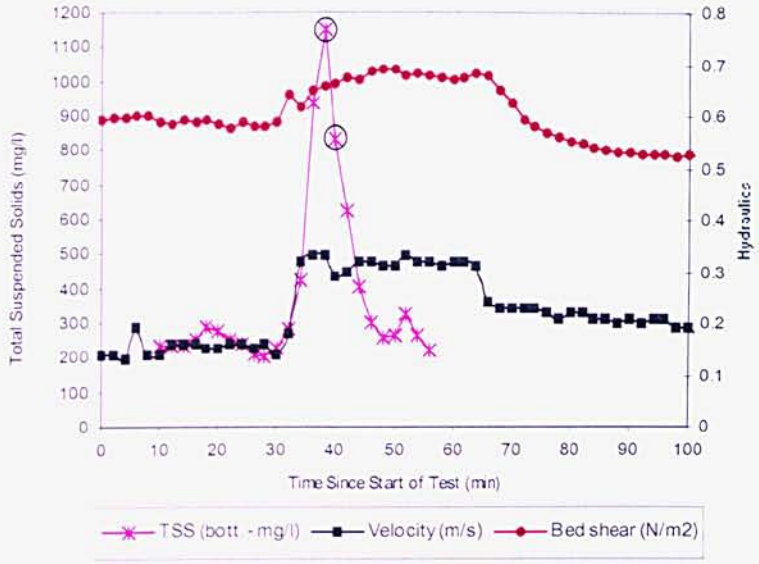

Figure 6.44: Location of fall velocity samples in flush test (circled)

6.7.2.2. *Fall Velocity Distributions from Test B (04/06/01)*

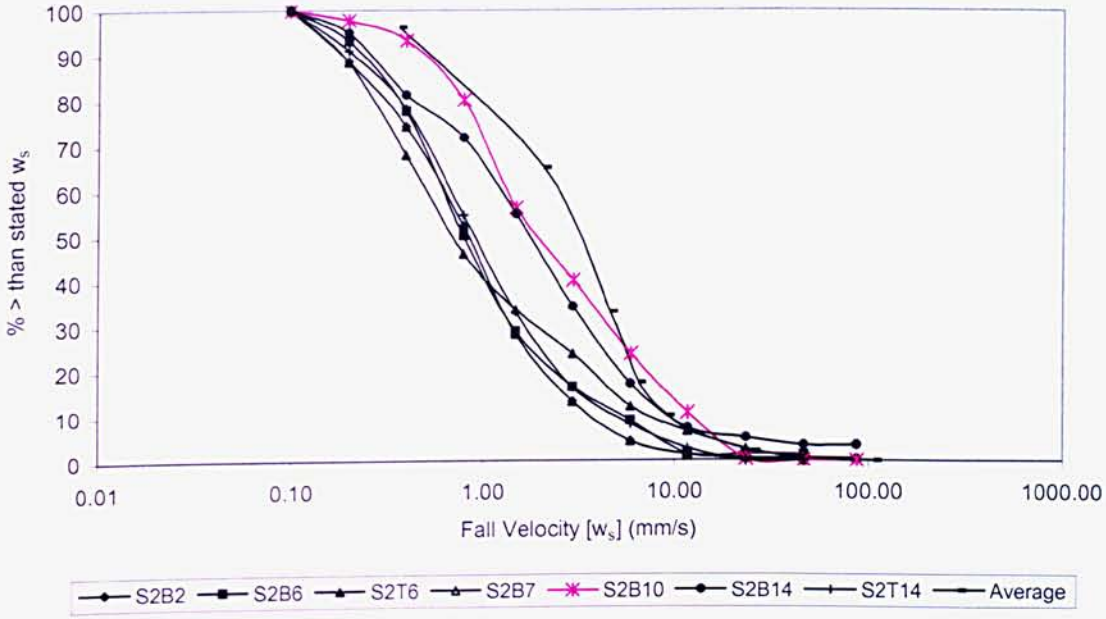

Figure 6.45: Fall velocity distributions from hydrant test (04/06/01)

The significant data pertaining to this test has been collated in Table 6.15 showing the changes in the w_{s50} relative to the prevailing shear stress at a particular time step.

Distribution	Test Time (min)	Sample Height (mm)	Prevailing τ (N/m^2)	w_{s50} (mm/s)
S2B2	24	30	0.529	1.39
S2B6	32	30	0.528	0.78
S2T6	32	50	0.528	0.71
S2B7	34	30	0.618	0.84
S2B10	40	30	0.718	2.01
S2B14	48	30	0.753	1.81
S2T14	48	50	0.753	0.93
Average	N/A	Bed sample	N/A	3.22

Table 6.15: Key fall velocity data from Forfar flush test (04/06/01)

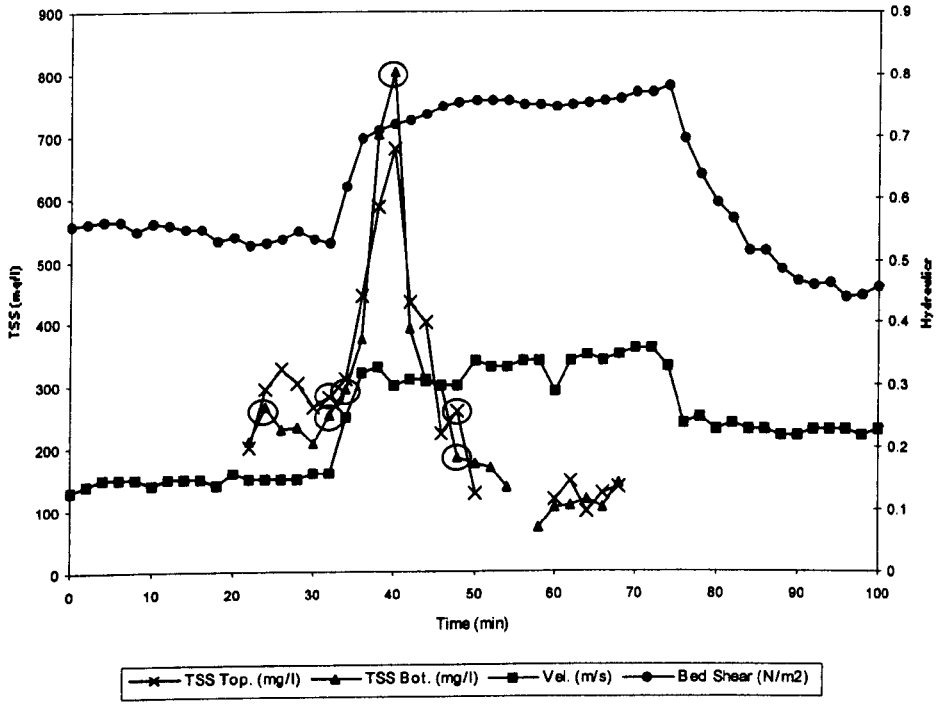

Figure 6.46: Location of fall velocity samples in flush test (circled)

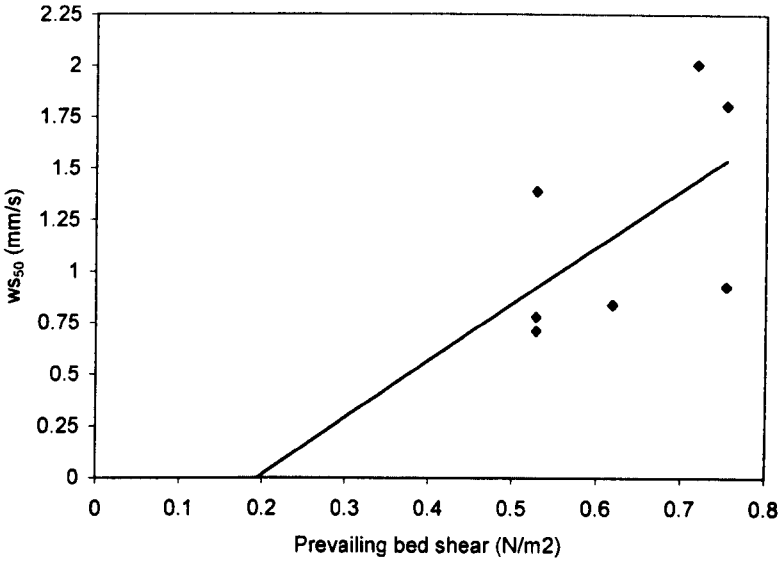

Figure 6.47: Relationship between w_{s50} and prevailing stress

Given that more samples from this test had been analysed for fall velocity it was possible to examine whether any trend existed between w_{s50} and the applied bed shear stress as shown in Figure 6.47. As outlined by the regression fit shown in Table 6.16 there was only a weak correlation between the two parameters.

Relationship	Regression Fit (R^2)
$w_{s50} = 2.7618.\tau - 0.5367$	0.313

Table 6.16: Relationship between w_{s50} and prevailing bed shear stress

6.7.2.3. *F all Velocity Distributions from Test C (09/07/01)*

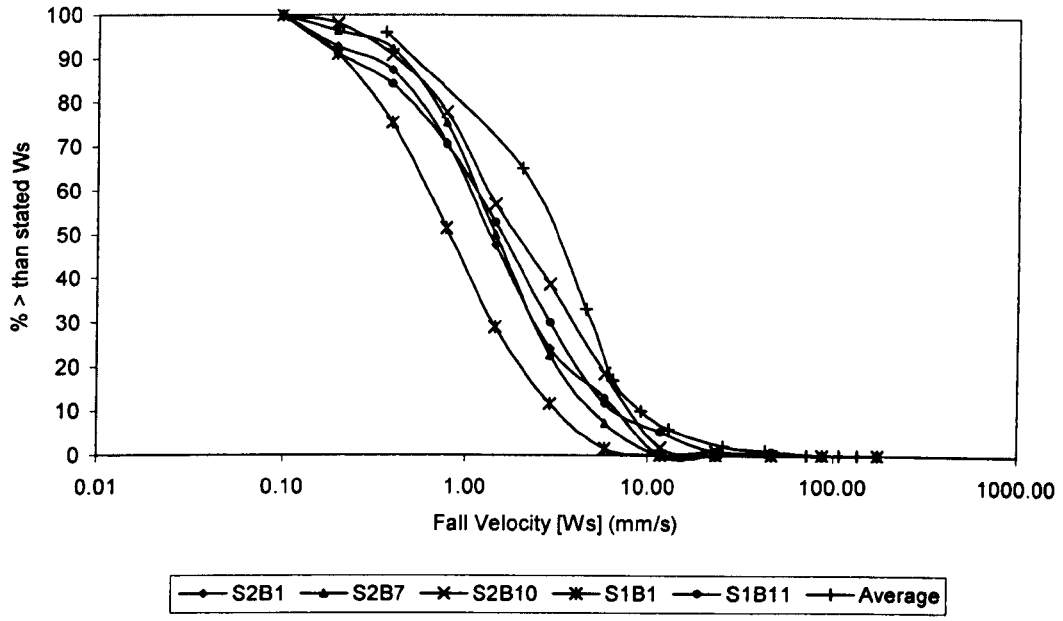

Figure 6.48: Fall velocity distributions from Test C (09/07/01)

The significant data pertaining to this test has been collated in Table 6.17.

Distribution	Test Time (min)	Sample Height (mm)	Prevailing Tau (N/m^2)	W_{s50} (mm/s)
S2B1	32	30	0.334	1.40
S2B7	44	30	0.337	1.46
S2B10	50	30	0.514	2.03
S1B1	34	30	0.296	0.81
S1B11	54	30	0.538	1.65
Average	N/A	Bed sample	N/A	3.22

Table 6.17: Key fall velocity data from Forfar flush test (09/07/01)

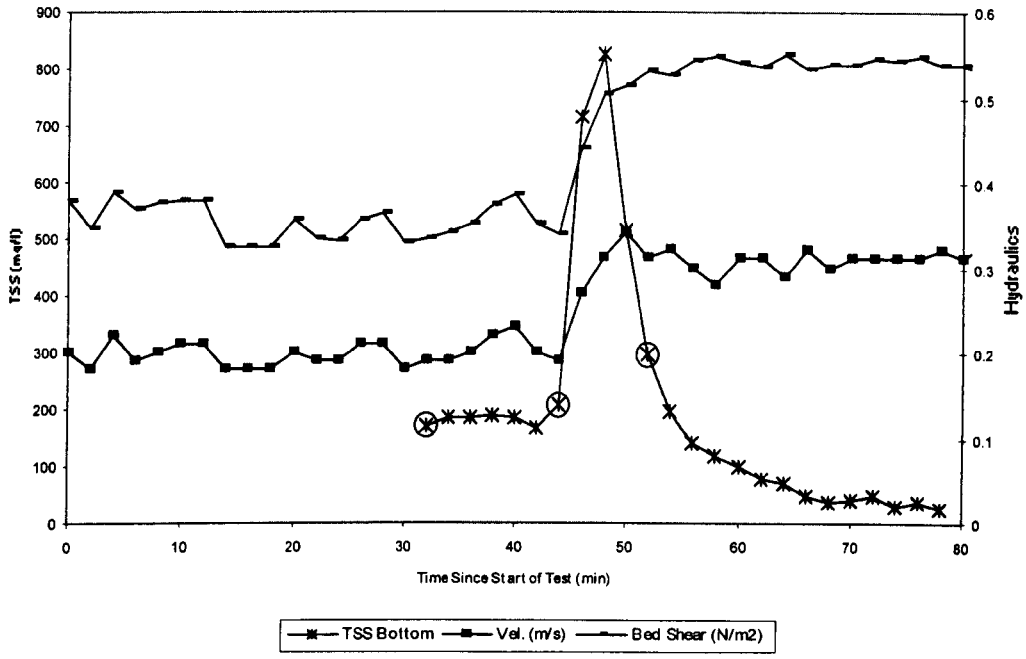

Figure 6.49: Location of Site 2 fall velocity samples in flush test (circled)

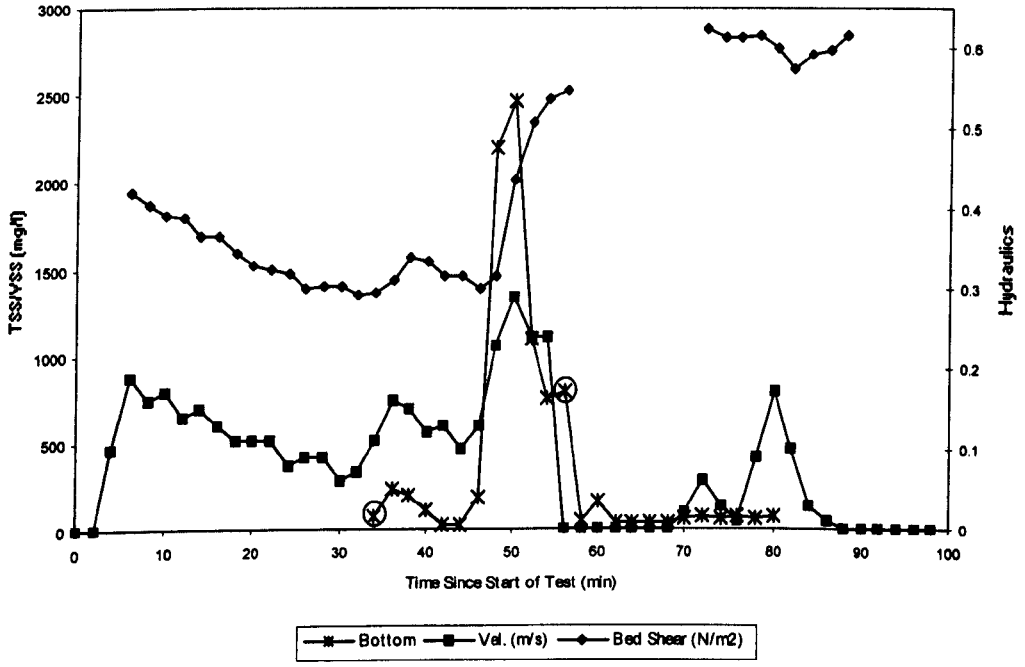

Figure 6.50: Location of Site 1 fall velocity samples in flush test (circled)

As with the previous test it was possible to examine whether any trend existed between w_{s50} and the applied bed shear stress as shown in Figure 6.51. Again when all points were considered there was a weak trend, and this did not intersect the τ axis. When the two outliers (circled in Figure 6.51) were removed, even though there were now only three data points, the fit was much stronger and did dissect the τ axis (see Figure 6.52). As before, two outlying points were sampled after the peak SSTR had been exceeded and therefore it was pertinent they be removed from the analysis (although as this only left 3 data points the resulting relationship was not deemed to be reliable).

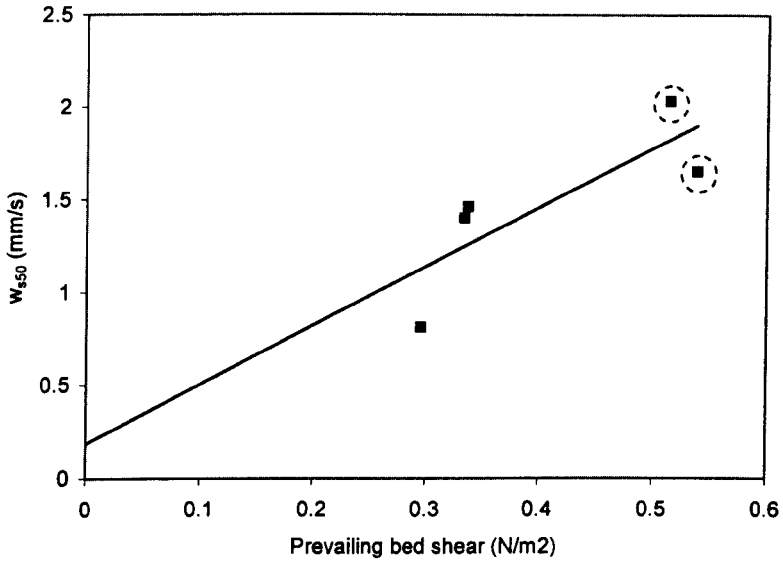

Figure 6.51: Relationship between w_{s50} and prevailing stress

The relationship between w_{s50} and the applied bed shear is summarised in Table 6.18 with the revised relationship (outliers removed) shown in Figure 6.52.

Trend Fit	Relationship	Regression Fit (R^2)
All data points	$w_{s50} = 3.1809.\tau - 0.1856$	0.657
Outliers removed	$w_{s50} = 15.715.\tau - 3.8421$	0.9997

Table 6.18: Relationship between w_{s50} and prevailing bed shear stress

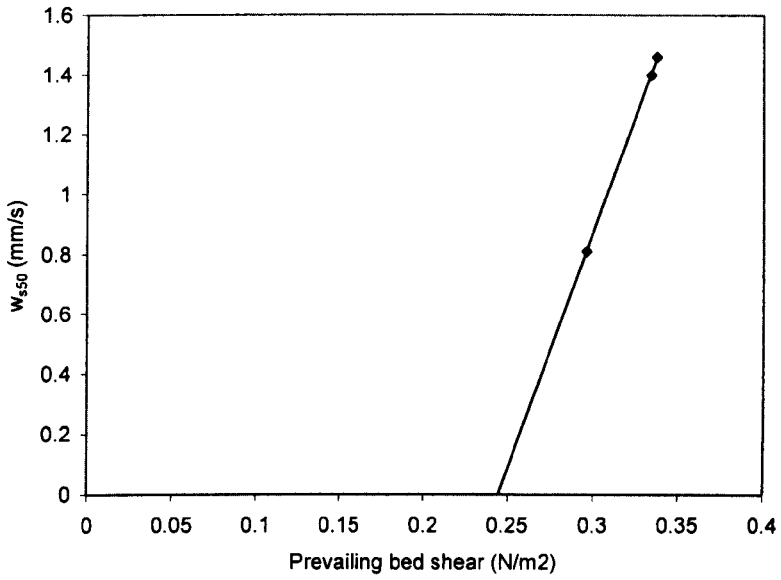

Figure 6.52: Relationship between w_{s50} and prevailing stress (outliers removed)

It was decided to look at the data (up to the peak transport rates) for all the tests. As can be seen in Figure 6.53, two distinct trends were evident. Given that the first trend (circled) corresponded with Test C which had a significantly longer ADWP, it may be that due to some physical or biochemical processes taking place within the sediment this may actually have contributed to a 'weaker' bed.

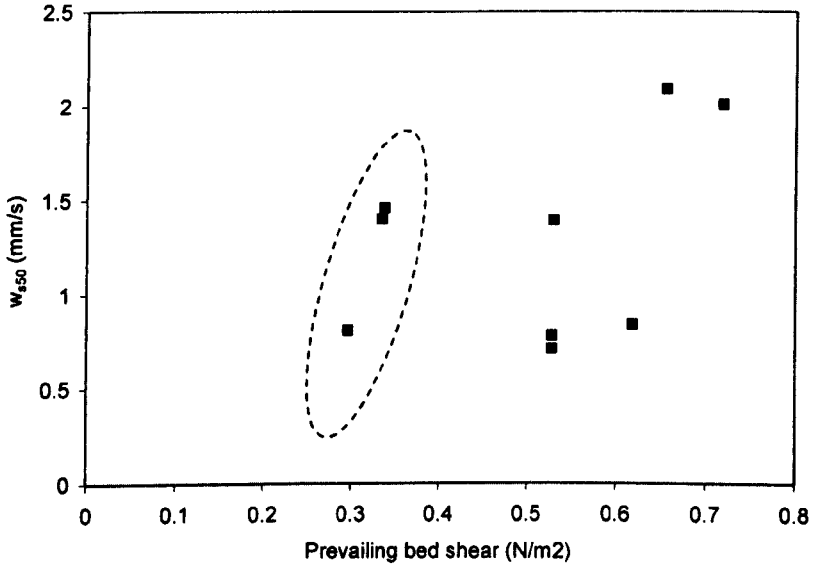

Figure 6.53: Relationship between w_{s50} and prevailing stress (all tests)

6.8. Further Particle Mobility Investigations

Section 6.4 illustrated how the SSTR results could be used to evaluate the manner in which the bed deposit behaved as an entire mixture. Given there was evidence available to suggest that the entrainment process was size selective it was decided to estimate the critical shear stresses at the threshold of motion for each of the individual size fractions within the mixture and see how this compared with the threshold value of shear stress for equivalent sizes of uniform sediment. Although the previous analysis was useful in determining whether there was any general trend between the applied bed shear stress and the w_{s50} values, it did not distinguish between the individual fractions within the mixture. In order to gain a better understanding of how the individual fractions were behaving within the mixture it was decided to check for any evidence of selective entrainment taking place. In an attempt to evaluate the threshold shear stresses for each of the individual fractions, the transport rate corresponding to each of the fall velocity fractions (i.e. the SSTRi) was plotted against the prevailing bed shear stress as shown in Figure 6.54, where ws1 to ws9 refers to a particular suspended material fraction as described in Table 6.19.

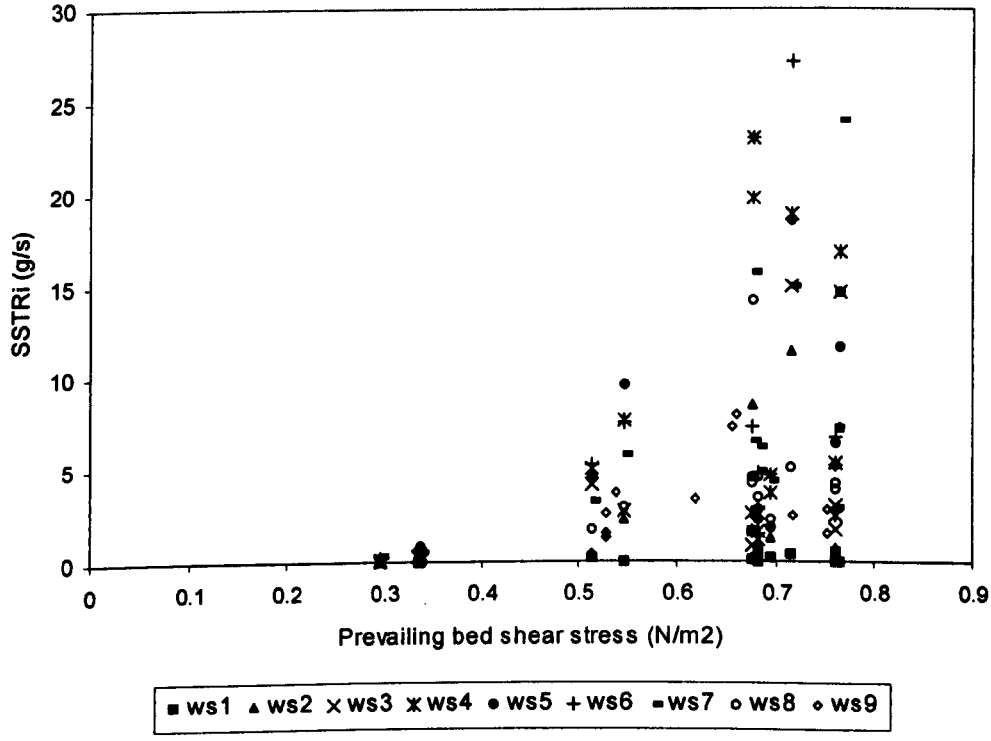

Figure 6.54: Relationship between fraction-wise SSTR and applied shear stress

The suspended material fractions ($ws_{i\,[1\text{-}9]}$) were distributed as shown in Table 6.19.

ws_i	w_s (mm/s)	Stokes Equivalent Particle Size (mm)
1	23.33	27.79
2	11.67	6.95
3	5.83	1.74
4	2.92	0.43
5	1.46	0.37
6	0.78	0.19
7	0.39	0.12
8	0.19	0.088
9	0.10	0.075

Table 6.19: Suspended material fractions

In order to investigate the mobility of the individual fractions within the mixture the settling velocity distributions were converted to equivalent particle sizes using Stokes Law (see Equations 6.10-6.12). As this methodology assigned a particular particle size to a corresponding settling velocity any flocs that may have formed would have been treated as an equivalent single particle size.

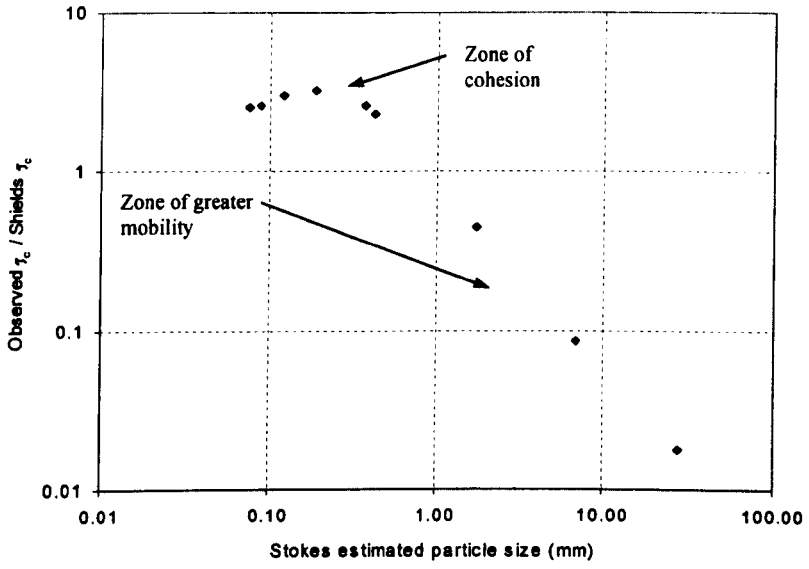

Figure 6.55: Fractionwise ratios of observed critical shear stress to Shields critical shear stress

The measured suspended sediment transport data from the Forfar tests was extrapolated to give the critical bed shear stress relative to each of the individual fractions. These were then plotted as a ratio of the equivalent Shields critical shear stress for that particular particle size had it been a uniform deposit. The results of this analysis (shown in Figure 6.55) showed two distinct zones of mobility. When the ratio of shear stresses was less than unity for a particular fraction this implied those particles were more mobile than would have been expected had those particles been present within a uniform deposit. As shown in Figure 6.55 this was the case for particles whose size exceeded 1mm, whereas particles finer than this value behaved in a more cohesive-like manner as they exhibited a lower mobility than would have been expected had they been part of a uniform deposit size.

6.9. Discussion of Results

The results of the tests highlighted the complexities associated with sediment transport within a combined sewer. Even in the relatively short test section (178m) it was demonstrated that the processes of erosion and net deposition occurred simultaneously during the flush tests. The results showed that pure erosion took place from the hydrant injection point to Site 1, with a *net* deposition of material occurring between Site 1 and Site 2. Figure 6.56 illustrates the particle size distributions estimated from the fall velocity distributions from suspended samples extracted during Test C. These samples, extracted after the peak SSTR had been exceeded (see Figures 6.49 and 6.50), demonstrated that the amount of fine material increased between Site 1 and Site 2; this material could only have been eroded from the bed. Given there was a net decrease in the amount of material in transport between Sites 1 and 2, this supported the supposition that deposition occurred as the coarser sediment must have been deposited in order to balance the increase in observed finer material in the flow. Given that the fall velocities were estimated however, it is acknowledged that this hypothesis should be treated with caution.

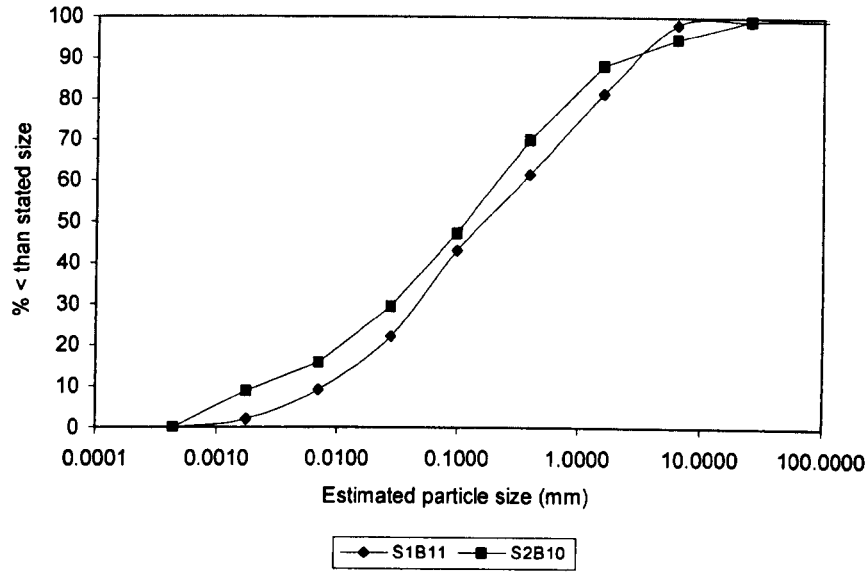

Figure 6.56: Composition of material in flow column (Test C)

It was evident from Figures 6.43, 6.45 and 6.48 that in all of the tests there was a tendency for the w_s values to increase as the test progressed in line with the increasing shear stress. The average w_s distribution of the deposit material was also higher than that for the material extracted from the flow column. This is to be expected, as this would suggest that the density and/or size of the material in the bed might have been greater than that in the flow column. This may also have been caused by the bed sample being extracted from the surface all the way through to the invert, whereas the material in suspension may possibly have originated from the surface of the bed only, depending on the prevailing shear at that time.

In addition, the results from this study exhibited a tendency for the critical bed shear stress to increase linearly, in line with an increase in the ADWP; however, as already acknowledged, this was based on only four data points. This apparent relationship between the ADWP and the 'strength' of an in-sewer deposit may in part be due to a bed stabilising effect due to bio-agglutination. As reported by De Sutter (2001), the influence of biology is believed to be capable of increasing the critical bed shear stress of a deposit by up to 0.13 N/m^2 due to the influence of algae and micro-organisms. However, it is recognised that a great deal more investigative work would be required before such a hypothesis could be supported.

In tests carried out by Rushforth (2001) it was found that a linear relationship existed between the SSTR and the bed shear stress. Rushforth's tests were conducted using deposit material which was comprised entirely of olivestone, and also mixtures of olivestone/sand and clay/sand. Conversely, from this study, the general form of the proposed relationship between SSTR and bed shear stress was represented by a power-law relationship as follows:

$$SSTR\ (g/s) = a\ [\tau_{bed}\ (N/m^2)]^{b} \qquad (6.13)$$

As reported in Table 6.20, from the analysis carried out using a combination of all available test data the values of the coefficient 'a' and the exponent 'b' in the proposed relationship were determined as 387.7 and 4.52 respectively.

Data Used	a	b	R^2
Site 1 (data available from Tests C & D only)	1016.3	5.5	0.64
Site 2 (data available from all tests)	322.3	4.3	0.84
Combined	387.7	4.52	0.8

Table 6.20: Coefficients established for transport rate/shear stress relationship

The form of this relationship is similar to that originally proposed by Mehta *et al.* (1989) for dense, uniform cohesive beds, as reported by De Sutter (2001); and, given this relationship was borne from tests carried out in real sewers, it is suggested that the coefficients from this relationship should form an integral part of any further investigations utilising real sewer sediments.

In order to test whether the proposed coefficients may be site specific, it would be a useful exercise to apply this form of relationship to a range of different sediments from sewers across Europe. This type of exercise would determine whether a series of coefficients could be derived for a range of sediment compositions and conditions, dependant upon variables such as w_{s50}, d_{50}, and ADWP.

Chapter Seven – Evaluation of the Ackers (1991) Model

7.1. Introduction

In order to model the erosion and transport of the Forfar bed deposit it was decided to use the transport capacity relationship as currently used in the InfoWorks sewerage simulation software produced by Wallingford Software. InfoWorks is the industry standard in drainage engineering and the quality simulation module (QSIM) within this package utilises the Ackers (1991) relationship (as outlined in Section 2.12.2.4) for modeling sediment transport. This is a total load relationship that differentiates between the modes of transport by the use of a mobility parameter (F_{gr}) that incorporates a coefficient (n). The coefficient 'n' is equal to '0' for coarse material (bedload) or '1' for fine material (suspended load) with a value between '0-1' for the so-called *transitional* material.

Rushforth (2001) showed that for coarse, granular material, this modified relationship severely underestimated the bedload transport of real sewer sediments in a test pipe at the UK National CSO Test Facility. The main objective of this study was to examine the validity of the Ackers relationship (as used in InfoWorks) for the prediction of suspended transport of sewer sediments in a combined sewer. If the results proved to be invalid when compared to the observed data then the objective would be to adjust the relationship in order to obtain improved results. If possible it would be desirable to achieve '*good*' results. In terms of a prediction accuracy considered accurate for the sediment transport field, both in sewers and fluvial hydraulics, this would mean that 50% of the predicted results should lie within the range of 0.5 to 2 times the observed values (White *et al.*, 1975).

In addition to using the 'standard' model it was also decided to investigate whether applying the relationship on a fractionwise basis would yield more accurate results. This approach follows the work carried out by White and Day (1982) on mixed-sized gravel in a recirculating flume and by Rushforth (2001) who used bedload data from real sewer sediments. The aforementioned studies used the Ackers-White relationship (modified for each sediment fraction) to model data collected using a

bedload trap but did not attempt to model the suspended load using the same methodology.

7.2. Modelling Strategy

Four different approaches were used to investigate the performance of the Ackers relationship for the prediction of suspended load transport in combined sewers. The data sets were initially modeled using the Ackers (1991) relationship in its unmodified form with a representative grain size (d_{35}), followed by the same method but with the effective bed width adjustment, as used in InfoWorks. The relationship was then applied in a fractionwise manner, with the final technique also involving a fractionwise application of the Ackers (1991) relationship, but with individually calibrated A_{gr} values (as detailed in Section 2.12.2.6) for each fraction. Additionally, the influence of the ADWP and the possible effects of cohesion on the transport rates were also investigated. The approach involving the modification of the A_{gr} values followed the work of White and Day (1982) and Rushforth (2001). This modelling strategy involved using data from two of Forfar tests (Tests B and C) to calibrate the model and then use two further data sets (Tests A and D) to validate the method. In order to develop modified A_{gr} values for each of the deposit fractions it was deemed necessary to choose suspended load timesteps for calibration purposes that were representative, not only of the various hydraulic conditions, but also the different responses exhibited by the bed deposit during the flush tests. With this in mind it was decided to choose a range of time intervals from the calibration tests (B & C) that accounted for the following conditions during each test:

- Pre-test ambient SSTR
- Middle of SSTR rising limb
- Peak SSTR
- Middle of SSTR receding limb
- Post-test ambient SSTR

As the Ackers-White formulation was derived from a series of experiments that were carried out using uniform sediments the resultant A_{gr} values were developed for particles that were present in a bed comprised of material of the same size. As shown in Figure 6.55 this would not be an appropriate methodology to adopt for

deposits comprised of mixed particle sizes. The field data showed that in mixed-sized sewer deposits the finer particles appeared to be less mobile than they would have been had they been part of a uniform bed. In addition, this work has also indicated that a deposit's propensity for erosion may also be related to the ADWP prior to the erosion event. With this in mind, it was deemed appropriate that not only should the Ackers-White relationship be applied in a fractionwise basis, but some adjustment should also be made to account for the ADWP of the event being modeled.

7.2.1. Calibration Strategy

As there were four sets of data available, it was decided to use two data sets for calibration purposes and then validate the method using the remaining data sets. When applying the Ackers relationship in the usual manner it is recommended that a single representative grain size should be used, with the d_{35} recommended by Ackers and White (1973) for graded sediments. Rather than using a representative grain size to compute the total load in transport, the relationship could be applied on a fractionwise basis. The resulting estimated transport rates could then be multiplied by the proportion of that fraction size in the original sediment bed to give an estimate of the amount of that particular size fraction in transport. Summation of the individual fraction loads would then yield the total estimated load in transport. This may be expressed as:

$$q_{stot} = \sum_{i=1}^{i=n} \Delta p_i q_{si} \qquad (7.1)$$

where: Δ_{pi} = % by weight of the ith size fraction present in the original bed deposit

q_{si} = predicted suspended sediment transport rate for the ith size fraction

The Ackers relationship utilises a general sediment mobility parameter (F_{gr}) the value of which at incipient motion is A_{gr}, that is, the particle threshold mobility parameter. By applying the relationship on a fractionwise basis as described above and adjusting the A_{gr} value until the predicted transport rate equaled the observed transport rate it was possible to derive relationships for each fraction size where the A_{gr} value was replaced by an A'_{gr} value. A mean A'_{gr} value was determined for each

size fraction using calibration data from representative timesteps as described in Section 7.2 from the Test B and Test C data sets.

As can be seen in Figure 7.1, by plotting the resultant ratios of A'_{gr} to A_{gr} against the fraction particle size (d_i) to the median grain size (d_{50}) ratios it was possible to examine how the various fractions would behave had they been present in a bed comprised entirely of material of that particular size fraction.

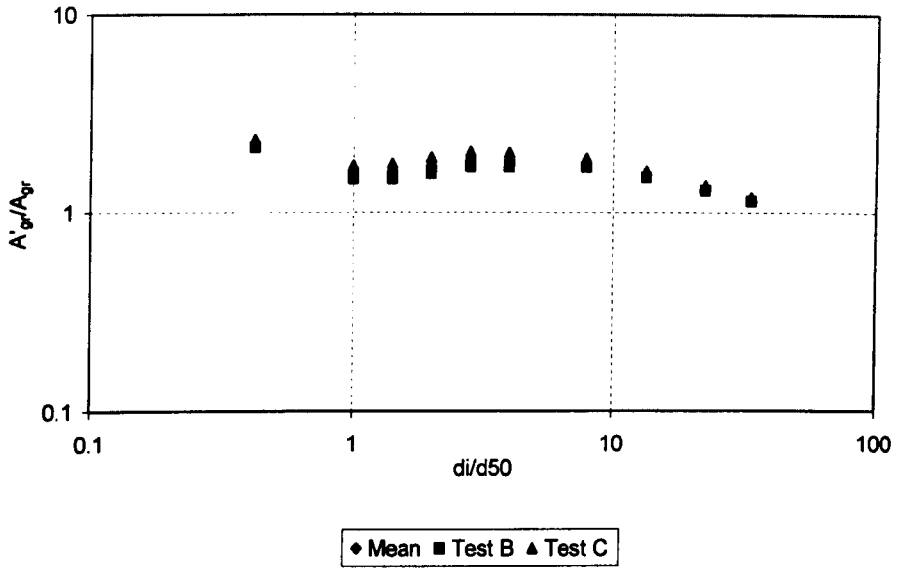

Figure 7.1: A'_{gr}/A_{gr} v d_i/d_{50} (from tests B and C)

An A'_{gr}/A_{gr} ratio equal to unity suggests that that particular size fraction behaves in the mixture as it would in a sediment bed comprised entirely of that size fraction. An A'_{gr}/A_{gr} value of less than one suggests that size fraction is less stable and hence more easily erodible in the mixture than it would be in a single-size deposit and vice versa. The mean A'_{gr}/A_{gr} values determined for each size fraction from the Test B and Test C calibration data sets are presented in Table 7.1.

Particle size fraction (mm)	A'_{gr}/A_{gr}
5	1.17
3.35	1.34
2	1.57
1.18	1.79
0.6	1.85
0.425	1.86
0.3	1.73
0.212	1.62
0.15	1.60
0.63	2.24

Table 7.1: Modified A_{gr} values from Forfar suspended fractions

7.3. Model Results

Figure 7.2 through to Figure 7.5 shows the individual transport rates obtained by applying the Ackers (1991) relationship using the following techniques:

Method 1 – Ackers (1991) with a characteristic deposit d_{35}

Method 2 – Ackers (1991) on a fractionwise basis without any A_{gr} correction

Method 3 – Ackers (1991) on a fractionwise basis using A'_{gr} values (i.e. recalibrated A_{gr} corrections)

7.3.1. Validation Results from Test A (23-05-01)

Figure 7.2 illustrates the results of the data set from Test A modelled using the Ackers (1991) relationship (Method 1) and also using the approach described in Section 7.2.1 (Method 3).

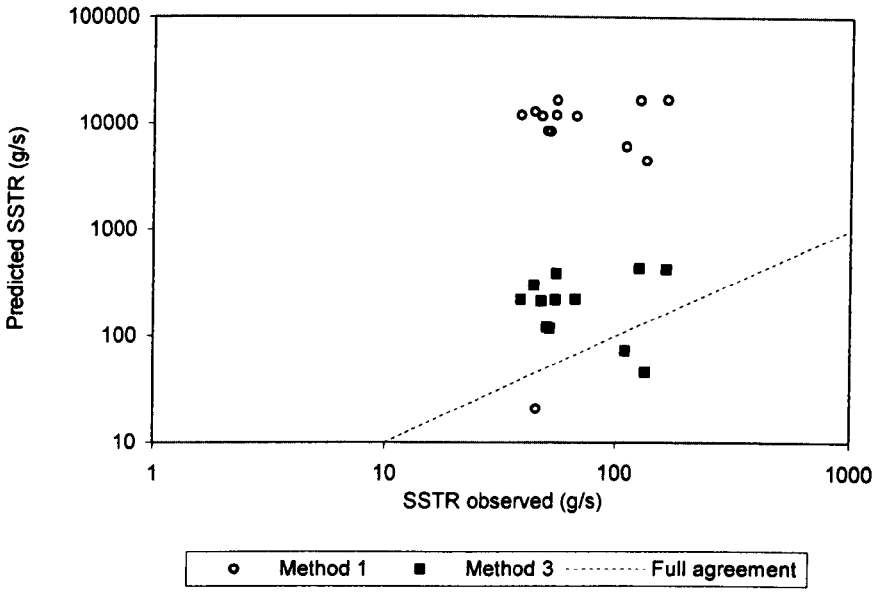

Figure 7.2: Test A prediction using modified and non-modified Ackers (1991)

It can be clearly seen that by using the relationship on a fractionwise basis (Method 3) with the A'_{gr} values presented in Table 7.1 there was a marked improvement in the predicted SSTR values.

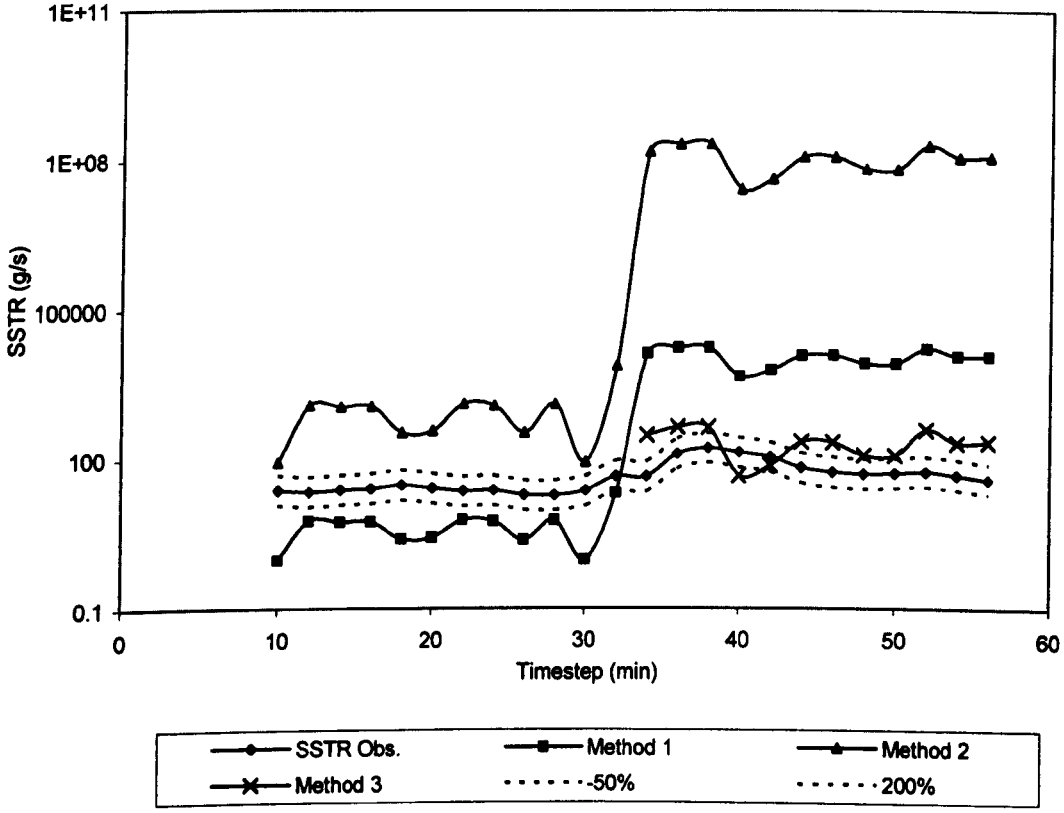

Figure 7.3: Results of Ackers (1991) Test A predictions

As can be seen from Figure 7.3 using the Ackers relationship in the traditional manner (Method 1) severely over-predicted the SSTR, while applying it on a fractionwise basis (Method 2) only served to compound the error. By using the A'_{gr} values on a fractionwise manner (Method 3) however it can be seen the predicted SSTR values are vastly improved, although they still lie outwith the generally accepted 50%-200% range of the measured data.

7.3.2. Validation Results from Test D (07-08-01)

Figures 7.4 illustrates the results of the data set from Test D modeled using both the original Ackers (1991) relationship (Method 1) and the approach described in Section 7.2.1 (Method 3).

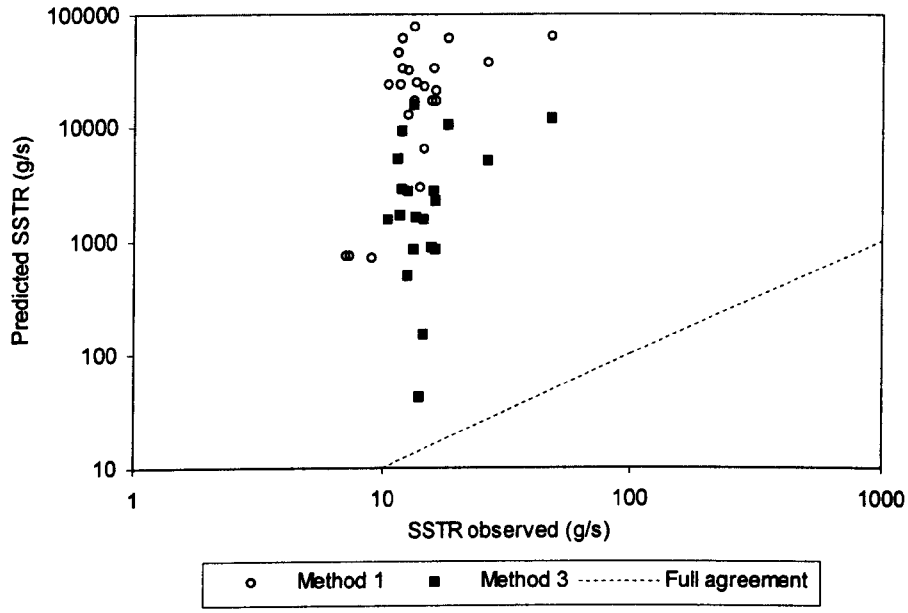

Figure 7.4: Test D prediction using modified and non-modified Ackers (1991)

Again, using the relationship on a fractionwise basis with the A'_{gr} values presented in Table 7.1, there was a marked improvement in the predicted SSTR values. In addition Figure 7.5 shows the individual transport rate results obtained by applying the Ackers (1991) relationship using Methods 1, 2 and 3 as described in Section 7.3. Of the three methods it is clear that Method 3, the fractionwise method with the A'_{gr} values produced the best results, which were a notable improvement on the results

obtained using the Ackers relationship in the traditional manner. The majority of the results still lay outwith the 50%-200% of observed values envelope.

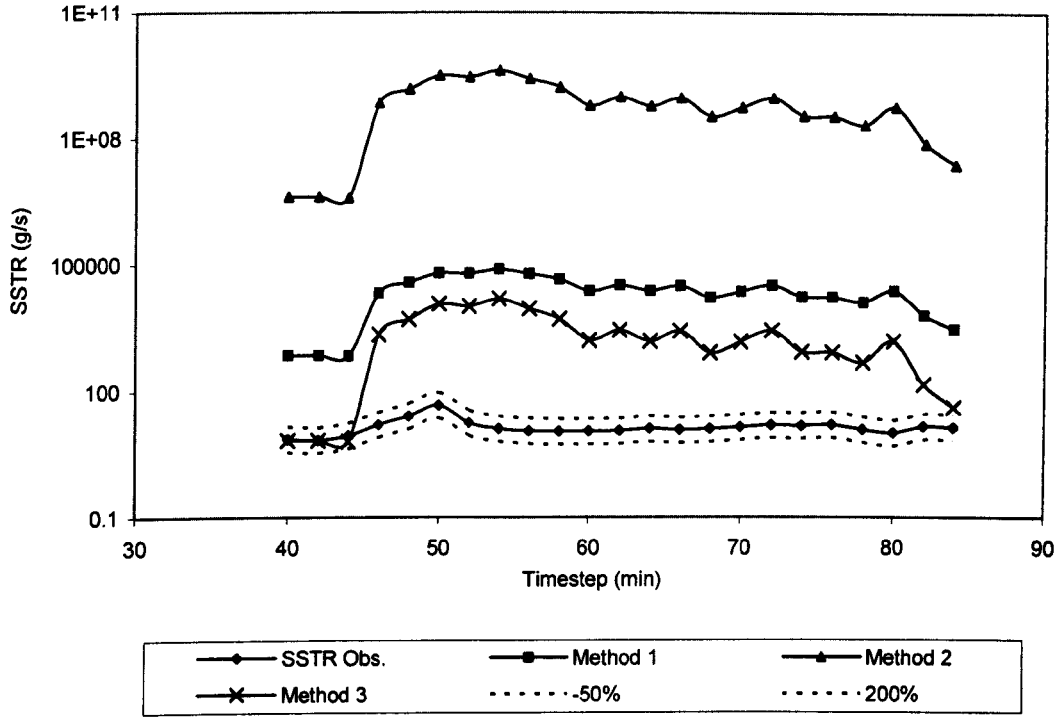

Figure 7.5: Results of Ackers (1991) Test D predictions

In general the modified Ackers method with recalibrated A'_{gr} values (Method 3) provided much better predictions of the suspended transport than those obtained by the original relationship. As illustrated by the vast over-prediction shown in Figure 7.5 the errors were clearly exacerbated by applying the relationship on a fractionwise basis without calibrating the A_{gr} values (Method 2); indicating that this was not a judicious manner in which to apply the model. The predictions were better for the Test A data than the Test D data. Given the significant difference in the deposit history for these tests, the Test A ADWP was 94.9 hours whereas it was only 16.93 hours for Test D, it was believed this factor may have had a bearing on the predicted results. In other words the modified Ackers relationship may not have been calibrated properly for deposits with relatively small ADWPs, resulting in gross over-prediction of the suspended transport rates for these tests. If this had been caused by the calibrations being carried out using data that originated from deposits with relatively long ADWPs (23.75 hours for Test B and 32.72 hours for Test C) it

was deemed pertinent to investigate the effect of modifying the model in order to take the effects of the ADWP into account.

7.4. Accounting for Influence of ADWP

To investigate the effect of the ADWP on the particle mobility of the individual fractions it was decided to use three of the data sets to derive a modified relationship for A'_{gr}/A_{gr} for each individual fraction and then use the final data set to validate the method. The data from Tests A, B and C were used for the relationship derivation purposes.

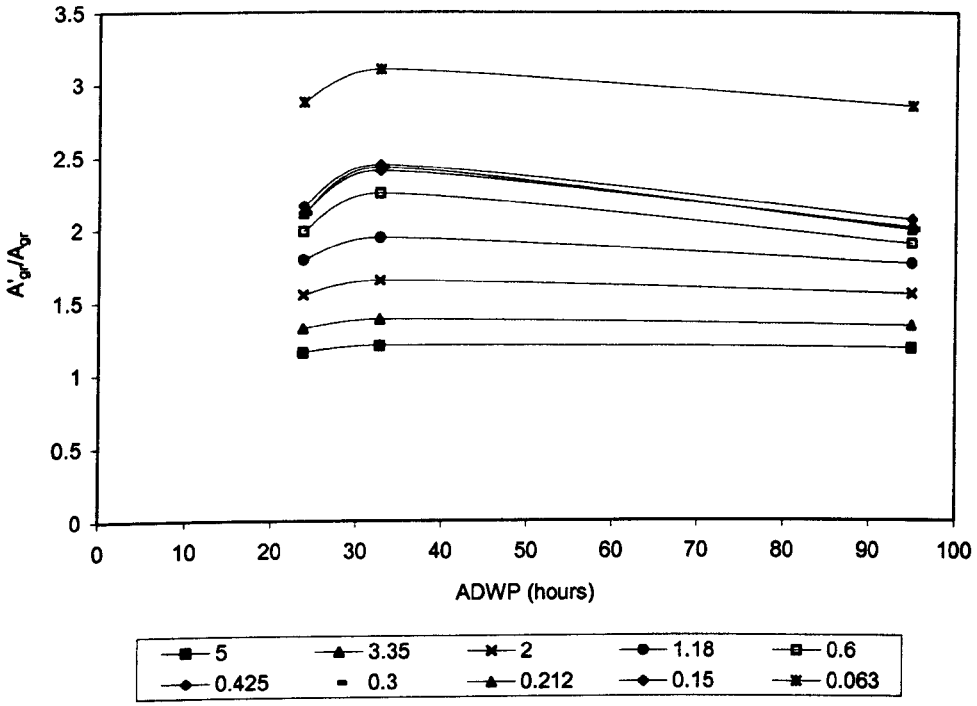

Figure 7.6: Fractional A'_{gr}/A_{gr} ratios v. ADWP (based on Tests A, B, & C)

Figure 7.6 illustrates the relationship between the A'_{gr}/A_{gr} versus ADWP for each of the size fractions (0.063-5 mm) within the bed deposit. Interestingly, it shows that for each of the size fractions there was an initial decrease in particle mobility with increased ADWP, which was then followed by an increase in particle mobility, possibly as a result of biochemical processes taking place within the deposit. Figure 7.6 also shows that this effect was more pronounced in the finer particles.

The resulting relationships that were used to compute the A'_{gr} values for the individual fractions based on the deposit history are presented in Table 7.2.

d_i (mm)	Relationship
5	$\frac{A'_{gr}}{A_{gr}} = -0.00008ADWP^2 + 0.0094ADWP + 0.9762$
3.35	$\frac{A'_{gr}}{A_{gr}} = -0.0001ADWP^2 + 0.0131ADWP + 1.0741$
2	$\frac{A'_{gr}}{A_{gr}} = -0.0002ADWP^2 + 0.0212ADWP + 1.1496$
1.18	$\frac{A'_{gr}}{A_{gr}} = -0.0003ADWP^2 + 0.0333ADWP + 1.1619$
0.6	$\frac{A'_{gr}}{A_{gr}} = -0.0005ADWP^2 + 0.0568ADWP + 0.9166$
0.425	$\frac{A'_{gr}}{A_{gr}} = -0.0005ADWP^2 + 0.0636ADWP + 0.9125$
0.3	$\frac{A'_{gr}}{A_{gr}} = -0.0006ADWP^2 + 0.0696ADWP + 0.8018$
0.212	$\frac{A'_{gr}}{A_{gr}} = -0.0006ADWP^2 + 0.0691ADWP + 0.8054$
0.15	$\frac{A'_{gr}}{A_{gr}} = -0.0005ADWP^2 + 0.0619ADWP + 0.9905$
0.063	$\frac{A'_{gr}}{A_{gr}} = -0.0004ADWP^2 + 0.0486ADWP + 1.9556$

Table 7.2: Revised fractional A'_{gr}/A_{gr} relationships based on ADWP

The relationships outlined in Table 7.2 were subsequently used to re-evaluate the fractional A'_{gr} values for Test D and the resultant transport rates. Given that these trends were derived from a three-point fit, it is acknowledged that the validity of these relationships cannot be taken for granted. Rather, this is an area of the research that requires further investigation to be carried out involving more field and/or laboratory testing using deposits with varying consolidation periods.

7.4.1. Results from Test D (07-08-01) using Revised A'_{gr} Values

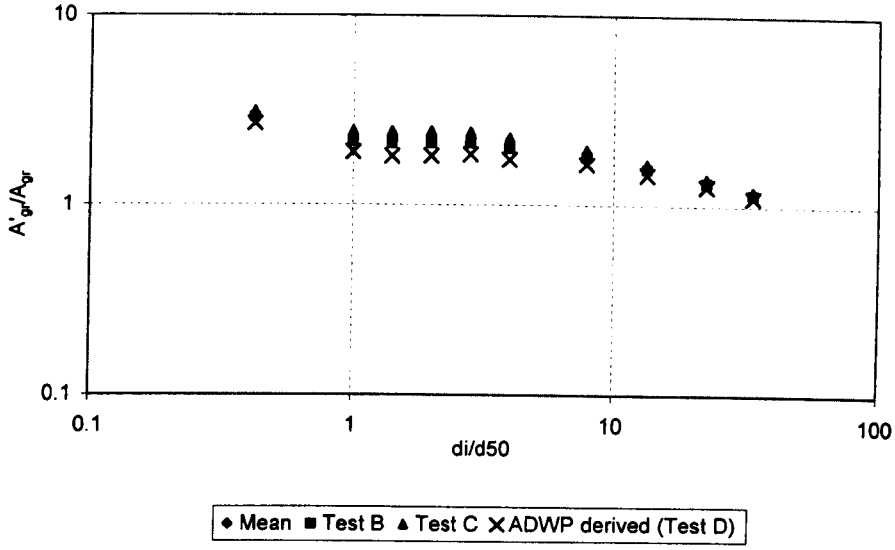

Figure 7.7: Effect of ADWP on A'_{gr}/A_{gr} v di/d_{50}

Given that the Test D suspended transport rates were grossly over-predicted it was hoped the revised A'_{gr} values based on taking the effect of the ADWP into account would yield lower predicted values. As shown in Figure 7.7 however, the revised A'_{gr} to A_{gr} ratios were actually lower than the mean ratios for all of the fractions. This implied greater mobility of the fractions and would thus result in even greater transport rates.

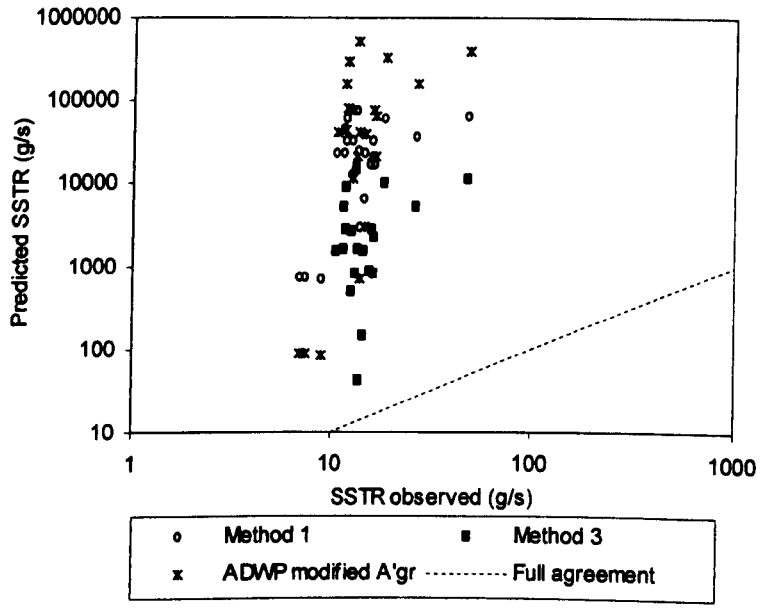

Figure 7.8: Effect of ADWP on predicted transport rate values

Figure 7.8 illustrated there was no improvement in the predicted transport rates by including an adjustment of the A'_{gr} values to take the ADWP into account, which was verified by Figure 7.9. This showed the predicted values with the ADWP taken into account were indeed of a greater magnitude than the predicted values obtained using the A'_{gr} values in Method 3.

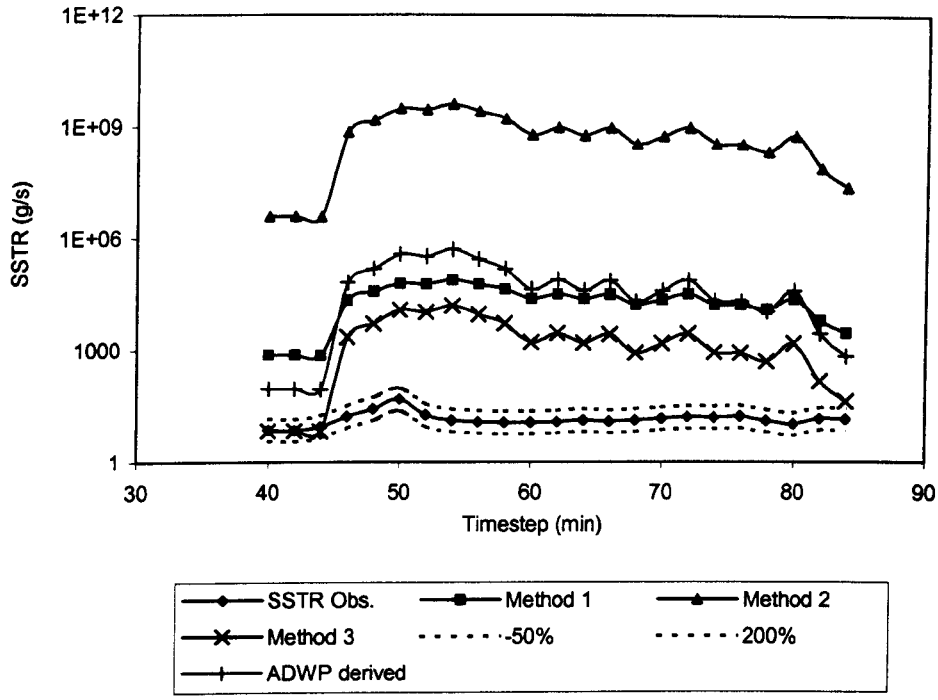

Figure 7.9: Test D suspended transport results including ADWP derived results

The fact that no improvement was attained may indicate that no relationship exists between the length of the ADWP and sediment mobility. However, given that the ADWP relationships were derived using only three data points for each sediment fraction this statement cannot be made with any great certainty. As already stated, it is recommended that further tests should be carried out with varying bed consolidation periods to establish whether this supposition may be discounted.

7.5. Modified A_{gr}s for Lower Mobility

As outlined in Section 7.4, by accounting for the history of the deposit in terms of the ADWP, no improvement was observed in the predicted suspended sediment transport values. It was clear that, as over-prediction was evident, particularly in the late stages of the flush events, modification of the A_{gr} values, although an improvement on the original Ackers method, was still not accurately representing the transport behaviour of the particle fractions at incipient motion. In order to reduce the mobility of the fractions it was decided to examine the modified Agr values from the various timesteps of the calibration data. As was to be expected, the highest modified A_{gr} values (that is, A'_{gr} values) were obtained from the timesteps at the end of the tests after the flush had passed. In other words when the easily erodible material would have been removed from the deposit surface there was a decrease in the particle mobilities. It was decided to re-model flush tests A and D using mean A'_{gr} values obtained from the post-test ambient timesteps of tests B and C to examine whether this would provide a more accurate representation of the material in transport.

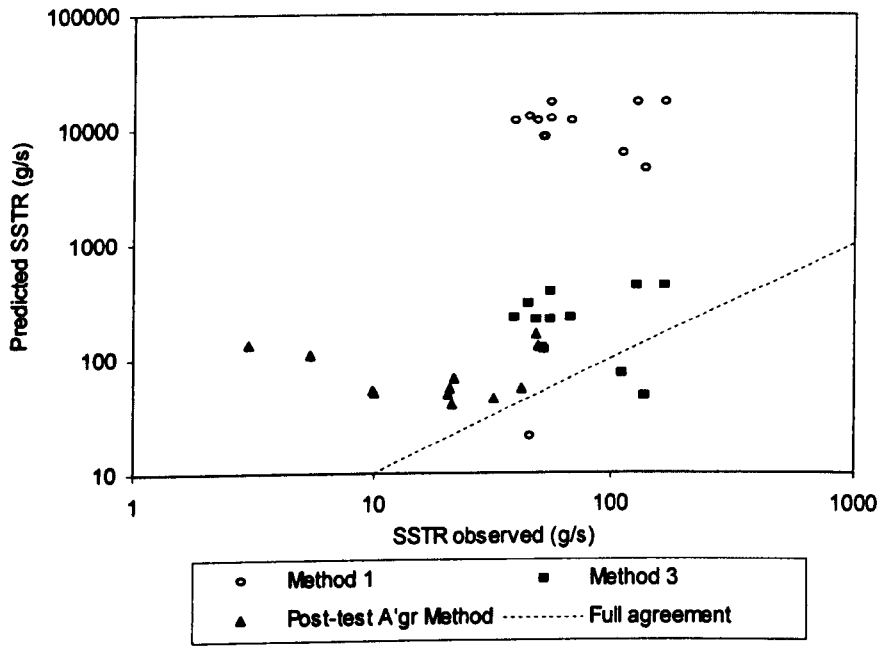

Figure 7.10: Effect of using post-test A'_{gr}s on predicted transport rates (Test A)

As illustrated in Figure 7.10 the post-test $A'_{gr}s$ resulted in improved predictions of the suspended transport rates observed in Test A. This becomes more apparent in Figure 7.11, which compares the results with those obtained from Method 3.

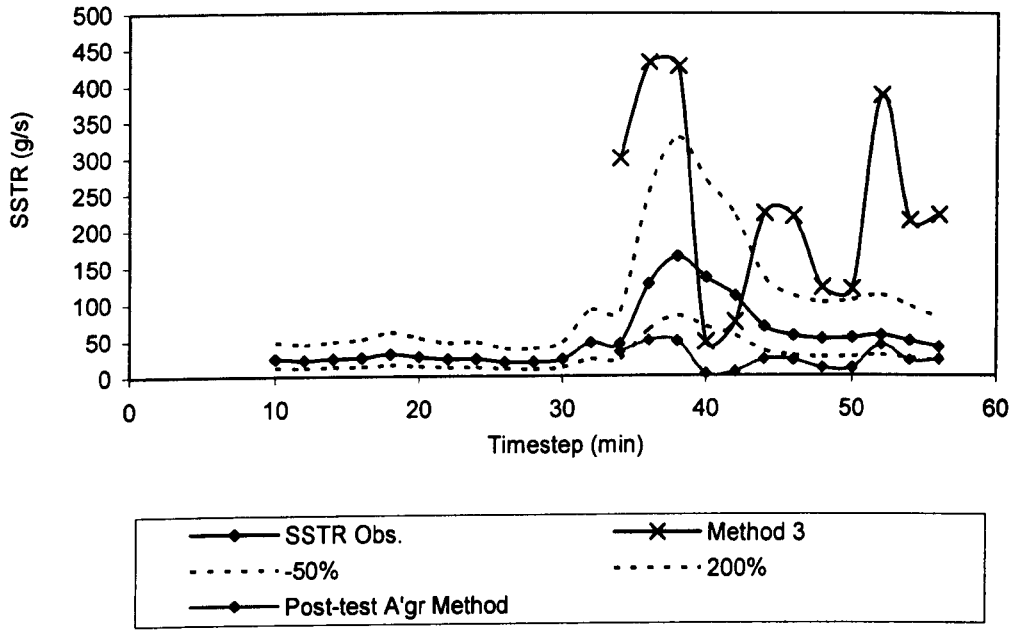

Figure 7.11: Predicted Test A suspended transport rates including post-test A'_{gr} results

As illustrated in Figure 7.11, whereas the previous methods over-predicted the observed suspended transport rates, the post-test A'_{gr} method actually under-predicted the transport rates, although in general the values were much closer to the observed values. The same method was applied to the Test D data set with the results presented in Figure 7.12 which shows the predicted values were again better than those obtained by using Method 3.

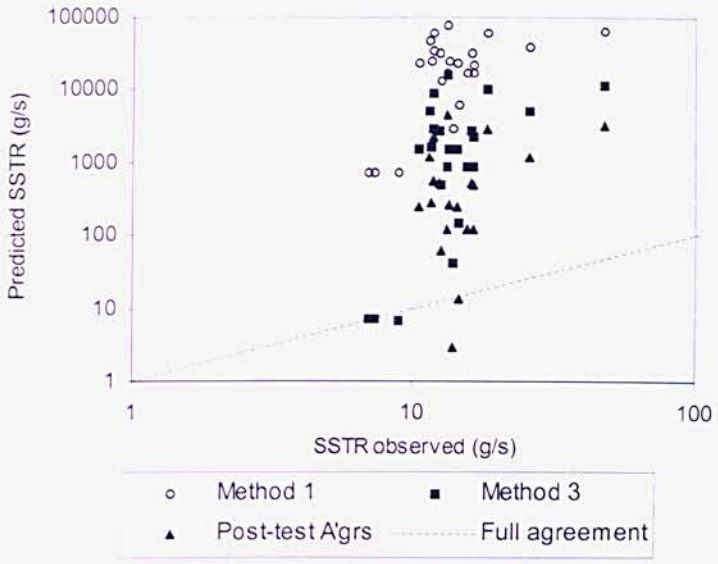

Figure 7.12: Effect of using post-test $A'_{gr}s$ on predicted transport rates (Test D)

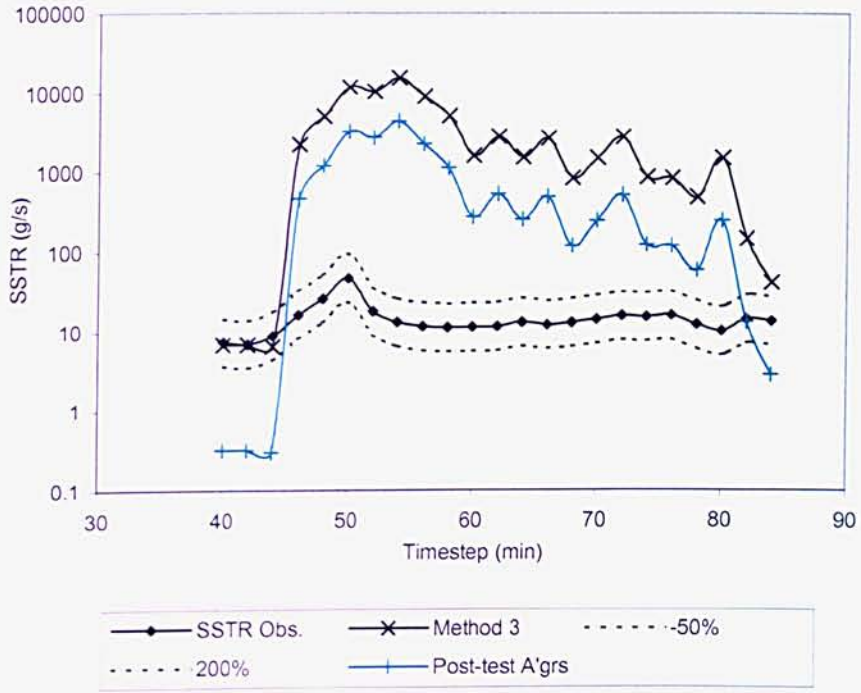

Figure 7.13: Predicted Test D suspended transport rates including post-test A'_{gr} results

Similar to the Test A results the predicted values were again reduced quite dramatically although the results remained outwith the '*good*' results sector.

7.6. Ackers (1991) with Effective Bed Width Adjustment

Given that the original Ackers (1991) relationship did not adequately model the suspended sediment transport rate, it was decided to examine the relationship used in InfoWorks that incorporated the bed width modification as recommended by Ackers *et al.* (1996).

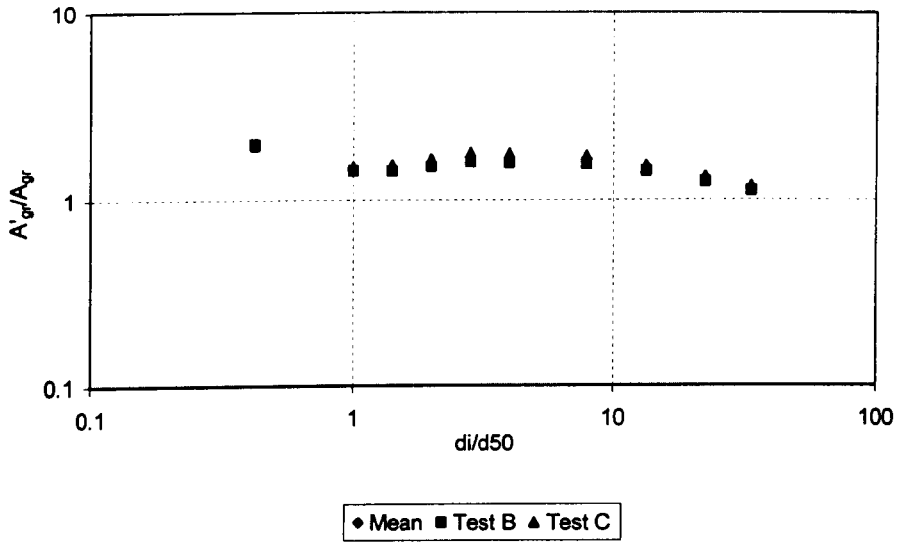

Figure 7.14: A'_{gr}/A_{gr} v di/d_{50} (from tests B and C using W_e)

With the same trend evident as that obtained with the original Ackers (1991) relationship it was clear that the finer fractions acted in a more stable manner within the sediment mixture than they would have had they been contained with a deposit comprised entirely of that fraction size. The mean A'_{gr}/A_{gr} values determined for each size fraction from Tests B and Test C are presented in Table 7.3.

Particle size fraction (mm)	A'_{gr}/A_{gr}
5	1.15
3.35	1.28
2	1.47
1.18	1.63
0.6	1.67
0.425	1.68
0.3	1.57
0.212	1.48
0.15	1.46
0.63	1.98

Table 7.3: Test B and C A'_{gr} values estimated from Forfar suspended fractions (W_e method)

7.6.1. Test A Results (Ackers 1991 with W_e adjustment)

The effect of using these modified mobility parameters and including the Ackers bed width adjustment factor on the Test A data is illustrated in Figure 7.15.

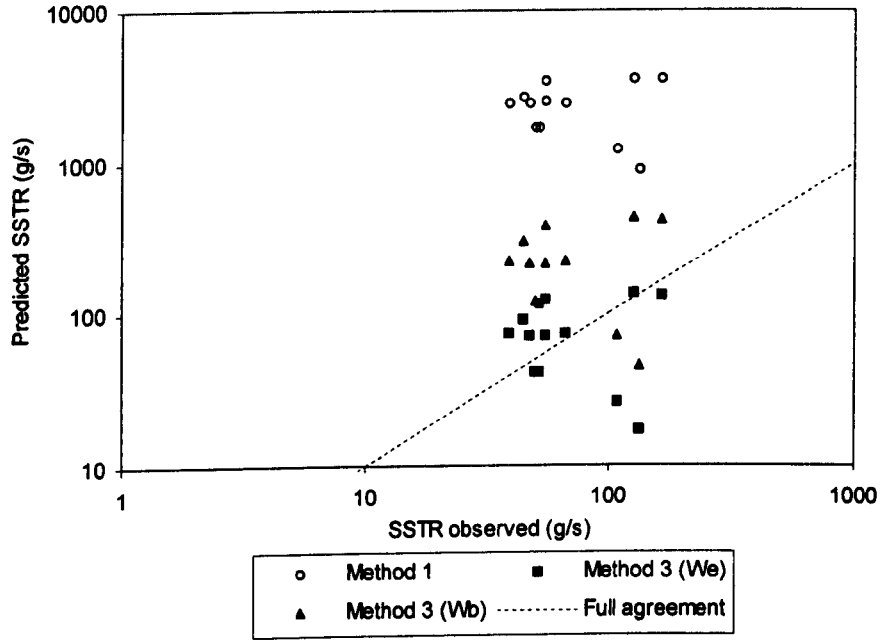

Figure 7.15: Effect of Ackers (W_e) with modified A_{gr}s on SSTRs (Test A)

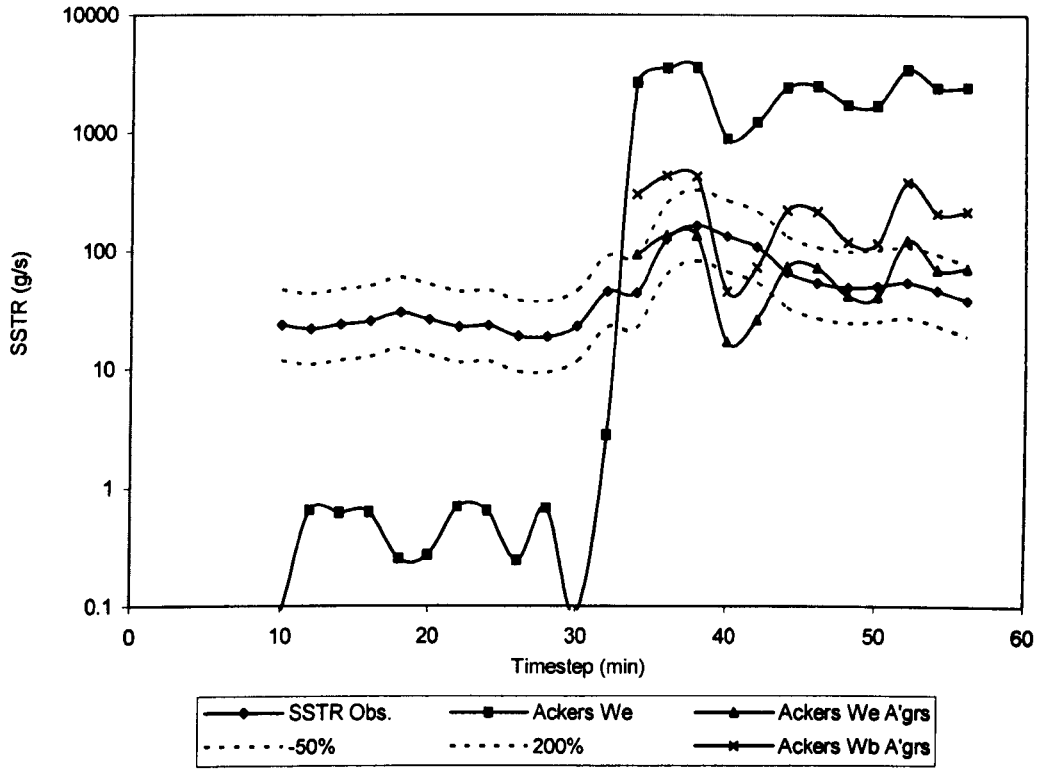

Figure 7.16: Comparison of predicted and observed SSTRs for models with modified A_{gr} and actual and effective bed widths (Test A)

During the early portion of Test A the bed shear stress remained under 0.59 N/m^2, prior to an increase to approximately 0.64 N/m^2 at time step 32. Figure 7.16 revealed interesting results, showing that for the Test A data set the Ackers (1991) relationship with an equivalent bed width (W_e) worked best for the lower values of bed shear stresses; whereas, using the same relationship on a fractionwise basis with modified $A_{gr}s$ produced the best results when the bed shear stress was in excess of 0.59 N/m^2.

7.6.2. Test D Results (Ackers 1991 with W_e adjustment)

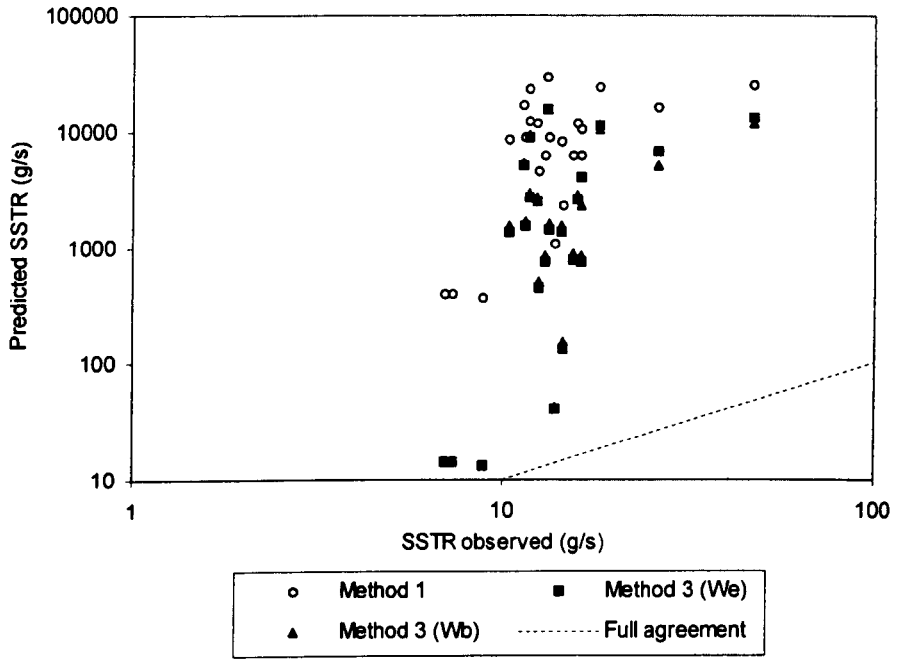

Figure 7.17: Effect of Ackers (W_e) with modified $A_{gr}s$ on SSTRs (Test D)

Figure 7.17 shows the effect of using the modified mobility parameter (A'_{gr}) with both the actual and the effective bed width on the Test D data. As shown by the results in Figure 7.18 improvements in the predicted results by using the relationships with an equivalent bed width (W_e) and the actual bed width (W_b) were obtained. However, the predictive performance was still very poor. Interestingly, the models' performances were much poorer for the data for Test A in comparison with Test D.

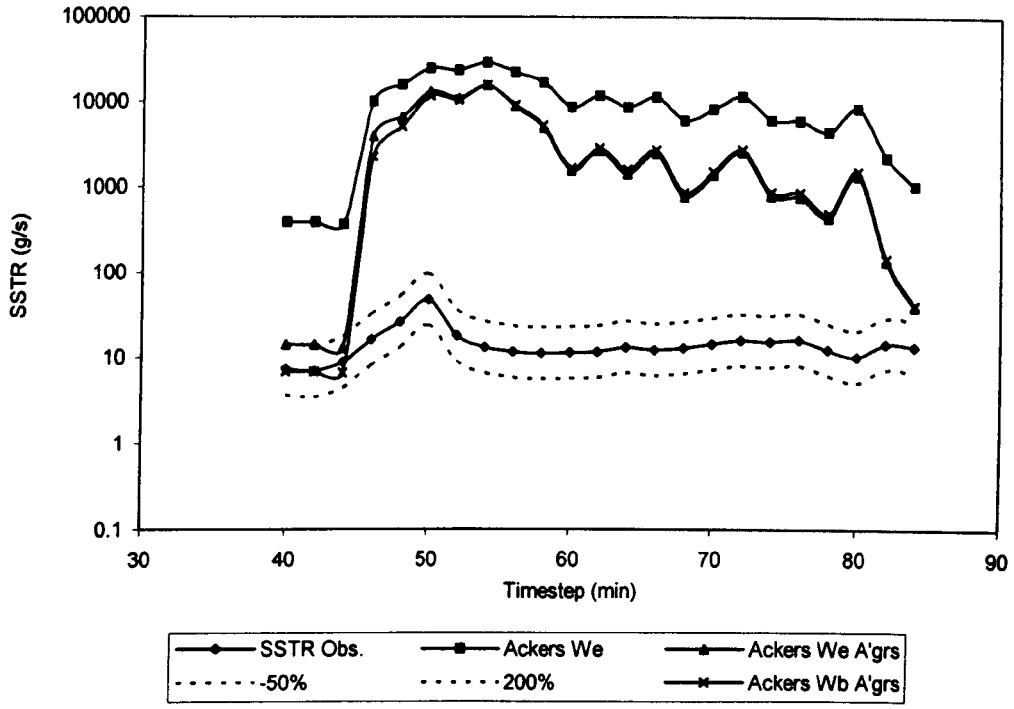

Figure 7.18: Comparison of predicted and observed SSTRs for models with modified A_{gr} and actual and effective bed widths (Test D)

7.7. Summary of Results

In summary, it can be seen that most of the modelling techniques substantially over-predicted the observed SSTR values. However, as illustrated in Figure 7.3 using the Ackers relationship on a fractionwise basis with modified $A_{gr}s$ for each fraction (i.e. Method 3) did significantly improve the predicted results. This was also the approach which yielded the best results for the Test D data set, which was further improved by modifying the A_{gr} values to account for the influence of the ADWP. This approach must be treated with caution however as ADWP relationships were only based upon three data points. Both the Test A and D results were further improved by applying modified A_{gr} values that were calibrated using data from the end of the flush events after the peak SSTR had been exceeded. However, it can be seen from Figure 7.16 and Figure 7.18 that improvements in the results obtained from the modification of the A_{gr} values in conjunction with an effective bed width were minimal.

7.8. Methodology to Account for Cohesive-like Sediment Properties

The problems with the over-prediction of the suspended transport values are clearly evident in Figure 7.19. It can be seen that the finest fraction (63-μm) was generally over-predicted by the greatest margin. Although the coarsest fraction was also over-predicted by a high percentage, this had a much less significant impact on the overall SSTR values as there was considerably less of this material in transport.

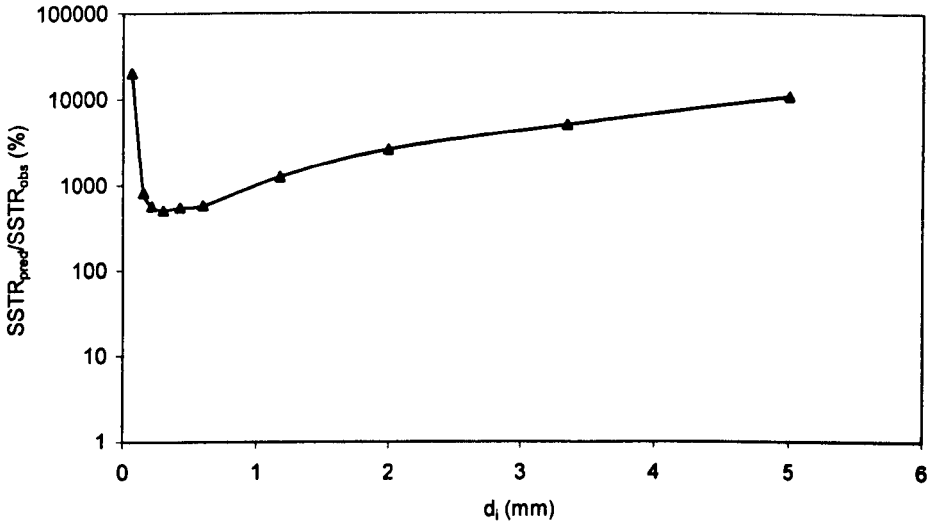

Figure 7.19: Mean percentage errors in predicted values of Forfar sediment fractions (Tests A & D)

It was decided to examine the D_{gr} values of the individual particle size fractions in order to investigate the possible cause.

Fraction size (mm)	Ackers D_{gr}
5	49.36
3.35	33.07
2	19.75
1.18	11.65
0.6	5.92
0.425	4.20
0.3	2.96
0.212	2.09
0.15	1.48
0.063	0.62

Table 7.4: Ackers D_{gr} values for suspended sediment fractions in the Forfar field tests

The calibrations of Ackers and White, 1973 are said to be valid in the non-dimensional grain size range:

$$1 < D_{gr} < 60 \qquad (7.2)$$

The size fraction with the greatest over-prediction was seen to be the 63-μm size. Assuming a particle density (ρ_s) of 1150 kg/m^3, based on deposit sampling carried out at Forfar, the D_{gr} value for this size fraction equated to 0.62, which was outwith the range of the data used to calibrate the transport capacity relationship. It was interesting to note that the lowest percentage error in the predicted suspended sediment transport rate occurred for the fractions whose D_{gr} values were contained within the 1.48-5.92 range. For the fractions with D_{gr} values outwith this range the observed errors increased proportionally as the D_{gr} value increased.

Ackers (1973) stated that, for fine sediments, his theory indicated very large changes in transport rates for small changes in shear. He noted that the lower limit of the dimensional particle size, that is, when D_{gr} = unity, was very close to the point at which sediments exhibit cohesive properties, when the laws of erosion and accretion are much more complex. The Ackers sediment mobility parameter (F_{gr}) was described by the ratio of the shear force on the unit area of the bed to the immersed weight of a layer of grains. Thus, predictive equations based on the Ackers theory would be meaningless for very fine sediments and no attempt was ever made to extend the optimisation curves below a D_{gr} value of 1. This is equivalent to a 40 μm sand particle with a density of 2650 kg/m^3. In InfoWorks the D_{gr} value for organic sediments equates to 0.692 when using the default d_{50} and specific gravity (s) values (0.04 mm and 1.7 respectively).

Clearly the Ackers relationship was never calibrated for sediments with D_{gr} values of less than unity, therefore there is a need for a different approach to be utilised when dealing with a mixture of non-cohesive and cohesive-like sediments. As stated by Ashley and Verbanck (1996), the definition of when a sewer deposit may behave as cohesive is not straightforward. When dealing with uniform sediment deposits it has been presumed the cohesive/non-cohesive boundary is marked by particle sizes less

than 20 μm (Alvarez-Hernandez, 1990). According to Clegg *et al.*, (1993), the proportion of fines may not be as important in sewer sediments as the organic content or the presence of biofilms for developing bed strength.

In the current study it was shown that the 63-μm fraction acted in a cohesive-like manner (see Figure 6.55) with the observed transport many times lower than that predicted by a granular transport relationship. Although the Nalluri and Alvarez (1992) relationship outlined in ??Equation 7.9 was developed for transport at the limit of deposition, given the need for a different approach to be used for the finest sediment fraction, it was decided to examine whether the above methodology could be applied to the 63-μm fraction of the Forfar deposit.

The results of applying this methodology to the 63-μm fraction of the Forfar sediment (from Tests B & C) is shown in Figure 7.21.

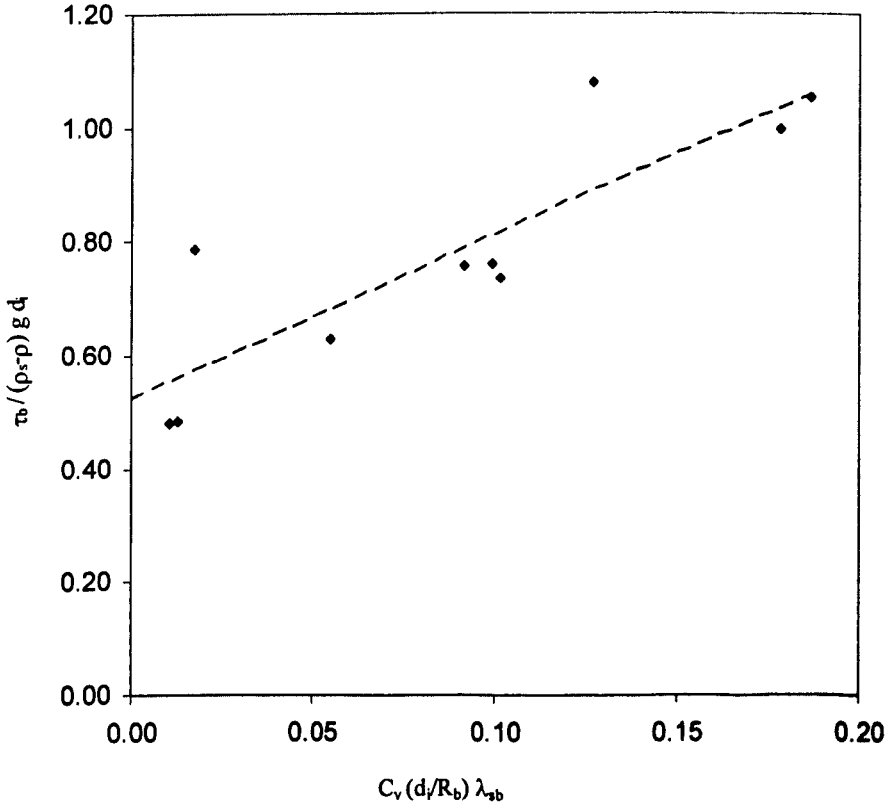

Figure 7.20: Cohesive transport of 63-μm Forfar sediment fraction

The resulting relationship for the transport of the 63-μm Forfar sediment fraction was as follows:

$$\tau_b / (\rho_s - \rho) g d_i = 2.8259 (C_v (d_i / R_b) \lambda_{sb}) + 0.5236 \qquad (7.3)$$

where:

d_i = particle size of the i^{th} fraction

7.8.1. Application of Cohesive Sediment Transport Relationship

The cohesive relationship was applied to the 63-μm fraction of the Test A data set with the results presented in Figure 7.22.

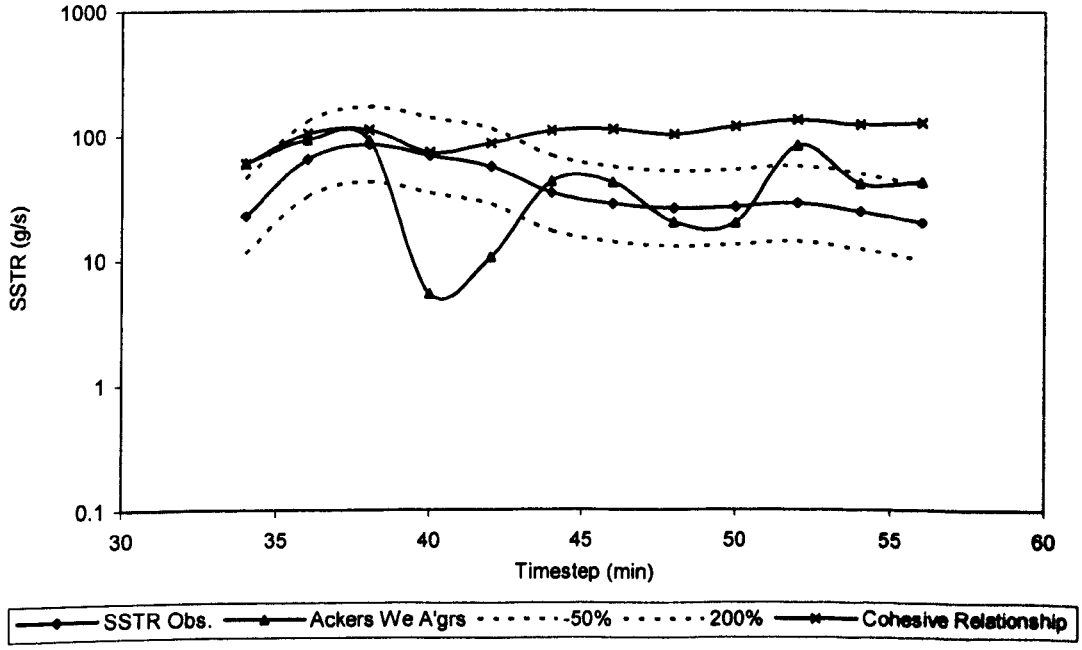

Figure 7.21: 63-μm fraction results from Test A

Figure 7.22 shows the results obtained using the Ackers (1991) relationship (with modified A_{grS}) with the effective bed adjustment and those obtained by using the cohesive relationship outlined in Equation 7.10. It can be seen that in general the cohesive relationship provided a better prediction than the Ackers relationship for this test.

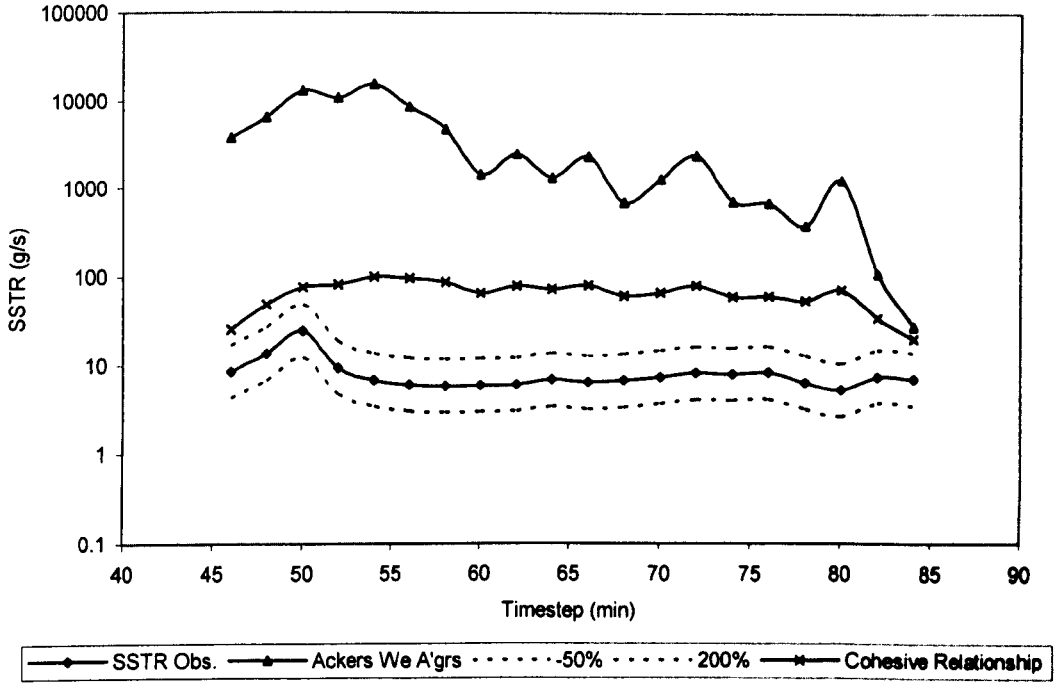

Figure 7.22: 63-μm fraction results from Test D

Figure 7.23 shows the results obtained using the Ackers (1991) relationship (with modified A_{grS}) with the effective bed adjustment and those obtained by using the cohesive relationship outlined in Equation 7.10. Again, it can be seen that for this test the cohesive relationship provided a significantly better prediction than the Ackers relationship. The effect on the overall transport rates of using a cohesive relationship for the 63-μm fraction is illustrated in Figure 7.24 overleaf. Use of the Ackers (1991) relationship with an effective bed width clearly overestimated the transport rates by a significant amount. Using this relationship on a fractionwise basis with individually calibrated fractional A_{gr} values greatly improved the predictions.

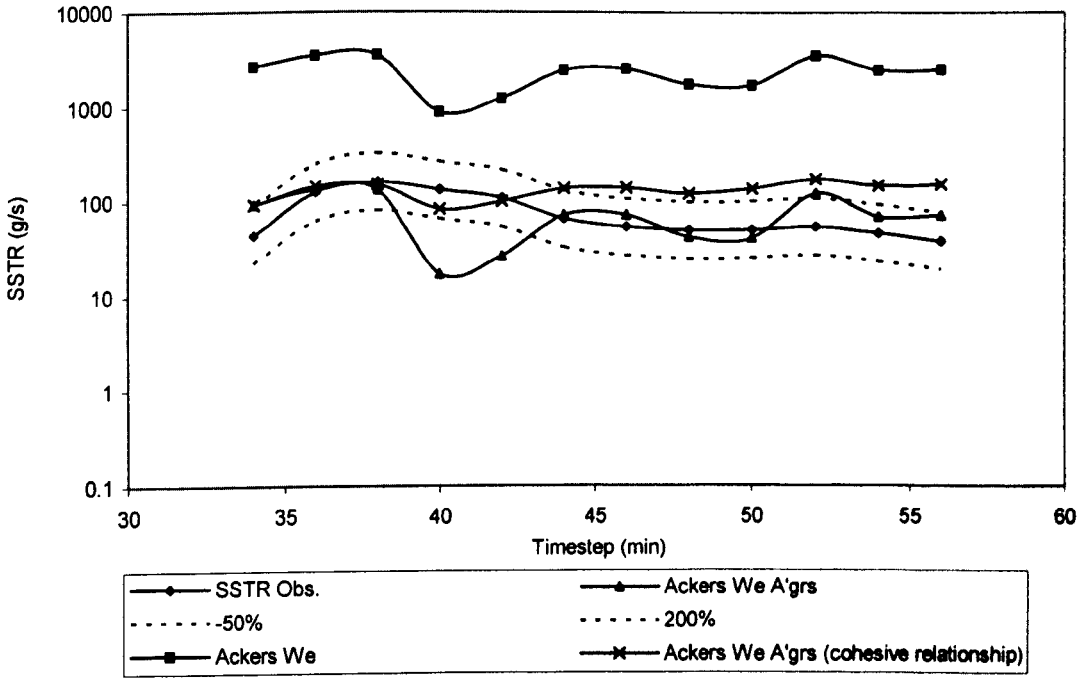

Figure 7.23: SSTR results from Test A

As illustrated by Figure 7.25, the inclusion of a cohesive relationship for the 63-μm fraction improved the predictions even further.

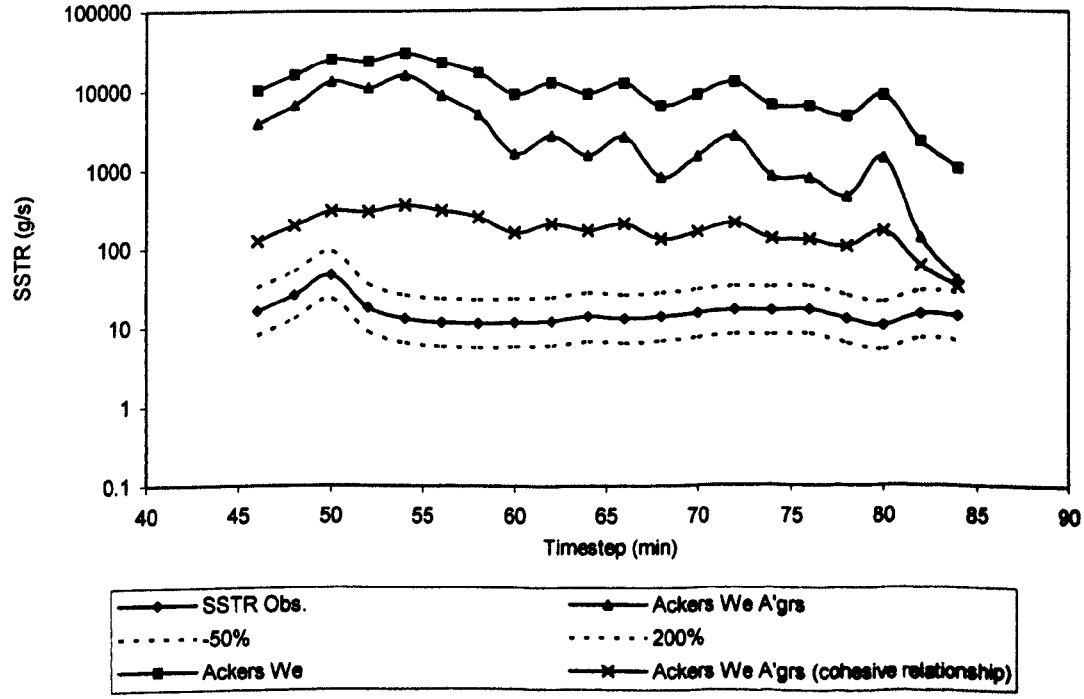

Figure 7.24: SSTR results from Test D

A similar trend was evident with the results from Test D. Again, use of the Ackers (1991) relationship with an effective bed width, overestimated the transport rates by a significant amount. Using this relationship on a fractionwise basis with individually calibrated fractional A_{gr} values again dramatically improved the predictions. Likewise, the inclusion of a cohesive relationship for the 63-μm fraction improved the predictions even further.

7.9. Discussion

The Ackers (1991) relationship is a total load relationship and is widely perceived by the UK Engineering community to be able to predict the transport of material from fine suspended material to coarser bedload. However, as shown by Rushforth (2001), the Ackers relationship underestimates bedload, while this study has shown that it greatly overestimates suspended load. For all of the tests carried out it has been shown that the Ackers (1991) relationship in its unmodified form is simply not suitable for the prediction of fine-grained sediments in combined sewers.

The results from this study have illustrated that, with regard to the prediction of suspended load transport, in order to obtain the best results and, dependant on the availability of data, the formulation should be applied in the following order (from best to worst):

- Hybrid Model [i.e. a cohesive relationship for the 63-μm fraction combined with the Ackers (1991) relationship for the remaining fractions]
- Ackers (1991) on a fractionwise basis using post-test A'_{gr} values
- Ackers (1991) on a fractionwise basis using A'_{gr} values
- Ackers (1991) on a fractionwise basis using We A'_{gr} values
- Ackers (1991) with a characteristic deposit d_{35}
- Ackers (1991) on a fractionwise basis with A'_{gr} values based on ADWP relationship
- Ackers (1991) on a fractionwise basis without any A_{gr} correction

As mentioned in Chapter 2, the Ackers (1991) relationship was derived from experiments involving solely non-cohesive sediments. The current tests however,

have demonstrated that the finer fractions acted in a more stable manner within the sediment mixture than they would have had they been contained with a deposit comprised entirely of that fraction size. To this end, the results have clearly shown that the Ackers (1991) relationship simply cannot deal with the fine material. Thus, in order to more accurately represent the suspended transport of this material it must be used on a fractionwise basis in conjunction with an alternative relationship for the cohesive-like 63-μm fraction. With this in mind, the current sediment transport module (QSIM) contained within the InfoWorks modelling package will never be able to accurately model the transport capacity of sewer flows, unless the relationship is used on a fractionwise basis and some modification is made to account for the finest fraction.

That is, in order to obtain the best results the equation must be used on a fractionwise basis with adjustments to the A_{gr} values for each size fraction. However, this means that a certain amount of fieldwork would be required in order to determine the particle size distribution of the deposit material and the SSTR for at least one event in order to 'calibrate' the A_{gr}s. For practicioners this may not always be practical as it might not be feasible to carry out field work due to time or economic constraints, but rather than simply use a default d35 (as is currently the case within InfoWorks) further research is required to assess whether, for cases where no fieldwork could be carried out, a table of the most likely deposit characteristics could be derived dependant on factors such as ADWP, contributing area type (urban/rural), likely hydraulic regime [e.g. based on network gradients, which could be derived from sewer record drawings or geographical information systems (GIS)]. The deposit 'most likely' to occur in a particular section of interest could then be used to estimate the particle size distribution which in turn could be used for the A_{gr} corrections. However, in an instance where a full urban pollution management (UPM) study was to be commissioned, then the additional data requirements would be low in relation to the already onerous data requirements of a UPM study.

Although inconclusive due to the limited amount of data, the study also illustrated that the effect of the ADWP could also be a possible source of improvement in the predicted SSTRs, and this would certainly be worthy of further research. Moreover, the methodology used in this study significantly reduced the error in the predicted

transport of the finest fraction (63 μm) which exhibited the greatest error, and this in turn reduced the error in the overall SSTR. With regard to the over-predictions of the coarser size fractions, the current study did not attempt to reduce these errors as, due to the amount of this material in transport, the overall effect on the predicted SSTRs was much less than that due to the finest size fraction. However, the findings of this study corroborated the work of Mitchener and Torfs (1996) who reported that the critical shear stress (τ_{cr}) required for the erosion of a non-cohesive bed (sand) was increased when mud was added to the deposit. The researchers found that the addition of 30% mud to a sand bed could increase τ_{cr} by as much as a factor of 10, and, if enough mud was added, the sediment behaved as if it were comprised completely of mud. This is a possible cause of the poor prediction of the coarser size fractions of the Forfar deposit material, as the impact of cohesion due to the fine material in the mixture may have resulted in a reduction in the transport rate of these fractions. This would form the basis for further research into the modelling of erosion from a mixed bed.

In conclusion, the results have suggested that in order to achieve the most accurate predictions of suspended sediment transport rates in a combined sewer, the most effective methodology would be to use a combined technique involving the application of a cohesive relationship for the finest fraction (63 μm), in conjunction with the Ackers (1991) relationship for the remaining fractions incorporating modified A_{gr}s to take account of the time-varying erodiblity of the deposit at different stages of the event.

Chapter Eight – Laboratory Transport Tests

8.1. Introduction

It has been noted (Tait *et al*, 2003) that carefully controlled experiments in which the antecedent depositional environment as well as the hydraulic conditions during the erosion test are controlled are extremely rare in sewer sediment studies. This chapter provides an overview and the results of tests that were carried out in an annular flume at WL Delft Hydraulics over the period November 2001 to January 2002. Sediment deposits were formed under carefully controlled and monitored environmental conditions and then subjected to a series of time steps in which the rotational speed of the flume's top and bottom plates was increased, progressively increasing the bed shear stress. The sediment deposits were formed using three different types of sediment. An artificial organic sediment (crushed olivestone), was selected as a surrogate sewer sediment and used in preliminary tests in order to gain qualitative information on the behaviour of the material in the flume under eroding conditions. The deposits used in the remaining experiments were real in-sewer sediments, from catchments in the UK (Dundee) and The Netherlands (Loenen). During the erosion tests, total and volatile suspended solids concentration, particle size distribution of the eroded sediment, and COD and DO levels were recorded. Where bed consolidation times were at least 24 hours a weaker surficial layer was observed to develop at the sediment/water interface. Deposit conditions (temperature and duration) were found to have a significant impact on the erosional resistance of the deposit.

8.2. Experimental Test Facility

The tests were carried out in an annular flume that had an external diameter of 2.2 metres and an internal diameter of 2.0 metres at WL Delft Hydraulics. The flume was placed in a room with climate controls and therefore some of the environmental parameters within the flume (such as DO and water temperature) could be controlled before and during the tests. The air temperature in this room was set to either 14°C or 4°C and the ability to control the environment within the flume meant that this facility had significant advantages over many other laboratory facilities. In addition, the annular flume was able to generate Reynolds numbers that were of the same order of magnitude as observed in real sewers. The flume was equipped to measure

bed shear stress, suspended sediment and dissolved oxygen concentrations and temperature at a frequency of 2 Hz. A web camera was installed on the lower plate and viewed a vertical section of the bed. Images from the web camera were recorded at one-minute intervals during the depositional and erosional phases of each test. This gave a visual record of what happened to the bed at one location and proved useful in examining the mechanisms of erosion.

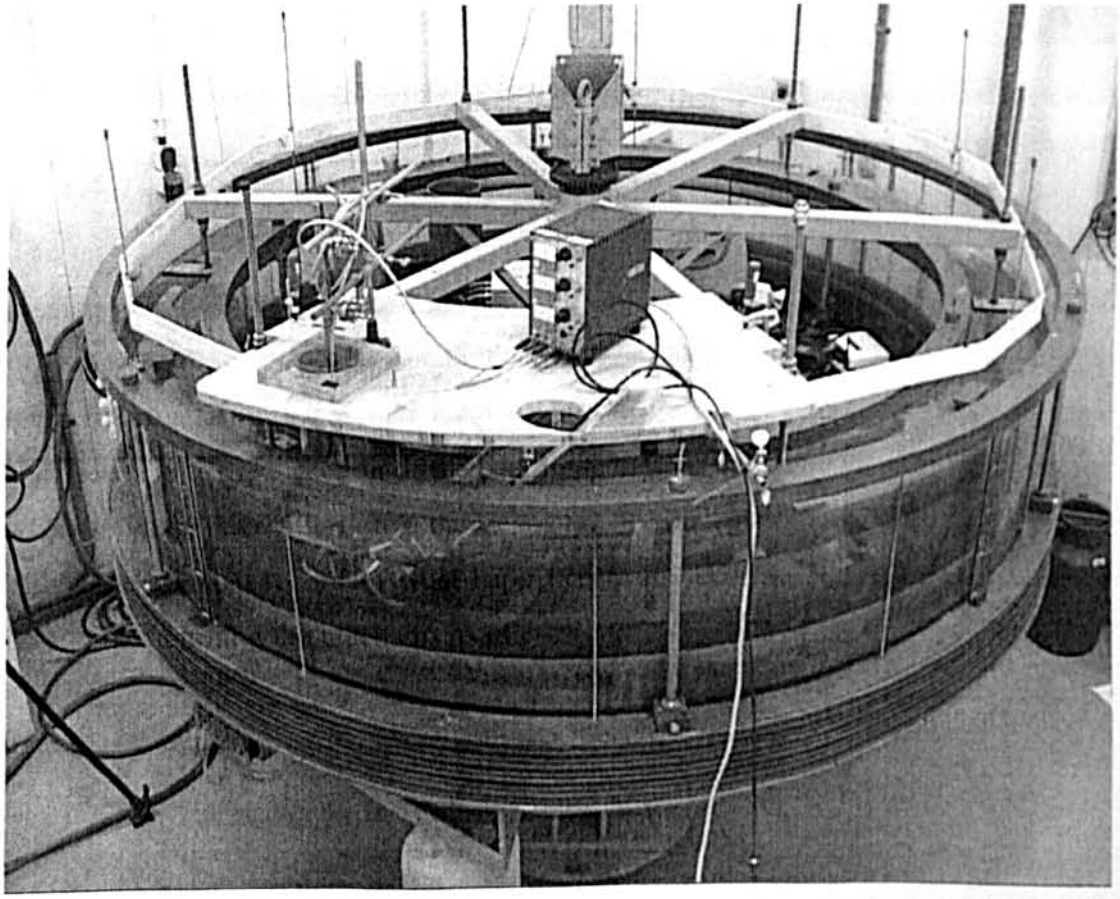

Plate 8.1: Rotating annular flume (WL Delft Hydraulics)

The flume was also equipped with an automatic sampling device that allowed recovery of discrete samples of 250 ml of fluid at any time. The draw off point for the suspended sediment concentration devices, the DO probe and the discrete samples was located approximately 30 mm above the sediment bed. As reported by Tait *et al.* (2003) this position was believed to provide depth-averaged values of suspended sediment and DO concentration.

8.3. Physical Characteristics of the Test Deposits

To enable the characterisation of the deposit material contained within the flume, samples were subjected to laboratory analysis. The results of these laboratory tests yielded values for the physical properties as described in Table 8.1.

Deposit Material	D_{50} (mm)	$\sigma_g = (d_{84}/d_{16})^{1/2}$	Organic content by mass (%)	Bulk density (kg/m^3)	Dry density (kg/m^3)	Moisture content (%)
Dundee sediment	0.601	4.2	3.26	1750	1309	25
Loenen sediment	0.270	1.8	2.42	1698	1225	28

Table 8.1: Average characteristics of original sediment mixes used to form deposits

8.4. Test Procedure

The tests comprised two parts, a deposit formation phase followed by a controlled erosion test. The second "erosion" part of the tests was carried out using a high level of control in order that a systematic data set was obtained. During the first part, the deposit formation phase, a 5 cm deep sediment bed was carefully placed in the flume base and then gently scraped flat. The flume was then slowly filled with tap water, with the water constituting a form of 'sewage', as there was some mixing with the placed sediment, although the filling of the flume did not significantly disturb the bulk bed. In each test the upper flume plate was set to be 270 mm above the level of the sediment bed. The temperature of the room had already been set as required. In each test the DO level in the flume was set at 70% of saturation. This was achieved as, when oxygen was utilised, the oxygen in the flume was replenished by recirculation of water through an oxygenation column that was continuously aerated. During the deposit formation phase the upper plate rotated slowly to ensure adequate mixing of the dissolved oxygen throughout the water column, as most oxygen depletion was thought to occur close to the bed. The deposit was then left for a pre-determined amount of time to consolidate.

After the consolidation period was over the deposit was then subjected to a controlled erosion test. The speed of the lower and upper plates of the flume were increased in a stepwise manner so that the bed was subjected to a series of steps in which the shear stress was steady but increasing from step to step. The suspended sediment concentration and dissolved oxygen levels were measured continuously during each step, which lasted approximately 30 minutes. An advantage of using an

annular flume as opposed to field studies to investigate erosion behaviour is that any sediment found in the water column must have been removed from the bed, whereas in the field it is difficult to isolate the influence of upstream sediment supply, as was the case in the Forfar field study. This means that any sharp increases in total suspended sediment concentration with time, in the flume, indicates high erosion rates from the deposited bed. Discrete samples (250 ml) of the 'sewage' containing eroded material were recovered approximately every 300 seconds and these were used to determine total and volatile suspended solids (TSS and VSS) concentrations. Images from the side viewing web camera were also recorded, at one-minute intervals, so that the response of the bed could be observed visually.

8.4.1. Test Programme

The levels of temperature and DO were selected to resemble the extremes encountered in a northern European sewer. The sediment deposits were left in these conditions for periods of approximately 18, 42 and 56 hours before being subjected to the stepwise increases in boundary shear stress to assess the erosional stability of the deposit. The sediment mixtures used were sourced in combined sewer systems, from Dundee in the UK and Loenen in The Netherlands. Table 8.2 summarises the initial conditions of each test.

		Deposit Formation Conditions		
Test no.	**Deposit Material**	**Temperature (°C)**	**DO Level (% of saturation)**	**Duration (hours)**
1	Dundee sediment	14	70	42
2	Dundee sediment	4	70	42
3	Loenen sediment	14	70	18
4	Loenen sediment	14	70	56

Table 8.2: Summary of experimental tests and deposit formation conditions

8.5. Determination of Velocity Profiles

Rotation of the top plate and the simultaneous counter-rotation of the main flume channel drove the flow within the flume. This counter-rotation minimised the cross-channel (radial) flow caused by water accelerating in a circular path. Minimisation of the lateral flow circulations within the flume resulted in a reasonably uniform shear stress pattern being applied to the sediment bed. The theoretical vertical

profiles of the flow velocity within the flume were determined using a methodology developed by Paganini (2002). As the flume was not instrumented with a velocity meter the accuracy of these profiles could not be verified. Given the quasi-2D nature of the flow, the profiles were assumed to follow logarithmic relationships, one for the lower zone of the water column (equation 8.1) and the other for the higher zone of the flow (equation 8.2). The flow was modelled two-dimensionally and the influence of any secondary flow was assumed to be insignificant.

$$\tilde{u} = \frac{u_*}{\kappa} \ln\left[\frac{y}{z_{0B}}\right] + V_B \qquad 0 < y \le y_1 \qquad (8.1)$$

$$\tilde{u} = -\frac{u_*}{\kappa} \ln\left[\frac{H-y}{z_{0T}}\right] + V_T \qquad y_1 \le y < H \qquad (8.2)$$

where: $\tilde{u} = \tilde{u}(y)$ = flow velocity (m/s) at a distance y from the bed

u_* = shear velocity (m/s)

κ = von Kármán constant

y = distance above the bed surface (m)

H = distance from bed to top plate (m)

Z_{0B} = sediment bed roughness (m)

Z_{0T} = top plate roughness (m)

V_B = bottom plate velocity [< 0] (m/s)

V_T = top plate velocity [> 0] (m/s); the positive flow direction was selected to be in the same direction as the top plate

The shear velocities at the sediment bed (u_{*B}) and at the top plate (u_{*T}) were assumed equal, as flow acceleration was nil during each step:

$$u_{*T} = u_{*B} = \sqrt{\frac{\tau_0}{\rho}} = u_* \qquad (8.3)$$

Given that the vertical velocity profiles (one for the lower zone and one for the higher zone) 'met' at height y = y1, with a corresponding velocity $\tilde{u}$(y1), then it followed that:

$$\tilde{u}_{\text{lower}}(y_1) = \tilde{u}_{\text{higher}}(y_1) \qquad (8.4)$$

and; $$\left(\frac{d\tilde{u}_{lower}}{dy}\right)_{y=y_1} = \left(\frac{d\tilde{u}_{higher}}{dy}\right)_{y=y_1} \quad (8.5)$$

The height, y1, was midway between the bed and the top plate; that is:

$$y_1 = \frac{H}{2} \quad (8.6)$$

At the mid-height (y = y1) equation 8.1 equals equation 8.2 thus, substituting y1 with $\frac{H}{2}$ leads to:

$$u_* = \frac{\kappa(V_T - V_B)}{\ln\left(\frac{\frac{H^2}{4}}{z_{0T}.z_{0B}}\right)} \quad \text{(where } V_T > 0 \text{ and } V_B < 0\text{)} \quad (8.7)$$

Hence, the bed shear stress can be estimated theoretically using the equation 8.8:

$$\tau = \rho_W u_*^2 = \rho_w \left[\frac{\kappa(V_T - V_B)}{\ln\left(\frac{\frac{H^2}{4}}{z_{0T} z_{0B}}\right)}\right]^2 = \rho_w \left[\frac{\kappa}{\ln\left(\frac{\frac{H^2}{4}}{z_{0T} z_{0B}}\right)}\right]^2 (V_T - V_B)^2 \quad (8.8)$$

where:

ρ_w = 1000 kg/m^3

κ = 0.40

H = 0.27m

z_{0T} = 0.03mm = 3x10^{-5}m (for smooth top plate)

$z_{0B} = 3d_{50}$

An example velocity profile generated using this approach is shown in Figure 8.1.

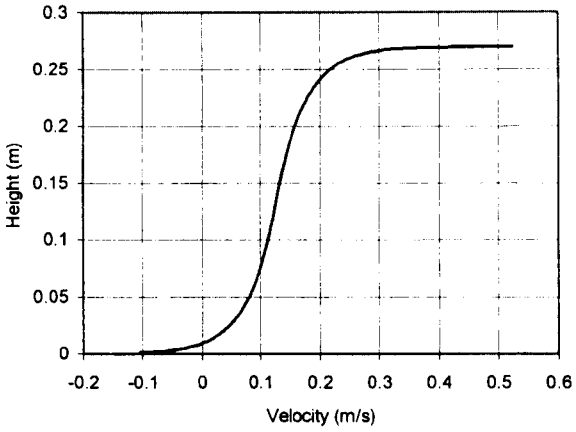

Figure 8.1: Illustration of a vertical velocity profile generated during Test 1 with a top plate speed of 0.524 m/s (5 rpm) and a bottom plate speed of –0.115 m/s (-1.1rpm)

8.6. Test Results

The results from the discrete sampling are summarised in Figure 8.2 (a-d) for Tests 1 to 4, with each of the tests exhibiting a steady increase in the average solids concentration within the flow column in line with the increased flow velocities that were generated.

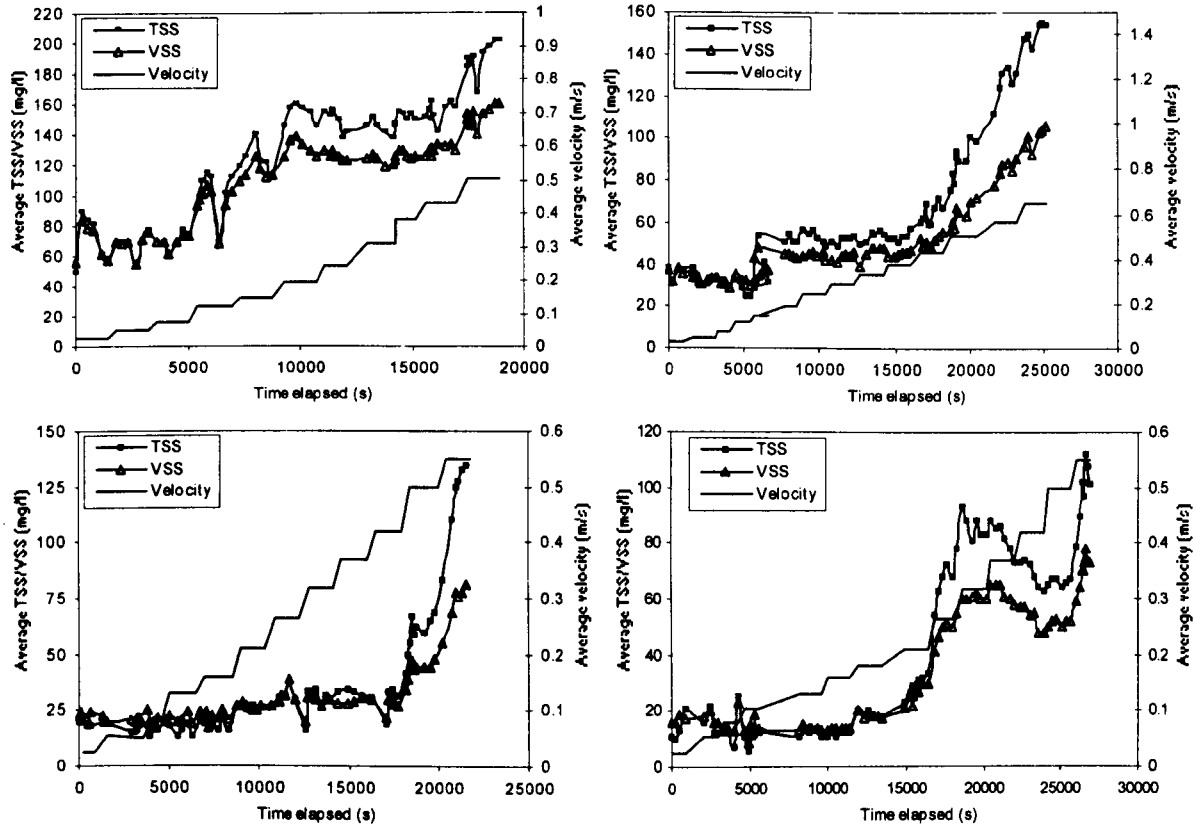

Figure 8.2: TSS/VSS measurements from discrete sampling, along with flow velocity (relative to the bed) for: (a - top left) Dundee deposit (14^{0}C, 42hrs); (b – top right) Dundee deposit (4^{0}C, 42hrs); (c – bottom left) Loenen deposit (14^{0}C, 18hrs) and (d – bottom right) Loenen deposit (14^{0}C, 56hrs)

8.7. Determination of SSTRs

The suspended sediment transport rate for each timestep (t) was determined by calculating the product of the mean flow velocity (v), the mean solids concentration (c) and the flow cross-sectional area (A):

$$(SSTR)_t = v_t c_t A \qquad (8.9)$$

The cross sectional area of the flow column was constant throughout the duration of each test.

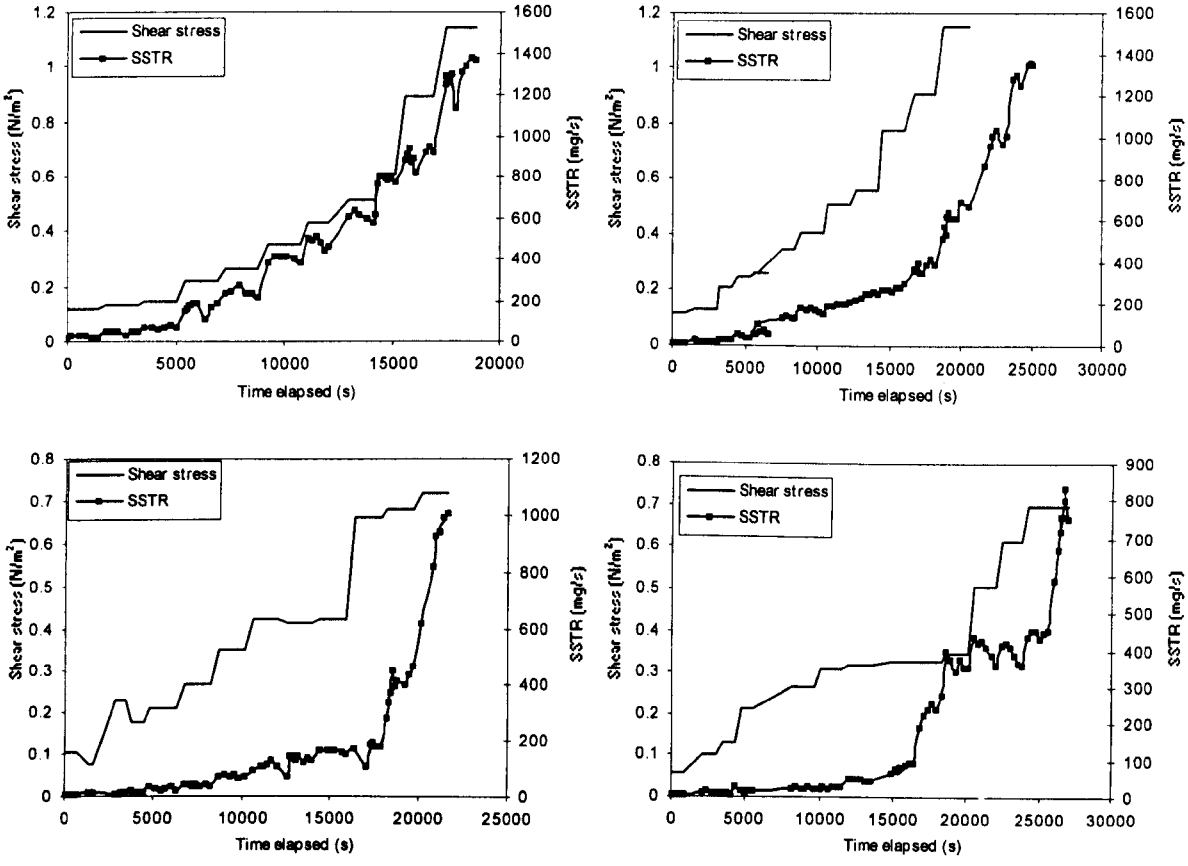

Figure 8.3: SSTRs and shear stresses for:
(a – top left) Dundee deposit (14^{0}C, 42hrs); (b – top right) Dundee deposit (4^{0}C, 42hrs);
(c – bottom left) Loenen deposit (14^{0}C, 18hrs) and (d – bottom right) Loenen deposit (14^{0}C, 56hrs)

8.8. Discussion of Test Results

The results of the tests provided, for the first time, comprehensive data on the influence that various environmental parameters may have on the development of deposit strength for in-pipe deposits composed of real sewer sediments.

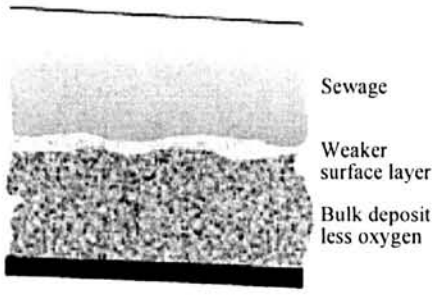

Figure 8.4: Typical deposit surface layer that developed in tests with a consolidation period of at least 24 hours at a temperature of 14^0C

The data also provided high quality observations necessary to understand how real in-sewer sediments transform in a sewer between high flow events. Similar surficial features could be observed for all deposits that had consolidated for at least 24 hours at 14°C. Figure 8.5 shows diagrammatically the existence of a weaker surface layer, the development of which was captured by the web camera as a lighter coloured material (discernible in Plate 8.2). This corresponds with field observations of sediment deposits where there is frequently a grey-whitish (aerobic) surface layer overlying a black (presumably anaerobic) bulk deposit. This grey-whitish layer was observed in all tests with sewer sediments at 14°C.

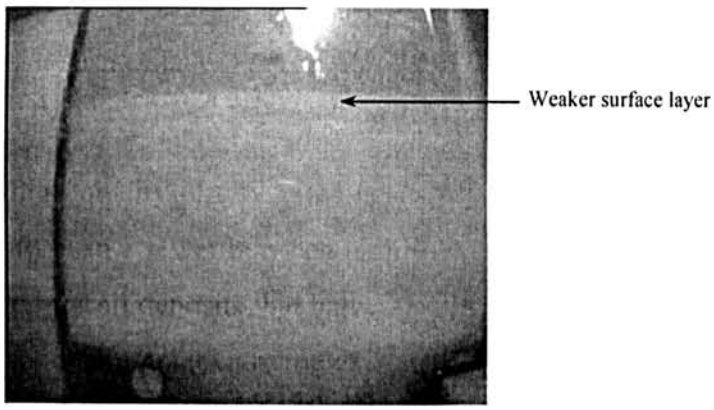

Plate 8.2: Deposit surface layer that developed in Test 4 (Loenen - 14^0C, 56 hours)

A characteristic pattern of erosion was observed in all of the sewer sediment deposit tests that were formed at 14°C, and in each case erosion was initiated at bed shear stresses of less than 0.5 N/m^2. As is evident from Figures 8.3 and 8.4, as the bed shear stress increased, the TSS values initially increased very slowly prior to a sharp increase. This increase was sustained for approximately 500 seconds after which the TSS values remained fairly constant even though the applied bed shear stress was still being increased in a stepwise fashion. In the final stage of the test the bed started to erode very rapidly and, as a consequence, the TSS values rose sharply. Comparison between Test 2 [see Figures 8.3(b) and 8.4(b)], which was conducted at 4°C, and Tests 1, 4 and 5, which were conducted at 14^0C, indicates that temperature has an influence on the development a sewer deposits erosion resistance. The sediment used in Test 1 was taken from the same location as that used in Test 2 (Dundee), and had very similar particle size distributions and organic content. It was also consolidated for an identical period of time and the DO level in the overlying water was maintained at 70% saturation for both tests. In terms of environmental conditions the sole difference was the temperature of the water. In Test 1 this was set to 14°C which was taken to resemble the conditions in a northern European sewer in summer, whereas in Test 2 a temperature of 4°C was selected in order that that the rate of the biochemical processes would be negligible. Although exposed to a similar pattern of shear stress steps it can be seen from Figure 8.3 that the overall mobility was lower, with the TSS values in the early part of the test approximately 50% lower, and the pattern of erosion of the deposit formed at 4°C is different. The grey-whitish surface top layer that was observed in the tests conducted at 14^0C did not form in Test 2. Additionally, in Test 2, after 5,000 seconds the TSS values rose slowly and then more quickly. Figure 8.3(b) also illustrates how, once the deposit had been mobilised the proportion of inorganic sediment in the suspension rose slowly as the shear stress increased. Further to the significance of the temperature effects, the impact of the different deposit durations was evident from the results of the tests carried out using the Loenen sediment. During these tests two types of process were postulated:

- physical consolidation, or
- transformation of the organic sediment due to biological processes

Suppression of the biological processes in Test 2 was achieved by running the test at 4°C and the comparative data from Test 1 indicated that when physical consolidation dominated, the sediment in suspension could be reduced by approximately 50%. Alternatively, the Loenen tests demonstrated a greater dependence on the biological processes which were much more important than physical consolidation. Comparison of the data from Test 3 [see Figure 8.3(c)] which was consolidated for 18 hours with the data from Test 4 [see Figure 8.3(d)], which was consolidated for 56 hours illustrate how the biological processes significantly weakened the bed with time. Although it may have been expected that the physical consolidation would have served to strengthen the bed, it would appear that the biological transformation processes seemed to dominate.

8.9. Performance of Applied Modelling Methodology

In order to test the veracity of the modelling methodology outlined in Chapter 7 and compare the results with the original Ackers (1991) relationship the following modelling techniques were applied:

Method 1 – Ackers (1991) with a characteristic deposit d_{35}

Method 2 – Ackers (1991) on a fractionwise basis without A_{gr} corrections

Method 3 – Ackers (1991) on a fractionwise basis with A_{gr} corrections as recommended by White & Day (1982)

Method 4 – Ackers (1991) on a fractionwise basis using A_{gr} corrections calibrated from the Forfar tests

As there was only data available from two tests using the Dundee and Loenen sediment mixtures respectively, it was considered there was not enough data on which to recalibrate the fractional A_{gr} values, as this would have left only 1 test upon which to validate the procedure. With this in mind it was decided to implement the relationship recommended by White and Day (1982) which linked the relative particle stability, A'_{gr}/A_{gr} to particle size, d_i/d_A:

$$A'_{gr}/A_{gr} = 0.4(d_i/d_A)^{0.5} + 0.6 \qquad (8.10)$$

where:

d_i = particle size of i^{th} fraction (m)

d_A = particle diameter of size fraction when $A'_{gr}/A_{gr} = 1$ (m)

White and Day also showed a relationship between d_A, and the range of particle sizes in a mixture:

$$d_A/d_{50} = 1.6(d_{84}/d_{16})^{-0.28} \qquad (8.11)$$

Using the approach outlined in Equations 8.10 and 8.11 the A'_{gr} values (for Method 3) were determined for the Dundee and Loenen sediment mixtures as outlined in Tables 8.3 and 8.4 respectively.

Particle size fraction (mm)	**(Dundee)** $\mathbf{A'_{gr}}$	**(Loenen)** $\mathbf{A'_{gr}}$
5	0.122	0.122
3.35	0.130	0.131
2	0.145	0.147
1.18	0.167	0.170
0.6	0.209	0.213
0.425	0.238	0.244
0.3	0.277	0.283
0.212	0.326	0.334
0.15	0.389	0.400
0.63	0.648	0.671

Table 8.3: Revised A'_{gr} values of Dundee and Loenen sediment mixtures

The results of all of the aforementioned modelling approaches (Methods 1-4) are presented in Figures 8.5-8.8.

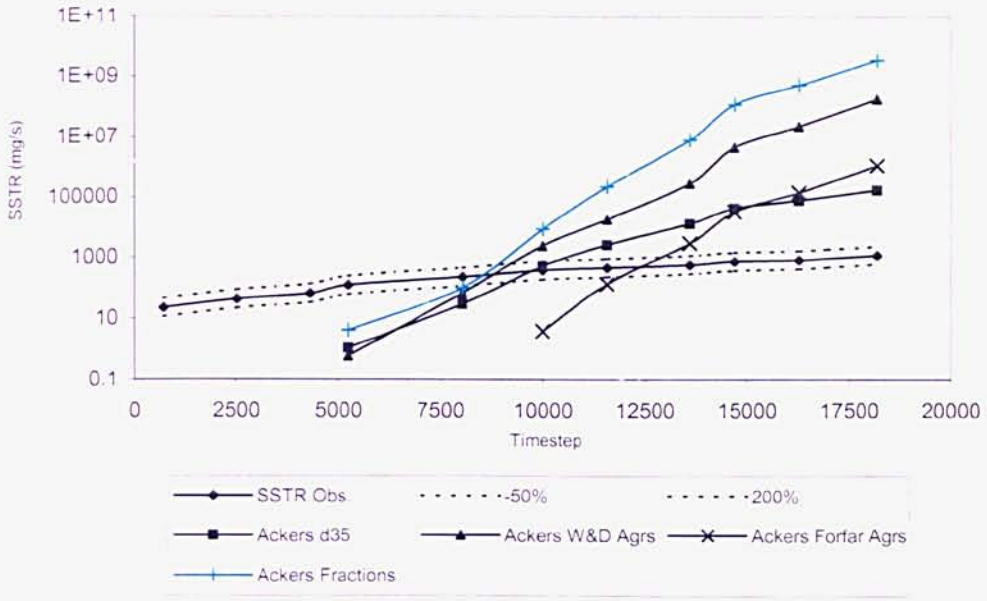

Figure 8.5: Model results from Test 1 (Dundee deposit, 42 hours consolidation at 14^0C)

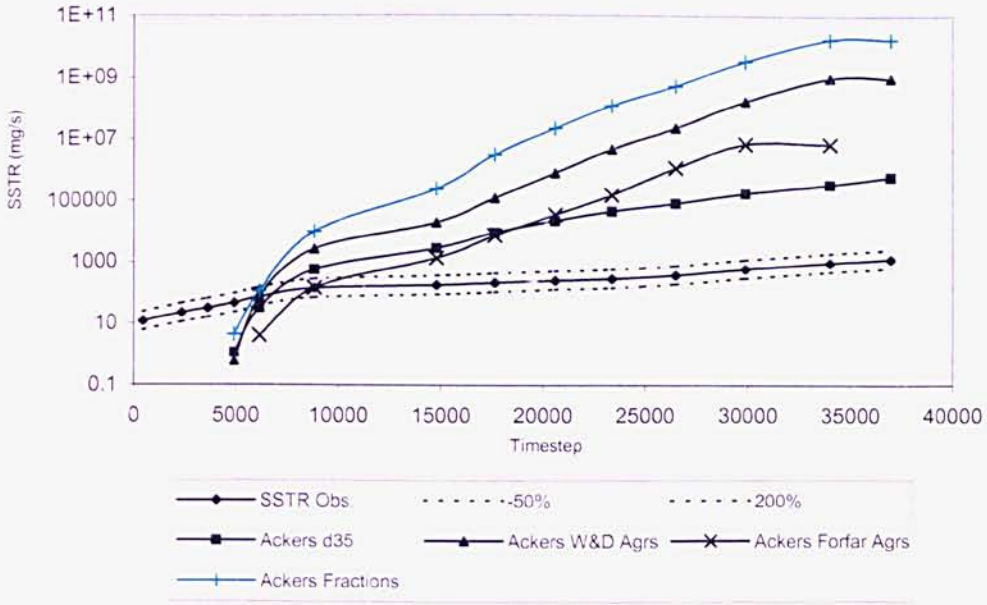

Figure 8.6: Model results from Test 2 (Dundee deposit, 42 hours consolidation at 4^0C)

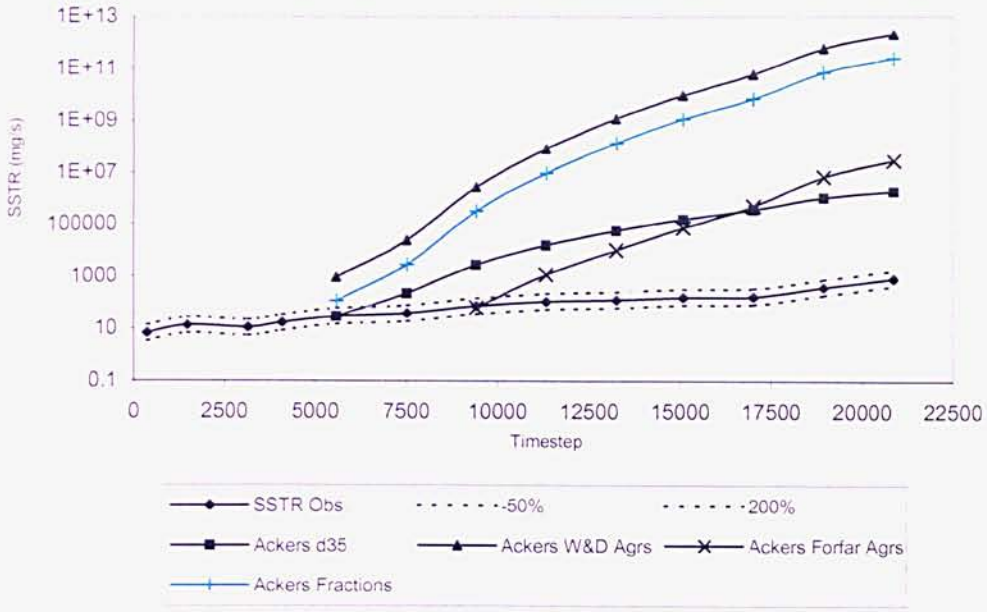

Figure 8.7: Model results from Test 3 (Loenen deposit, 18 hours consolidation at 14^0C)

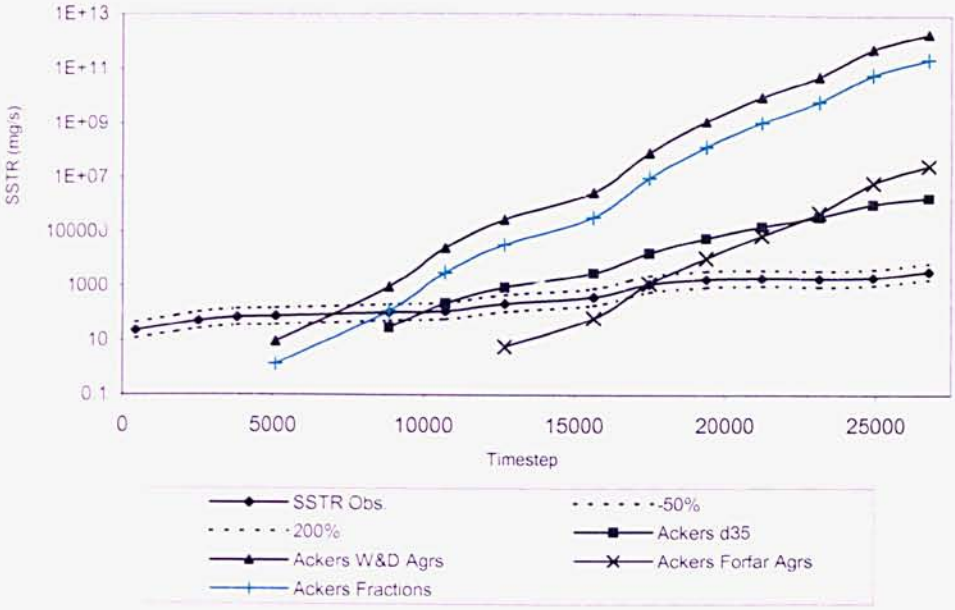

Figure 8.8: Model results from Test 4 (Loenen deposit, 56 hours consolidation at 14^0C)

Quite clearly the Ackers relationship (Method 1) over-predicted the observed SSTRs in the laboratory just as it did in the field. For the tests carried out on the Dundee deposits in general it can be seen from Figures 8.5 and 8.6 that the SSTRs observed from the 4^0C test were over-predicted to a greater degree than those from the 14^0C test. This was not surprising, as the Ackers relationship does not account for temperature effects that caused the overall mobility to be lower in Test 2. Similarly, although there was severe over-prediction for the results of both tests carried out on the Loenen deposit material, the errors were not as severe for Test 4 which had been consolidated for 56 hours as opposed to 18 hours for Test 3. As discussed in Section 8.8 the longer consolidation period at 14^0C actually served to weaken the bed, leading to enhanced SSTRs; again the Ackers relationship does not make any allowances for ADWP or deposit consolidation time. By plotting the observed and predicted (Method 1) SSTRs against the shear stress as shown in Figure 8.10 overleaf it was noted that, in all of the tests, the predictions worsened as the rate of shear increased in magnitude. This provided an indication as to why the Ackers (1991) relationship, the general form of which is shown in Equation 8.12, performed poorly.

$$G_{gr} = H\left(\frac{F_{gr}}{A_{gr}} - 1\right)^m \qquad (8.12)$$

where: G_{gr} = sediment transport rate

F_{gr} = sediment mobility

A_{gr} = value of F_{gr} at threshold of movement

H and m are empirical calibration coefficients

Had the predictions been excessively poor at the lower values of shear stress this would have indicated a problem with the threshold values. In contrast, as the worst predictions actually occurred at the higher values of shear stress, this indicated that the problem was associated with the calibration of the 'm' coefficient.

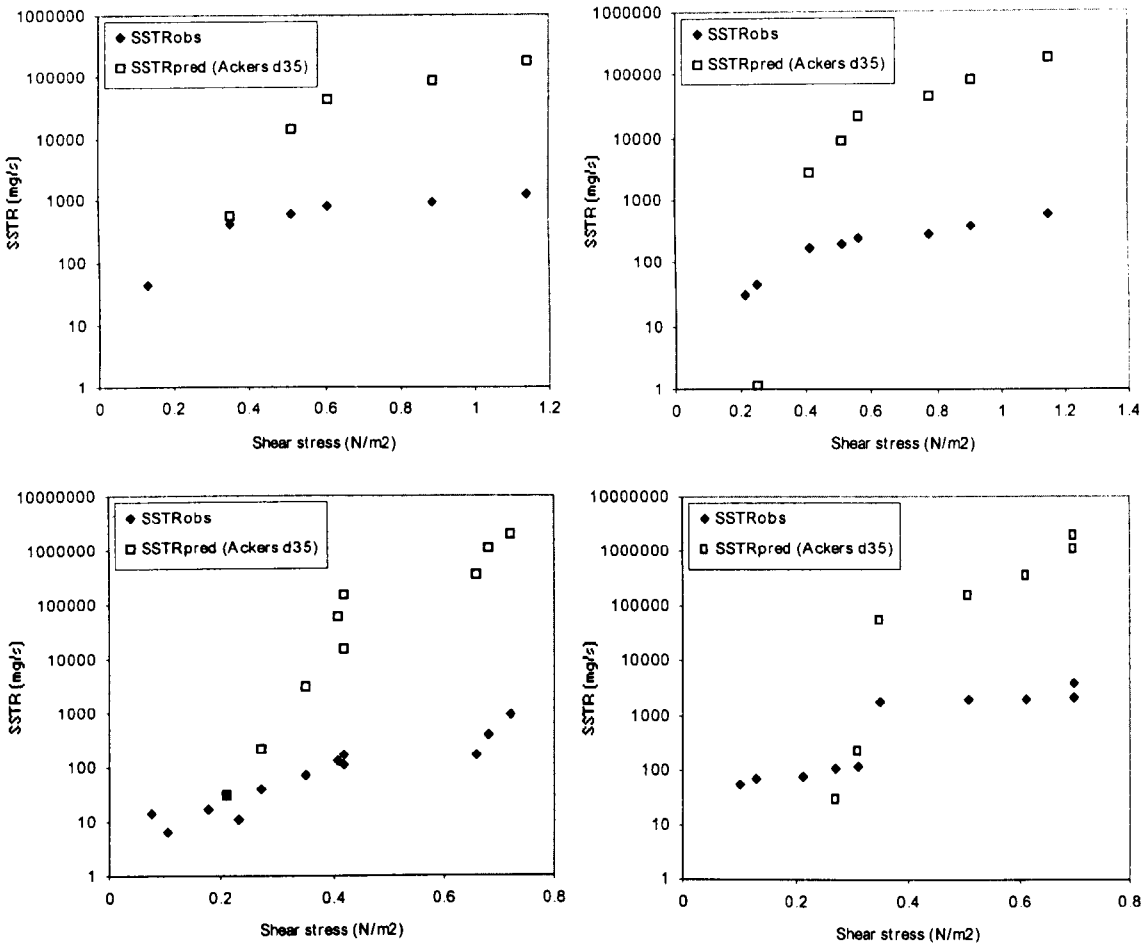

Fig 8.9: SSTRs (observed and predicted) versus bed shear stress for:
(a - top left) Dundee deposit (14^{0}C, 42hrs); (b – top right) Dundee deposit (4^{0}C, 42hrs);
(c – bottom left) Loenen deposit (14^{0}C, 18hrs) and (d – bottom right) Loenen deposit (14^{0}C, 56hrs)

8.9.1. Accounting for Cohesive-like Properties of the Deposit

Although as seen in Figures 8.6-8.9 some improvement could be gained by using the $A_{gr}s$ calibrated from the Forfar sediment on a fractionwise basis, the results were still very poor. It was decided to apply the Nalluri and Alvarez (1992) cohesive relationship (Equation 2.67) as derived in Section 2.12.3.2 in an attempt to improve the results. The results from this analysis for each of the tests are presented in Figures 8.10-8.14.

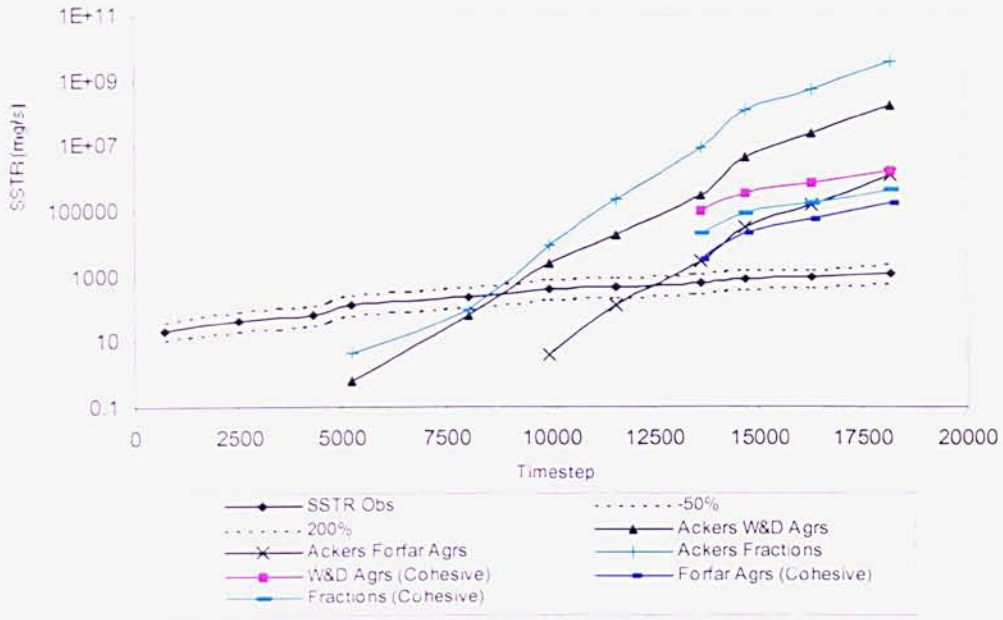

Figure 8.10: Test 1 (Dundee deposit, 42 hours consolidation at 14^0C)

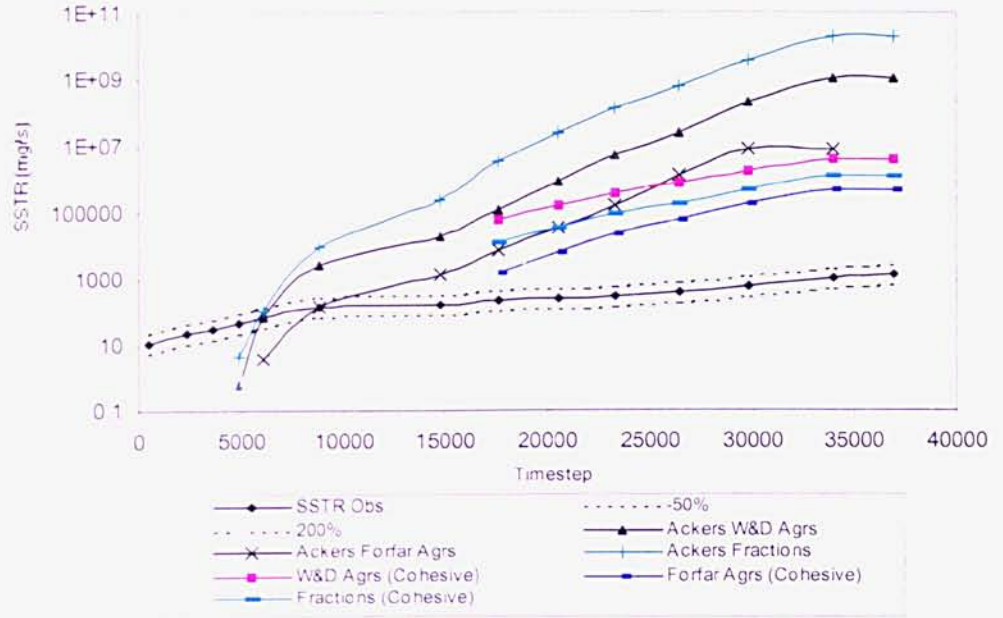

Figure 8.11: Test 2 (Dundee deposit, 42 hours consolidation at 4^0C)

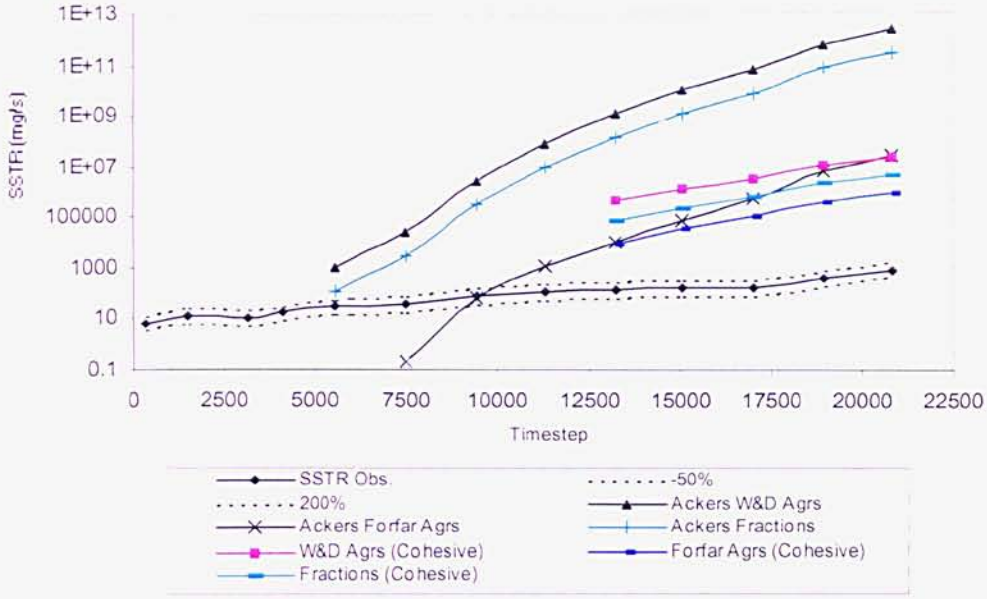

Figure 8.12: Test 3 (Loenen deposit, 18 hours consolidation at 14^{0}C)

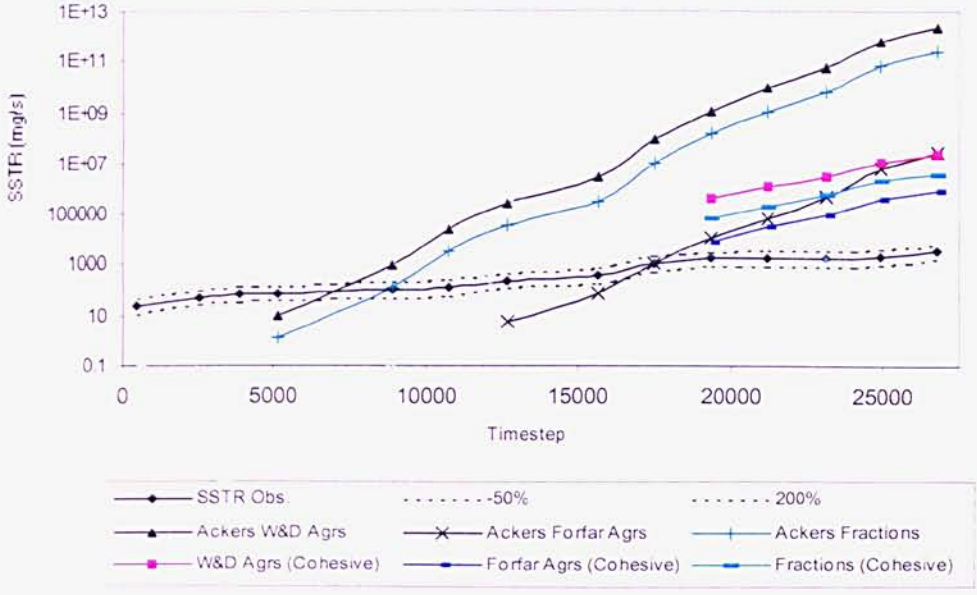

Figure 8.13: Test 4 (Loenen deposit, 56 hours consolidation at 14^{0}C)

It is clear from Figures 8.10-8.13 that incorporating a cohesive relationship to cater for the finest fraction did produce some improvement in the results. However, the cohesive relationship only predicted transport at shear stresses in excess of 0.5 N/m^2 and clearly required to be recalibrated for the deposit material it was being used to model. As with the computation of the A'_{gr} values, as there was only data available for two tests for each deposit material, there was not considered sufficient data upon which to recalibrate the cohesive relationship. Using the cohesive relationship it can be seen from Figure 8.13 that the deposit material that had been consolidated for the greatest amount of time (at 14^0C) achieved the best results.

8.10. Conclusions

The evidence from the Delft laboratory tests illustrated that sewer sediment deposits formed under different environmental conditions exhibit different resistances to erosion. Specifically, in conditions in which the biochemical processes are inhibited (due to low temperatures) deposits behave in a manner as though they were composed of entirely inorganic sediments. Conversely, when biochemical processes are present deposits are generally weaker and appear to exhibit a two-stage erosion process.

These tests have shown that surficial biochemical processes are likely to have a measurable impact on the erosional resistance of a sewer sediment deposit. This was corroborated by examination of the results from Tests 1 and 2 in which the Dundee deposit formed at 4°C proved significantly stronger when subjected to similar hydraulic conditions as the deposit formed at 14^0C. When the deposits were consolidated at the higher temperature images obtained from the side-view web camera indicated that a surface layer developed during the consolidation period. Of note is the fact that the thickness of this layer was seen to increase in the early parts of the tests as the shear stress increased, until a stage was reached when particles were observed to be eroded from the surface layer. Indeed, the high proportion of organic material in the early stages of these tests confirmed the highly organic nature of this surface layer. As the TSS values started to increase rapidly later in the tests it was observed that the surface layer no longer covered the whole surface but had been breached, releasing material from below it. This would suggest that perhaps the use

of a single 'continuous' equation is not the most sensible approach and perhaps a 'layered' model would be more appropriate. That is, it may be that an approach, which takes into account the more easily erodible surface layer, may yield better results.

In addition, the results of the modelling have shown that, although the $A'_{gr}s$ that were calibrated from the Forfar tests did improve the predicted SSTR values somewhat, the $A'_{gr}s$ that were determined from the White and Day (1982) method offered minimal improvement on the original Ackers (1991) results. This illustrated the importance of calibrating the A'_{gr} values using the actual material being modelled; and it is believed that, had this process been carried out with the Dundee and Loenen mixtures, then the predicted SSTR values from the experimental data could have been improved further. Similarly, the cohesive relationship was also calibrated for the Forfar material and ideally should also have been recalibrated for the individual deposits being modelled.

Chapter Nine – Conclusions

9.1. Introduction

This programme of research highlighted the importance of obtaining good quality data from both field studies and laboratory testing, and illustrated how the outputs from both can be combined in order to further knowledge in the field of sediment transport. The research has highlighted the need for a new modelling approach to be adopted by the UK Water Industry to deal with sediment transport. Existing sewer sediment modelling approaches are generally too simplistic and the current methodology employed in the InfoWorks industry standard drainage modelling package yields unreasonably high over-predictions, and thus cannot be used with any degree of confidence to predict water quality that may be spilled to receiving waters via CSOs. This shortfall is due to the use of the Ackers (1991) sediment transport model, which was developed from a study of non-cohesive deposits. This approach is flawed due to a lack of detailed consideration of the bed properties (e.g. cohesiveness, controlled by finest particles/organics; and consolidation time, controlled by the length of the ADWP). The study has also illustrated the need for further research to be carried out, both field and laboratory based, although it is acknowledged that good quality field data is difficult to obtain. This is due to a combination of health and safety considerations and the inhospitable conditions under which samples must be obtained and instrumentation must be installed, maintained and operated.

9.2. Field Instrumentation Reliability Problems

Obtaining good quality field data proved to be a major obstacle that had to be overcome during this study. Due to the harsh operating conditions experienced within combined sewers, the equipment often malfunctioned as a result of sewage ingress and condensation affecting the electronic components. Apart from these malfunctions the main problem experienced was the build-up of sediment and rags against the sensor head of the flow monitors. There is nothing that can be done to resolve this problem apart from regular manual cleaning of the equipment. Unlike laboratory studies, fieldwork operations often require a high complement of staff due to health and safety regulations

and the requirement for several separate items of equipment to be operated simultaneously, often over relatively large distances.

9.3. Primary Outcomes of Field and Laboratory Testing

The main objective of this study was to test the veracity of the Ackers (1991) modelling approach for the prediction of suspended sediment transport in combined sewers and suggest ways in which the approach could be improved. Rushforth (2001) reported that the Ackers relationship generally underestimates bedload whereas this study has shown that it greatly overestimates suspended load, and, in its unmodified form, is not suitable for the prediction of fine-grained sediment transport in combined sewers. The main reasons for these shortcomings with the modelling approach may be summarised as follows:

- The Ackers (1991) relationship evolved as a result of research into the transport of non-cohesive deposit material and as such does not account for the cohesive-like properties exhibited by fine-grained sewer sediments.
- The relationship does not make any allowance for deposit formation conditions such as consolidation time (governed by the antecedent dry weather period), or biochemical processes (temperature controlled) which have been shown by this study to actually lower the erosion resistance of the bed.

From the results of this study it is suggested that improvements to the predicted results could be obtained by the following means (in order of greatest improvement obtained):

- Use the model on a fractionwise basis with the Ackers predicted $A_{gr}s$ for each size fraction
- Use the model on a fractionwise basis in conjunction with modified A_{gr} values that have been specifically calibrated for the deposit material being modelled.

- Use the model on a fractionwise basis in conjunction with modified A_{gr} values that have been specifically calibrated for the deposit material being modelled in conjunction with a cohesive relationship for the prediction of the finest fraction.

In addition, it would be pertinent to revise the empirical calibration coefficient 'm' based on experimental data specifically from cohesive mixed deposits. As discussed in Section 8.9 this was a likely source of error at high rates of bed shear stress.

9.4. General Observations Regarding Transport Phenomena

The results of the tests highlighted the complexities associated with sediment transport within a combined sewer. The results of the field testing demonstrated that the processes of erosion and net deposition occurred simultaneously during the flush tests with all of these providing evidence that there was a tendency for the fall velocity values to increase as the test progressed in line with the increasing shear stress.

The evidence from the Delft laboratory tests highlighted the importance of the deposit history to its erosional resistance. Surficial biochemical processes have a demonstrable impact on the erosional resistance of a sewer sediment deposit and it may be inferred that:

- Inhibition of the biological processes (by consolidating the bed at low temperatures) causes deposits to behave in a manner as though they were composed of entirely inorganic sediments.
- Conversely, when biological processes are present deposits are generally weaker and appear to exhibit a two-stage erosion process.
- While the deposit is biologically 'active' it tends to get weaker with time.
- Consolidation of a bed that is not biologically 'active' increases its erosional resistance.

These findings have illustrated the need for a holistic modelling strategy, which takes into account deposit formation conditions as well as the 'usual' hydraulic factors.

9.5. Recommendations for Further Research

In order to improve the results obtained by using the Ackers (1991) relationship it has been shown that it is necessary to apply the model on a fractionwise basis with modified A_{gr} values (A'_{gr}) for each of the size fractions. As shown from the Delft results it is necessary to carry out this calibration process on the material being modeled as the relationship put forward by White and Day (1982) for evaluating A'_{gr} values did not produce satisfactory results. Although relatively straightforward, it is nonetheless a time consuming operation to calibrate these A'_{gr} values for individual deposit materials. Thus it would be beneficial if more research was carried out to recommend either:

(i) A generic set of modified A_{gr} values (A'_{grs}) that could be used with different types of deposit material, that is, in terms of particle size ranges and densities.

(ii) A new relationship based on extensive field data and/or laboratory data that could be used to evaluate A'_{gr} values more successfully than that proposed by White and Day (1982).

Of further importance is the fact that the fractional calibrations of A'_{gr} were achieved by modifying the $A_{gr}s$, so that the amount of material per fraction in suspension was in the same proportion as the fractions in the parent bed deposit. This could be a possible source of error as, if the particle size distribution of the bed were changing during the event this would affect the results later in the test, as there would be different proportions of material available for erosion and hence different proportions of material in suspension. Additionally, the current study did not attempt to reduce the error of the larger fractions, which also exhibited a large degree of error; this would also form the basis for further research and may have been due to the changing composition of the bed as previously discussed.

In terms of suspended sediment transport prediction, this work has shown the importance of taking into account the environmental conditions under which the sewer deposit was formed. With this in mind, further research is also required to investigate the effect of the antecedent dry weather/consolidation period, as this could also be a source of improvement in the predicted suspended sediment transport rates. Historically researchers have had a tendency to quantify the polluting potential of a sewer flow by the value of the total suspended solids, however a more elaborate approach is required, whereby the solids in transport are 'broken down' into fractions in order to look at their polluting potential. Indeed, different pollutants could be associated with different fractions, therefore different storm events could actually have different polluting potentials. Again, this could also be associated with the deposit history, in terms of what was deposited during the antecedent dry weather period, and what microbiological activity could have taken place depending on the length of the antecedent dry weather period. Indeed, as shown in this study, these biological aspects undoubtedly have an effect on the structure of the sediment bed and as such are inextricably linked to the physical processes involved in the onset of erosion and transport. An approach that could be used for the development of a suitable holistic modelling strategy for combined sewerage systems is outlined in Figure 9.1.

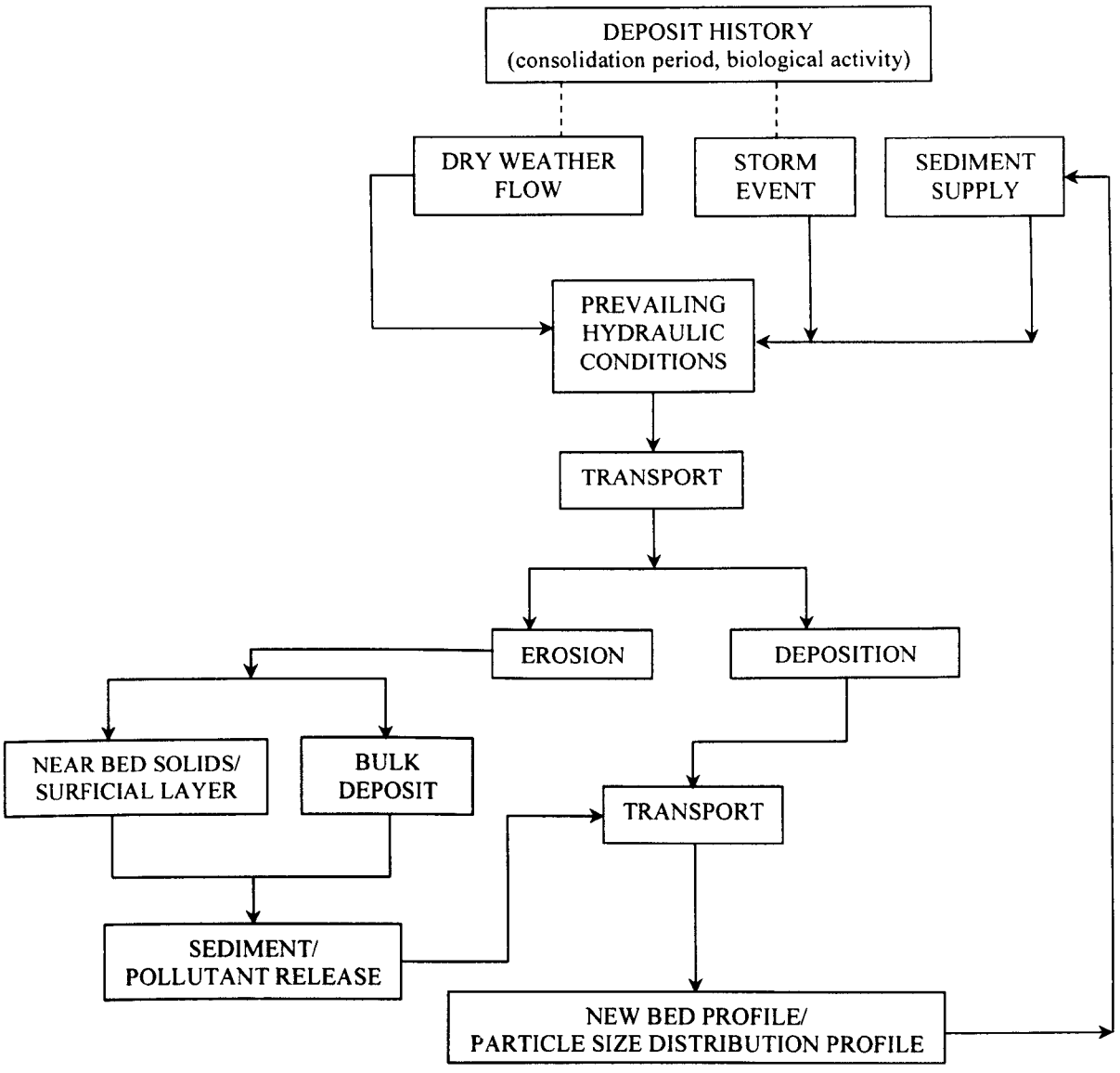

Figure 9.1: Proposed integrated modelling strategy

Contrary to the findings of previous studies it is proposed that the origins of the material in suspension should be considered, rather than simply modelling it as either a granular or cohesive-like mixture. That is, field and laboratory work should be undertaken in an attempt to ascertain whether the material in the flow column has been eroded from the bed or is primarily comprised of near bed solids and/or the organic surficial layer such as that observed in the Delft tests. This study has shown the importance of the deposit

history in terms of consolidation time and temperature on erosional resistance. Thus it follows that any approach used to predict solids transport must account for the ambient flow conditions and take into account whether there has been a long duration of low flow velocity; that is, the antecedent dry weather period should be accounted for. To this end an approach should be adopted that relates the total solids in transport with the consolidation time, and microbiological processes as a function of the bed strength.

To develop an integrated modelling approach as previously described would require a significant collaborative research programme to be undertaken between those involved in the physical processes of sediment transport and microbiologists. If such a model should be developed that catered for the aforementioned processes this would be a significant step forward for the prediction of sediment transport and associated pollutants in combined sewers.

References

Ab Ghani, A. (1993). Sediment transport in sewers. *PhD Thesis*. University of Newcastle upon Tyne, Dept. of Civil Engineering.

Ackers J.C., Butler, D. and May, R.W.P. (1996). Design of sewers to control sediment problems. *Report CIRIA141*, Construction Industry Research and Information Association, London, UK

Ackers, P. (1984). Sediment transport in sewers and the design implications. *Proc. Int. Conf. on Planning, Construction, Maintenance and Operation of Sewerage Systems*. BHRA (Cranfield), Reading, UK, 215-230.

Ackers, P. (1991). Sediment aspects of drainage and outfall design. *Proc. of the Int. Symp. on Environmental Hydraulics*, J.H.W. Lee and A.A. Cheung (Eds.) Hong Kong.

Ackers, P. and White, R.W. (1973). Sediment transport: new approach and analysis. *J. Hydr. Div.*, ASCE, 99(HY11), pp2041-2060.

Ackers, P., Harrison, A.J.M. and Brewer, A.J., (1968). The hydraulic design of overflows incorporating storage. *Jou. Inst. Municipal Eng.*, 95, pp31-37.

Ahyerre M. (1999). Bilan et mécanismes de migration de la pollution organique en réseau d'assainissement unitaire. *PhD thesis*. Université de Paris.

Alvarez-Hernandez, E.M. (1990). The influence of cohesion on sediment movement in channels of circular cross-section. *PhD Thesis*. University of Newcastle upon Tyne.

Angus Council. (1999). Finalised Angus Local Plan, 1999. *Angus Council Report*.

Arthur S. (1996). Near bed solids transport in combined sewers. *PhD Thesis*. University of Abertay Dundee

Arthur, S. and Ashley, R.M., (1998). The influence of near bed solids transport on first foul flush in combined sewers. *Wat. Sci. Tech.*, Vol. 37, No. 1, pp131-138.

Ashley, R.M., Wotherspoon, D.J.J., Coghlan, B.P. and Ristenpart, E. (1993). Cohesive sediment erosion in combined sewers. *Proc. 6ICUSD*, Niagara Falls, Sept

Ashley, R.M., Vollertsen, J., McIlhatton, T. and Arthur, S. (1999). Sewer solids erosion, washout, and a new paradigm to control solids impacts on receiving waters. *Proc. 8ICUSD*, Sydney.

Ashley, R.M. and McIlhatton, T.D. (1998). The importance of near bed solids. *Proc. Conf. on Alleviating Stormwater & CSO Problems*. Bristol, UK, Dec.1998.

Ashley, R.M. and Verbanck, M. (1996). Mechanics of sewer sediment erosion and transport. *J. Hyd. Res.* 34 pp753-769.

Ashley, R.M. (1993). Sediment behaviour in combined sewers. *Report for WRc*. WWTC, Dundee Institute of Technology.

Ashley, R.M. (1994). The Dundee central area sewer model. *Report for Tayside Regional Council - Department of Water Services*. University of Abertay Dundee.

Ashley, R.M., and Crabtree, R.W., (1992). Sediment origins deposition and build-up in combined sewer systems. *Wat. Sci. Tech.*, 25, pp1-12.

Ashley, R.M., Arthur, S., Coghlan, B.P., and McGregor, I., (1994). Fluid sediment in combined sewers. *Wat. Sci. Tech.* 29, pp113-123.

Ashley, R.M., Saul, A.J., Nalluri, C., Arthur, S. and Skipworh, P., (1995). Behaviour of sediments in sewers. *Final EPSRC Grant Report (No. GR/H/13373)*. Wastewater Technology Centre, University of Abertay Dundee, Dundee, Scotland, UK.

Ashley, R.M., Wotherspoon, D.J.J., Goodison, M.J., McGregor, I., and Coghlan, B.P. (1992). The deposition and erosion of sediments in sewers. *Wat. Sci. Tech.*, 26, pp1283-1293.

Bagnold, R.A. (1966). Approach to the sediment transport problem from general physics. *US Geological Survey Professional Paper* 422.

Ashley R M., Bertrand-Krajewski, J.L., Hvitved-Jacobsen, T. and Verbanck, M. (2003). Solids in Sewers. *IWA Scientific and Technical Report*. IAWQ/IAHR Joint Committee on urban Storm Drainage.

Batchelor, G.K. (1965). The motion of small particles in turbulent flow. *Proc. 2nd Austr. Conf. on Hyd. And Fluid Mech.* University of Auckland.

Berlamont J. and Torfs H. (1996). Modelling (partly) cohesive sediment transport in sewer systems. *Wat. Sci. Tech.*, Vol. 33, No. 9.

Bertrand-Krajewski J.L., Madiec H., and Moine O. (1995). Study of two experimental sediment traps : operation and solids characteristics. *Proc. Int. Conf. on Sewer Solids - Characteristics, Movement and Control.* Dundee.

Black K.S., Tolhurst T.J., Paterson, D.M. and Hagerthey S.E. (2002). Working with natural cohesive sediments. *Journal of Hydraulic Engineering. 7 (1), 67-82*

Bonnefille, R. (1963). Essais de synthese des lois de debut d'entrainment des sediments sous l'action d'un courant en regime uniforme bull. *Du CREC*, no. 5. Chatou.

BSI - British Standards Institution. (1990). British standard methods of test for soils for civil engineering purposes, *BS 1377.*

Butler, D., Friedler, E. and Gatt, K. (1995). Characterising the quantity and quality of domestic wastewater inflows. *Wat. Sci. Tech. 31 (7),* pp13-24.

Butler, D., May, R.W.P., and Ackers, J.C., (1996). Sediment transport in sewers - Part 1: Background. *Proc. Institution of Civil Engineers*, Wat., Marit. & Energy, 113, 8.

Chebbo G. (1992). Solides des rejets pluviaux urbains, caractéristaion et traitabilité. *PhD thesis.* Ecole Nationale des Ponts et Chaussées. Paris.

Chebbo G., Ashley, R. and Gromaire, M-C. (2002). The nature and pollutant role of solids at the water-sediment interface in combined sewer networks. *Proc. Int. Conf. on Sewer Processes and Networks.* Paris.

Clegg. S, Foster, C.F. and Crabtree, R.W. (1993). An examination of the ageing of gully pot sediments. *Environmental Technology*, 14, pp453-461.

Coghlan, B.P. (1995). Solids transport in combined sewerage systems. *PhD Thesis.* University of Abertay Dundee.

Coleman, N.L. (1969). A new examination of sediment suspension in open channels. *Journal of Hydraulic Research. 7 (1), 67-82*

Coleman, N.L. (1982). Discussion of paper 16313. *J. Hydraul. Div.*, ASCE, Vol. 108, Nr. HY1, pp164-165.

Crabtree, R.W. (1989). A classification of combined sewer sediment type and characteristics. *WRc Report* ER324E.

Craig, R.F., (1987). Soil Mechanics. 4th Edition, *Van Nostrand International*, ISBN 0-278-00019-3.

Dade, W.B., Nowell, A.R.M. and Jumars, P.A. (1992). Predicting erosion resistance of muds. *Mar. Geol.* 105, 285- 297.

Davies, J.W. (1990). Laboratory study related to the modelling of stormwater quality in combined sewers. *Proc. 5th ICUSD* pp215-219.

De Sutter, R. (2001). Erosion and transport of cohesive sediment mixtures in unsteady flow. *Ph.D. Thesis*. University of Gent, Belgium.

De Sutter R., Rushforth P.J., Tait S.J., Huygens M., Verhoeven R. and Saul A. J. (2000). The erosion of cohesive mixed deposits: implications for sewer flow quality modelling. *Urban Water* 2(4) pp285-294.

Dinckelacker, A. (1992). Cleaning of sewers. *Wat. Sci. Tech.* 25 (8), pp37-46.

Ellis, J. B. (1986). Pollutional aspects of urban runoff. *Urban Runoff Pollution,* NATO ASI Series Vol. G10, edited by H.C. Torno, J. Marsalek, and M. Desbordes, Springer-Verlag, Berlin, 1-38.

Engelund, F.A and Hansen, E. (1966). A monograph on sediment transport in alluvial streams. *Technical Press*, Copenhagen.

Fraser, A.G. (1998). The prediction of near bed solids (NBS) movement using suspended solids profile methods. *Internal report.* UWTC, University of Abertay Dundee.

Fraser, A.G. and Ashley, R.M. (1999). *A model for the prediction and control of problematic sediment deposits.* Proc. 8ICUSD, Sydney.

Geiger, W. (1987), *Flushing effects in combined sewers. Proc. 4ICUSD.* pp40-47.

General Register Office for Scotland (2001). The registrar general's annual review of demographic trends. *The Scottish Office.*

Grass, A.J. (1970). The initial instability of fine sand. *Proc. ASCE*, 96(HY3), pp619-632.

Gromaire, M.C., Garnaud, S., Saad, M., and Chebbo, G. (2001). Contribution of different sources to the pollution of wet weather flows in combined sewers. *Water Res.* Vol.35, No.2, pp521-533.

Gupta K. and Saul A J. (1996) Specific relationships for the first flush load in combined sewer flows. *Water Res.* Vol.30, No.5

Harrison A J M. and Holmes D W. (1967). The movement of storm water in combined sewers. *Report INT 73.* Hydraulics Research Station, Wallingford.

Hyder Consulting. (2002). Forfar DAP scoping study. *Report for Scottish Water.*

Jefferies, C., and Ashley, R.M. (1994). The behaviour of gross solids in sewer systems. *Jou. European Water Pollution Control Association.* Vol. 4, No.5. pp11-17

Jubb S., Guymer I., Licht G. and Prochnow J. (2000). Relating oxygen demand to flow: development of an in situ sediment oxygen demand measurement device. *Proc. 1st. World Water Congress of IWA*, pp79- 86. Paris.

Kandiah, A. (1974). Fundamental aspects of surface erosion of cohesive soils. *PhD thesis.* University of California, Davis, California.

Kirby, J.M. (1988). Rheological characteristics of sewage sludge: a granuloviscous material. *Rheologia Acta*, 27, pp326-334.

Kleijwegt, R.A. (1992). Sediment transport in circular sewers with non-cohesive deposits. *Ph.D. Thesis.* Delft University of Technology.

Lavelle, J.W. and Mofjeld, H.O. (1987). Do critical stresses for incipient motion and erosion really exist? *Jou. Hyd. Eng.*, ASCE, Vol 113, pp389-393.

Licht, G. (1998). Effects of sediment oxygen demand during storm conditions. *Diploma dissertation.* Lehrstuhl und Institut fur wasserbau und wasserwirtschaft. RWTH Aachen.

Liem, R., Spork, V. and Koengeter, J. (1997). Investigations on erosional processes of cohesive sediment using an in-situ measuring device. *Int. Jou. of. Sed. Res.*, ASCE, Vol 12, no. 3, Dec.

Lindholm, O. and Aaby, L., (1989). In-pipe flushing and its implication for overflow quality. *Wat. Sci. Tech.* 22, pp17-25.

Mantz, P.A., (1977). Incipient transport of fine grains and flakes by fluids - Extended Shields diagram. *ASCE*, J.E.E.D. 103, pp601-615.

May, R.W.P. (1993). Sediment transport in pipes and sewers with deposited beds. *Report SR 320*, HR Wallingford.

May, R.W.P. (1994). Transport of sediments in pipes – application to design of self-cleansing sewers. *Jou. European Water Pollution Control.* Vol.4, No.5.

Mayerle, R., Nalluri, C. and Novak, P. (1991). Sediment transport in rigid bed conveyance. *J. Hydraulic Res.*, 29(4), pp475-495.

Mehta, A.J., and Partheniades, E. (1982). Resuspension of deposited cohesive sediment beds. Proc. 18th Coastal Engineering Conference. pp1569-1588.

Metcalf and Eddy Inc., (1991). Wastewater engineering - Treatment, disposal and reuse. *London: McGraw-Hill International.*

Michelbach, S. and Weiss, G.J., (1995). Settleable sewer solids in stormwater tanks with clarifier for combined sewage. *Proc The International Conference on Sewer Solids - Characteristics, Movement and Control*, Dundee.

Michelbach, S. and Wohrle, C. (1992). Settleable Solids in a Combined Sewer System - Measurement, Quantity, Characteristics. *Wat. Sci. Tech.*, 25, pp181-188

Mitchener, H. and Torfs, H. (1996). Erosion of mud/sand mixtures. *J. Coastal Eng.*, Vol 29, pp1-25.

Nalluri, C. and Ab Ghani, A. (1993). Bedload transport without deposition in channels of circular cross section. *Proc. 6ICUSD.* Niagra Falls, Canada.

Nalluri, C. and Alvarez, E. (1990). The influence of cohesion on sediment behaviour in pipes and open channels. *Final report to SERC.*

Nalluri, C. and Alvarez, E.M.. (1992). Influence of cohesion on sediment behaviour. *Wat. Sci. Tech.*. Vol. 25, No. 8, pp151-164.

Nikuradse, J. (1933). Stromungsgetze in rauhen Rohern. *V.D.I. – Forschungsheft*, no. 356.

Oms, C. (2003). Nature, localisation et dynamique de l'interface eau-sédiment en réseau d'assainissement unitaire. *PhD thesis*. Université de Paris.

Oms, C., Gromaire-Mertz M.C., DeSutter R. and Chebbo G. (2001). Measurement of local bed shear stress in combined sewers. *Proc. UDM symposium*, Orlando, Florida, May 20-24, 2001.

Oms, C., Sakrabani, R., McIlhatton, T., Chebbo, G. and Ashley, R. (2002). Near bed solids in combined sewers. *Proc. 9ICUD*, Portland, USA, September 2002.

Paganini, M. (2002). Variability of sewer sediment properties in different site specific environmental conditions. *Diploma dissertation.* Facolta di Ingegneria, Universita Degli Studi di Padova.

Parchure, T.M. and Mehta, A.J. (1985). Erosion of soft cohesive sediment deposits. J. Hyd. Eng pp1308-1326

Parenthiades, E. (1965). Erosion and deposition of cohesive soils. *Jou. Hyd. Div.*, ASCE, 91, HY1, pp105-139.

Paterson, D.M. (1997). "Biological mediation of sediment erodibility: Ecology and physical dynamics." *Cohesive Sediments,* Burt et al.,eds. Wiley Interscience, New York, pp215-230.

Parzonka, W., Verhoeven, R. and Huygens, M. (1997). *From non-cohesive to cohesive sediment transport. Proc. 9th Int. Conf. On Transport & Sedimentation of Solid Particles.* J. Szobota (Eds.), pp41-60, Krakow.

Pearson, L.G., Thorton, R.C., Saul, A.J. and Howard, K., (1986). An introductory analysis of the factors affecting the concentration of pollutants in the first foul flush of a combined sewer. *Proc. 1ICUSD.* pp93-102.

Perrusquia, G. and Nalluri, C. (1995). *Modelling of bedload transport in pipe channels. Proc. Int. Conf. On the transport and sedimentation of solid particles.* Prague.

Perrusquia, G.S. (1991). Bedload transport in storm sewers. Stream traction in pipe channels. *A22. Report.* Chalmers University of Technology.

Pisano, W.C. (1995). Summary: US 'Sewer Solids' settling characterisation - methods, results, uses and perspective. *Proc The International Conference on Sewer Solids - Characteristics, Movement and Control*, Dundee.

Prandtl. L, (1952). Essentials of fluid dynamics. *Blackie publishers.*

Panagiotopoulos, I., Voulgaris, G. and Collins, M. (1997). The influence of clay on the threshold of movement of fine sandy beds. *Jou. Coast. Eng.*, 32, pp19-43.

Raudkivi, A.J. (1990). Loose boundary hydraulics. *Pergamon Press.* London:

Rennet, R.J. (1995). Sewerage management in Dundee. *Proc. Int Conf. on Sewer Solids - Characteristics, Movement and Control.* Dundee.

Ristenpart, E. (1995). *Sediment Properties and Their Changes in a Sewer.* Wat.Sci.Tech., Vol.31(7), pp77-83.

Ristenpart, E. and Uhl, M. (1993). *Dynamic behaviour of sewer sediments.* In proceedings of the sixth international conference on urban storm drainage. (pp.748-753). Niagra Falls, Canada.

Ristenpart, E., Ashley, R.M., and Uhl, M. (1995). *Organic near-bed fluid and particulate transport in combined sewers.* Wat. Sci. Tech.31(7), 61-68.

Rouse, H. (1937). Modern conceptions of the mechanics of sediment suspension. *transactions, ASCE*, Vol 102, pp463-543.

Rushforth, P.J., Tait, S.J and Saul, A.J. (2003). Modeling the erosion of mixtures of organic and granular in-sewer sediments. *Jour. Of Hyd. Eng. ASCE 129(4)* April 2003 pp308-315.

Rushforth, P.J. (2001). The erosion and transport of seer sediment mixtures. *PhD Thesis.* University of Sheffield.

Saget, A., Chebbo, G. and Bertrand-Krajewski, J.L. (1995). The first flush in sewer systems, *Proc The International Conference on Sewer Solids - Characteristics, Movement and Control.* Dundee.

Shields, A. (1936). Anwendung der Ahnlichkeitsmechanik und der Turbulenzforschung auf die Geschiebebewegung, Heft 26. *Preuss. Vers. für Wasserbau und Schiffbau*, Berlin.

Simons, D.B., and Senturik, F. (1992). Sediment transport technology - water and sediment dynamics. *Water Resources Publications.*

Skipworth, P.J., Tait, S.J. and Saul A.J. (1999). Erosion of sediment beds in sewers; Jour of Environmental Engineering ASCE 125(6) pp566-573.

Skipworth, P.J. (1996). Laboratory Investigations into cohesive sediment transport in pipes. *PhD Thesis*, University of Sheffield.

Smith, G.N. (1990). Elements of soil mechanics. *BSP Professional Books*, ISBN 0-632-02616-2.

Stokes G.G. (1851). Transactions of the Cambridge Philosophical Society (9):8 27

Stotz, G. and Krauth, K. (1984). Factors affecting first flushes in combined sewers. *Proc. 3ICUSD.* pp869-878.

Tait S.J., Ashley R.M., Verhoeven R., Clemens F. and Aanen L. (2003). Sewer sediment transport studies using an environmentally controlled annular flume. *Wat. Sci. Tech.* Vol 47, No.4, pp51-60.

Thorton, R.C. and Saul, A.J. (1986). Some quality characteristics of combined sewer flows. *The Public Health Engineer*, pp35-38.

Tito, L. (1995). Etude theorique et experimentale du transport des materiaux partiellement cohesifs. *PhD Thesis*. University of Gent, Belgium.

Torfs, H. (1995). Erosion of mud-sand mixtures. *PhD Thesis*. Catholic University of Leuven, Belgium.

Van Rijn, L.C. (1982). Equivalent roughness opf alluvial bed. *J. Hydr. Div.*, ASCE, no. HY10, 1982.

Van Rijn, L.C. (1984). Sediment transport: Part 1 Bedload transport. *J. Hydr. Eng.* 110(10), pp1341-1356.

Van Rijn, L.C. (1993). Principles of sediment transport in rivers, estuaries and coastal seas. *Aqua publications*. The Netherlands.

Verbanck, M A. (1995a). *Transferts de la charge particulaire dans l'egout principal de la ville de bruxelles. PhD Thesis*. Universite Libre de Bruxelles

Verbanck M.A. (1995b). Capturing and releasing settable solids - the significance of dense undercurrents in combined sewer flows. *Wat.Sci.Tech.*, Vol.31(7), pp.85-93.

Verbanck M.A. (1996). Assessment of sediment behaviour in a cunette-shaped sewer section. *Wat.Sci.Tech.*, Vol.33(9), pp.49-60.

Verbanck, M.A. (2000). Computing near-bed solids transport in sewers and similar sediment-carrying open-channel flows. *Urban Water*, Vol. 2, Issue 4, pp277-284

Wallingford Software. (2001). InfoWorks CS technical review. Available from: http://www.wallingfordsoftware.com/products/infoworks_cs/technical_review.asp.htm

White, S.J. (1970). Plane bed threshold of fine grained sediments. *Nature*, 228 (5267), pp152-153.

White, W.R. and Day, T.J. (1982). Transport of graded gravel beds. *Gravel Bed Rivers*. Ed. by R.D. Hey, J.C. Bathurst and C.R. Thorne, John Wiley & Sons Ltd., pp181-213.

White, W.R., Milli, H. and Crabbe, A.D. (1975). Sediment transport theories: a review. *Proc. Instn Civ. Engrs*, Part 2, 59, June, pp265-292.

Wilkinson, R. (1956). The quality of rainfall runoff water from a housing estate. *Jour. Of Inst. of Pub. Health. Eng,* 55.

Williams, D.J.A., and Williams, P.R. (1987). Rheology of sewer sediments. *Report for WRc.*

Williams, D.J.A., Williams, P.R., and Crabtree, R.W. (1989). Preliminary investigation into the rheological properties of sewer sediment deposits and the development of a synthetic sewer sediment material for laboratory studies. *FWR Report No FR0016.*

Williams, P.R., and Williams, D.J.A. (1989). Rheometry of concentrated cohesive sediments. *Jou. Coastal Res.*, Special issue no. 5.

Wöhrle, C., and Brombach, H. (1991). Sampling in sewers. *Wasserwirtschaft.*

Wotherspoon, D J J. (1994). The movement of cohesive sediment in a large combined sewer. *PhD thesis.* University of Abertay Dundee.

Wotherspoon, D.J.J., & Ashley, R.M. (1992). Rheological measurement of the yield strength of combined sediment deposits, *Wat. Sci. Tech.* 25, pp165-169.

Yalin, M.S. (1972). Mechanics of sediment transport. *Pergamon Press.*

Yang, C.T. (1996). Sediment Transport: theory and practice. *McGraw-Hill.*

APPENDIX A: FORFAR INORGANIC PARTICLE SIZE DISTRIBUTIONS

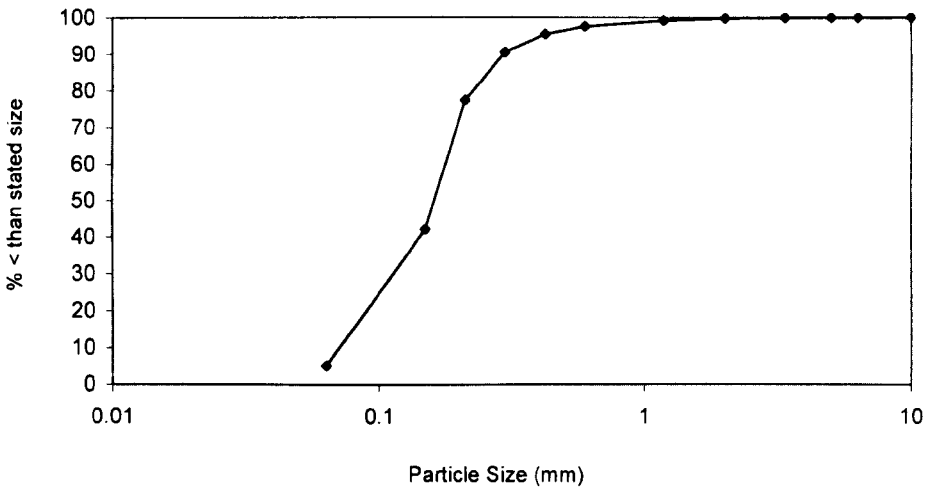

Figure A1: Particle size distribution of bed deposit (Site 2, 14/06/01)

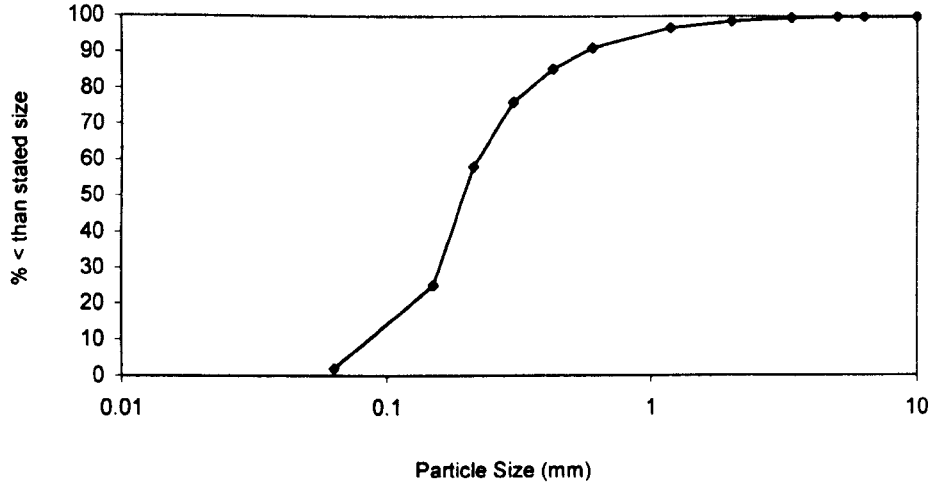

Figure A.2: Particle size distribution of bed deposit (Site 1, 14/06/01)

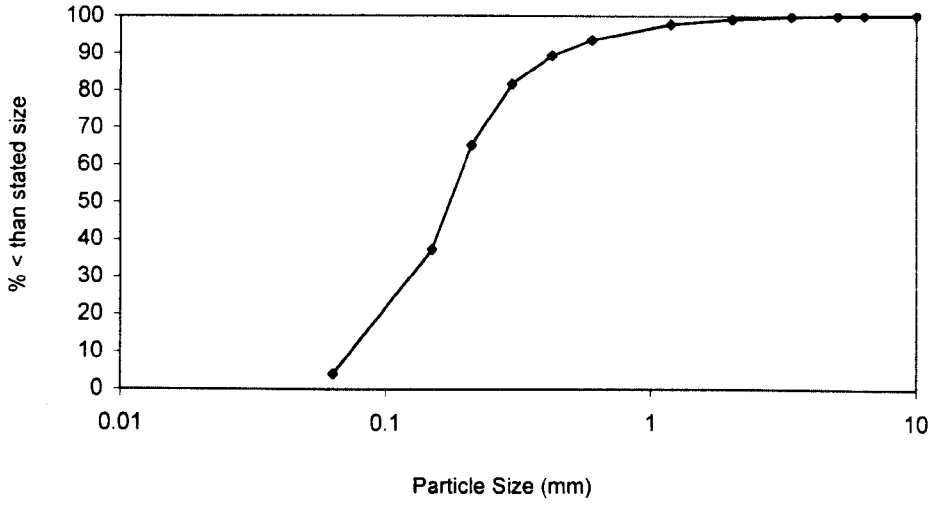

Figure A.3: Particle size distribution of bed deposit (Site 1, 16/07/01)

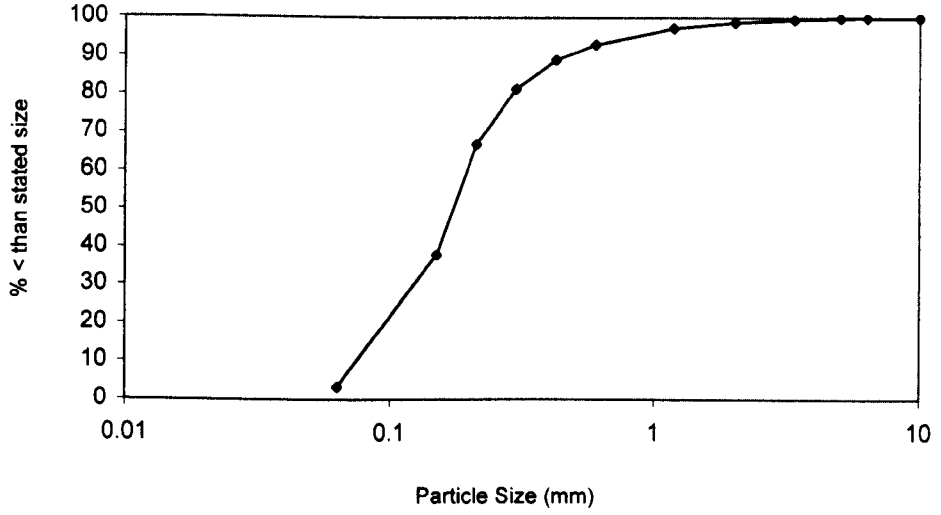

Figure A.4: Particle size distribution of bed deposit (Site 1, 24/07/01)

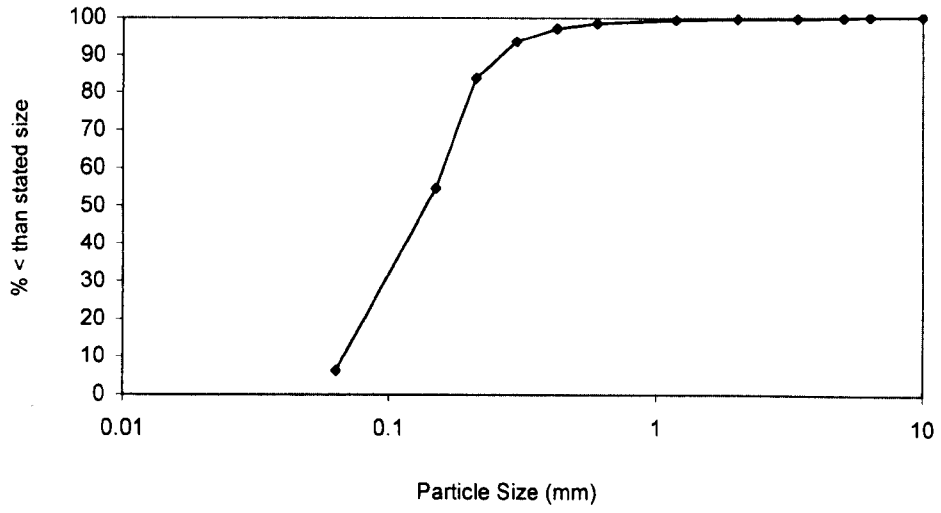

Figure A.5: Particle size distribution of bed deposit (Site 2, 24/07/01)

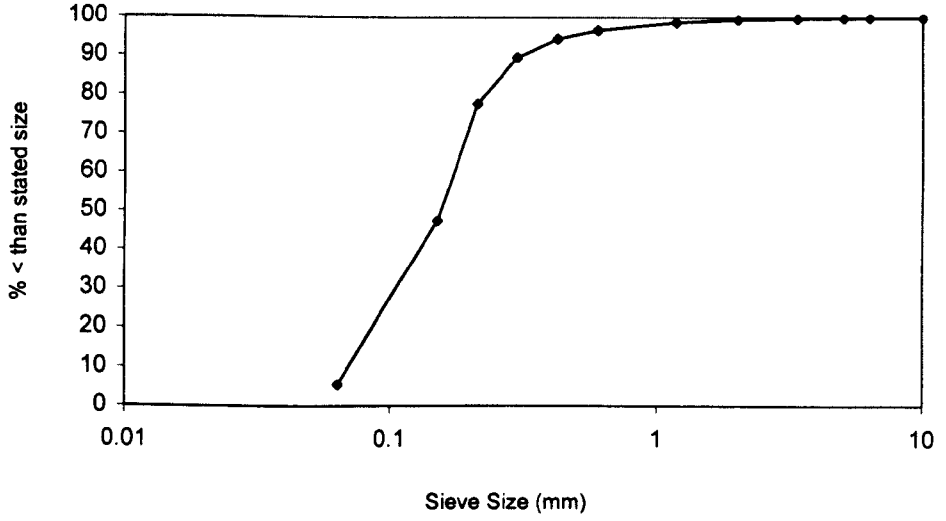

Figure A.6: Particle size distribution of bed deposit (Site 2, 01/08/01)

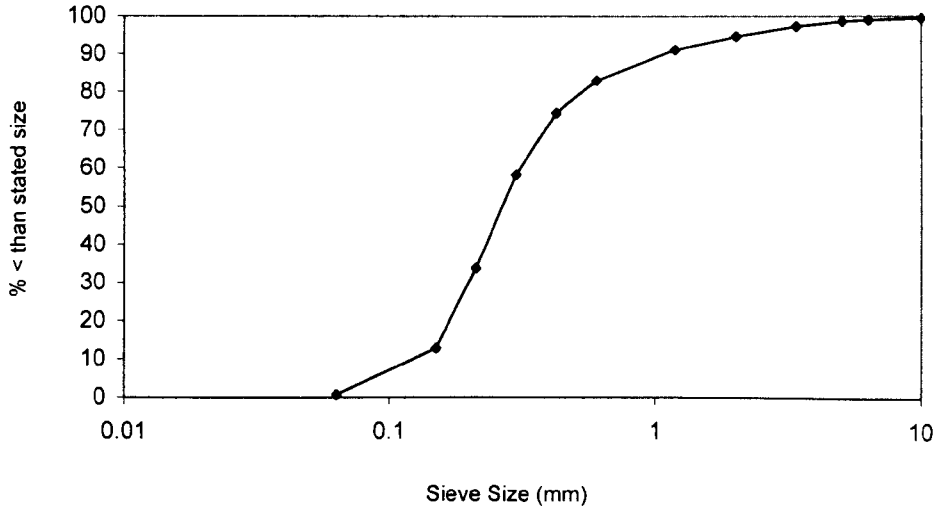

Figure A.7: Deposit size distribution from manhole upstream of Site 1 (01/08/01)

APPENDIX B: FORFAR FALL VELOCITY DISTRIBUTIONS

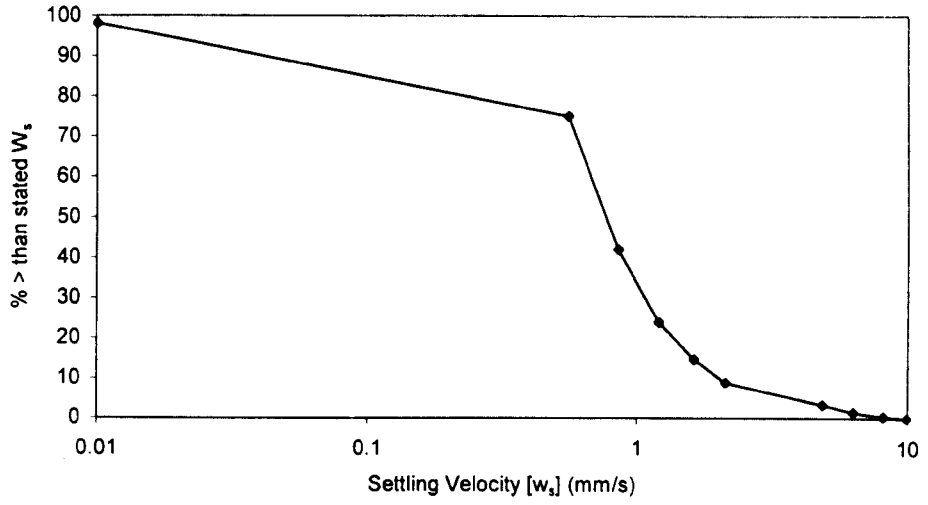

Figure B1: Fall velocity (w_s) distribution (Site 1, 14/06/01)

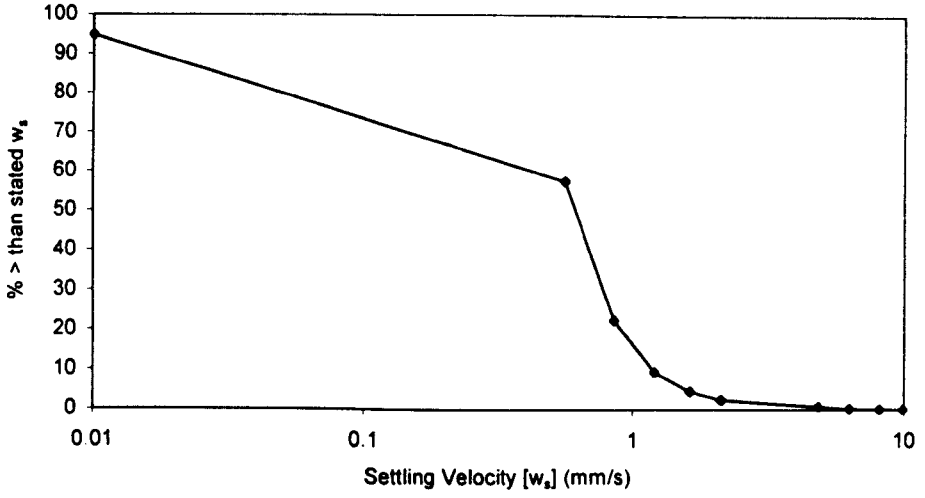

Figure B2: Fall velocity (w_s) distribution (Site 2, 14/06/01)

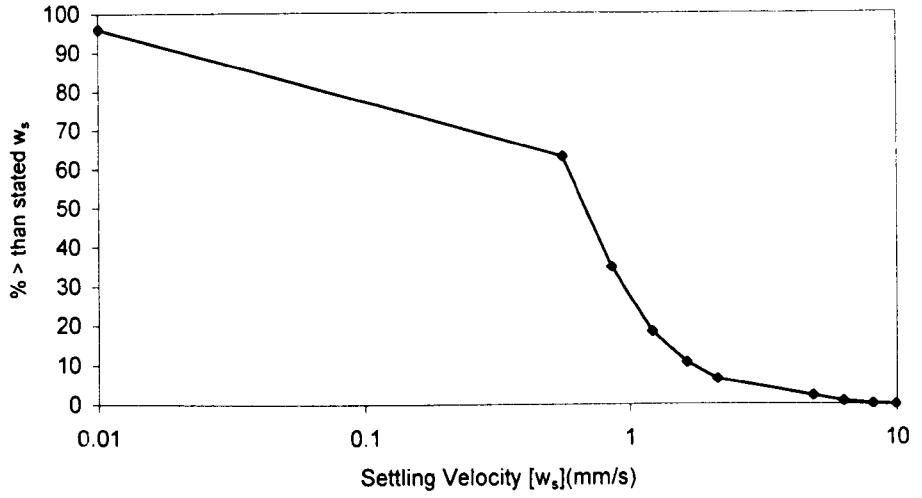

Figure B3: Fall velocity (w_s) distribution (Site 2, 16/07/01)

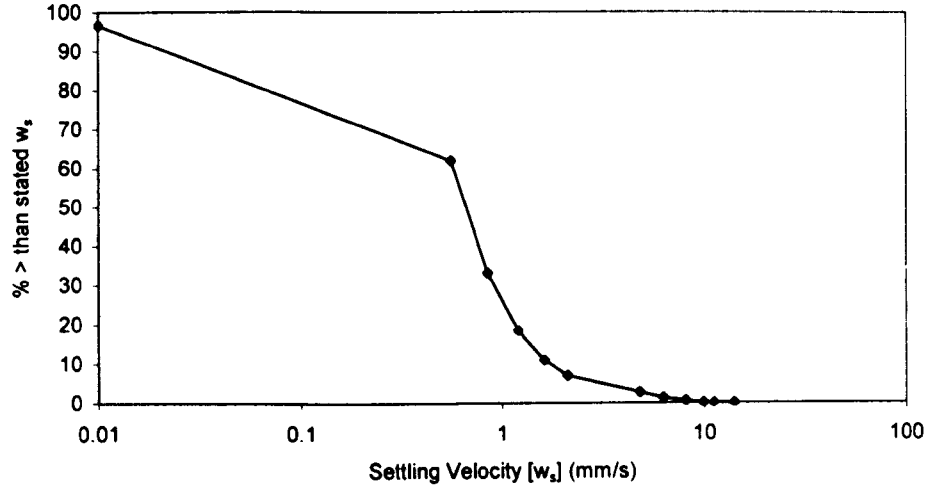

Figure B4: Fall velocity (w_s) distribution (Site 1, 24/07/01)

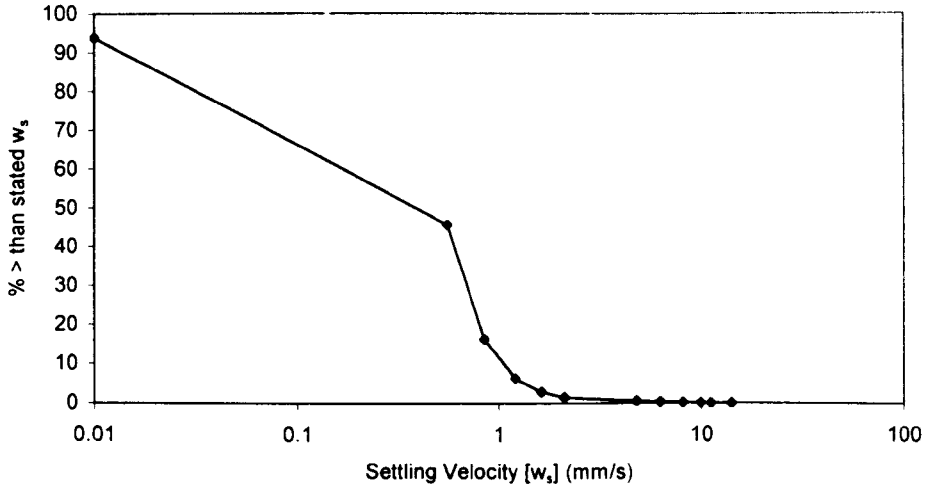

Figure B5: Fall velocity (w_s) distribution (Site 2, 24/07/01)

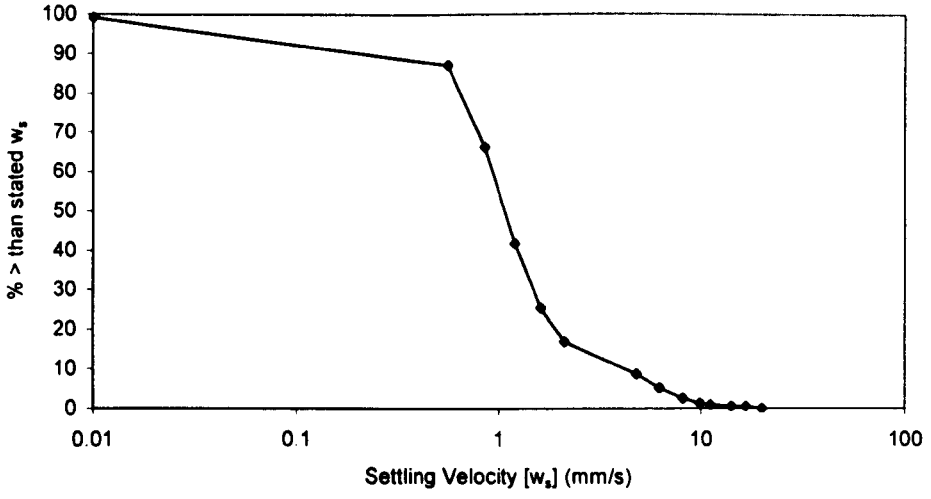

Figure B6: Fall velocity (w_s) distribution (USM, 24/07/01)

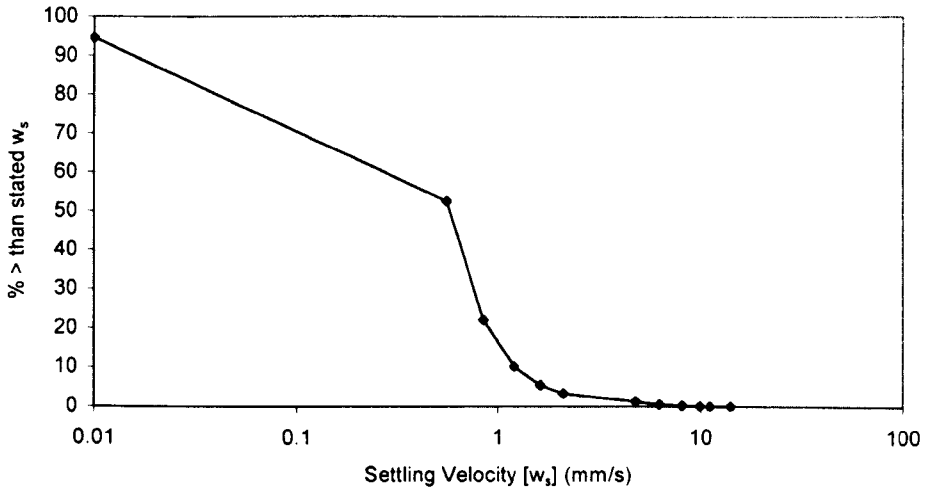

Figure B7: Fall velocity (w_s) distribution (Site 2, 01/08/01)

APPENDIX C: PUBLICATIONS

McIlhatton, T.D., Ashley, R.M., and Tait, S.J. (2004). Improved formulations for rapid erosion of diverse solids in combined sewers. *Proc. 6th International Conf. on Urban Drainage Modelling*, 15-17 September, Dresden, Germany, 2004

Oms, C., McIlhatton, T., Sakrabani, R., Chebbo, G. and Ashley, R. (2002). The nature of near bed solids in combined sewers. *Proc. 9ICUD*, 8-13 September 2002, Portland, USA.

McIlhatton, T.D., Sakrabani, R., Ashley, R.A., and Burrows, R. (2001). Erosion mechanisms in combined sewers and the potential for pollutant release to receiving waters and water treatment plants. *Proc. 2nd International Conf. on Interactions between Sewers, Treatment Plants and receiving Waters in Urban Areas*, Lisbon, Portugal, 2001.

Ashley R M., Hvitved-Jacobsen, T., Vollertsen, J., McIlhatton, T. and Arthur, S. (1999). Sewer solids erosion, washout, and a new paradigm to control solids impacts on receiving waters. *Proc. 8ICUSD*, Sydney, 1999.

Ashley, R.M., Tait, S., Fraser, A., McIlhatton, T.D., Phelan, D., Arthur, S., and Saul, A.J. (1998). Towards a model to understand foul flushes in combined sewers. *Proc. 2nd Int. Symp. on Environmental Hydraulics*. Hong Kong, 1998.

Ashley, R.M. and McIlhatton, T.D. (1998). The importance of 'near bed solids'. *Proc. Conf. on Alleviating Stormwater & CSO Problems*. Bristol, UK, 1998